E85 Optimized Engine
End of Project Technical Report
Ford Motor Company

Recipient: Ford Motor Company
Award Number: DE-FC26-07NT43276

Working Partners: Ford Motor Company, AVL, and Ethanol Boosting Systems (EBS)
Cost-Sharing Partners: Ford Motor Company and EBS

Contact: Stanley Bower 313-337-1169, sbower@ford.com
DOE Manager: Ralph Nine 304-285-2017 RALPH.NINE@NETL.DOE.GOV

Project Title: E85 Optimized Engine

Project Period: Oct 1, 2007 - Dec 31, 2011
Date of Report: March 31, 2012

Project Objectives:

- Develop a roadmap to demonstrate a minimized fuel economy penalty for an F-Series FFV truck with a highly boosted, high compression ratio spark ignition engine optimized to run with ethanol fuel blends up to E85.
- Reduce FTP 75 energy consumption by 15% - 20% compared to an equally powered vehicle with a current production gasoline engine.
- Meet ULEV emissions, with a stretch target of ULEV II / Tier II Bin 4.

Background:

This program was undertaken in response to US Department of Energy Solicitation DE-FC26-07NT43276, resulting in a cooperative agreement with the Ford Motor Company and EBS to demonstrate improvement of fuel efficiency using E85 fuel in a highly turbocharged direct injection engine. Direct injection of E85 is extremely effective in suppressing knock, enabling higher compression ratio and greatly increased torque per unit of engine displacement. The latter enables downsizing of the engine displacement and/or downspeeding of the engine rpm, which moves the operating regime of the engine in the vehicle to a more efficient part of the engine speed-load map.

In addition to demonstrating the benefits of an E85 optimized FFV engine, an integral part of the project was assessment of the Dual Fuel concept, which combines port fuel injection of gasoline with direct injection of E85 in the same engine (Figure 1). In this concept, gasoline is used at low to medium torque, and direct injection of E85 is used at high torque only in the amount required to prevent knock. The concept combines the heating value per volume advantage of gasoline with the high load knock suppression advantage of E85. Because direct injection of E85 enables higher compression ratio and downsizing / downspeeding, gasoline is used more efficiently in the vehicle, thereby leveraging the benefit of ethanol in reducing the consumption of gasoline. The vehicle owner realizes high mpg fuel economy because gasoline, with its high heating value per volume, is the fuel that is primarily used for most driving modes in an engine which operates at high efficiency in the vehicle.

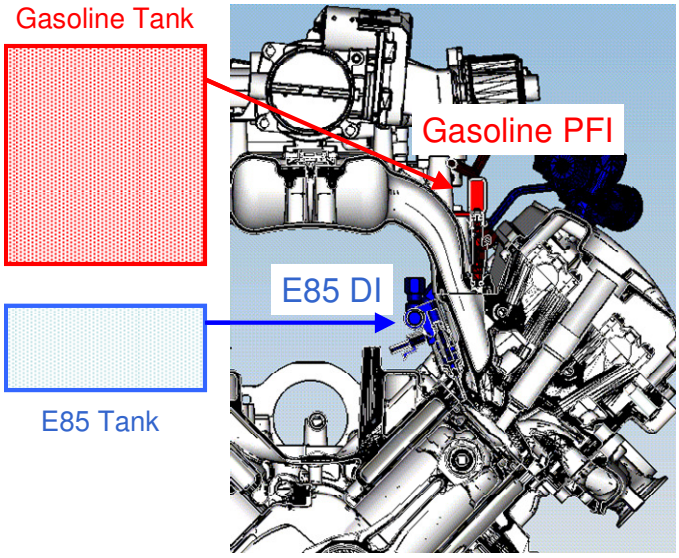

Figure 1 - Dual Fuel engine concept.

Summary of Results:

A 5.0L V8 twin-turbocharged direct injection engine was designed, built, and tested for the purpose of assessing the fuel economy and performance in the F-Series pickup of the Dual Fuel engine concept and of an E85 optimized FFV engine. Additionally, production 3.5L gasoline turbocharged direct injection (GTDI) "EcoBoost" engines were converted to Dual Fuel capability and used to evaluate the cold start emissions and fuel system robustness of the Dual Fuel engine concept. All project objectives were met or exceeded.

Full Load Performance

The Dual Fuel and E85 optimized FFV engines provide greatly increased full load torque and power compared to an equal displacement GTDI engine due to the highly knock resistant properties of E85. Peak BMEP (a measure of torque per unit of engine displacement) increased from 23 bar with gasoline running with enrichment to 32 bar with E85 at stoichiometry (Figure 2). This enables downsizing of the engine displacement and/or downspeeding (running lower engine speed), which moves the engine operating range in the vehicle to a more efficient region, providing improved vehicle fuel economy.

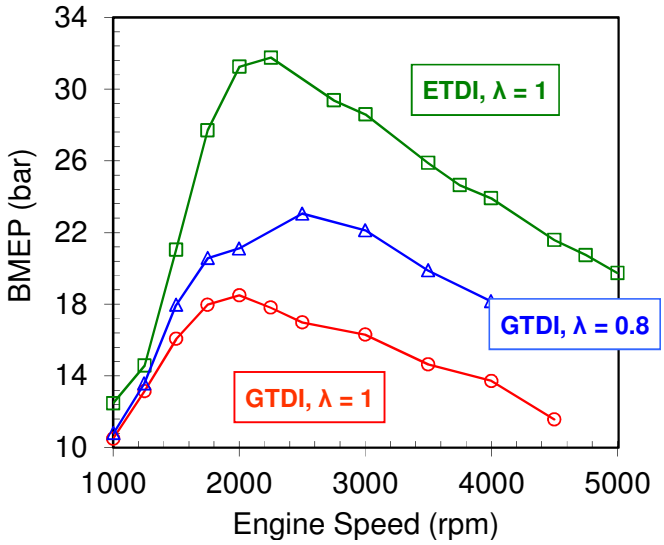

Figure 2 - Full load BMEP for ETDI and GTDI.

Fuel Economy

Using 5.0L engine dynamometer data scaled to various engine displacements as input, vehicle simulation analysis for the F150 indicates that a 3.0L Dual Fuel or E85 optimized FFV engine can replace the 6.2L displacement naturally aspirated gasoline engine (the baseline at project initiation) and provide equivalent or greater vehicle acceleration and towing performance, with the following results (Figure 3):

- The E85 optimized FFV engine using E85 fuel results in a mpg fuel economy penalty of about 8% on the combined M-H cycle. This compares favorably with the reduced energy content of E85 compared to gasoline of 29%.
- The Dual Fuel engine results in a mpg fuel economy improvement of about 20% on the combined M-H cycle.
- The E85 optimized FFV engine using E85 fuel and the Dual Fuel engine result in reductions of energy consumption on the FTP75 cycle of 26% and 21%, respectively, exceeding the project objective of 15 - 20%.
- The E85 optimized FFV engine using E85 fuel and the Dual Fuel engine result in reductions of CO_2 emissions on the M-H cycle of 23% and 17%, respectively.

For reference, simulation results for a 3.5L GTDI engine based on scaled 5.0L engine data are also shown in Figure 3.

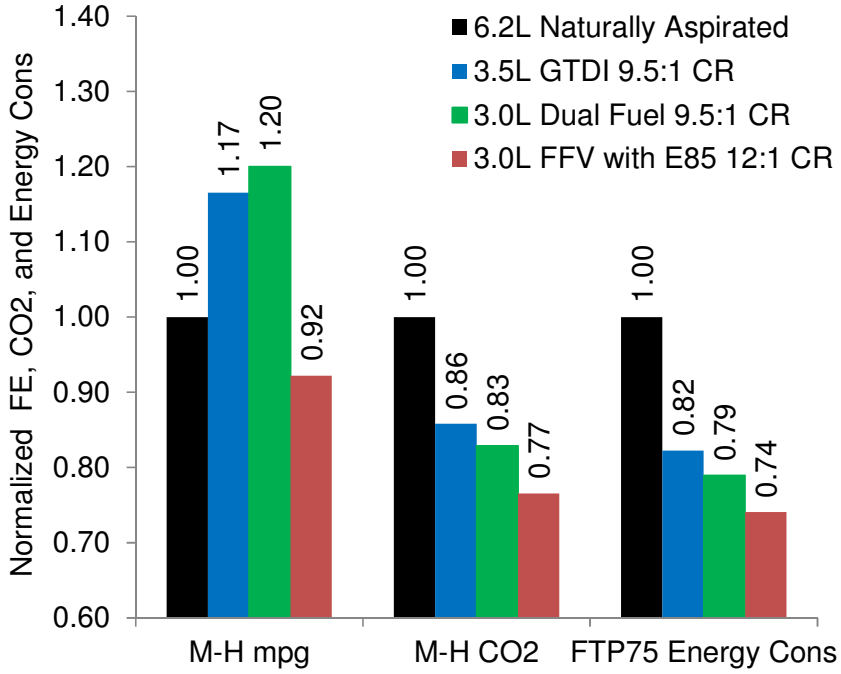

Figure 3 - M-H fuel economy, M-H CO_2 emissions, and FTP75 energy consumption normalized to values for 6.2L naturally aspirated baseline engine.

The above results assume the Dual Fuel engine maintains the compression ratio of the baseline GTDI engine (to increase driving range on the E85 fuel tank, as described below), and that the E85 optimized FFV engine has an increased compression ratio of 12:1(to utilize the high effective octane of E85 fuel). However, the performance of the E85 optimized FFV engine will be adversely affected by the high compression ratio when the engine is operated on gasoline, and thus implementation of an E85 optimized FFV engine at high compression ratio would be dependent upon the availability of E85.

Leveraging of Ethanol to Replace Gasoline

Because direct injection of E85 enables very high BMEP and downsizing of the engine displacement, gasoline is used more efficiently in the vehicle with the Dual Fuel engine concept, thereby leveraging the use of ethanol in reducing the consumption of gasoline. For the vehicle simulation results for the F150 on the M-H cycle, the reduction in gasoline consumption for the 3.0L Dual Fuel engine compared to the 3.5L GTDI engine is equivalent to one gallon of E85 replacing 2.5 gallons of gasoline (Figure 4).

The reduction in gasoline consumption for the 3.0L E85 optimized FFV engine is equivalent to one gallon of E85 replacing 0.8 gallon of gasoline. Note that this is still a significant improvement compared to the heating value of E85 relative to that of gasoline; on an equal heating value basis, one gallon of E85 would replace 0.71 gallons of gasoline. The improvement from 0.71 to 0.8 is due to the increase in thermal efficiency in the vehicle as a result of higher compression ratio and downsizing of the engine displacement.

Thus, the Dual Fuel engine concept provides greater leveraging of ethanol in reducing gasoline consumption and greater mpg fuel economy than the E85 optimized FFV engine. The E85 optimized FFV engine provides lower CO_2 emissions and energy consumption than the Dual Fuel engine (Figure 3), but full load performance is more severely degraded due to higher compression ratio if E85 is not available.

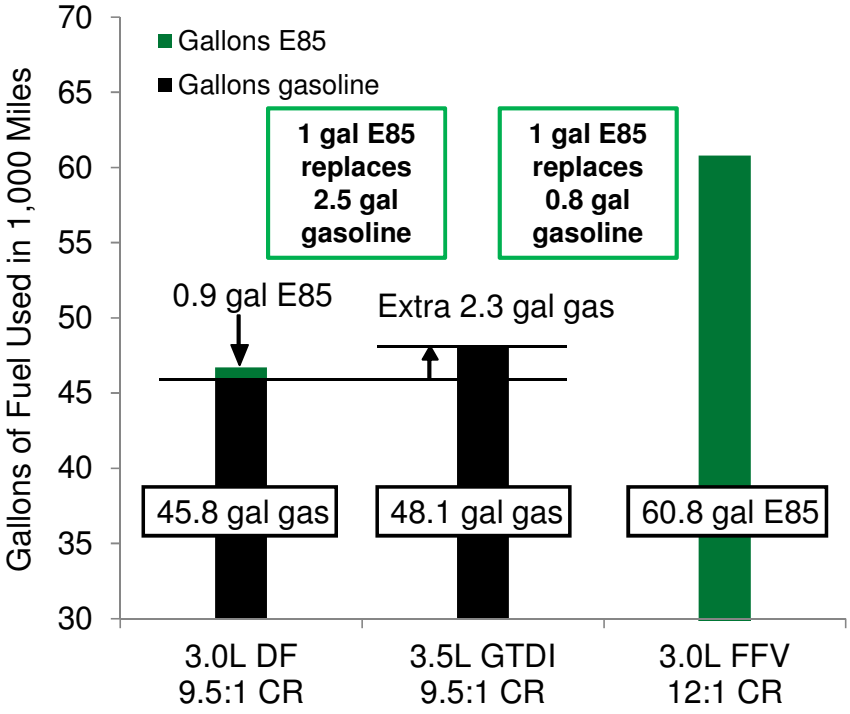

Figure 4 - Dual Fuel engine leveraging of ethanol to reduce gasoline consumption.

Emissions

The Dual Fuel engine concept provides cold start NMOG and NOx emissions comparable to a well-developed "EcoBoost" gasoline turbocharged direct injection (GTDI) baseline engine and meets the cold start emission targets for the project stretch objective of ULEV II / Tier II Bin 4. The Dual Fuel engine and E85 optimized FFV engine provide near zero particulate emissions, but the cold start NMOG emissions for the E85 optimized FFV engine are higher than the baseline GTDI engine (Figure 5).

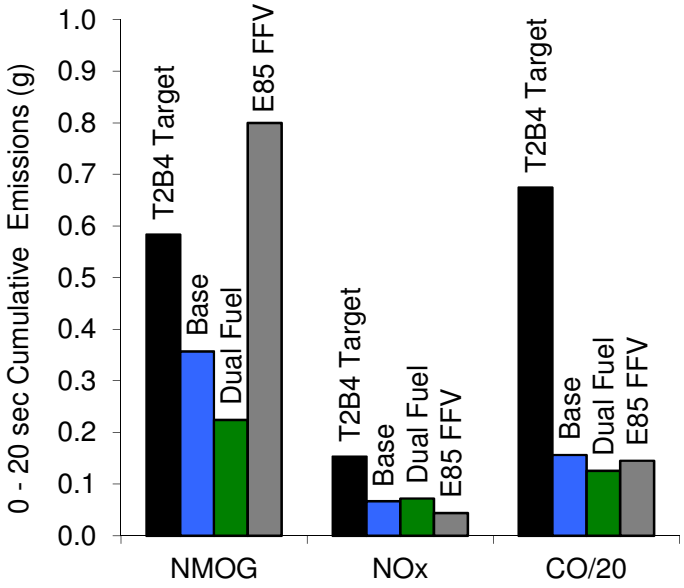

Figure 5 - Cold start emissions for base GTDI, Dual Fuel, and E85 FFV.

The Dual Fuel and E85 FFV engines are also able to run with stoichiometric air-fuel ratio over the entire engine operating range, which enables three way catalyst function for all operating conditions, including off-cycle. This is in contrast to gasoline engines which run with significant enrichment at full load.

E85 Tank Range for Dual Fuel Concept

The E85 tank for a 3.0L Dual Fuel engine in a F-Series pickup would need to be filled about every 17th time that the gasoline tank is filled for driving conditions typical of the M-H cycle and about every 11th time for towing a 10,000 pound trailer at 65 mph up a 1% grade, with the following assumptions:

- The E85 tank is one third the size of the gasoline tank.
- Moderate combustion phasing retard is applied to reduce E85 usage under heavy load conditions such as towing a trailer.
- The compression ratio of the engine is maintained at that of the baseline GTDI engine.

Increasing compression ratio improves the fuel efficiency and CO_2 emissions of the engine in the vehicle, but dramatically increases E85 usage and the refill frequency of the E85 tank relative to that of the gasoline tank. Thus, selection of compression ratio for a Dual Fuel engine will be dependent upon the duty cycle of the intended vehicle application and the availability of E85. Additionally, the above refill frequencies only include the use of E85 for knock suppression, and do not take into account other uses of E85 such as for the reduction of cold start emissions, use of 100% E85 fueling for enhancement of turbocharger response and vehicle launch performance, and potential use of additional E85 for direct injector robustness. The cumulative effect of these uses of E85 for an actual vehicle implementation of the concept has not yet been quantified.

Durability/Robustness

No technical issues have been encountered to date which would preclude implementation of the Dual Fuel concept. However, production of the concept would require assessment of long term durability/reliability and analysis of potential failure modes in addition to those investigated during this project.

Project Overview:

The E85 Optimized Engine Project was undertaken to demonstrate and assess the use of ethanol as a fuel for direct injection turbocharged engines when used in conjunction with smaller engine displacement (downsizing), higher gear ratios (downspeeding), and increased compression ratio (CR), in order to achieve improved vehicle fuel efficiency. As an integral part of this project, the Dual Fuel "ethanol on-demand" concept was evaluated. In this concept, port fuel injection (PFI) of gasoline is combined with direct injection (DI) of E85. Gasoline PFI is used for starting/cold start emissions and low-medium load operation, and ethanol is directly injected as a function of load only in the amount required to suppress knock.

The first phase of the project included design and development of the combustion system for the engine. After an initial design was specified based on prior experience, the in-cylinder air motion and direct injection fuel spray were optimized using a single cylinder engine with optical access (Figure 6), and the combustion system function was verified using a single cylinder test engine (Figure 7). This phase of the project was documented in SAE paper 2010-01-0585.

The multi-cylinder engine design was based on the architecture of the Ford Motor Company V8 modular engine family, incorporating the bore centers and deck height of the production 5.4L engine. An all new cylinder head was designed based on the results of the single cylinder combustion system optimization. New lower end components (cylinder block, crankshaft, pistons, connecting rods, etc.) were designed to support a peak cylinder pressure of 150 bar, in order to enable evaluation of the highly knock resistant properties of ethanol fuel. A new air system (intake manifold, intercoolers, etc.) and twin turbocharger system with new exhaust manifolds were also designed. A picture of the multi-cylinder engine without the intercoolers is shown in Figure 7.

As part of the multi-cylinder engine development, the effects of exhaust "blowdown interference", a phenomenon which occurs on a V8 engine with outboard exhaust manifolds, were quantified and two methods of mitigating these effects were investigated. This work was documented in SAE paper 2011-01-0337. As a result of this investigation, twin-scroll turbochargers were incorporated for the final phase of the engine dynamometer testing, in order to make the results more generic and applicable to other engine configurations.

Multi-cylinder engine development included optimization of twin independent variable cam timing (TiVCT) settings, turbocharger matching, DI fuel injection pressure and timing, and other engine parameters. Engine maps and full load performance curves were then developed based on steady state data taken on the multi-cylinder engine for the following cases: gasoline turbocharged direct injection (GTDI) at 9.5:1 CR, an E85 optimized FFV using E85 fuel at 9.5:1 CR and at 12:1 CR, and Dual Fuel at 9.5:1 CR and at 12:1 CR. Due to the high knock resistance enabled by direct injection of ethanol, the E85 optimized FFV and Dual Fuel cases result in large improvements in full load performance compared to the GTDI case, thereby enabling downsizing of the engine displacement. Using the above data scaled to various engine displacements as input, vehicle level fuel efficiency and performance were assessed using the AVL-CRUISE vehicle simulation model.

To facilitate assessment of cold start emissions of the Dual Fuel concept utilizing a production three way catalyst aftertreatment system and to allow comparison to an optimized production baseline GTDI ("EcoBoost") calibration, a production 3.5L V6 EcoBoost engine was converted to Dual Fuel capability. The cold start emissions of the Dual Fuel engine as well as a FFV version of the engine using E85 were then assessed on a dynamometer capable of replicating cold start transient conditions. The 3.5L Dual Fuel engine was also used to assess fuel system robustness with the Dual Fuel concept.

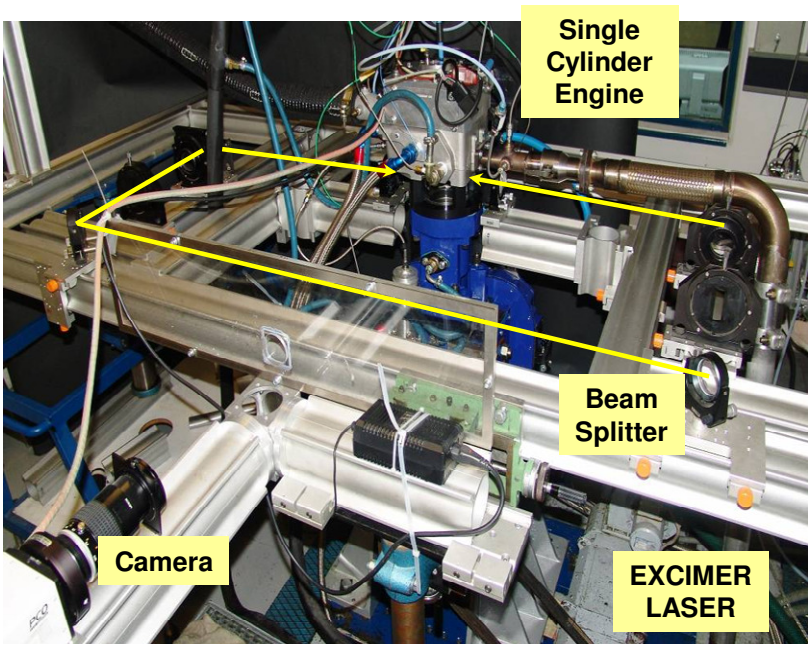

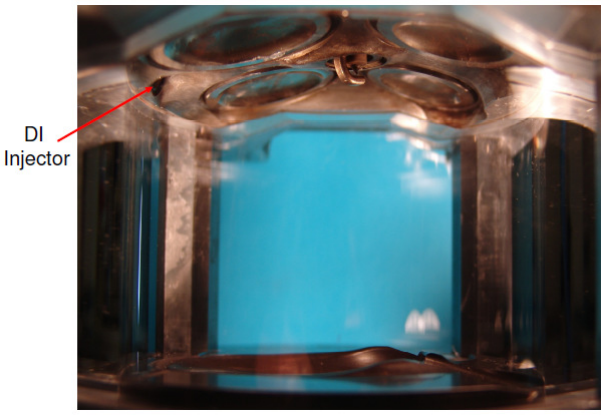

Figure 6 - Single cylinder engine with optical access.

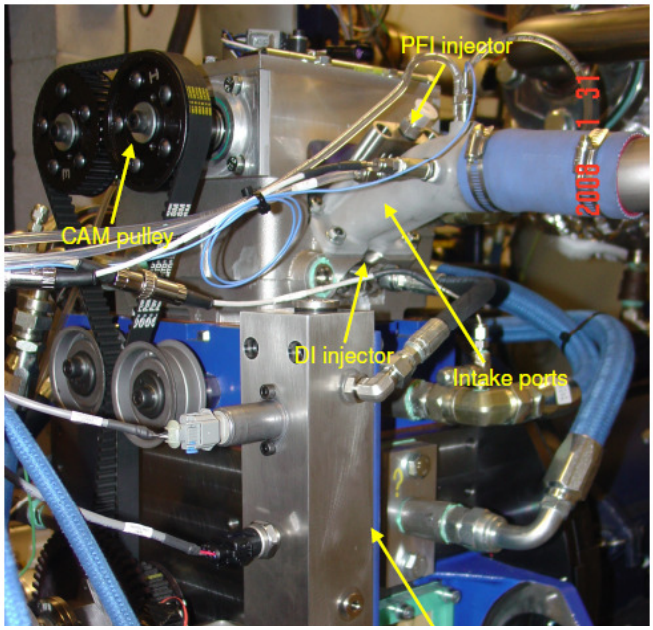

Figure 7 - Single cylinder engine (left) and multi-cylinder engine (right).

DISCLAIMER

Table of Contents

List of Figures

Technical Discussion

(Phase and Task Numbers Defined in the Statement of Project Objectives)

Phase 1 – Concept Definition

Task 1 – Cylinder Head

The cylinder head concept is based on the existing Ford modular engine family. A 3-dimensional CAD view of the cylinder head is shown in Figure 8. The first major decision was to place the DI injectors at the side of the combustion chamber rather than in a central location between the valves, close to the spark plug. This reduces the exposure of the DI injectors to excessive heat, which is especially important when there is zero or low fuel flow through the injectors at part load with the Dual Fuel concept.

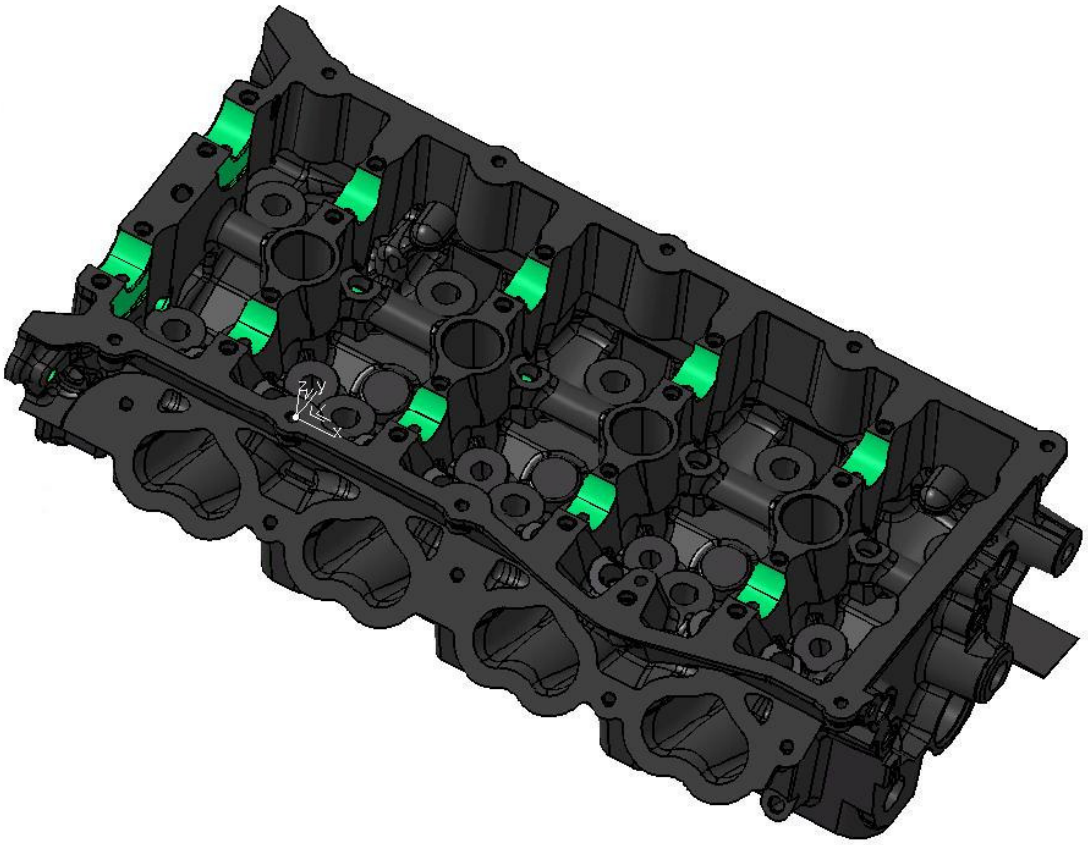

Figure 8 - CAD 3-dimensional view of multi-cylinder head design.

Valve train geometry and major components were carried over from an existing Ford engine design. Ports were designed to provide high levels of tumble air motion which has been found to improve the detonation tolerance of gasoline turbocharged direct injection (GTDI) engines and also provide improved mixture preparation and reduced cylinder wall wetting. The high tumble ports were developed to optimize the flow-tumble trade-off and to ensure the tumble flow field was symmetric and well-centered in the combustion chamber. Flow box analysis of the ports is described later in this report.

To achieve the necessary cooling requirements, a series of different cooling strategies were analyzed. Care was taken to ensure sufficient coolant flow between the valve bridges and spark plug towers and under the lower sides of the intake ports. The first refinement of this layout was to increase the flow in front of the first

cylinder bolt boss and in the back of the last cylinder bolt boss, plus the addition of a second crossover at the rear of the cylinder head. The flow was further optimized to ensure adequate flow velocities between the cylinder bores.

Task 2 – Air System

The program assumed boost air would be supplied by twin turbochargers mounted on the outboard sides of the engine. Minimum pressure drop and velocity gradient requirements for efficient operation must also be considered when routing compressor and turbine inlet and outlet ducting.

An issue with uneven firing order V8 engines identified at the outset of the program is that two cylinders on each bank fire within 90 crankshaft degrees of each other, so the exhaust blowdown from the first cylinder influences the gas exchange process of the next firing cylinder by causing a backflow of exhaust gas into the cylinder. This leads to increased levels of residual gas which can lead to lower IMEP levels and higher combustion instability in those cylinders, but more importantly, especially for a turbocharged engine, this can lead to reduced detonation tolerance in the two affected cylinders, which limits the ignition timing setting for the entire engine and reduces efficiency.

With cam phasing it is possible to increase valve overlap and use the boosted high intake pressure to scavenge the cylinders of exhaust gas and increase mass flow to the turbines. This can be used to great advantage to improve low speed torque. At low speed full load operation, torque is normally limited by low available boost pressure and is the reason for the phenomenon known as ‘turbo lag’, where the engine feels unresponsive due to low torque until the turbocharger begins to generate boost and torque increases. With a port fuel injected (PFI) engine, the scavenge air would also contain fuel, which would lead to high engine-out hydrocarbon emissions and would lead to a damaging thermal reaction in the catalysts. With DI, the fuel injection event can be separated from air delivery and this scavenging strategy can be employed to improve low speed torque and improve responsiveness and driveability. However, the issue of uneven firing order and residual gas effects can be exacerbated with high levels of overlap for scavenging, so a low residual solution was required to enable scavenging. The possibilities identified included optimization of valve events and optimization of the exhaust manifold design to separate the offending exhaust pressure pulses from the affected cylinders. This is described in detail later in this report.

Two alternative configurations were explored to overcome some of the package challenges and help overcome the residual gas issues; conventional outboard exhaust manifolds with a single larger turbocharger packaged in the valley and inboard exhaust with twin-turbochargers. Both alternatives were excluded due to various technical and timing implications. The decision to move forward with the conventional twin turbocharger outboard configuration was made.

GT-POWER (1-dimensional intake and exhaust dynamics simulation) studies were performed to identify a single turbocharger specification that would meet three performance target levels. This work was supported by the turbocharger supplier who provided a number of compressor and turbine maps based on their own analyses. GT-POWER simulations were run with agreed assumptions on pressures and temperatures throughout the intake and exhaust system, and various valve timing strategies were investigated using a design of experiments process to optimize airflow performance while reducing residual exhaust gas levels.

A schematic of the air system layout is shown in Figure 9. With a conventional twin turbocharger configuration, air is fed to each compressor from a separate air cleaner and zip tube in a symmetric layout to ensure even air distribution and pressure drop to each bank. From each compressor, air is then fed up to two air-water heat exchanger units cooled by a low temperature coolant circuit. Each heat exchanger or intercooler is responsible for cooling the air from each compressor so as to achieve high cooling effectiveness with a low pressure drop. The cooled air meets in a central reservoir where it flows through the throttle and enters the intake manifold which is packaged below and supporting the intercooler modules. This package arrangement again relies on symmetry to provide even airflow to each bank. On the exhaust side, exhaust gas flows through a cast log type exhaust manifold and into the turbine housing with an integrated wastegate. After exiting the turbine,

exhaust gas flows through a close-coupled three way catalyst (TWC) and then through a dual exhaust system to the tailpipe. Boost pressure is controlled on each bank by wastegates integral to the turbine housings, and surge valves are fitted to the compressors to bleed boost from the high pressure side of the compressor to the inlet to protect against compressor surge on throttle tip-out maneuvers.

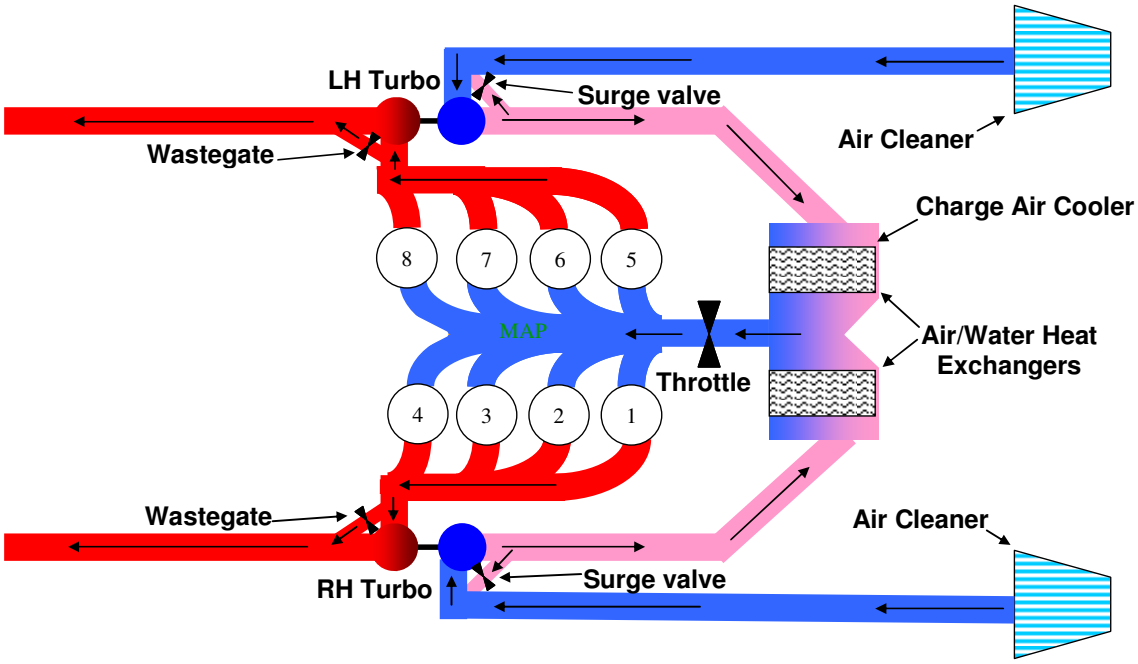

Figure 9 - Air system layout.

Intake Ports

Intake ports were designed to provide high levels of tumble air motion. The high burn rates resulting from high tumble motion help to suppress detonation and provide earlier end of combustion timing. Both of these factors are important in a turbocharged gasoline engine as it allows stable operation at increased BMEP levels. Fuel economy is improved and at higher speeds where fuel enrichment is typically required to control maximum turbine inlet temperatures due to retarded spark timing, the fuel enrichment requirement is reduced, which further improves fuel economy. High tumble also helps the fuel-air mixture preparation process in a direct injection engine and helps reduce bore washing that can lead to smoke and oil dilution. However, the positive effects of tumble ratio must also be balanced with NVH concerns as the high burn rates may lead to high pressure rise rates in the combustion chamber.

A high tumble intake port was designed to package around the DI injector and optimized for the valvetrain layout and valve sizes. A PFI injector was packaged and optimized to target the intake valves while minimizing inlet port wall wetting. A water jacket was designed to provide cooling around the DI injector, spark plug, and combustion chamber, the lower part of the intake and the top and bottom of the exhaust port.

A model of the intake port, valves, valve guides and seats was produced for testing. A flow box was used to develop the port to produce a symmetric flow field and optimize the tumble/flow tradeoff while achieving the target high tumble ratio. The tumble flow field was measured on the AVL laser Doppler anemometry (LDA) rig, which provides velocities in the vertical direction at 250 points across the bore area measured at a distance equivalent to half the bore diameter down from the top of the liner. This provides a complete measurement of the air motion generated by the port, and by taking measurements at various valve lifts, the instantaneous flow field along with a cycle averaged tumble ratio can be derived. This technique also allows for measurement and assessment of the symmetry of the air motion field and an estimate of flow coefficient. Initial results showed

that the port generated a very high tumble ratio. To reduce the tumble, the throat of the port was modified by reducing the tumble generating lip at the interface between the port leg and the throat with a control cutter. This modification reduced the tumble ratio, provided adequate flow coefficient with good flow field symmetry centered in the combustion chamber and satisfied the turbocharged GDI engine requirements.

Task 3 – Fuel System

Placement of the DI injector for this engine was a critical design decision with the options of central or intake side location. A central injector location would be required should the engine need to operate in a stratified combustion mode for lean burn operation and future additional fuel economy improvements. However, the central location is the hottest location for the injector and the location that is most problematic in terms of packaging an adequate coolant jacket around the injector and spark plug, compounding injector cooling issues.

DI injector cooling was considered an important issue for this engine, not only because of the high BMEP targets, but because under the Dual Fuel operating regime fuel flow to the DI injector would be shut off at part load with fuel supplied by the PFI injector only. GDI injectors are temperature limited to reduce fouling, which can deteriorate spray, and rely on fuel flow through the injector to cool the injector tip. Previous results have shown that operating conditions around mid-speed, light-load result in the hottest injector tip temperatures. At these conditions engine fuel demand is low relative to combustion temperatures, and under Dual Fuel operation all fuel would be delivered by the PFI injector with zero flow through the DI injector.

To minimize cost and complexity and increase the applicability of the design to other engines, the decision was made to package the injector on the intake side. This location satisfied all current performance and emissions requirements with minimum risk to injector durability and tip temperature concerns.

The DI injector was packaged in the cylinder head with the tip located between the intake valves. The body of the injector was inclined to the cylinder head face at an angle which provided a 360° water jacket around the injector with a well-targeted fuel spray and minimum impact on the intake port. As the cylinder head and intake port design evolved, a requirement to reduce the installed injector angle was adopted to facilitate removal of the injector. This modification had no impact on injector spray targeting as the spray could be retargeted in the new position; however this compromised injector cooling as it closed off the area under the injector required for cooling underneath the injector body. The impact of this change was assessed on a running engine, and injector cooling was found to be acceptable. These results are shown later in this report.

Injectors were sized using the maximum permissible injection duration under peak power conditions and the minimum injector duration required for idle operation. Sizing must ensure the injector operates in the linear region of its flow versus pulse width duration curve at all conditions with a high degree of cycle-to-cycle repeatability. The number of injector holes was optimized for targeting as well as specified flow rate to maintain required L/D (L=length of each injector hole, D=hole diameter) limits which influences atomization and penetration.

Injector sprays were designed by AVL based on knowledge and experience gained from many other GDI programs and injector spray development in CFD, optical single cylinder, and conventional engine development work. Two injector sprays were designed with variations of spray targeting based on two recent and similar engine programs where the injectors had performed very well. The fuel injector supplier also provided an injector design derived from applying their standard methodologies.

Piston bowls were designed to work in combination with these injectors to support very late ignition timing for catalyst heating by creating a rich mixture at the spark plug with a split injection strategy. The piston bowl was designed to be as open as possible so as not to negatively impact normal homogenous combustion by hindering flame propagation.

DI fuel pump options were reviewed in terms of fuel flow requirements, pressure requirements, and ethanol compatibility. Three pumps that met the functional requirements were identified: a six-piston radial pump, a

dual piston plunger pump, and two single piston plunger pumps. The two single piston plunger pumps mounted on the cam covers and driven by an additional lobe on each cam were chosen.

PFI injector flow rate was influenced by Dual Fuel operation where it would operate at light load with the DI injector shut off. The PFI injector would contribute less than 50% of the total fuel requirement at full load where the DI injector would deliver the majority of the fuel. The PFI injector specification, defined by assuming a maximum flow of half the total fuel flow at peak power, helped bias the PFI injector to a lower flow rate to improve fuel flow control at idle. A PFI spray pattern was selected from the range of available production injectors to target closed intake valves with a wide spray angle for best spray quality while minimizing port wetting.

Task 4 – Performance Development and Analysis

Target performance curves were defined for conventional GTDI, ETDI and Dual Fuel operation. Performance capability will be similar for Dual Fuel and ETDI, however, Dual Fuel will minimize E85 usage to extend the E85 range of the vehicle between E85 tank refills.

GT-POWER Modeling

A GT-POWER performance simulation model of the engine, air induction system, turbocharger, and exhaust systems was built. Temperature and pressure boundary conditions were agreed and combustion metrics were taken from AVL test bed data. The GT-POWER model was then correlated to the measured AVL engine data. The validated model was then exercised to investigate the following:

- Performance with the initial turbocharger match provided by turbocharger supplier
- Trapped residual gas estimates for a number of turbocharger package configurations and manifolding schemes
- Turbocharger match optimization at the three performance levels with various compressor and turbine options
- Optimization of cam duration and timing for full load performance, with and without scavenging optimized for low trapped residual gas levels
- Investigation of part load fuel economy differences between the two alternative sets of cams optimized for full load performance
- Effect of 6000 ft altitude on performance and turbocharger match

For all cases the GT-POWER model was run assuming either direct injection of 91 RON gasoline or E85. No attempt was made to model combined E85 DI and gasoline PFI as the critical combustion characteristics needed for modeling were considered similar to those of single fuel direct injection. The main requirements for the initial GT-POWER work was to define airflow requirements to meet targets, and turbocharger match optimization; these would not have been greatly influenced by an E85 DI/gasoline PFI model.

Figure 10 shows residual gas levels at full load as a function of engine speed at the start of combustion. The residual levels are very high in the two cylinders that are affected by exhaust pulsations from adjacent firing cylinders. These high residual levels would lead to elevated end gas temperature which would result in detonation at earlier ignition timing than the remaining cylinders. This would limit the ignition advance that could be realized for the engine and would reduce engine efficiency and possibly lead to a combustion stability deterioration. As such, residual levels must be managed at low and high engine speeds.

Figure 11 shows residual levels that could be achieved if the engine was configured so that the turbocharger system operated like two 4-cylinder engines with the exhaust pulses for each cylinder separated by 180° from the adjacent cylinders in the firing order. This eliminates the pressure pulse from one cylinder affecting the adjacent cylinder and increasing residual fraction. Valve timing was the same for this case as for the standard case.

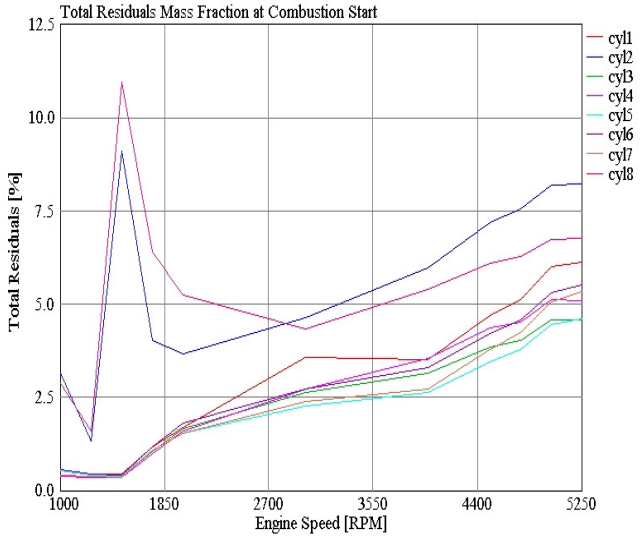

Figure 10 - Trapped residual gas levels for each cylinder vs. engine speed at full load.

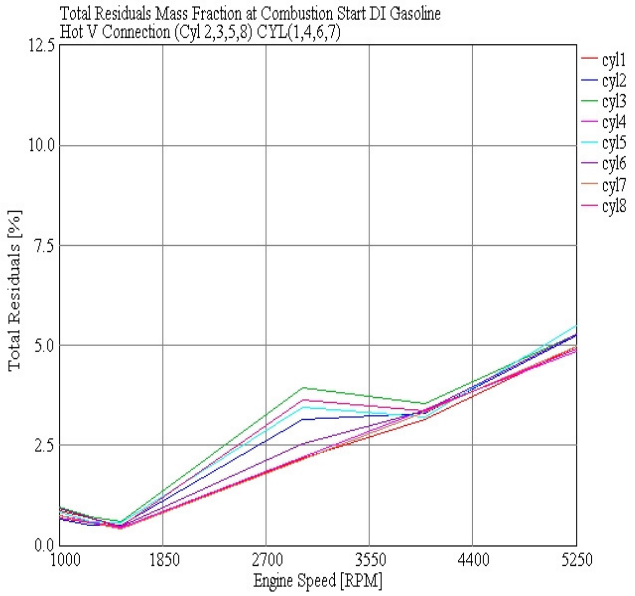

Figure 11 - Trapped residual gas levels for each cylinder vs. engine speed at full load for an alternate configuration with manifolding to separate the engine into two 4-cylinder engines.

Intake cam duration and phasing were studied to investigate the effect on residuals. Figure 12 shows three different intake camshaft phasings where the duration of the intake cam was reduced and then increased giving the five duration cases plotted on the three phasing graphs. Case number 1 shows high residuals in cylinders 2 and 8. However, cases 2-5 show alternative cam durations provide a reduction in residual levels in cylinders 2 and 8 but at the expense of increasing residuals in the other cylinders.

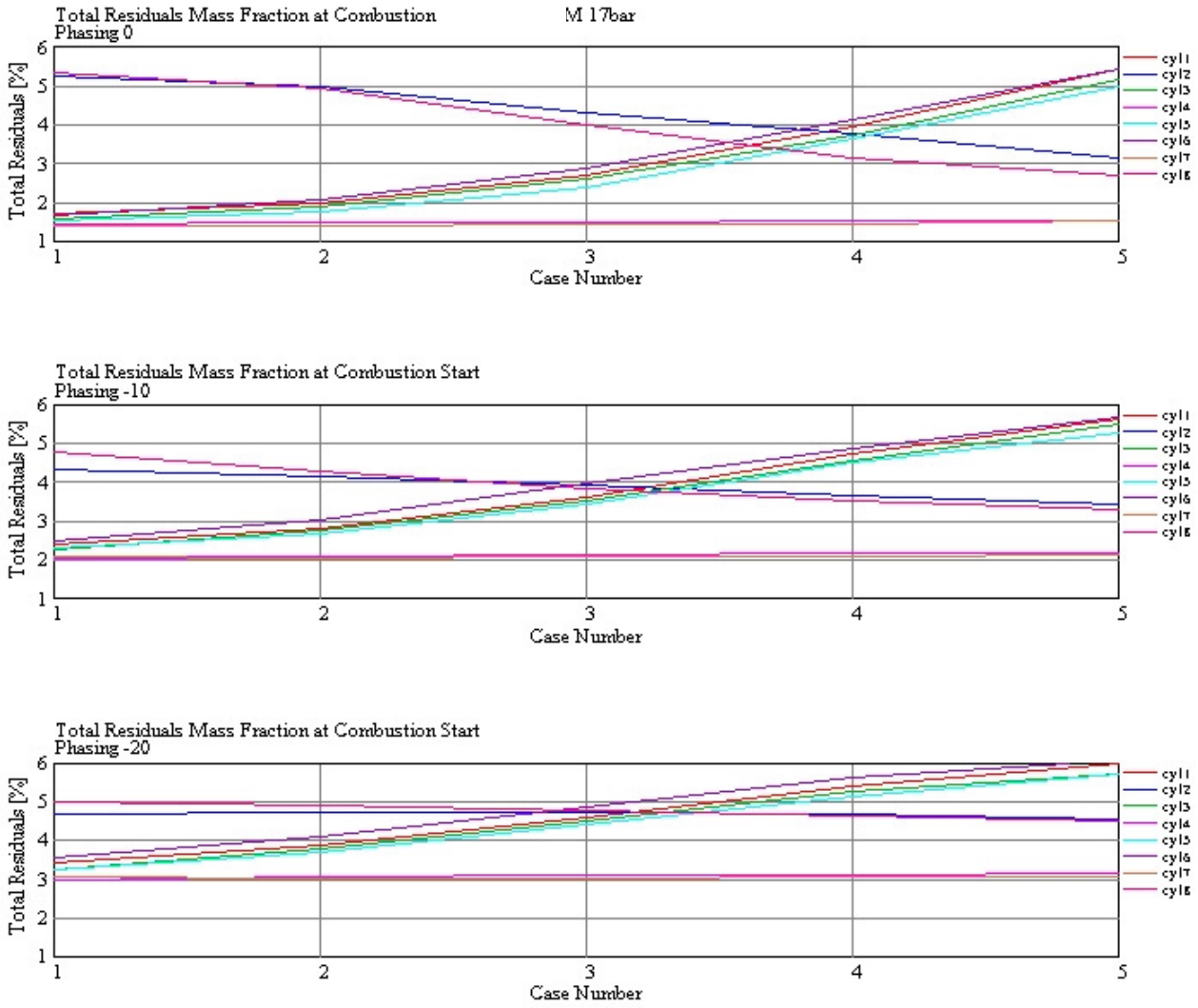

Figure 12 - Effect of intake duration and phasing on individual cylinder residual levels.

The issue with this approach is that for any change in intake cam timing and duration, there must be a corresponding optimization of exhaust cam timing and duration, and the impact on all cylinders must be observed. Furthermore, optimization will be engine speed dependent due to the changing dynamic behavior of the gas exchange process with engine speed. Due to these complex interactions, a DOE (Design of Experiments) plan was executed. The five DOE variation parameters were:

- Exhaust valve closing timing
- Exhaust valve duration
- Intake opening timing
- Intake valve duration
- Combustion phasing (CA50)

The range of cam phaser authority and corresponding valve lift curves for the DOE are shown in Figure 13. The DOE analysis illustrates the interactions between all five variation values and leads to a better understanding for valve timing definition. DOE results helped define two camshaft profiles to be tested in the single cylinder engine, a 240° exhaust duration combined with a 242° intake duration, and a 254° exhaust duration combined with a 254° intake duration. The 240/242 camshaft combination shows advantages at WOT and low engine speed (lower residuals, better transient response). The 254/254 camshaft combination shows approximately 1% higher residual gas content. At rated power the two camshaft combinations show very similar results.

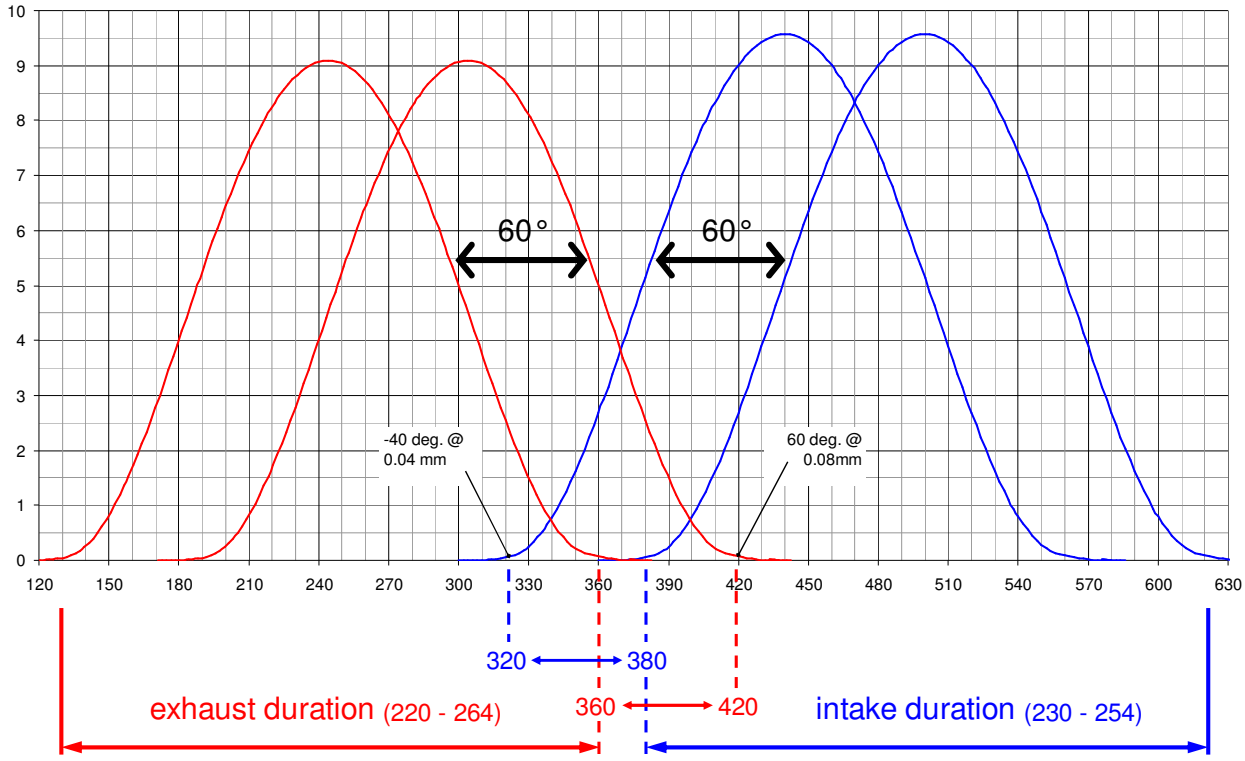

Figure 13 - Range of cam phaser authority and corresponding valve lift curves for the engine.

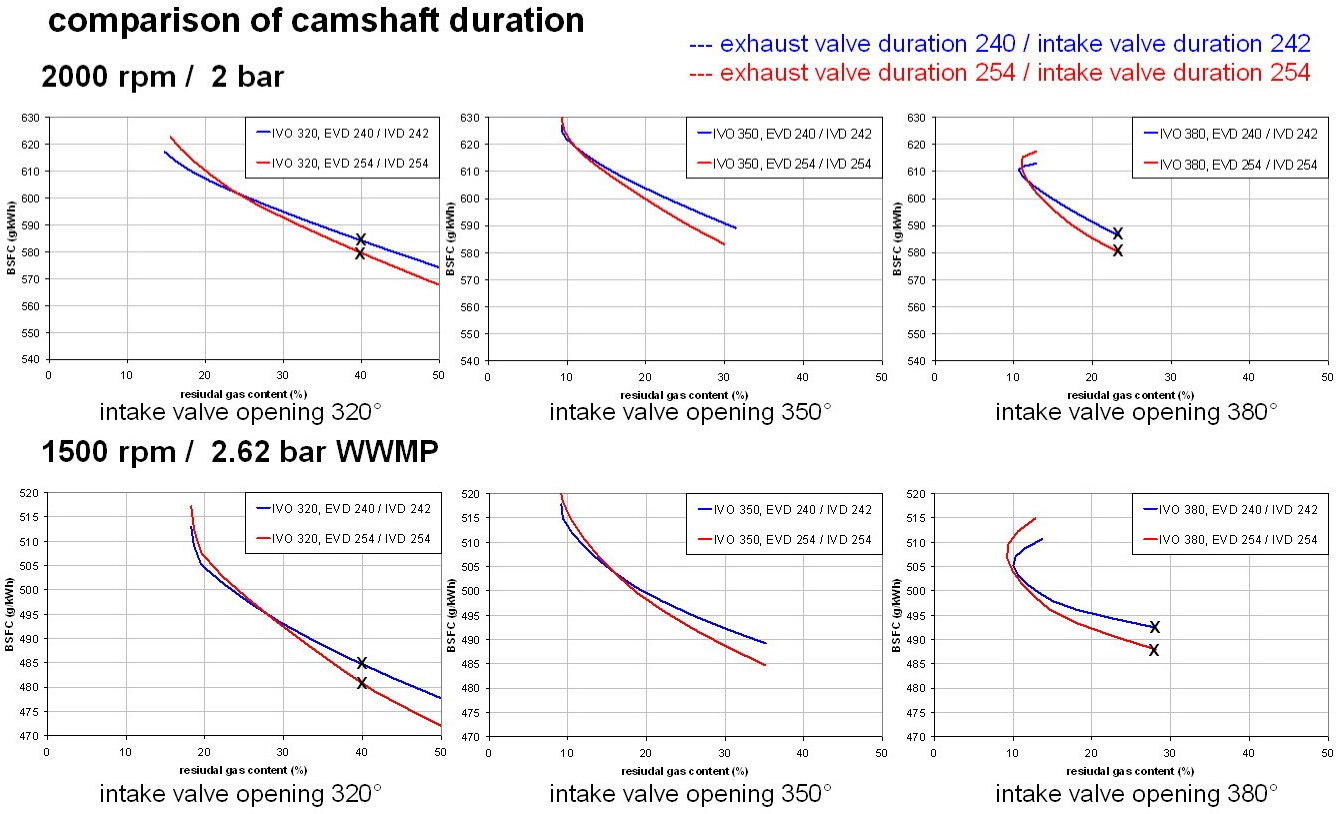

Figure 14 - Comparison of DOE optimized cam duration solutions showing BSFC at part load for different cam timing and overlap settings.

Investigation of part load fuel economy differences between the two alternative sets of cams optimized for full load performance has been done for direct injection of E85. The analysis was based on variation of residual gas content to perform a comparison of the two alternatives. At part load (Figure 14 and Figure 15), the 254/254 cam combination shows reduced pumping losses and consequently lower BSFC. The cam timing strategy for the 254/254 cam combination is retarded exhaust and retarded intake (late/late strategy).

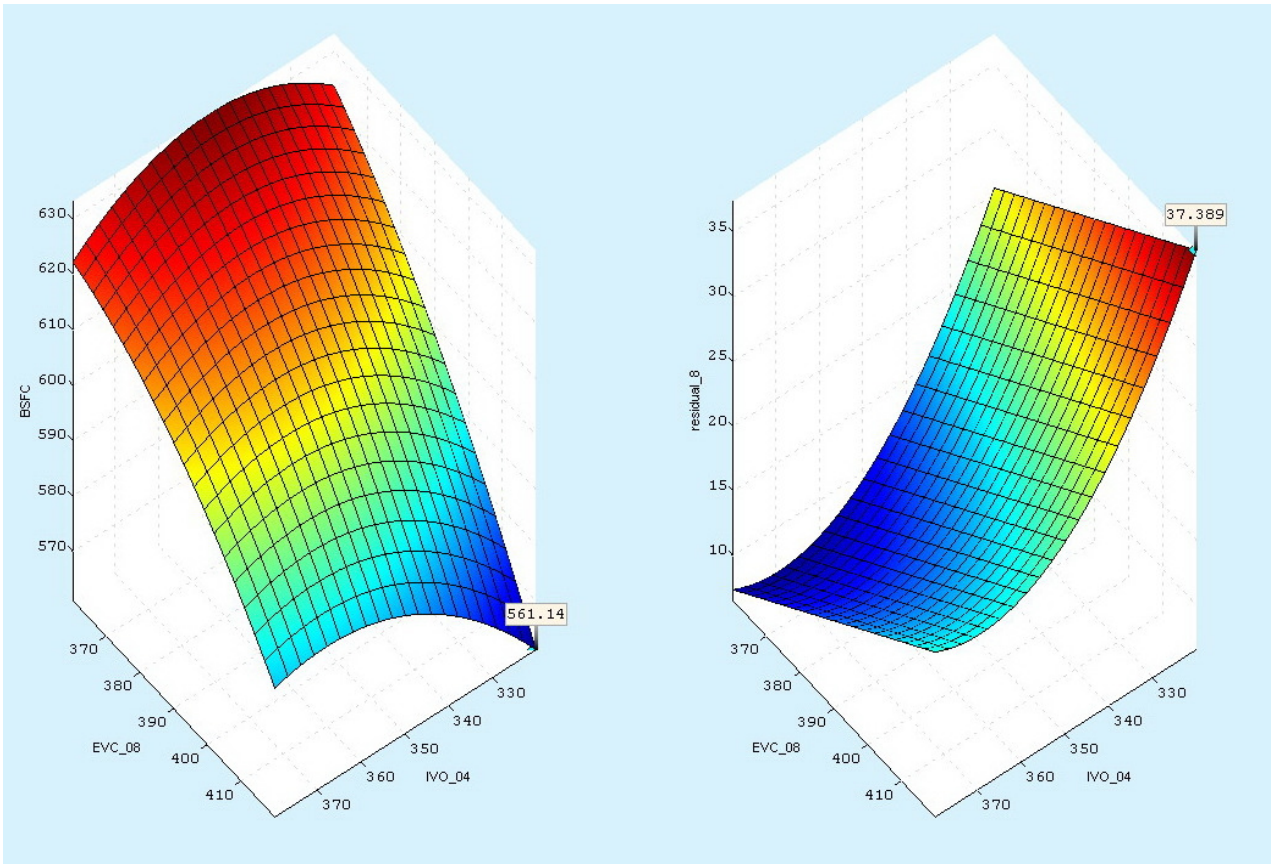

Figure 15 - Surface plots showing the effect of cam timing on part load BSFC and residual levels for the 254/254 cam combination.

To ensure good compressor matching, the chosen compressor map was overlaid with BMEP performance curves. The target curve was easily accommodated by the compressor, with sufficient margin to the surge and choke lines, and with margin for altitude. The operating point curve also passes through the maximum efficiency point of the map.

Compressor matching was achieved through an iterative process whereby each successive map suggested by the turbocharger supplier was evaluated using GT-POWER until an adequate solution was achieved. The impact of the match on packaging size was also considered.

Task 5 – Single Cylinder Engine

The single cylinder engine (SCE) was used to perform combustion studies for different piston configurations. Engine performance was then optimized using this piston study in combination with different cylinder head combustion chambers, valve timings, and various injection patterns.

Drivetrain Assembly

The drivetrain assembly includes all of the parts below the fire deck including crankshaft, piston assembly, connecting rod, and liner. There is also an oil nozzle for piston cooling located in the crankcase. The SCE will

receive a custom-designed drivetrain. The 580 series single cylinder base engine is provided by AVL and is suitable for this size of single cylinder engine. A trigger wheel is mounted on the crankshaft and the crankshaft sensor is mounted on a bracket located on the front of the engine.

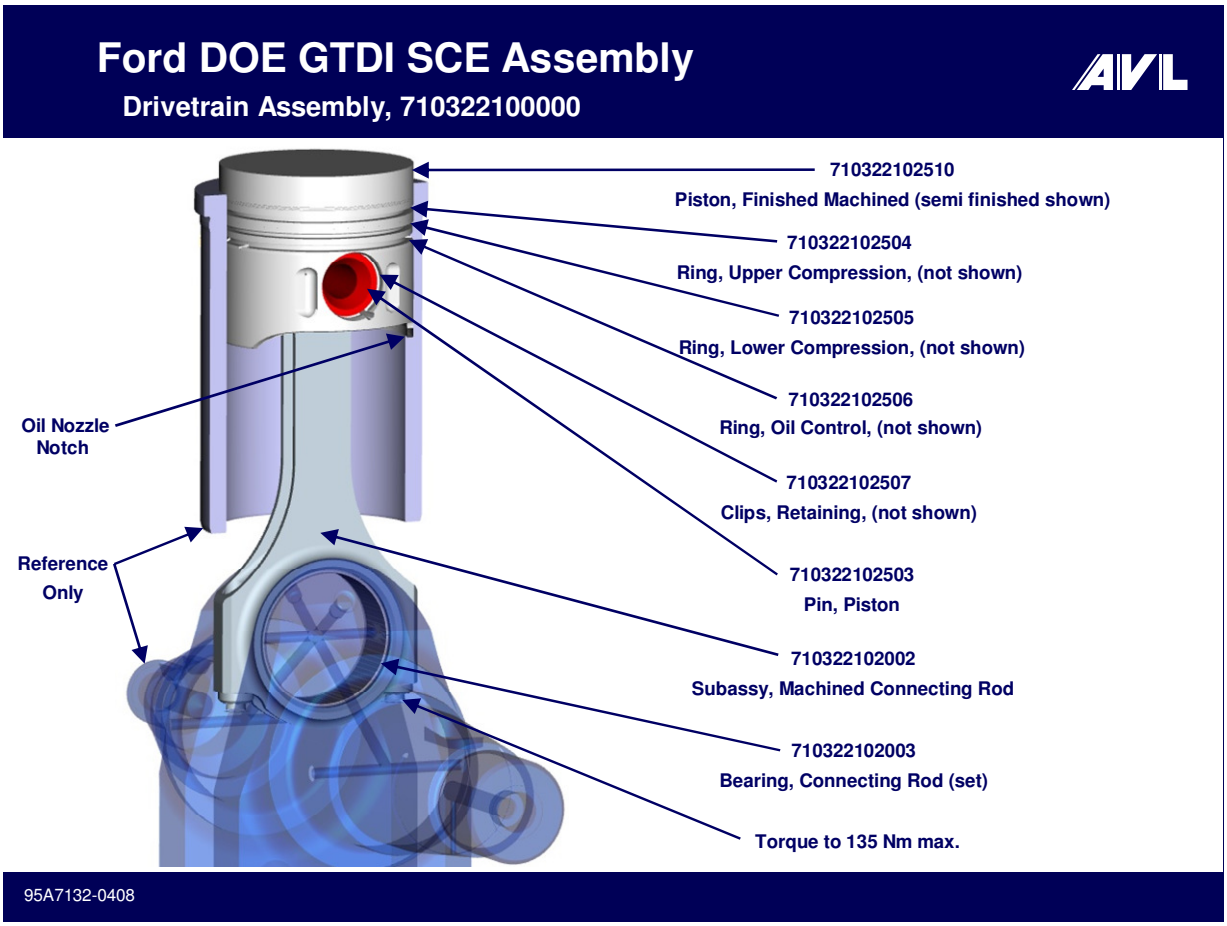

Figure 16 - Single cylinder engine drivetrain assembly.

Cylinder Head Assembly

The complete cylinder head assembly (Figure 17) matches the engine layout and is available in several configurations in terms of combustion chamber geometry, fuel delivery and flow characteristics. For faster prototype delivery, some existing production parts were used (i.e. springs, roller followers, valve guides etc).

Valves, seats and the aluminum casting head are custom made. Intake and exhaust ports were developed by AVL Graz and will be optimized in the testing process. The head assembly includes a direct injector and pressure transducer. The port injector is part of intake manifold assembly.

Valvetrain Assembly

The valvetrain assembly includes two camshafts (intake and exhaust) with separate cam sensors, a cam carrier and a cover. For easy disassembly the cam carrier is a separate part. The cam carrier has provisions for oil supply, camshaft locking pins, bearings and crankcase vents. A modified production ignition coil goes through an adapter and reaches down to the spark plug in the cylinder head. Two O-rings seal the spark plug tube from the cam carrier and cylinder head. Using a combination of camshaft geometry and sprocket position, different timing configurations can be tested on the single cylinder.

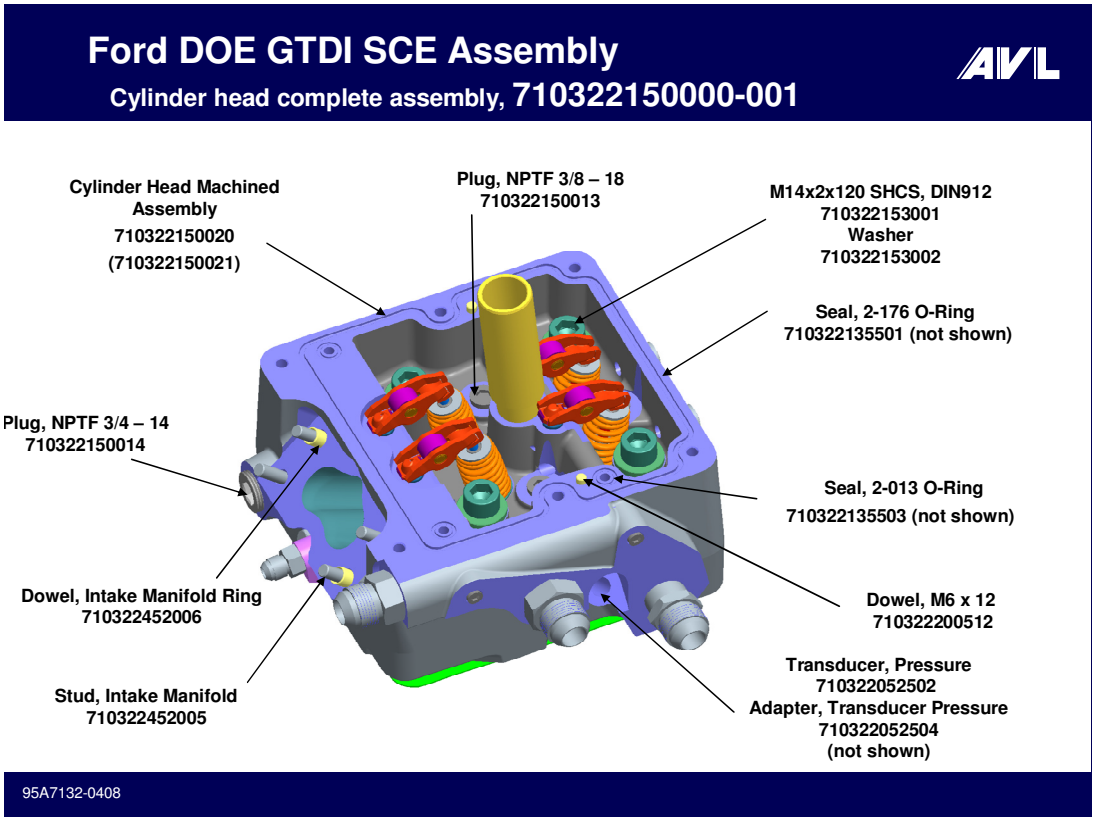

Figure 17 - Single cylinder engine cylinder head complete assembly.

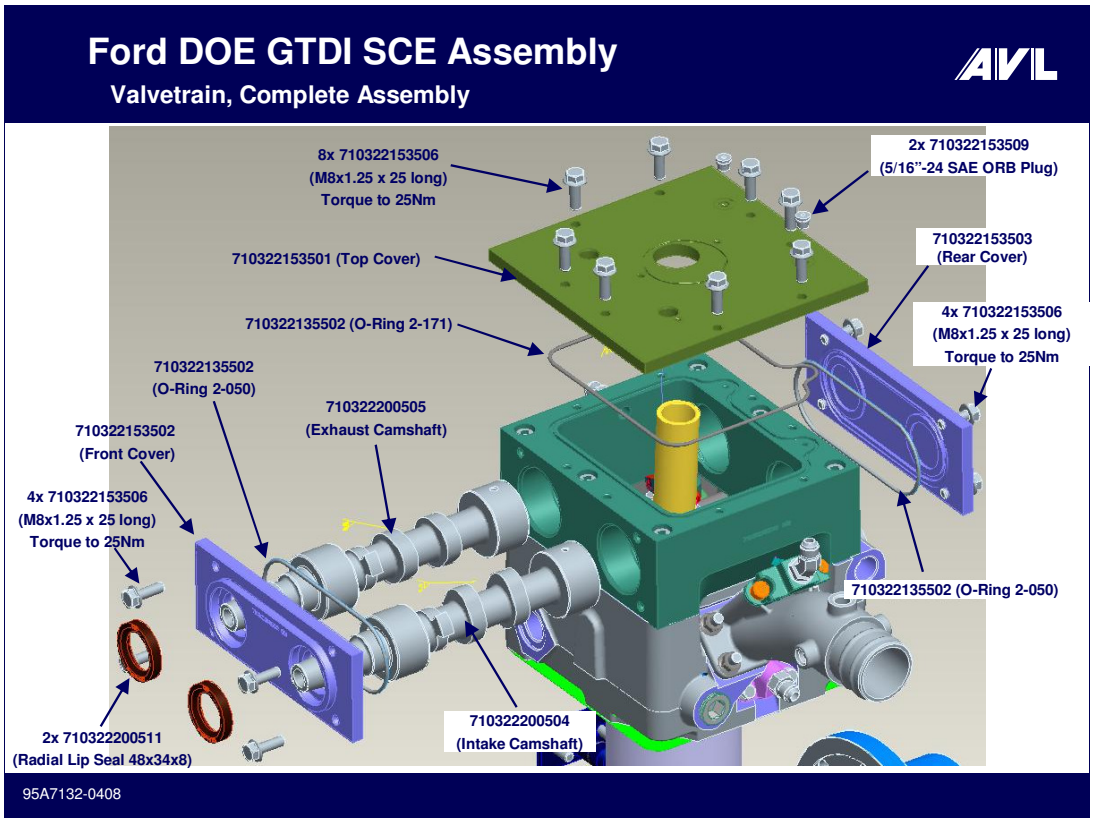

Figure 18 - Single cylinder engine valvetrain complete assembly.

Intake Manifold Assembly

The intake manifold is an aluminum cast part with provisions for temperature and pressure sensors (Figure 19). It holds the port fuel injector assembly and is bolted to the cylinder head by four studs. For easy disassembly, the manifold is sealed to the cylinder head with an O-ring.

Exhaust Manifold Assembly

The exhaust manifold is a fabricated steel part, bolted by four studs to the cylinder head (Figure 20). It has provisions for pressure and temperature sensors and is sealed by a Grafoil gasket.

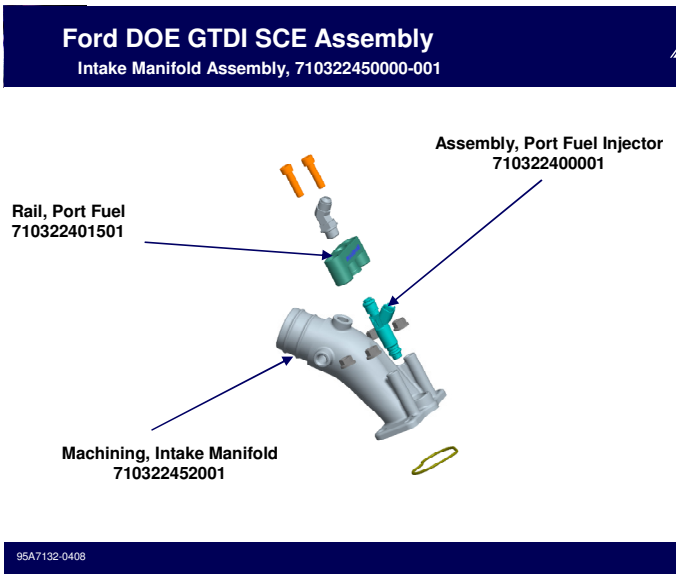

Figure 19 - Single cylinder engine intake manifold assembly.

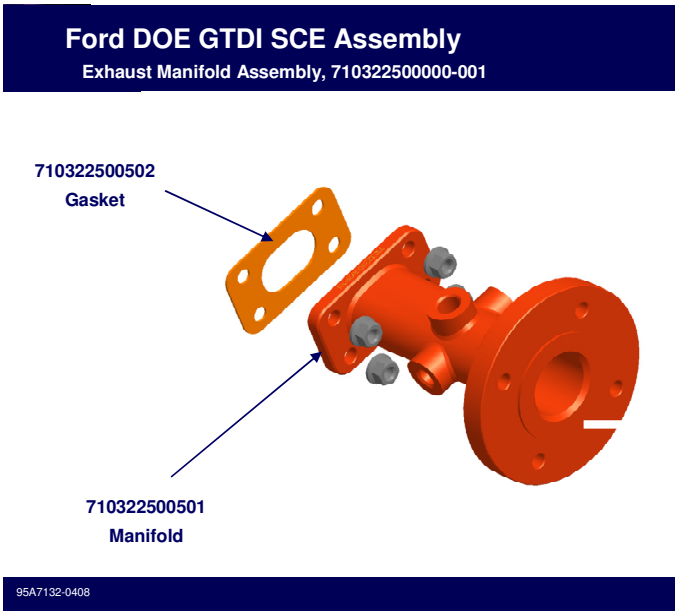

Figure 20 - Single cylinder engine exhaust manifold assembly.

Timing Belt Assembly

The timing belt drives the camshafts through a series of sprockets and pulley (Figure 21).

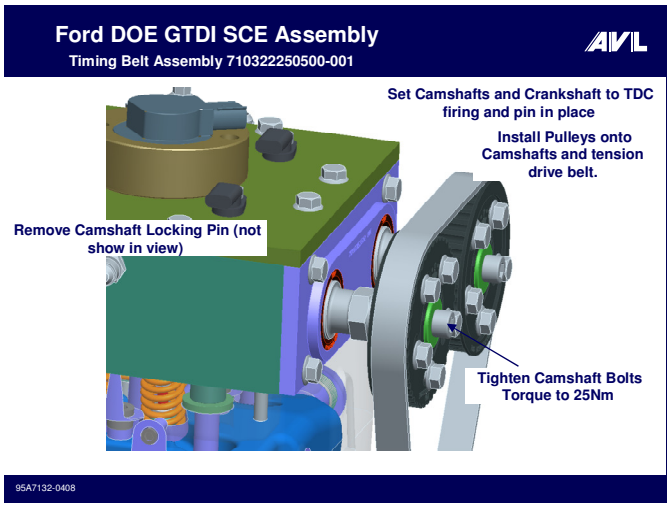

Figure 21 - Single cylinder engine timing belt assembly.

For each camshaft, the relative position of the crankshaft can vary to a maximum of 15 degrees cam angle in each direction. In this way the real engine cam phasing can be replicated without the complexity of a production solution. The camshaft, crank sprockets, timing belt, and pulleys are custom made parts, while the idlers and the crankshaft hub are part of the base single cylinder engine.

Task 6 – Optical Engine

The purpose of the transparent engine was to conduct optical studies to enable the visualization of the interaction of the ethanol fuel spray with the in-cylinder tumble motion induced by the intake ports. The single cylinder head is used in both optical and conventional single cylinder test engines. Special optical engine design considerations are required:

- Position of cylinder head screws must be outwards of the glass liner (thickness 19 mm), see Figure 22.
- Positioning dowels have to be in the area of the posts of the glass ring housing.
- Extra material is needed in the area of the “hat” of the glass ring.
- No oil or water outlets in the plane of the cylinder head gasket; these connections must be outside the glass, using hoses.

These design modifications were included in the design process of the test bed engine.

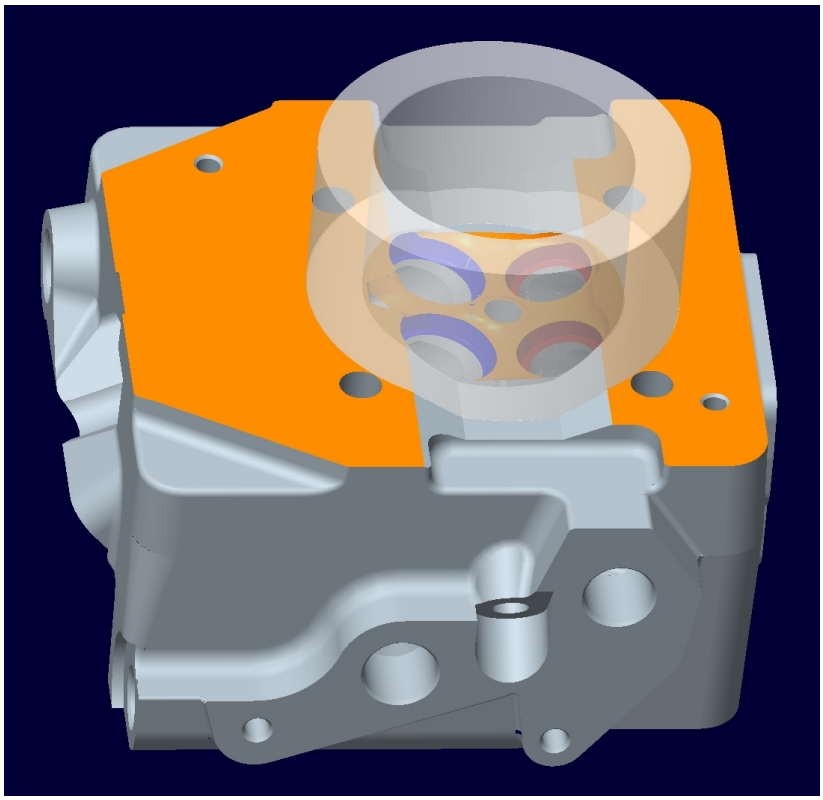

Figure 22 - Cylinder head with glass liner.

The machining of the single cylinder head for the optical engine is different from that of the test bed engine in the following locations:

- The head bolt threads will be smaller to ease making of new threads.
- Positioning dowels have to be added.

Lead time constraints require that the first step in designing the optical engine is the glass liner. The glass ring consists of a cylindrical part of standard height and a ”hat” that extends into the cylinder head to enhance

visibility of the spark plug area (Figure 22 and Figure 23). The glass liner is positioned between the cylinder head and engine body via a large housing (Figure 24). Positioning dowels are used on both sides.

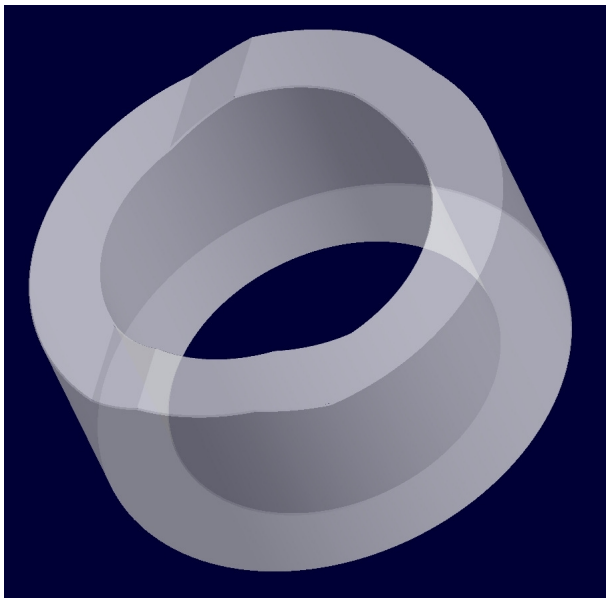

Figure 23 - Glass liner.

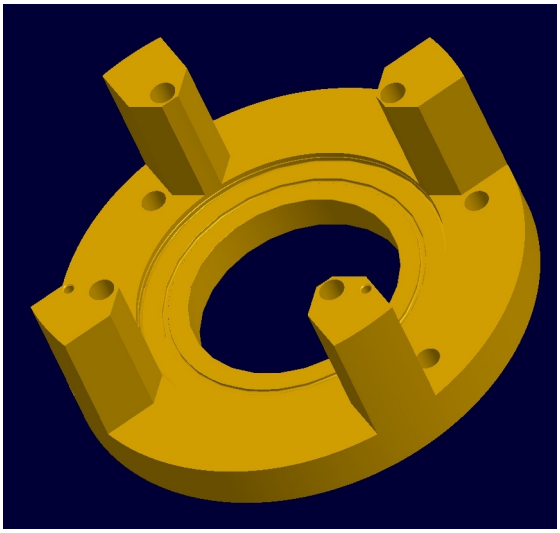

Figure 24 - Glass liner housing.

Figure 25 shows the optical engine assembly: cylinder head, glass liner, and housing. The piston does not touch the glass liner or housing. A sketch of the optical engine assembly is illustrated in Figure 26. The base engine and piston are not shown. The plate in front of the lower part of the cylinder head is the upper part of the drivetrain for the camshafts.

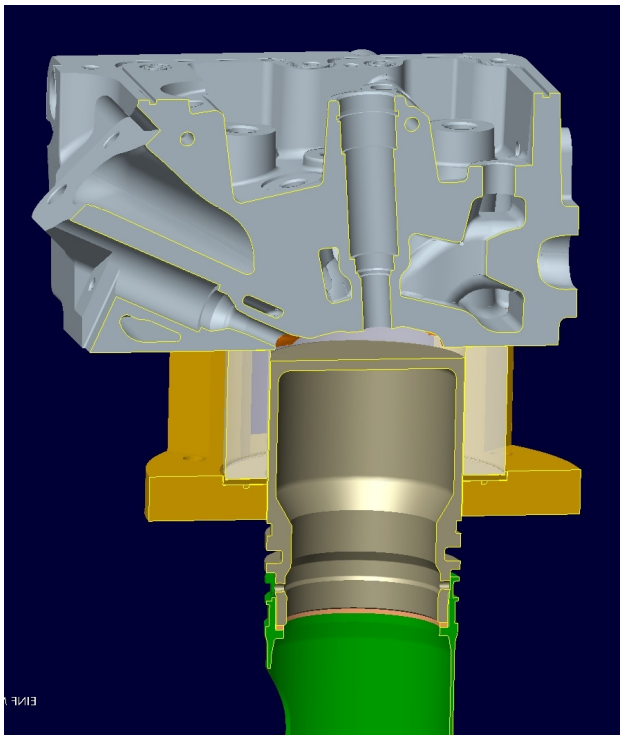

Figure 25 - Glass liner assembly and piston.

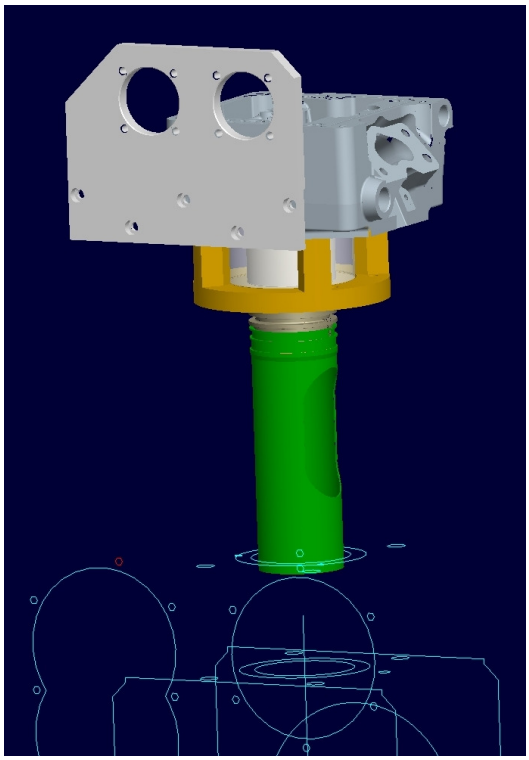

Figure 26 - Assembly for optical engine.

Phase II – Single Cylinder Engine Exploratory Development

Task 5.0 – Single Cylinder Engine and Task 6.0 – Optical Engine

These tasks are described in SAE 2010-01-0585 [3]. This section incorporates text and figures from that publication.

Specifications

The combustion system is a 4-valve per cylinder pent roof high tumble design with variable cam timing for both intake and exhaust valves. The engine will employ split injection in conjunction with a shallow piston bowl for rapid catalyst heating as a cold start emissions reduction strategy. Each cylinder has both DI and PFI fuel injectors to support a Dual Fuel concept whereby under most conditions gasoline is delivered through the PFI injectors and E85 is delivered through the DI injectors at higher load in the quantity required to mitigate knock [1,24]. This concept was studied during this program in addition to single fuel DI only operation and will be reported in detail in a separate paper to be published at a later date. The DI injector is side mounted for a number of reasons including more favorable thermal conditions for the injector which will not be flowing fuel during part load operation for the Dual Fuel concept. Turbochargers are utilized to generate boost pressure to improve specific torque and power output, and are appropriately sized for fast transient response.
Figure 27 shows two performance curves for the engine. For gasoline, the target peak BMEP was 17 bar for 91 RON US regular grade gasoline. Target peak BMEP for E85 was 27 bar.

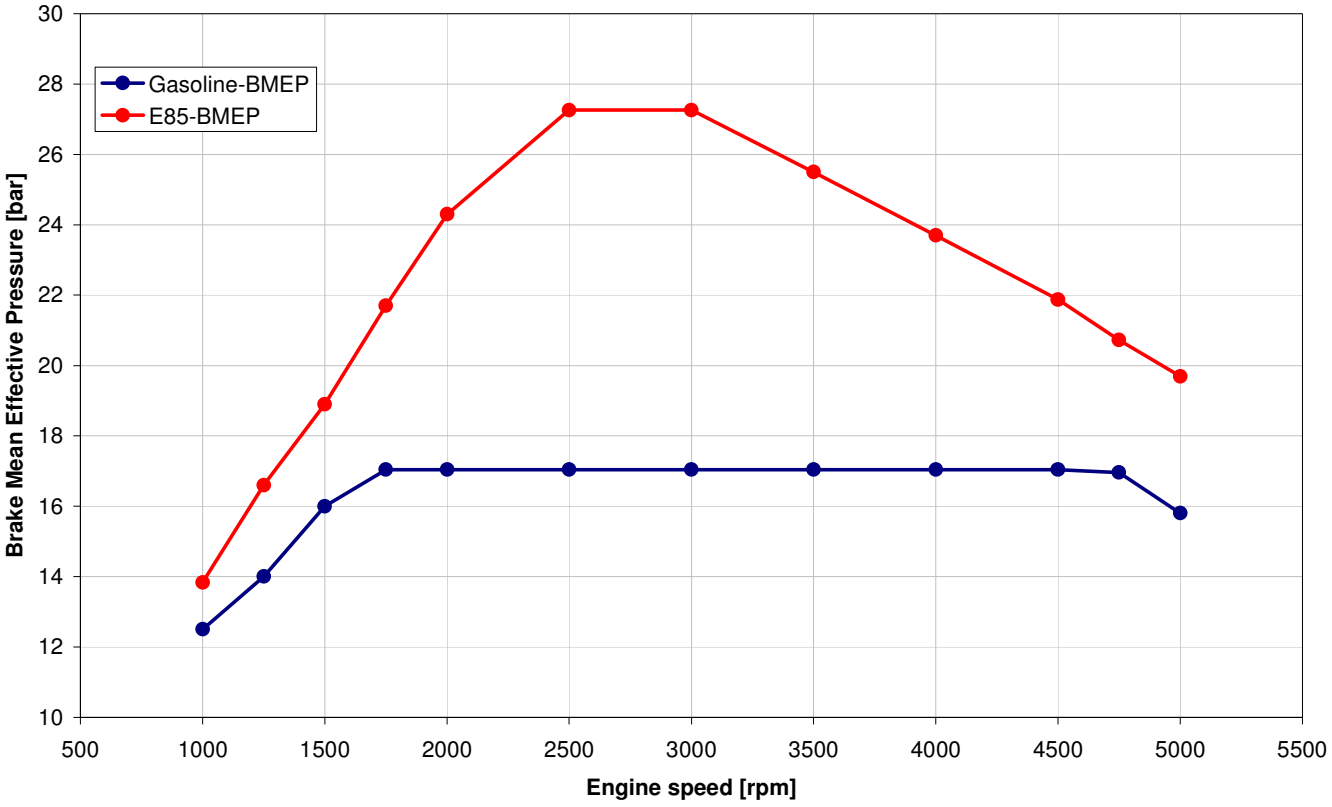

Figure 27 - Initial full load performance targets.

A single-cylinder research engine was used for initial performance and emissions work as this allowed the combustion system to be developed months before the first multi-cylinder engine was available. It was also

more cost and time effective to use a single cylinder engine to define the major combustion system specifications such as tumble ratio, injector spray, piston bowl design, and compression ratio as the number of prototype components required for each build was reduced and rebuilds were quicker. Following single cylinder development, a batch of multi-cylinder engines were built with confidence that further combustion system changes would not be required, and multi-cylinder development focused on optimization of valve events, fine tuning of compression ratio, and turbocharger matching.

Multi-cylinder engine FMEP was estimated to provide NMEP levels that could be used for single cylinder testing. FMEP for a single cylinder engine is generally higher than for a multi-cylinder engine due to added friction from a balance shaft system and timing drive friction which is carried by a single rather than multiple cylinders. Controlling to NMEP set points also provides consistency for testing and development if friction levels change from one build to the next due to variations in timing belt tension, etc.

Single cylinder development focused on full load operation at low, mid and high speed, part load operation at 1500 rpm 2.62 bar BMEP and the operating point that is typical for catalyst heating . These development points are shown in Table 1.

Table 1: Development points

Point	Engine speed	NMEP for gasoline	NMEP for E85	Description
2	2000 rpm	18.50 bar	25.70 bar	Full load low speed
3	3500 rpm	18.70 bar	27.10 bar	Full load mid speed
4	4750 rpm	18.80 bar	22.60 bar	Full load high speed
1	1500 rpm	3.32 bar		Part load
5	1200 rpm	1.70 bar		Catalyst heating

Combustion System Development

Combustion Chamber

Figure 28 shows the layout of the combustion system as packaged for the single cylinder engine. The DI injector is side mounted between the intake valves and the spark plug is at the center of the combustion chamber slightly tilting towards the intake side. Also shown is a sleeve on the intake and exhaust bridge for a pressure transducer for cylinder pressure measurement, which is used to calculate NMEP, heat release, and other combustion parameters. The PFI injector is located in the intake manifold targeting the intake valves. The targeting of the injector was optimized using an endoscope and simulated air and fuel delivery conditions on a test rig at AVL. This was done to minimize port wall wetting to improve transient air-fuel ratio control for emissions reduction. Shown in Figure 29 is a CAD model of the piston. The piston has a shallow bowl to support split injection for catalyst heating.

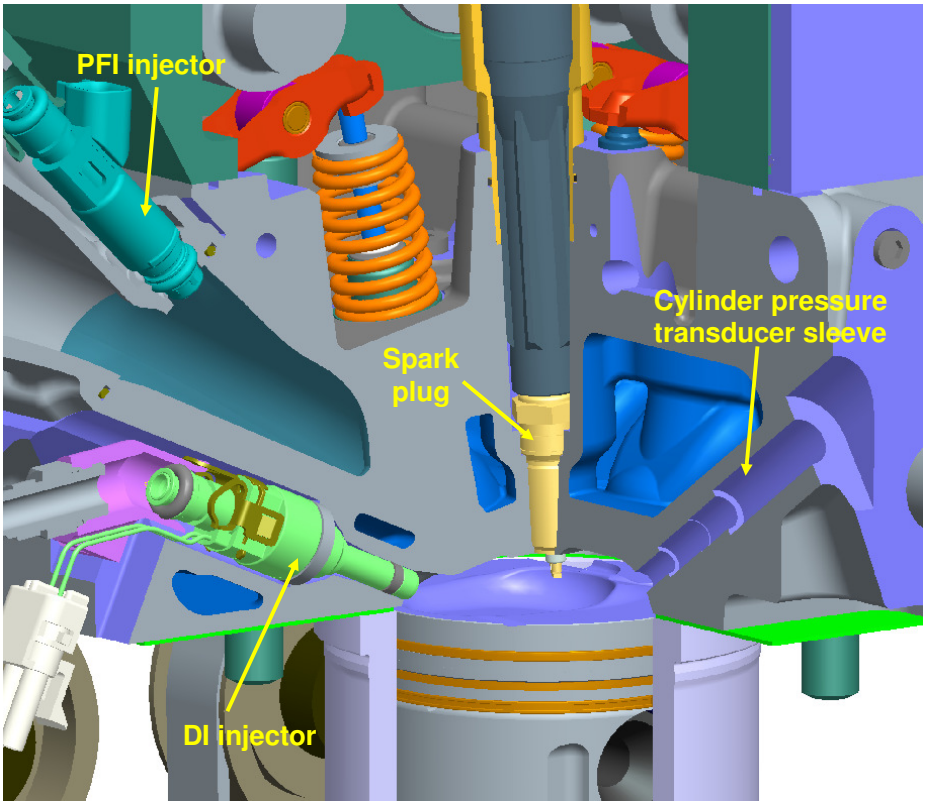

Figure 28 - CAD Model of the combustion chamber.

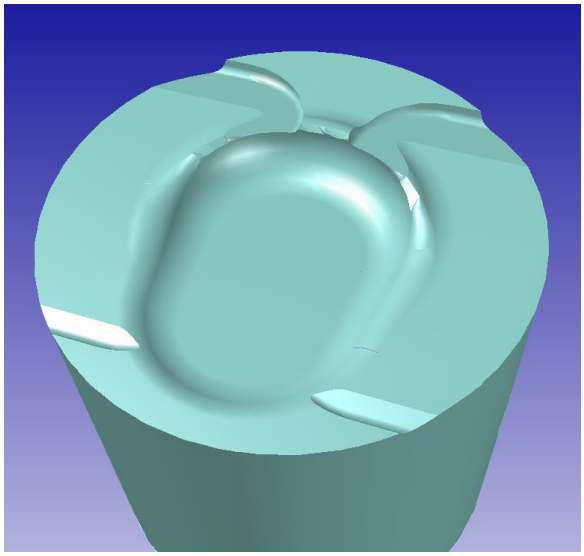

Figure 29 - CAD model of the initial piston design.

Port Design

R&D experience has shown that increased tumble can provide significant combustion benefits for a GTDI engine, and in the past two decades of GTDI development, tumble levels have been increasing continuously. High tumble provides a number of benefits for a GTDI engine [26]:

1. High tumble helps fuel/air mixing which helps reduce CO and smoke emissions, improving efficiency and combustion stability.

2. In a side injector engine, strong tumble air motion can help reduce or eliminate liner wetting by deflecting the fuel spray from the liner.
3. High tumble has been shown to provide octane benefits allowing more advanced combustion phasing. This provides efficiency benefits due to more optimum combustion phasing and improves combustion stability and combustion system robustness. Advanced combustion phasing also reduces exhaust temperature reducing fuel enrichment requirement to maintain turbine inlet temperature limits, and improved thermodynamic efficiency reduces boost requirements to achieve a target torque level.
4. High tumble provides increased dilution tolerance due to faster burn rates which enables increased efficiency due to ability to use higher internal or external EGR at part load or cooled external EGR for exhaust temperature and fuel enrichment reduction at full load.
5. Differences in tumble for individual cylinders of a multi-cylinder engine resulting from manufacturing variability can lead to burn rate and knock borderline differences between cylinders causing one cylinder to knock before the others which limits spark advance for the engine even though the other cylinders are operating knock free. With high tumble ports, manufacturing variability results in lower percentage tumble variation between ports so all cylinders are more closely matched in burn rate and knock borderline ignition timing, which allows more advanced ignition timing.

Figure 30 shows the high tumble intake ports that were designed for this engine. These ports were designed not only to provide a high tumble ratio, but also to provide a centered tumble field within the cylinder that would provide an even turbulence distribution throughout the cylinder for symmetrical flame propagation to mitigate knock. The ports and throat cut were designed to minimize tumble variation from casting core shift to provide a similar tumble level and flow field for all cylinders. The top side of the intake flange has a bulge to accommodate the fuel spray from the PFI injector which is located in the intake manifold, and the bottom side of the flange has a relief to accommodate the DI injector and fuel rail connection.

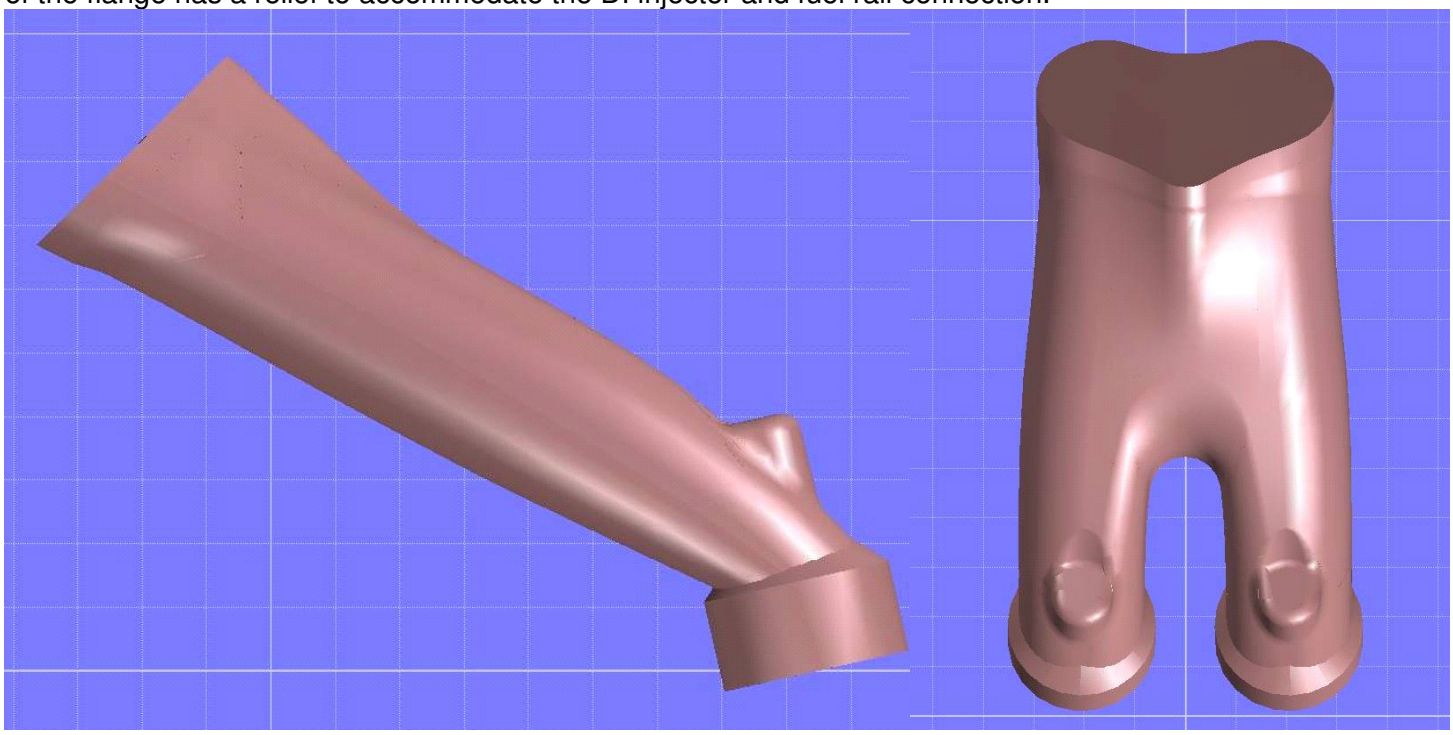

Figure 30 - Side and front views of the intake ports.

Port Development

In order to ensure that the tumble generated by the ports was not only of the magnitude required, but symmetric and centered, port development was conducted in an LDA port development laboratory at AVL. LDA measurement provides velocities of the air stream (seeded with particles) in the vertical direction at 250 points

across the bore area, measured at a distance equivalent to half the bore diameter down from the top of the liner [28]. This provides a complete measurement of the air motion field generated by the port, and by taking measurements at various valve lifts, the instantaneous tumble and a cycle average tumble ratio can be derived for a given valve lift curve corresponding to the intake cam profile. This also provides a qualitative and quantitative assessment of the symmetry of the air motion field, determination of the location of the tumble field axis, and an estimate of flow coefficient. A schematic of the AVL Laser Doppler anemometry (LDA) rig is shown in Figure 31.

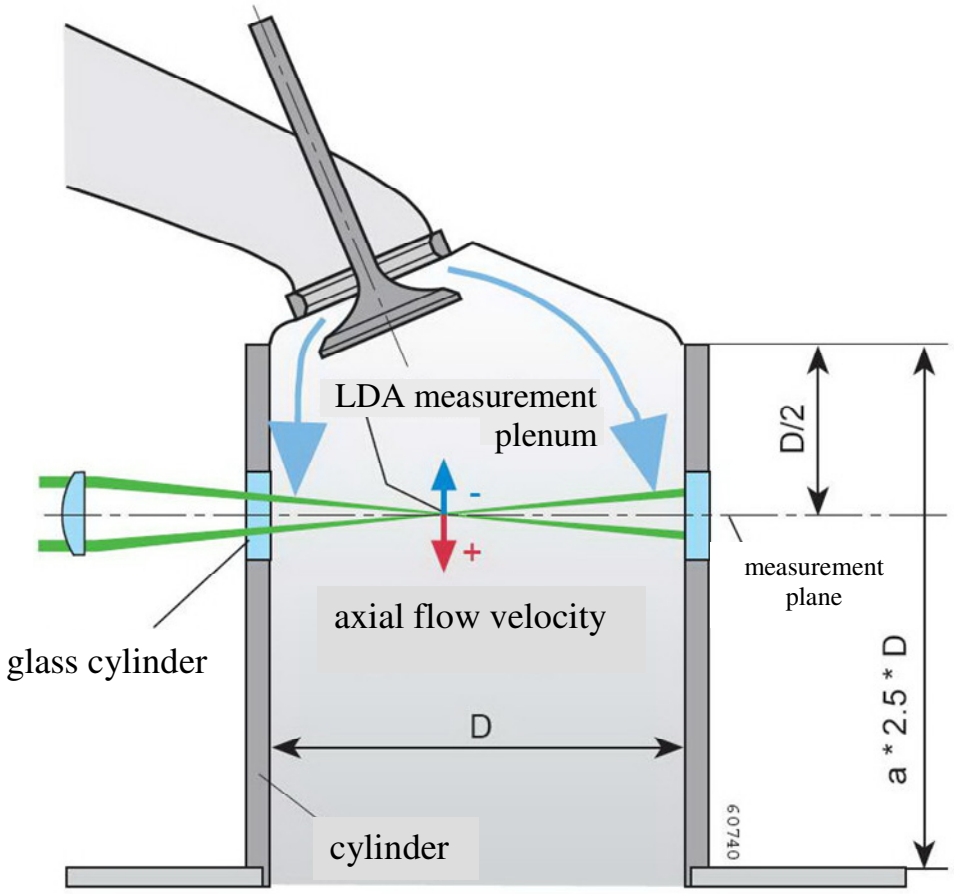

Figure 31 - Schematic of AVL Laser Doppler anemometry (LDA) rig.

Figure 32 shows LDA measurement results of the in-cylinder tumble flow at different valve lifts from the tumble port with tumble ratio of 1.93. Red dots denote the charge air at the measuring element flowing downwards with high velocity, while blue dots denote air flowing upwards (towards the cylinder head) with high velocity. It is shown that a tumble flow field with good symmetry is established by the time the intake valves are wide open. On the rig, at lower valve lifts small differences in valve lift can produce an asymmetric tumble field pattern. Also shown in the figure are angles of the tumble plane relative to the cylinder center plane between intake and exhaust, which quantifies the symmetry of tumble flow. At the time when intake valves are wide open, the angle of the tumble plane is only 4 degrees rotated clockwise from the cylinder center plan, indicating good symmetry of the flow field.

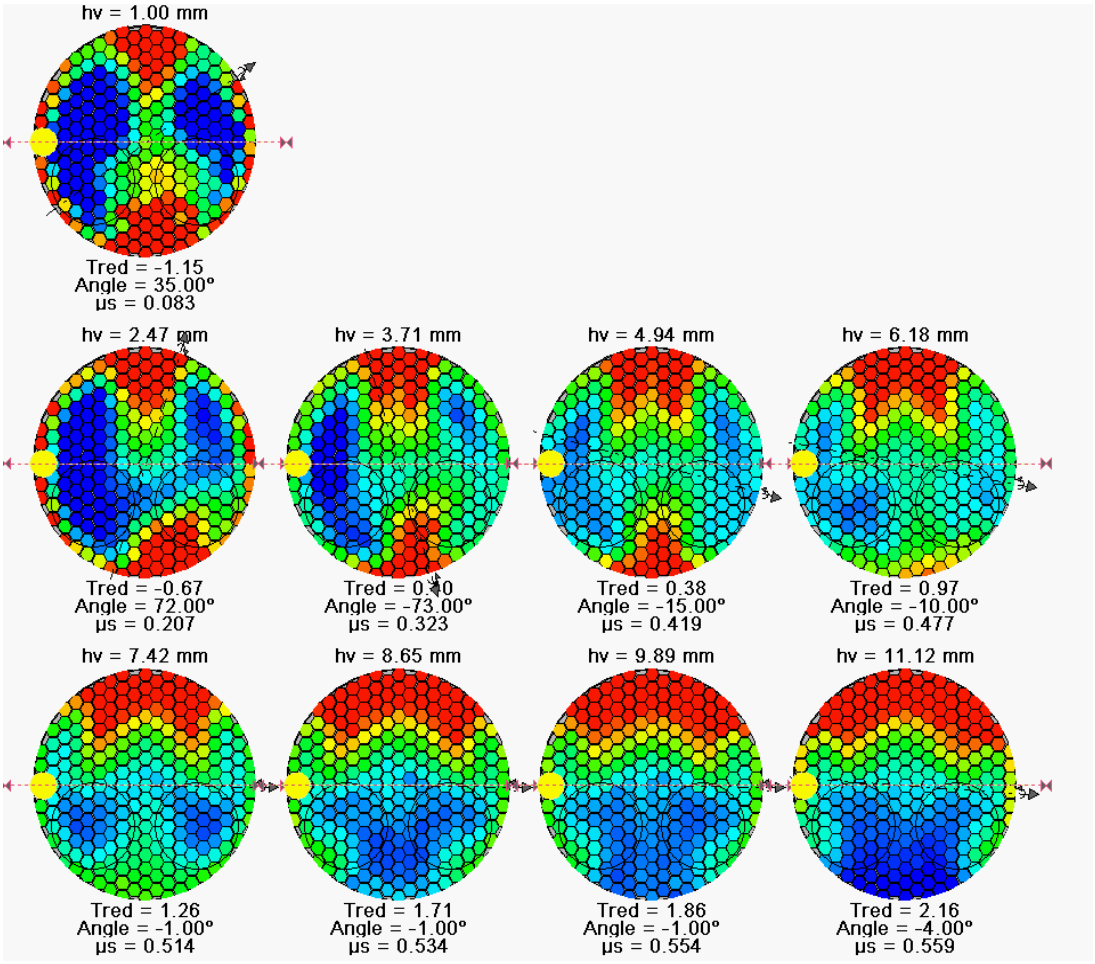

Figure 32 - LDA intake port measurement results at valve lift increments.

Tumble ratio is defined as:

$$TR = \frac{1}{\pi}\int_{\alpha=0}^{\pi} \frac{\omega_a}{\omega_E}\left(\frac{c(\alpha)}{c_m}\right)^2 d\alpha \quad \text{.....(Equation 1)}$$

Where:

TR	=	Tumble ratio
α	=	Crank angle
c(α)	=	Instantaneous piston speed
c_m	=	Mean piston speed
ω_a	=	Angular velocity of charge air in the combustion chamber
ω_E	=	Angular velocity of engine crankshaft

As shown in Equation 1, tumble ratio is the cycle integral of instantaneous tumble ratios at each crank angle, weighted by the instantaneous piston speed. Flow coefficients (µs) at each valve lift are also measured and shown in Figure 32. At the highest valve lift the flow coefficient is 0.559. Shown in Figure 33 are the mean flow coefficients and tumble ratios of the intake ports tested during the program compared to other engines in the AVL engine database. This shows that the port designs are very efficient as they provide above average flow capacity for the high levels of tumble generated.

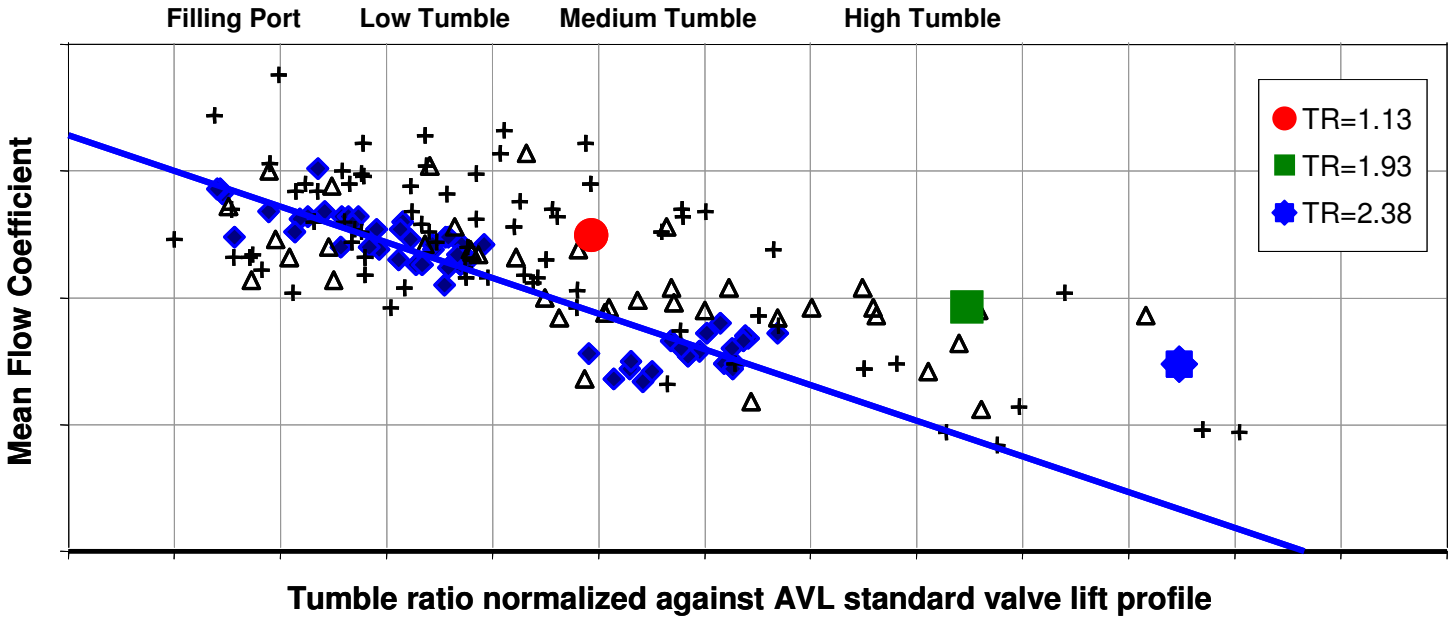

Figure 33 - Flow coefficient versus tumble ratio trade-off plot showing ports tested during development.

Injector Spray Design

Injector spray targeting is one of the most challenging design and development tasks for a new DI combustion system. The fuel spray must be designed so that it provides excellent homogenous mixture preparation for part and full load operation while the same spray must target the piston bowl to support split injection for catalyst heating and produce the required level of stratification in this mode. Under part and full load operation, piston impingement must be minimized to maximize charge cooling benefits and to avoid smoke, and under all conditions, bore washing must be avoided to reduce oil dilution, smoke and to avoid cylinder system wear. Flow rate must be specified so that there is time for the fuel to vaporize and mix under the highest flow rate conditions (usually peak power), however, the flow rate must be low enough so that under the lowest fuel flow conditions the injector will continue to operate within its linear flow range. The minimum fuel flow condition is unloaded idle during evaporative canister purge.

Injector flow rate can influence individual spray plume cone angle, droplet size and fuel spray penetration, which all influence spray targeting and mixture preparation. Two alternative 7-hole spray designs were designed and procured for performance and emissions development. These were designated DT1 and DT2, which had spray patterns as shown in Figure 34 and Figure 35, respectively. These designs were based on prior design and development experience with similar combustion system layouts (injector placement, installation angle, tumble level and bore size) from prior projects and the learning from optical and conventional combustion development on those engines was incorporated into these designs. Figure 36 shows the DT1 spray layout in the combustion chamber.

The difference between DT1 and DT2 injectors is the arrangement of fuel jets. Seven fuel jets for the DT1 injector are arranged in a 2-3-2 pattern, while those for DT2 injector are 1-3-3. Also, the top two rows of sprays are lower for the DT1 injector, compared to those for DT2 injector.

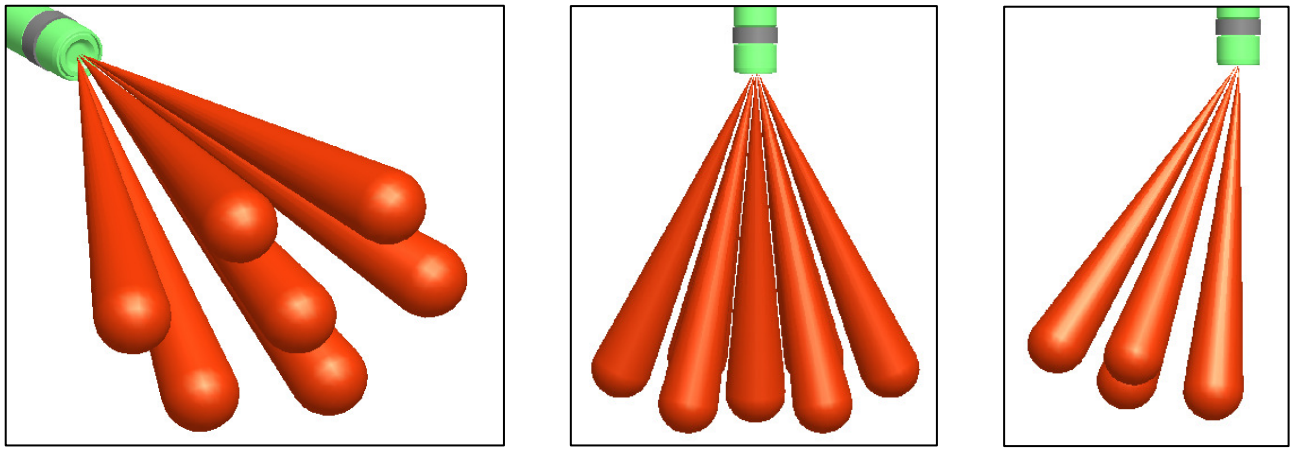

Figure 34 - DT1 injector spray patterns (isometric, front, and side views).

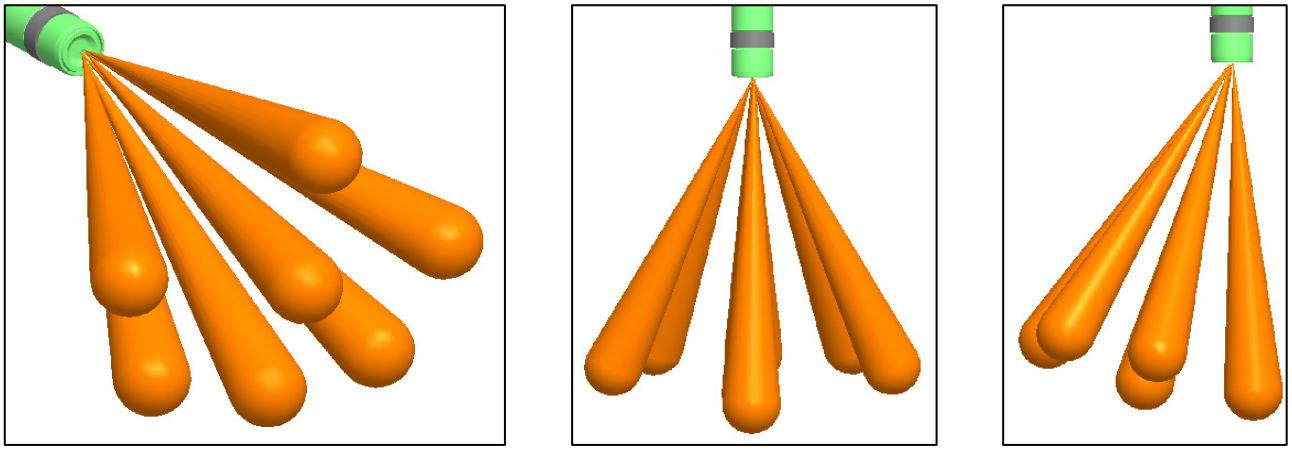

Figure 35 - DT2 injector spray patterns (isometric, front, and side views).

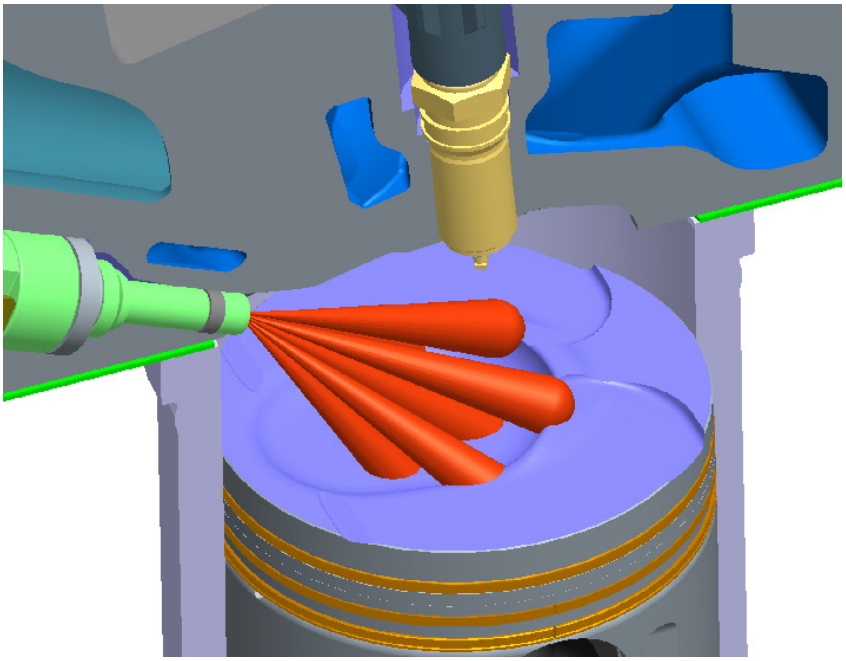

Figure 36 - DI fuel spray targeting.

Single Cylinder Development

Test Engine

Performance and emissions development was conducted on an AVL 580 single-cylinder research engine, shown in Figure 37. Boost air was supplied externally by a test cell system, which was controlled for temperature, pressure, and humidity. The static and dynamic back pressure in the exhaust of the turbocharged multi-cylinder engine was emulated by orifices in the exhaust pipe set to levels defined by 1D simulation. Three uncooled GU21C piezoelectric high-speed transducers were installed on the engine to monitor intake port, in-cylinder, and exhaust port pressures. All three pressure traces were captured on an Indi-master/Indicom system, and then used as input to AVL Gas exchange and Combustion Analysis (GCA) which among other parameters provided an estimate of residual gas fraction. NMEP and knock intensity were evaluated based on the in-cylinder pressure trace.

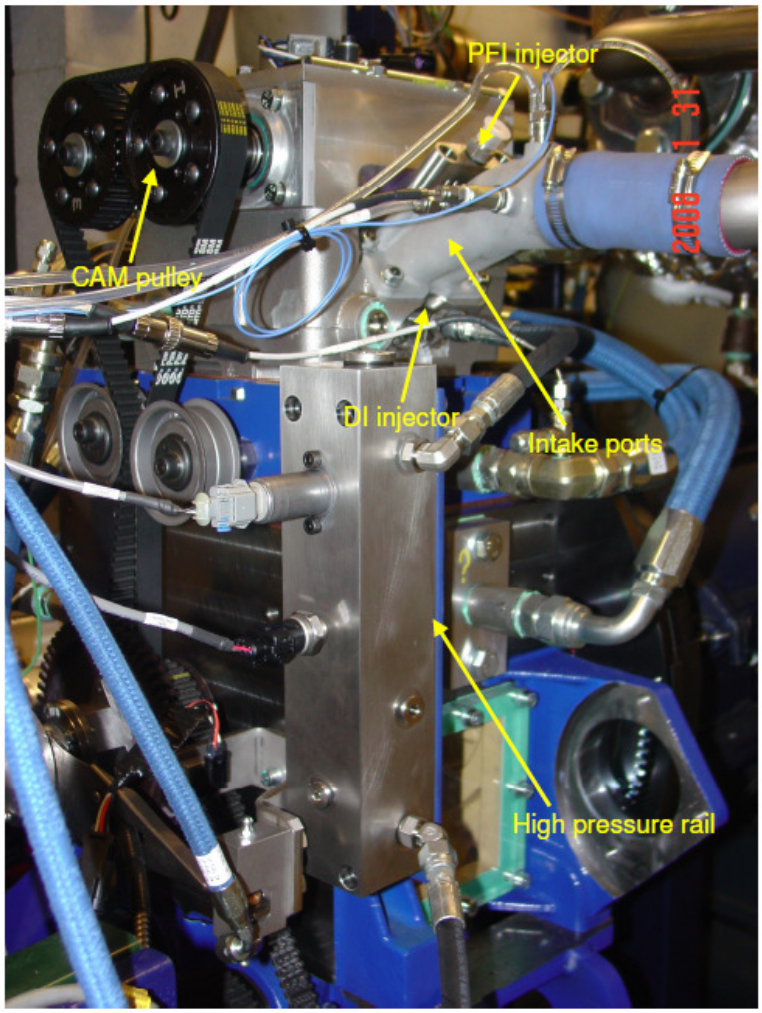

Figure 37 - Single cylinder setup in the test cell.

Tumble Ratio Optimization

Fuel economy, emissions, octane requirement, combustion stability and NVH can all be influenced by tumble ratio and all these factors have to be considered when determining the optimum tumble ratio requirement. However, this is one of the areas where different solutions could be reached for gasoline compared to E85, and operation on both fuels had to be considered when selecting tumble ratio.

The target tumble ratio for this engine was between 1.75 and 2.00, however, the initial port as designed and packaged into the single cylinder head had a tumble level of 2.38. Due to concerns over initial data with this high tumble ratio showing very high rates of pressure rise and high combustion noise at high BMEP operation with E85, the intake ports of a second cylinder head were modified to produce much lower tumble for testing. The tumble ratio of this second cylinder head was measured at 1.13. Results for these two tumble ratios are shown in Figure 38.

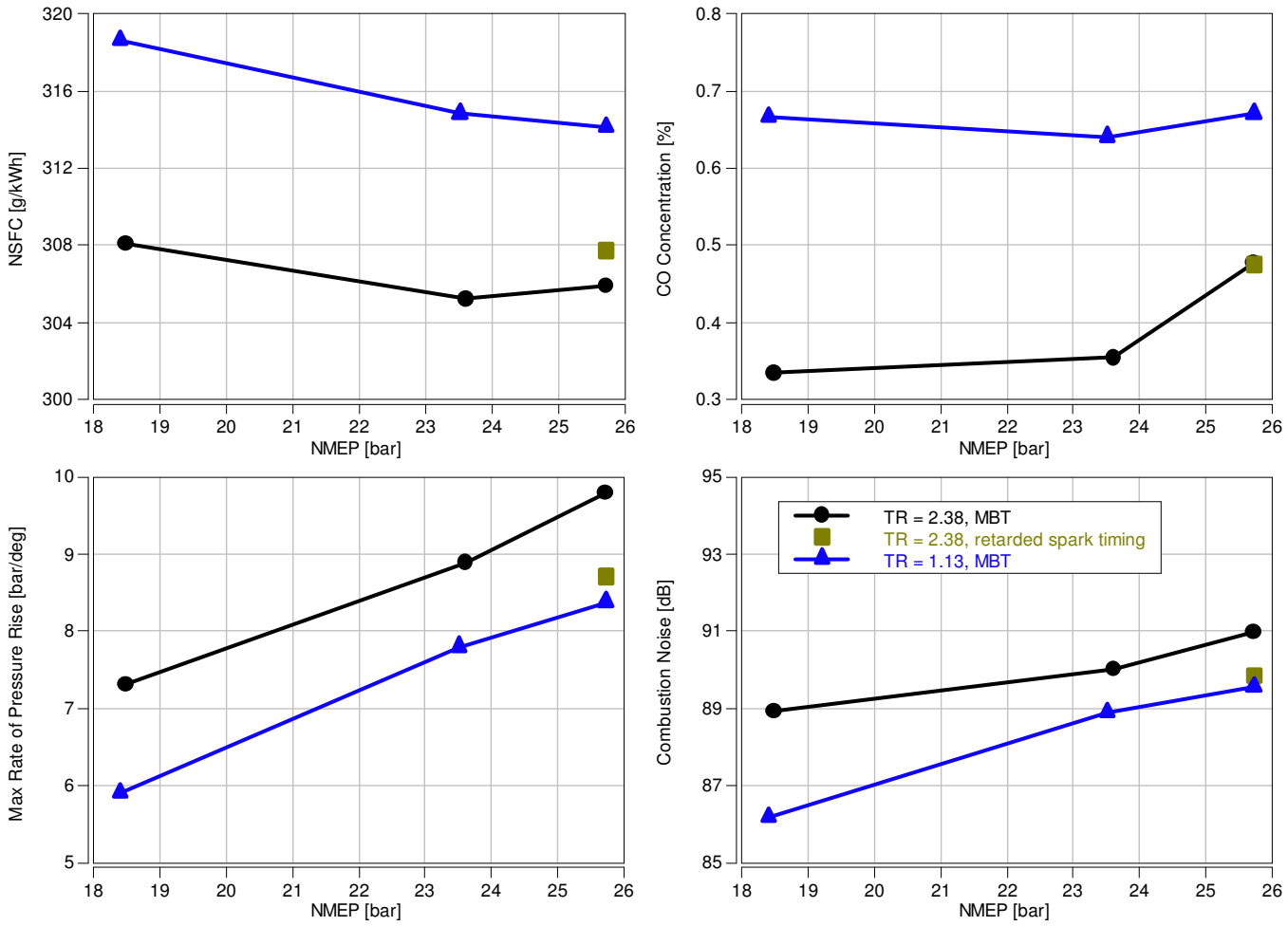

Figure 38 - Tumble effects at 2000 rpm high load with E85 at stoichiometric air-fuel ratio (λ=1).

As shown in Figure 38, maximum rate of pressure rise with 2.38 tumble was close to 10 bar/deg at 25.7 bar NMEP. This is due to a combination of very high load operation at MBT ignition (enabled by knock free operation due to the increased octane number and charge cooling benefits of E85 and high cylinder pressure capability) and high burn rates due to the high tumble ratio. Combustion noise estimated by an AVL combustion noise analyzer (which provides an estimate of combustion noise based on cylinder pressure measurement and a user selectable transfer function) showed a combustion noise level of 91 dB at this condition - which is comparable to a diesel engine. With lower tumble, rates of pressure rise and combustion noise reduced, however CO increased - indicative of poorer mixing - and NSFC increased. Therefore higher tumble appeared beneficial to mixture preparation and fuel economy at high load. High fuel flow rates are required with E85 at high NMEP, so high tumble helps fuel/air mixing especially at lower engine speeds where the effective air motion is lower. As rates of pressure rise are also a function of advanced combustion phasing which increases cylinder pressure and burn rates, the effect of combustion phasing was investigated with the 2.38 tumble ratio head. Ignition timing was retarded from MBT to a timing where rates of pressure rise were similar to those measured with the 1.13 tumble head. This required only 2 degrees of ignition retard leading to

less than 1% increase in NSFC which remained much lower than for the low tumble case. This showed that it is more beneficial to run high tumble but retard ignition timing to control noise than to reduce tumble level.

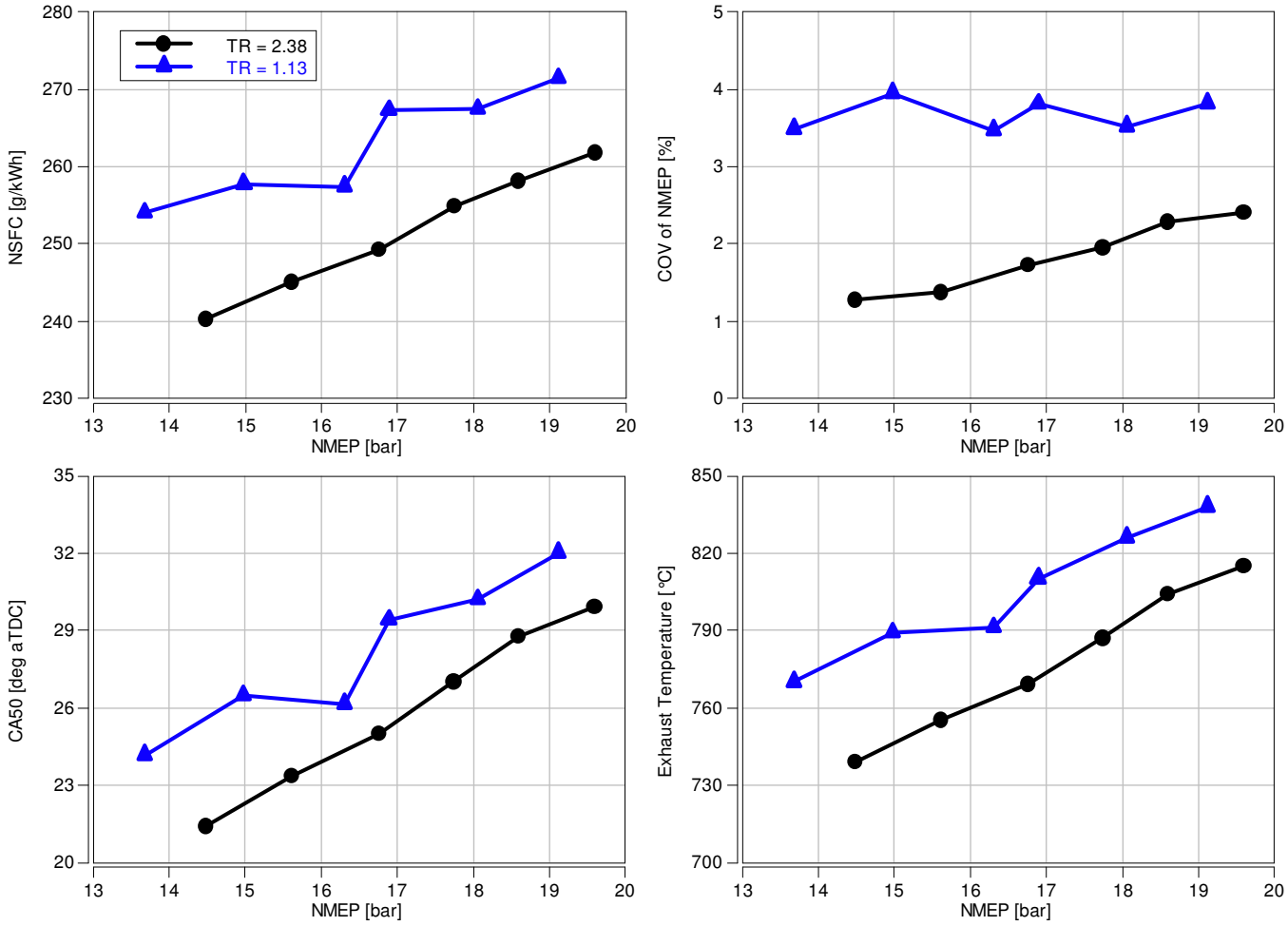

Figure 39 - Tumble impact on engine performance at 2000 rpm with 91 RON gasoline.

Figure 39 compares full load operation on 91 RON gasoline with high and low tumble. High tumble provides an octane benefit as combustion phasing is 2 - 3 degrees advanced at detonation borderline (DBL) for tumble of 2.38 compared to the 1.13 tumble case. With the low tumble, COV of NMEP is above the 2.5 % limit, primarily due to retarded combustion phasing. With high tumble, acceptable stability was achieved all the way up to 19.5 bar NMEP. This illustrates a key difference in requirements for E85 and gasoline - while high tumble was beneficial at full load with E85, it is essential at full load with gasoline as combustion stability targets cannot be met with low tumble.

The two other impacts of retarded combustion phasing due to increased octane requirement with low tumble were increased fuel consumption and increased exhaust temperature. Exhaust temperature would lead to a further increase in fuel consumption at high speed full load as more fuel enrichment would be required for turbine inlet temperature control.

At part load, although high tumble showed a benefit in reduced COV of NMEP, combustion stability was also acceptable with low tumble, even under retarded IVC conditions (Figure 40). 1.13 tumble ratio is still high compared to NA engine tumble levels. High tumble provided benefits at part load in the form of reduced CO emissions due to improved mixture preparation which also provided reduced fuel consumption. These benefits would appear to more than compensate for increased heat transfer losses due to the higher air motion.

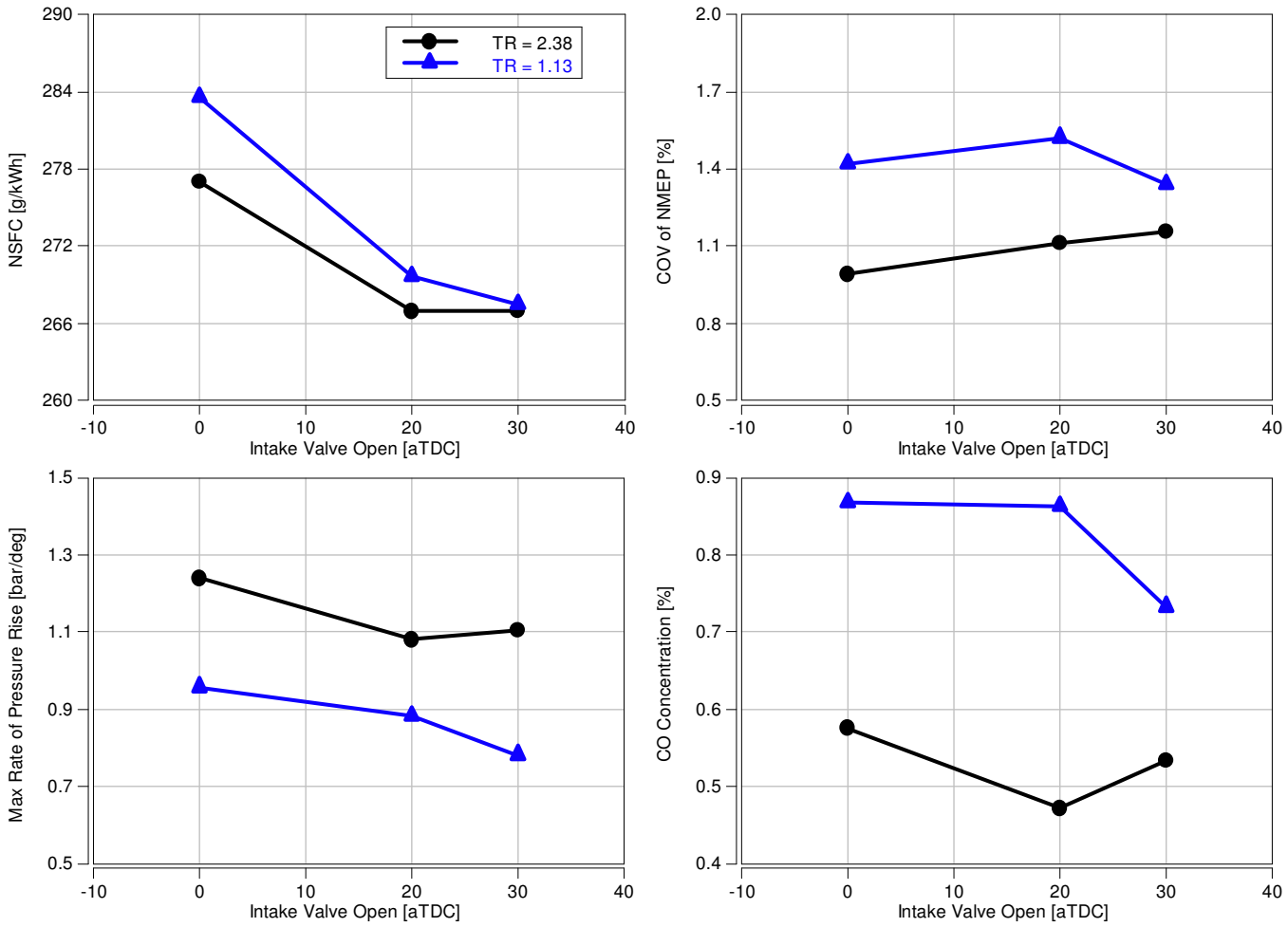

Figure 40 - Tumble impact on engine performance at 1500 rpm, 3.32 bar NMEP with 91 RON gasoline for intake cam phasing sweep with constant 20° overlap.

Full Load Comparison Gasoline versus E85 with 1.93 Tumble ratio

Following port development for the multi-cylinder engine aimed at reducing tumble to within the 1.75 - 2.0 target range and improving flow capability, a confirmation flow box for the multi-cylinder intake port was manufactured and tested. The tumble level of this port was measured at 1.93. Due to the negative impact on mixture preparation and octane requirement that had been observed when tumble was reduced from 2.38 to 1.13, the intake port of the single cylinder head was modified to match the multi-cylinder port, and performance on 91 RON gasoline and E85 was evaluated.

Figure 41 and Figure 42 compare full load operation on 91 RON gasoline and E85, with 1.93 tumble ratio and 9:1 compression ratio. Ignition timing was set to MBT/DBL or to control cylinder pressure to a limit of 150 bar (mean + 3σ) and equivalence ratio was set at λ=1 or rich as required to maintain an exhaust temperature of 950°C. NMEP was set to the target levels for the engine. With 91 RON gasoline, CA50 at 2000 rpm, 18.5 bar NMEP was close to 30 degrees and COV of NMEP was close to the limit of 2.5%, any further increase in NMEP would result in further retardation of combustion phasing and a corresponding increase in COV of NMEP, therefore 18.5 bar NMEP was the maximum load that would give acceptable combustion stability at 9:1 compression ratio with 91 RON fuel. This showed that 1.93 tumble was acceptable for 91 RON operation, however higher tumble may have provided a small octane improvement which would improve stability and/or allow increased NMEP. The impact of reduced tumble ratio on mixture preparation was studied in detail on the optical engine and is presented later in this report.

There is a significant difference between 91 RON (regular grade) and 98 RON (premium gasoline); at 18.5 bar NMEP, 98 RON gasoline would allow several degrees more ignition advance with improved combustion stability, which would therefore allow much higher NMEP operation. Likewise, knock free operation on E85 allows very high NMEP operation as combustion stability is excellent due to advanced combustion phasing. The limiting factors for performance on E85 are thermal and mechanical loading on the base engine and airflow capability which is defined by the turbocharger match. For this engine, maximum BMEP for the multi-cylinder engine on E85 was set at 27 bar BMEP between 2500 - 3000 rpm, the single cylinder operated at 26, 27 and 22 bar NMEP at 2000, 3500 and 4750 rpm respectively. At all of these conditions the engine ran knock free. At 2000 rpm the engine ran with MBT ignition, but at 3500 rpm ignition timing was retarded slightly to control cylinder pressure.

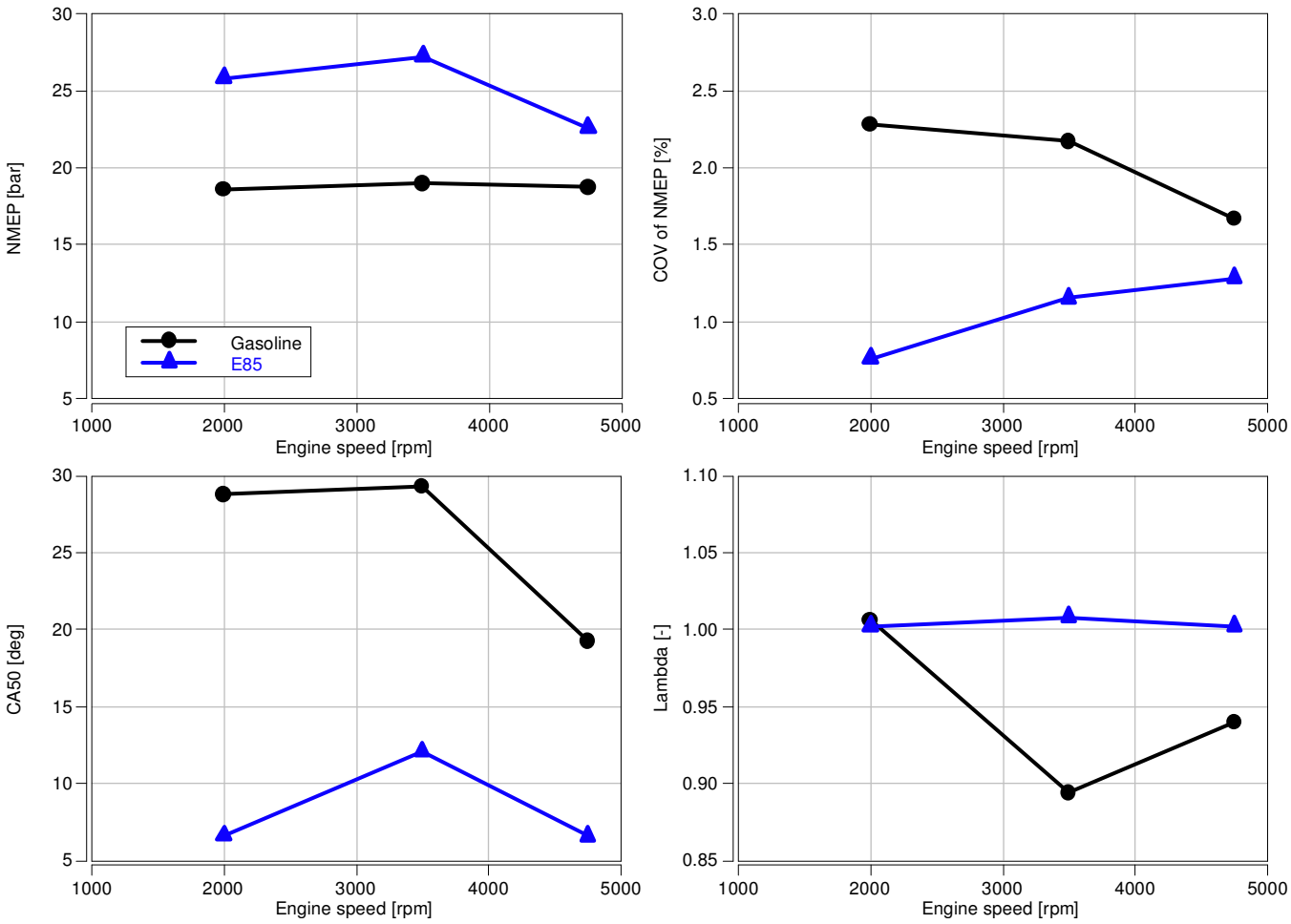

Figure 41 - Full load results with gasoline and E85 and a tumble ratio of 1.93.

With E85 the engine operated with an equivalence ratio of λ=1 but with gasoline, even though the NMEP was significantly lower, enrichment was required at 3500 rpm and above to control exhaust temperatures.
While fuel consumption was higher for E85 than gasoline, the increase was less than the difference in heating value between the two fuels due to combustion phasing and λ=1 operating benefits with E85. At 3500 rpm E85 NSFC was only 12% higher than for gasoline despite the 33% reduction in heating value. On a thermal efficiency basis E85 showed 34% higher net thermal efficiency than gasoline at 3500 rpm, and at 2000 rpm net thermal efficiency was 41%. This could be increased further by increasing compression ratio if the engine were to be optimized for E85 operation rather than being required to run on either gasoline or E85 as a flex fuel application. There would be some trade-off between thermal efficiency benefit from compression ratio increase and reduced efficiency due to combustion phasing retard for cylinder pressure control at full load as higher compression ratio would increase cylinder pressure, however increased compression ratio would provide fuel

efficiency benefits under part load operating conditions which is more critical for most drive cycle and real world conditions.

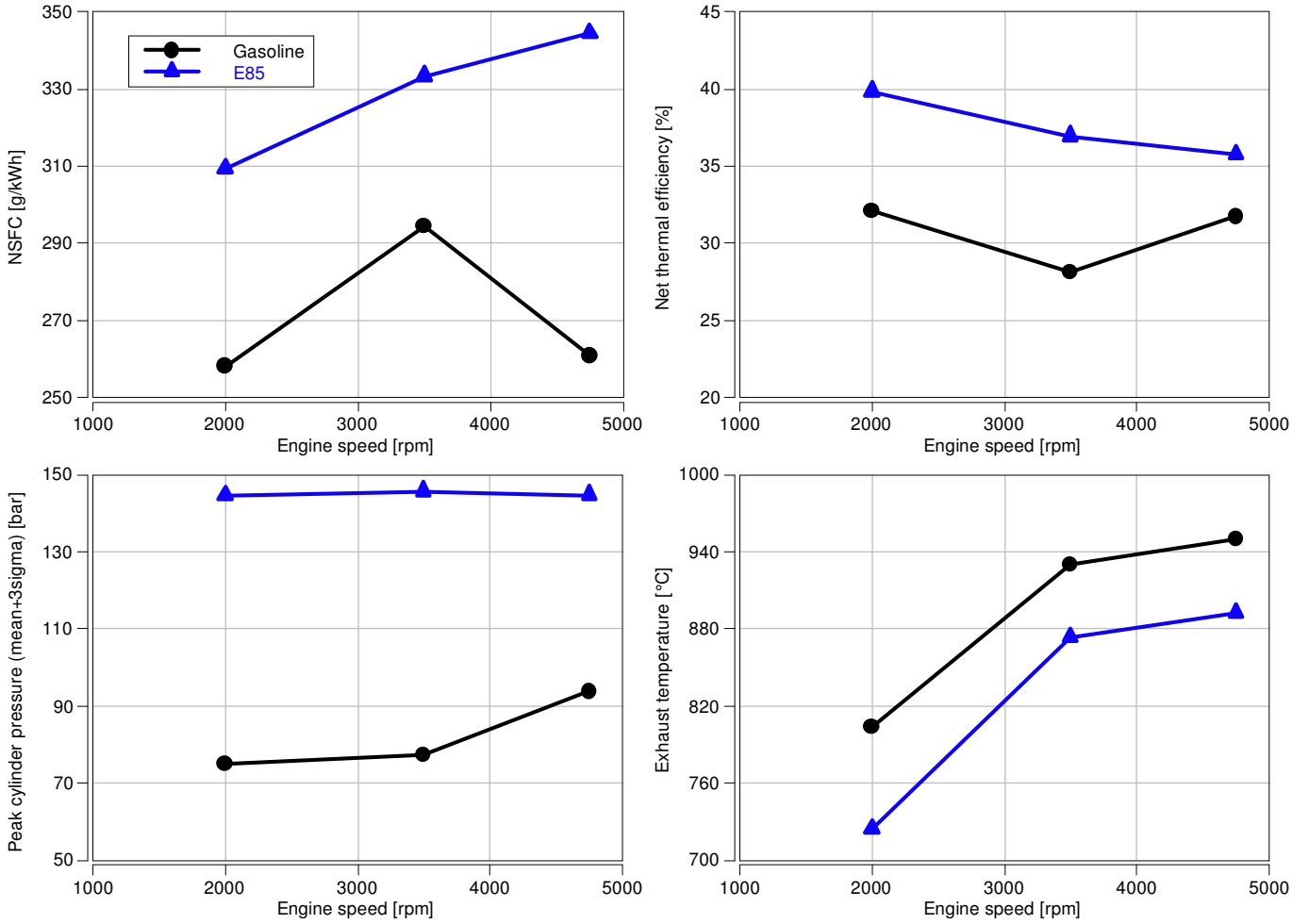

Figure 42 - Full load results with gasoline and E85 at a tumble ratio of 1.93.

Residual Fraction Impact at Full Load

Trapped residual gas can increase the propensity to knock as it raises unburned gas temperature. Increased valve overlap can help scavenge residual gas from the cylinder as intake pressure is higher than exhaust pressure under boosted conditions at lower engine speeds, however on I4 or V8 engines, overlapping exhaust pulses can lead to backflow from the exhaust to the cylinder and from the cylinder to the intake manifold, as exhaust blowdown from the next cylinder in the firing order sequence will increase exhaust pressure during valve overlap.

Figure 43 shows the impact of residual gas at 2000 rpm, 18.5 bar NMEP. When residual gas fraction was increased (by changing cam timing) from 1.0% to 2.6% (determined from GCA), knock-limited combustion phasing retarded by almost 10 degrees. As a result, combustion stability deteriorated, fuel consumption increased by almost 7%, and exhaust temperature increased by 110°C which would lead to increased fuel enrichment requirements. With E85, due to its anti-knock properties, residual gas content is not expected to lead to knock-limited combustion.

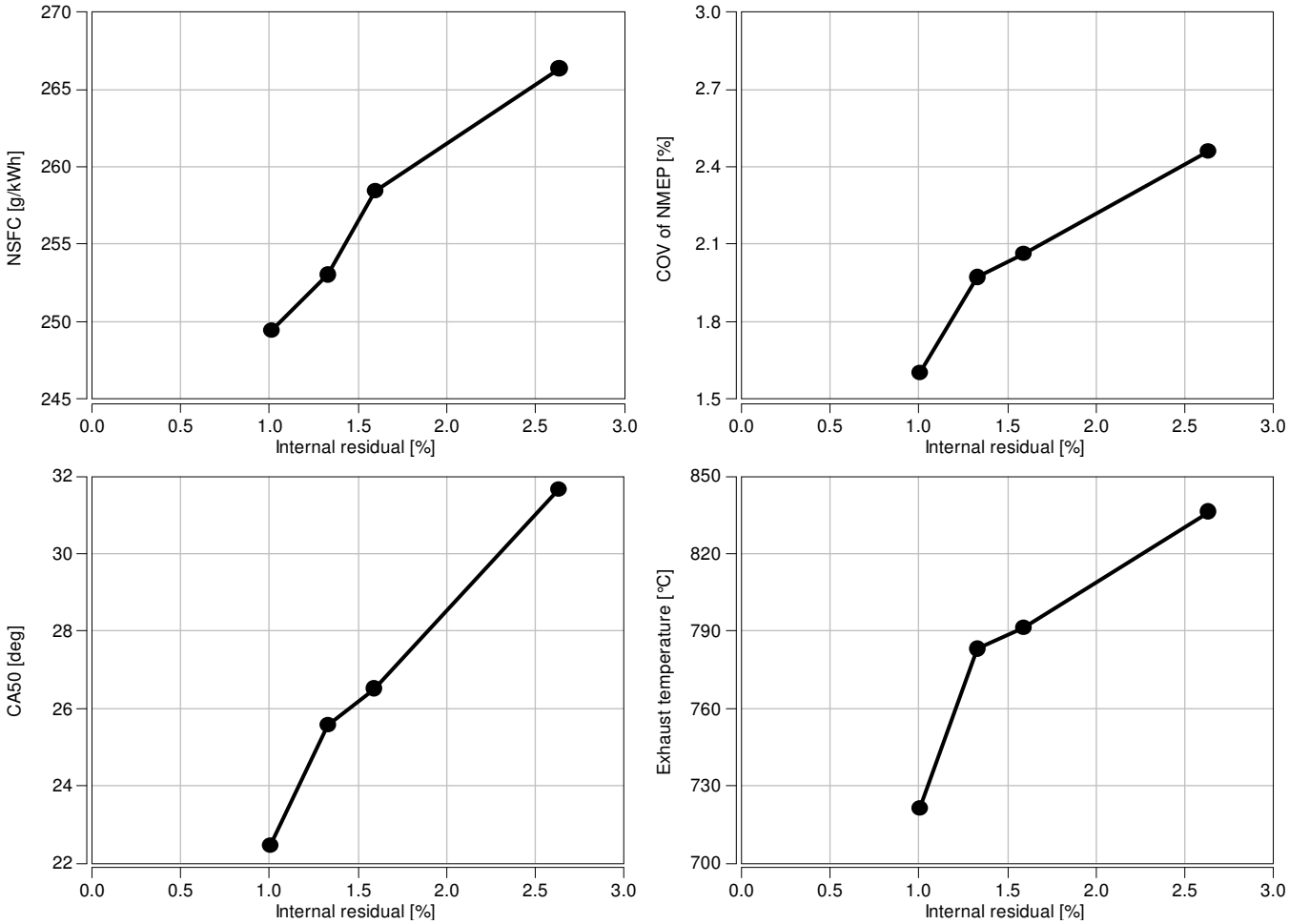

Figure 43 - Internal residual impact on combustion with regular gasoline at 2000 rpm, 18.5 bar NMEP.

Split Injection for Catalyst Heating

Following a cold start, it is important to heat the catalyst rapidly as the majority of drive cycle emissions are produced while the catalyst is warming up and operating at low efficiency. Also, during catalyst heating, engine-out emissions must be reduced to a minimum. Catalyst heating is achieved by using a split injection strategy in a direct injection engine.

Figure 44 shows a comparison of catalyst heating mode operation for DT1 and DT2 injectors. Following optimization of the primary and secondary injection timings for each injector the fraction split between the primary and secondary injection pulse was optimized. These results show improvements in all areas for the DT1 injector with improved combustion stability, reduced emissions and lower fuel consumption. The differences between the injection split fraction for the two injectors relates to poorer stratification with the DT2 injector which favors more fuel injected in the first pulse to produce a richer background homogenous mixture.

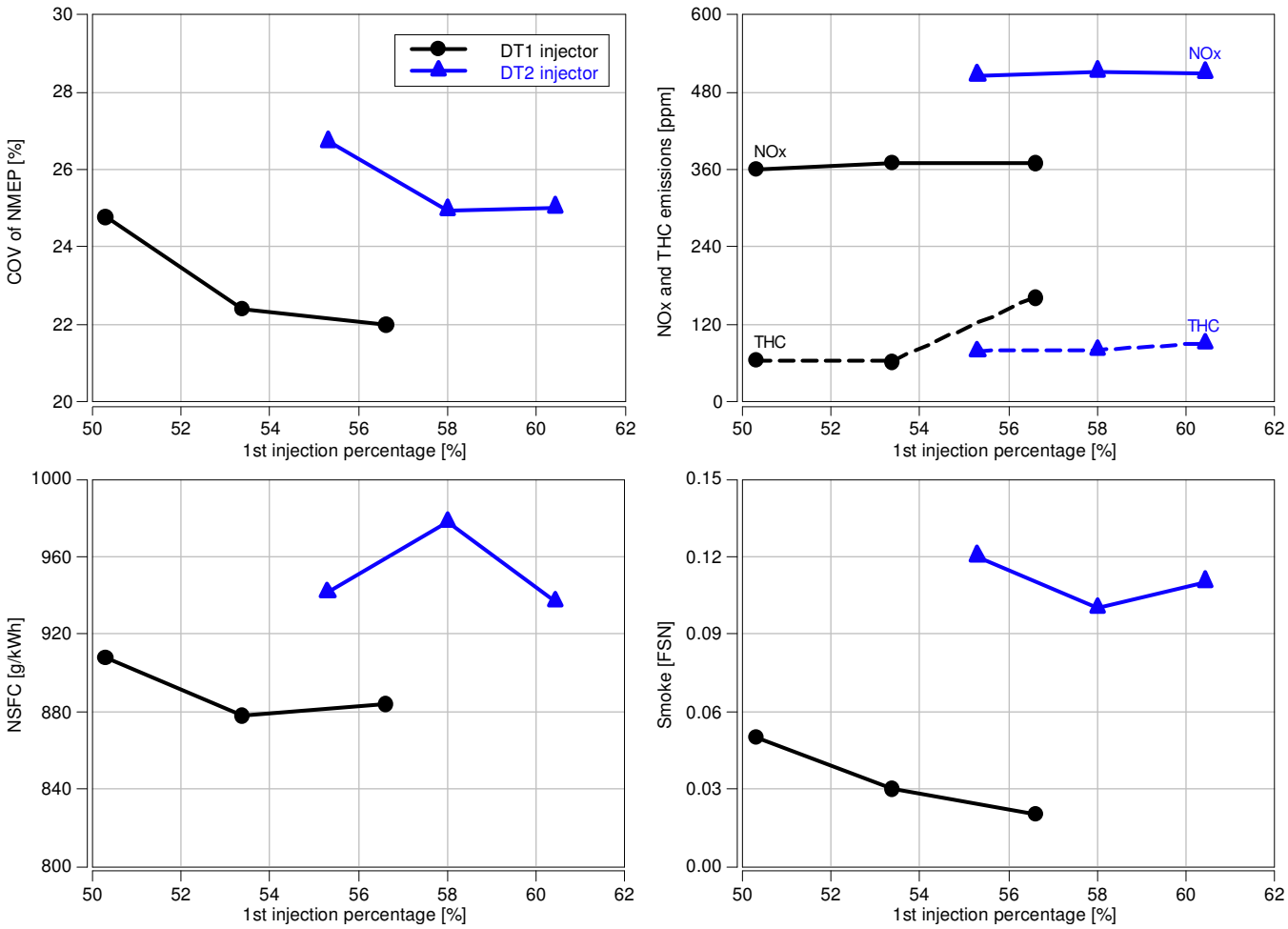

Figure 44 - Comparison of DT1 and DT2 injectors in catalyst heating mode, TN=2.38, CR=9.7:1, gasoline.

Optical Engine Development

DI combustion systems offer a variety of opportunities, but at the same time have to meet a number of requirements, as mentioned previously:

- At part load, a well-mixed homogenous charge is required, otherwise fuel energy will be lost in the form of increased CO or HC emissions.
- During catalyst heating a rich stratified mixture must be created at the spark plug with low cyclic variability and low engine-out emissions.
- At full load, a well-mixed homogeneous charge is required to mitigate knock and fuel impingement on the piston must be minimized to maximize the DI charge cooling benefit.
- Under all conditions, liner impingement must be eliminated or reduced to a minimum to avoid liner wear, smoke, and oil dilution.

With conventional engine development some of these issues can be inferred from emissions, fuel economy or cylinder pressure results, however other potential issues such as liner wetting are difficult to identify with conventional engine testing. AVL routinely uses a single cylinder engine with optical access for GTDI development programs as this helps identify and resolve any potential issues early on in a program. This process has a number of advantages compared to CFD analysis as the results require no correlation, the process does not rely on assumptions or fuel spray models (which are difficult to obtain), and the process

accounts for cyclic variability rather than providing a mean cycle result which has limited value for a gasoline engine.

For the current program, E85 operation increased the risk of wall wetting due to increased fuel flow that would be required due to the lower heating value and higher BMEP target. Fuel spray penetration increases in proportion to injection pulse width, so the risk of liner wetting and resultant liner wear and oil dilution increases with higher fuel flow requirements.

The optical engine is a single cylinder engine with the upper part of the liner made from quartz glass, providing valuable insight into the fuel injection and combustion processes. Figure 45 shows the combustion chamber of the optical engine. Laser Induced Fluorescence (LIF) is used to observe the fuel-air mixing process and flame photography is used to observe combustion[1]. The engine is operated on iso-octane (with 10% 3-pentanone as a tracer for LIF measurement) rather than regular gasoline in order to reduce deposits on the glass liner which deteriorate visual observation. For LIF an EXCIMER laser with KrF is operated at a wavelength of 248 nm.

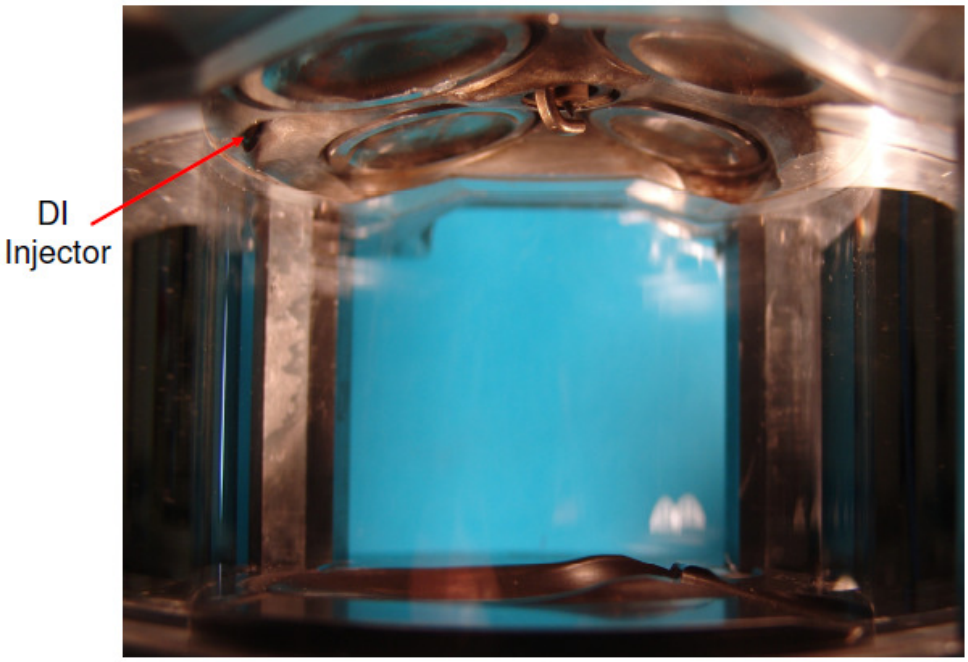

Figure 45 - Combustion chamber of the optical engine.

At each measurement point, 35 images are captured from consecutive cycles taken at the same crank angle timing. These single images (fuel spray or combustion flame) are statistically evaluated, replacing the fuel (or flame) intensity by the probability to find fuel of low or high density (or sooting versus premixed (no soot) flames for flame images), see Figure 46.

[1] The compression ratio on the optical engine is lower than the development engine, however the difference in the compression ratio has minimal impact on the optical engine results.

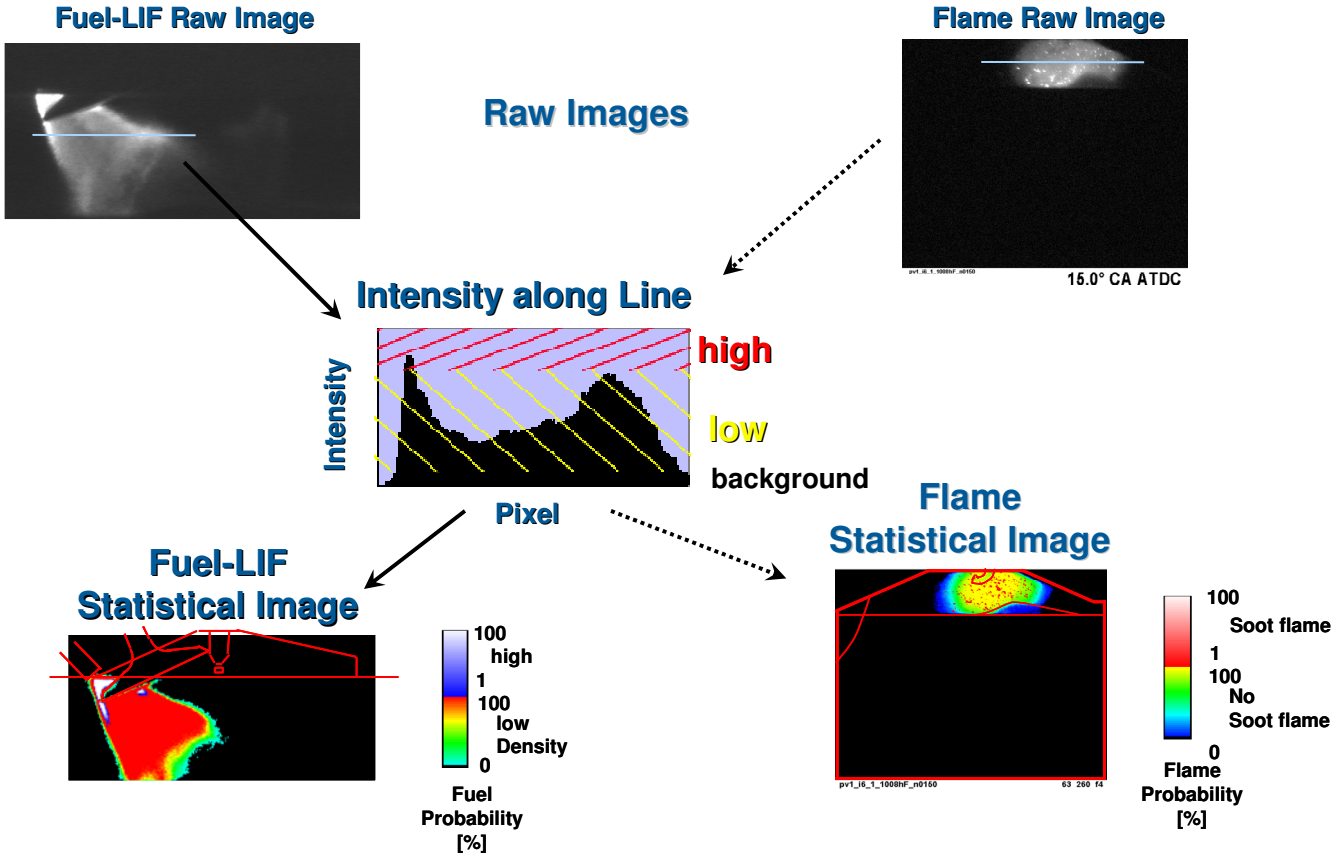

Figure 46 - Statistical evaluation of fuel and flame images.

Table 2 lists the operating conditions evaluated on the optical engine. Low speed full load conditions were selected for evaluation as mixing can be more problematic at these conditions due to lower in-cylinder air motion combined with high fuel flow rates. At full load, the engine operated with intake manifold conditions matching boosted multi-cylinder conditions, however ignition timing was retarded to reduce cylinder pressure to protect the glass liner. This has no effect on the air/fuel mixing process which is the focus of the investigation.

Table 2 - Development points on the optical engine.

	Speed	NMEP	Description	Investigation focus
1	1500 rpm	3.32 bar	World-wide mapping point	Fuel/air interaction
2	1000, 1500, 2000 rpm	14.7 bar	Low speed, high load	Fuel penetration, piston/liner wetting
3	1200 rpm	1.70 bar	Catalyst heating	Fuel stratification

Optical engine testing was run in parallel with conventional single cylinder engine development so that the optimum hardware and control settings defined by single cylinder testing could be evaluated on the optical engine and vice versa.

Fuel-air interaction and fuel penetration results were similar for both DT1 and DT2 injectors at part and full load, however differences were observed in catalyst heating modes which are described in detail below. Statistical images of fuel distribution for the first injection in catalyst heating mode at different crank angle degrees are shown in Figure 47 and Figure 48 for DT1 and DT2 injectors respectively. The upper spray of the DT2 injector separates from the main spray and results in increased liner wetting. At the start of the second injection (75 degrees BTDC), mixture homogeneity is similar for both injectors.

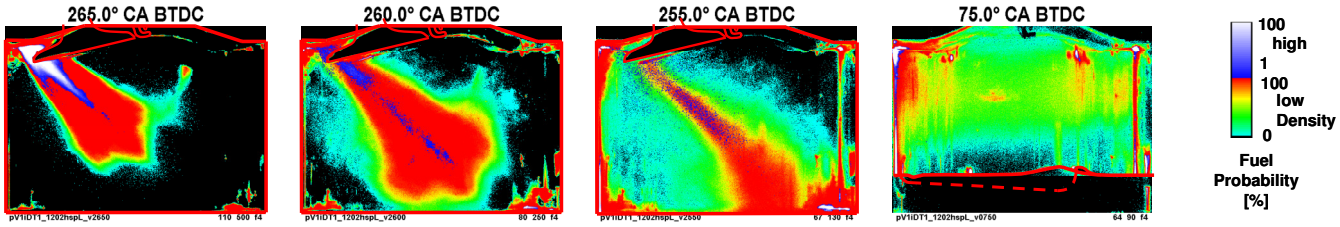

Figure 47 - Fuel spray distribution of the 1st injection (SOI=275 BTDC) with DT1 injector in CSER mode.

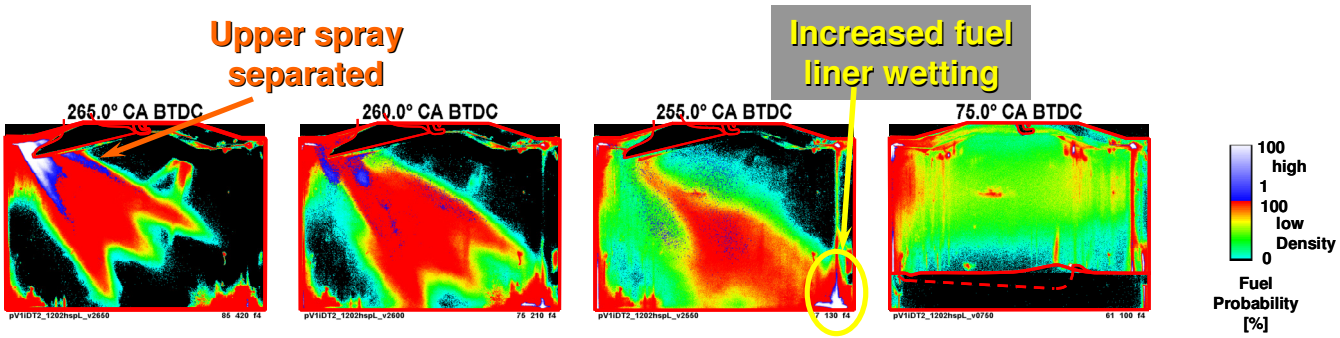

Figure 48 - Fuel spray distribution of the 1st injection (SOI=275 BTDC) with DT2 injector in CSER mode.

Statistical images of fuel spray distribution for the second injection at different crank angle degrees with both injectors are shown in Figure 49 and Figure 50. The top spray from the DT2 injector - which again separates from the main spray - overshoots the piston bowl and impinges the rear of the piston. Due to this poor targeting, stratification is reduced leading to a leaner mixture at the spark plug with the DT2 injector which resulted in reduced combustion stability. The first two frames of Figure 49 (70 and 65 ° CA BTDC) show what looks to be fuel to the right of the spark plug (circled in blue) where fuel would not be expected at these timings. This is an optical reflection of the fluorescing fuel spray onto the quartz liner and therefore has no meaning in terms of the results.

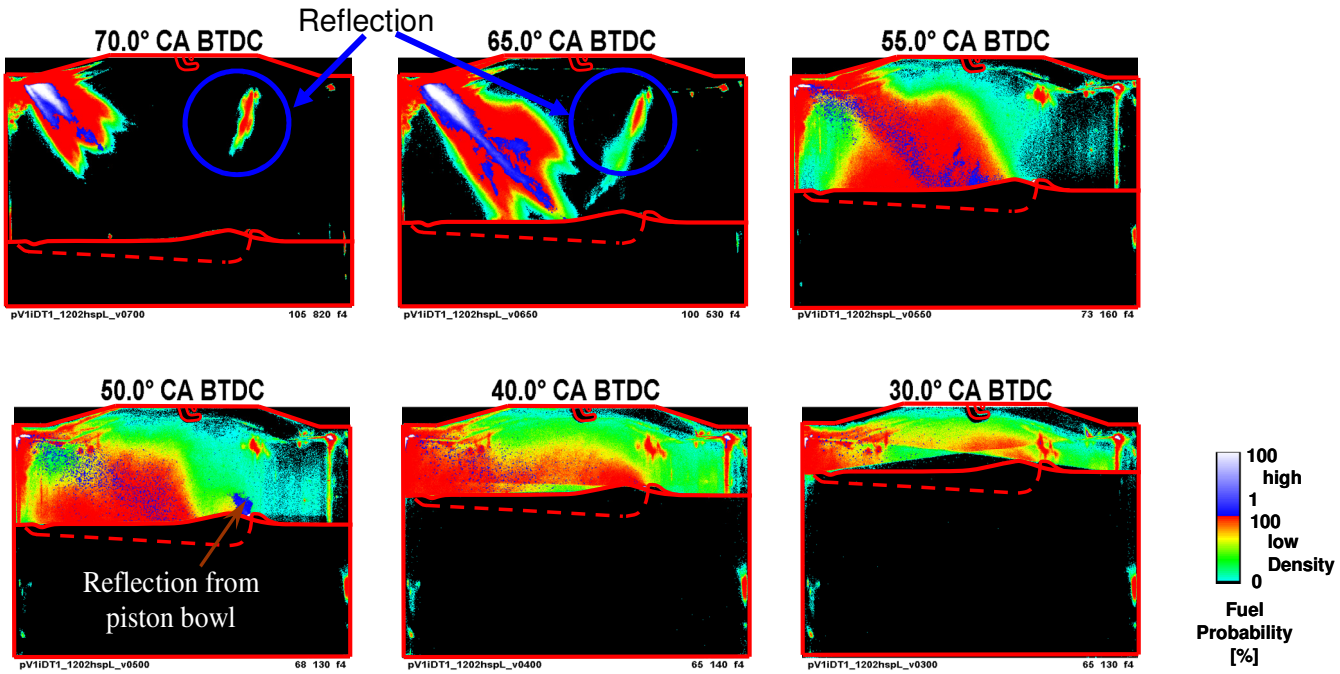

Figure 49 - Fuel spray distribution of the 2nd injection (SOI=75 BTDC) with DT1 injector in CSER mode.

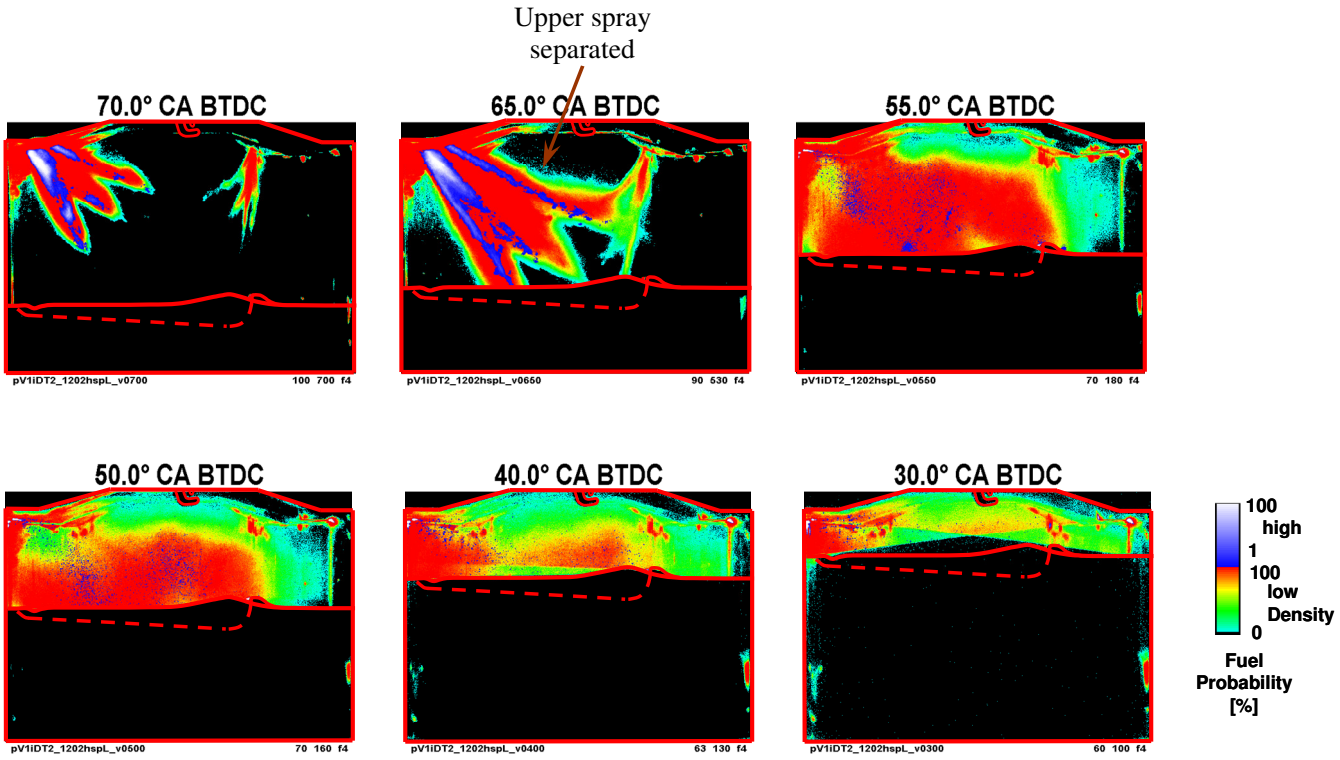

Figure 50 - Fuel spray distribution of the 2nd injection (SOI=75 BTDC) with DT2 injector in CSER mode.

Figure 51 and Figure 52 show the statistical flame images at 40 and 60 degrees ATDC for both injectors in catalyst heating mode. Due to the improved fuel stratification of DT1:

- The engulfed flame volume at the same time is larger
- Cyclic variability is significantly reduced

The slightly increased soot flame probability of DT1 is not significant, as tailpipe smoke measurements showed very low smoke levels. Based on these findings and similar advantages measured on the single cylinder engine, the DT1 injector was chosen.

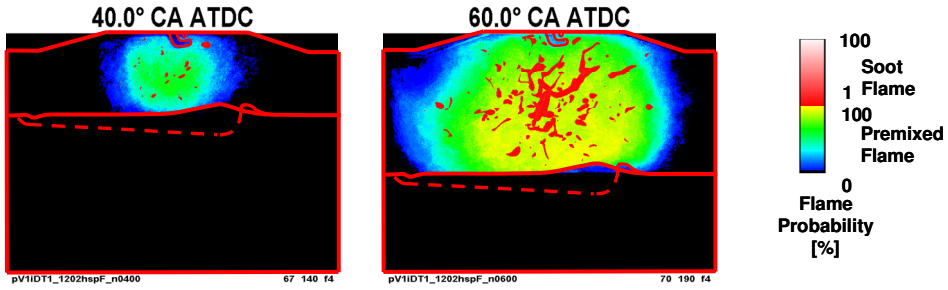

Figure 51 - Flame propagation with DT1 in catalyst heating mode.

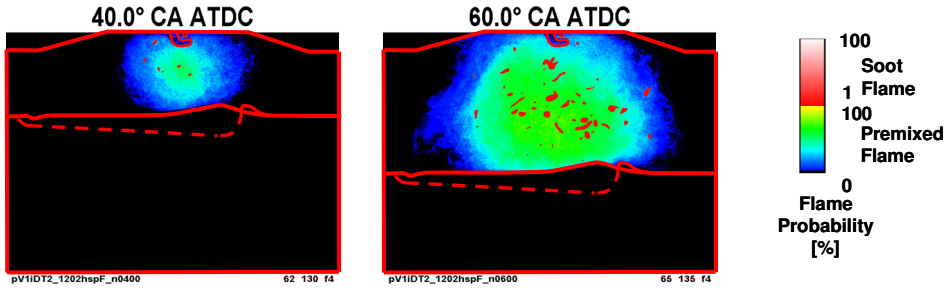

Figure 52 - Flame propagation with DT2 in catalyst heating mode.

Figure 53 shows statistical flame images at 30 and 90° ATDC in catalyst heating mode on gasoline and E85. With gasoline, soot producing flames were measured, especially in the region close to the piston where fuel impingement would have created a fuel film. When the engine was operated on E85 at the same conditions, the soot producing flames disappeared and only premixed combustion flames were observed. As ethanol is oxygenated, oxygen contained in the fuel reduces or eliminates soot formation in rich regions. Also ethanol is a single component fuel with a single boiling point of 78.3℃. E85 is a mixture of ethanol and high volatility gasoline components (to aid cold starting). Gasoline is a multi-component fuel with a range of boiling temperatures for its various constituents, typically with boiling points up to 200℃. Therefore it is likely that more complete evaporation of an E85 fuel film on a hot piston crown will occur than for gasoline and that that the heavier components that do not evaporate as readily are the source of soot producing flames with gasoline.

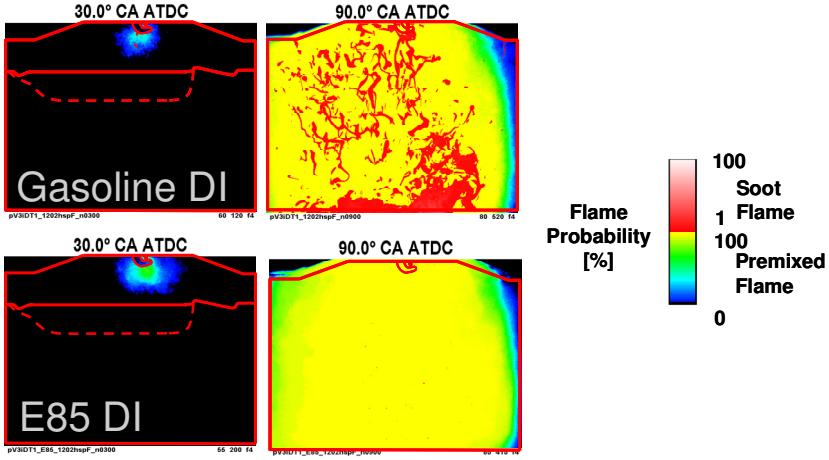

Figure 53 - Flame images in catalyst heating mode comparing E85 operation with gasoline.

Figure 54 shows statistical fuel images at full load for 2000, 1500, and 1000 rpm with a tumble ratio of 2.38. At 2000 rpm there is a beneficial interaction of the high tumble air motion with the fuel spray, effectively deflecting the fuel spray away from the exhaust side of the liner and eliminating bore washing. Early injection is preferable as the air motion decays at later crank angles. However injection timing earlier than 300 deg BTDC led to an increase in smoke due to increased fuel impingement on the piston crown. At lower engine speeds, air motion is lower but fuel spray velocity remains unchanged due to almost unchanged injection duration. At 1000 rpm some degree of bore and piston wetting is evident as the air motion is insufficient to deflect the fuel spray.

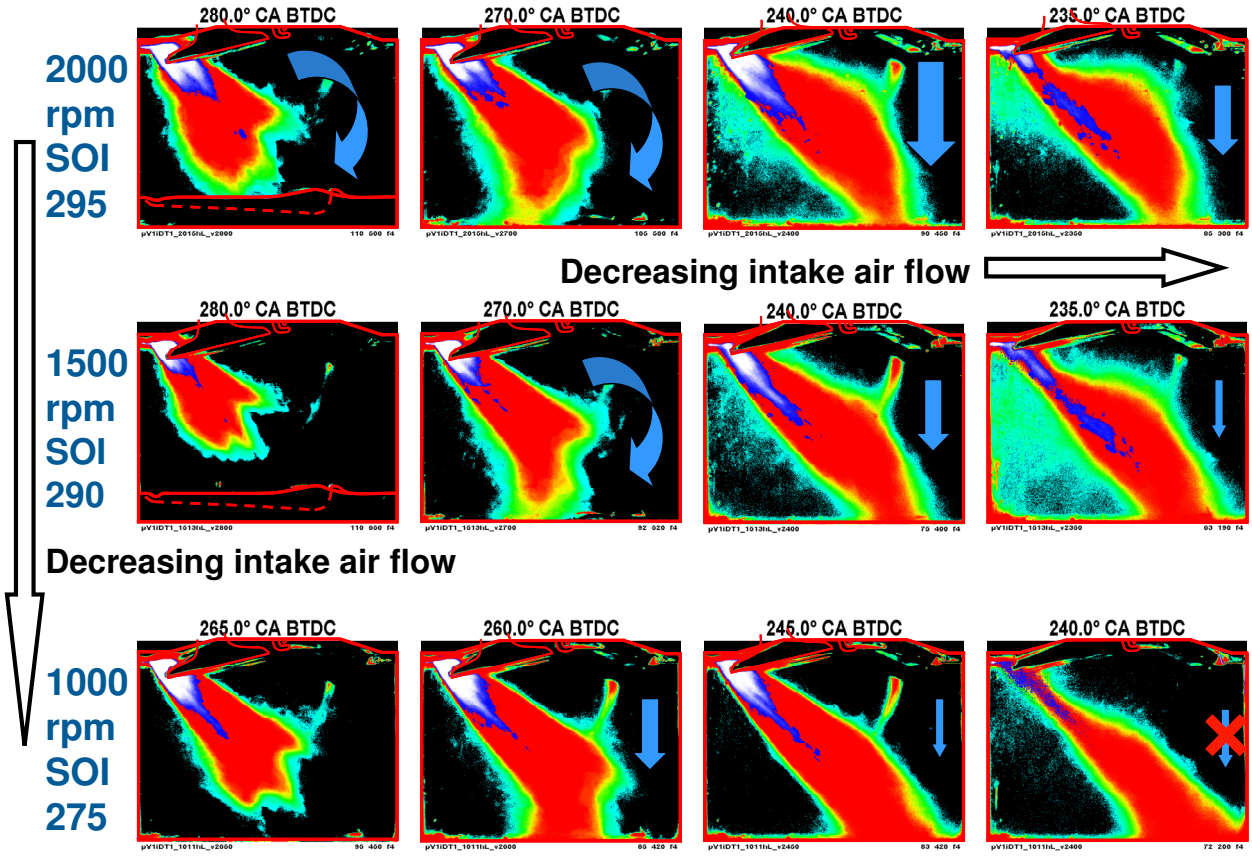

Figure 54 - Full load LIF measurements with a tumble ratio of 2.38.

Figure 55 shows the statistical flame images that result from the fuel delivery effects shown in Figure 54. At 2000 rpm where there was a strong air and fuel spray interaction, wall wetting was reduced and mixture preparation was good resulting in very few soot producing flames. At 1000 rpm there were more soot producing flames due to increased liner and piston wetting. Inspection of the piston following measurement showed fuel spray impingement witness marks confirming that fuel had wet the piston.

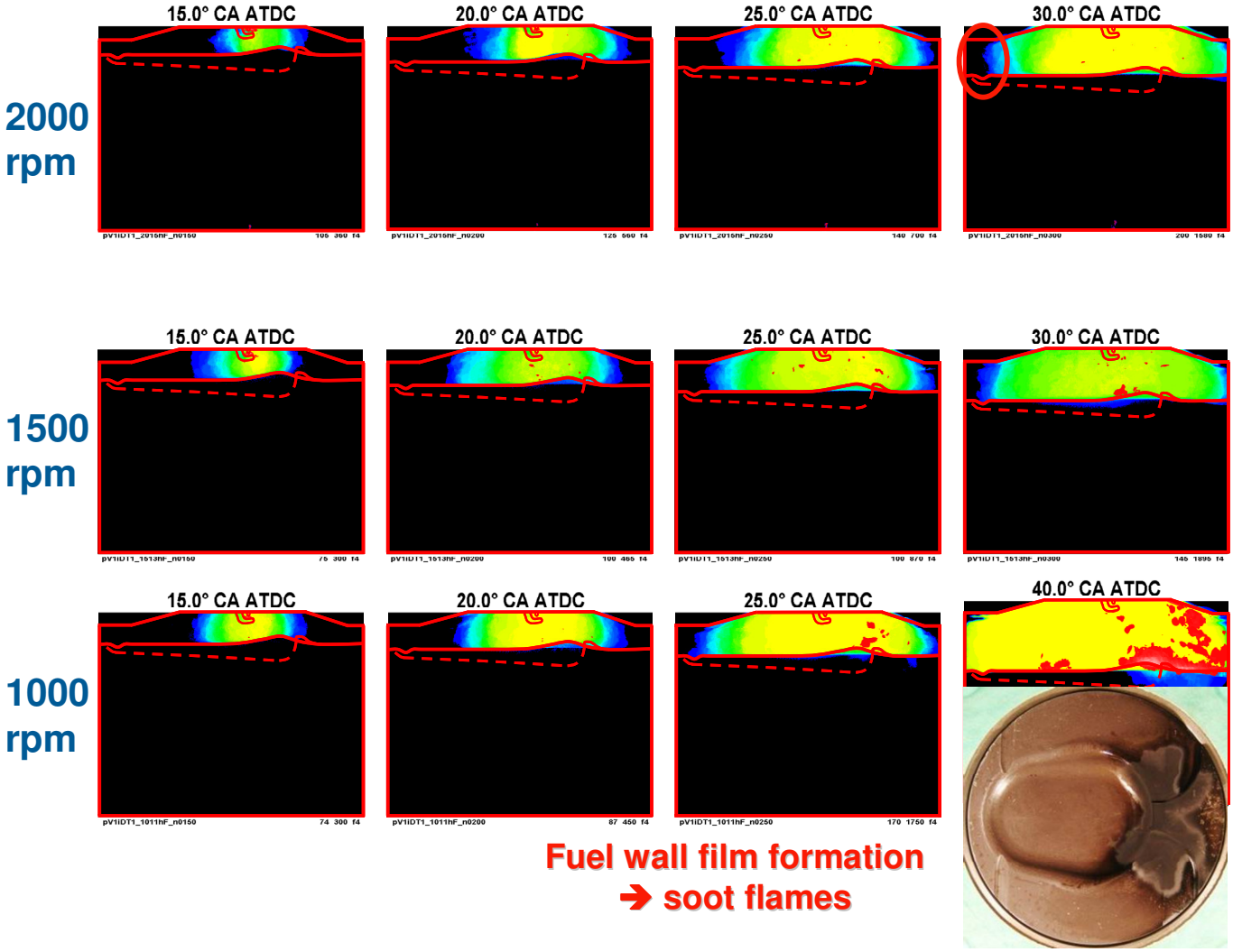

Figure 55 - Statistical flame images corresponding to the statistical fuel images in Figure 47 at full load with a tumble ratio of 2.38.

Therefore high tumble was very effective in eliminating bore washing and providing good mixture preparation at 1500 rpm and above, however despite the high tumble it was difficult to eliminate liner wetting below 1500 rpm at full load. It was noticed that fuel spray penetration with the DT1 and DT2 injectors was higher than expected for DI injectors of similar specification from other suppliers, which is probably due to design differences between suppliers. The higher penetrating spray forced later injection timings to avoid piston wetting and smoke and as a result injection was forced to a later timing where the tumble field intensity was reduced and the air motion was less effective at deflecting fuel from the liner.

The same tests were repeated with the multi-cylinder intake ports with a tumble ratio of 1.93. With reduced tumble ratio the interaction of the air motion and fuel spray was reduced and increased liner and piston wetting was noticed at 1500 and 1000 rpm with increased soot producing flames (Figure 56). As this was undesirable, reduced fuel pressure and advanced injection timing was investigated as a means of reducing liner wetting and soot producing flames.

Figure 57 shows that by reducing fuel pressure it was possible to advance start of injection by 10 degrees which reduced liner wetting and soot producing flames. Earlier injection timing ensured that the fuel was injected into stronger tumble motion while the lower fuel pressure reduced fuel spray impingement reducing piston wetting at the earlier injection timing. Inspection of the pistons after these tests confirmed reduced piston

fuel impingement with 7 MPa fuel pressure and 300° SOI. It was agreed that these adjustments had provided an acceptable solution for the lower tumble level and that no further changes were necessary.

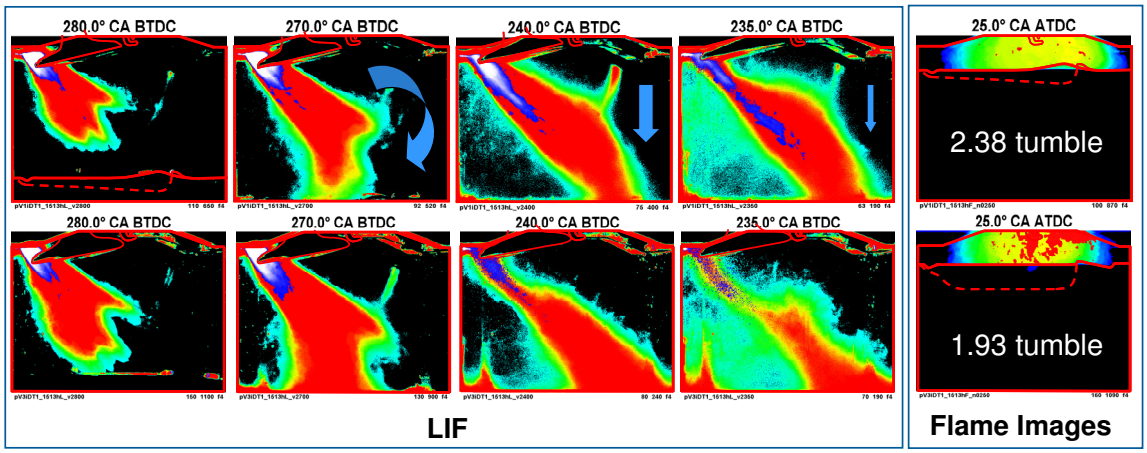

Figure 56 - Statistical fuel and flame images at the same 290 deg injection timing and 13 MPa fuel rail pressure at 1500 rpm full load comparing tumble of 2.38 and 1.93.

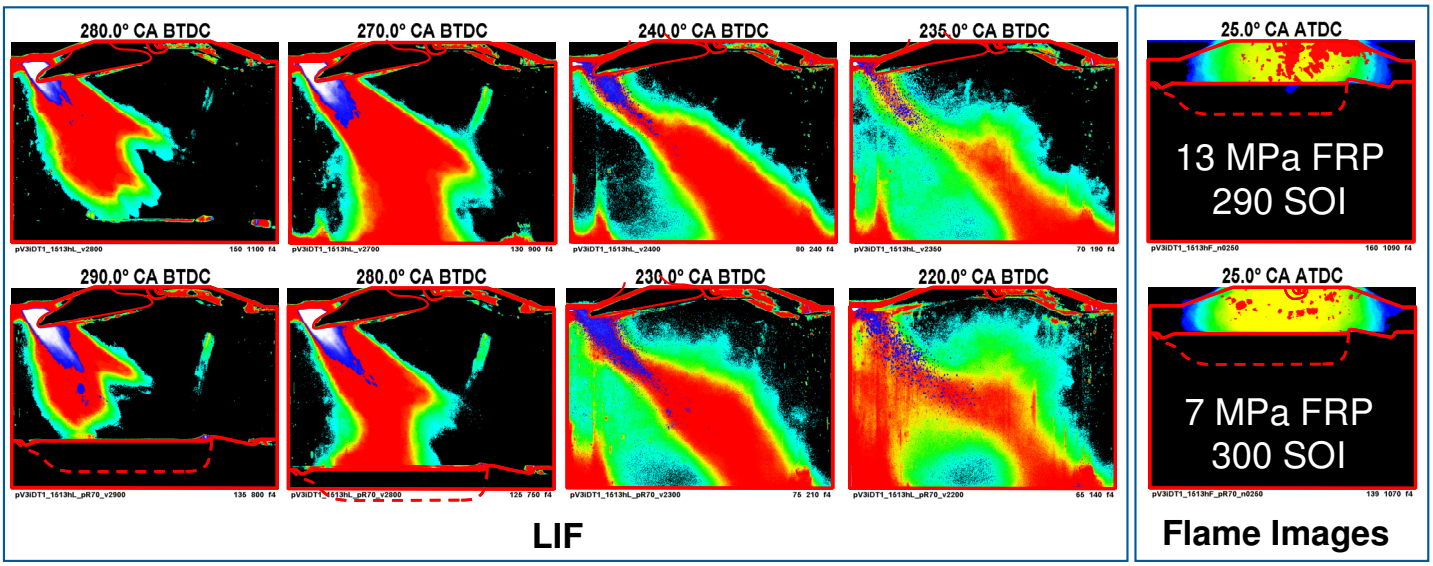

Figure 57 - Statistical fuel and flame images at 1500 rpm full load for a tumble ratio of 1.93 showing the influence of fuel rail pressure (FRP) and injection timing (SOI) on liner wetting and sooting flames.

Figure 58 shows the results of fuel spray measurements for operation on E85 at 2000 rpm for the 26 bar NMEP target with a tumble ratio of 1.93. At this condition there is a 64% increase in fuel flow relative to gasoline due to a 41% increase in target NMEP and 33% reduction in heating value - less the efficiency benefit of E85 operation at MBT ignition. This leads to increased injection duration and a higher penetrating fuel spray. However as E85 operation significantly reduces smoke, it was possible to operate with injection 20 degrees advanced of the gasoline case. This allowed the fuel to be injected at time when there was a strong air motion interaction which deflected fuel and prevented liner wetting.

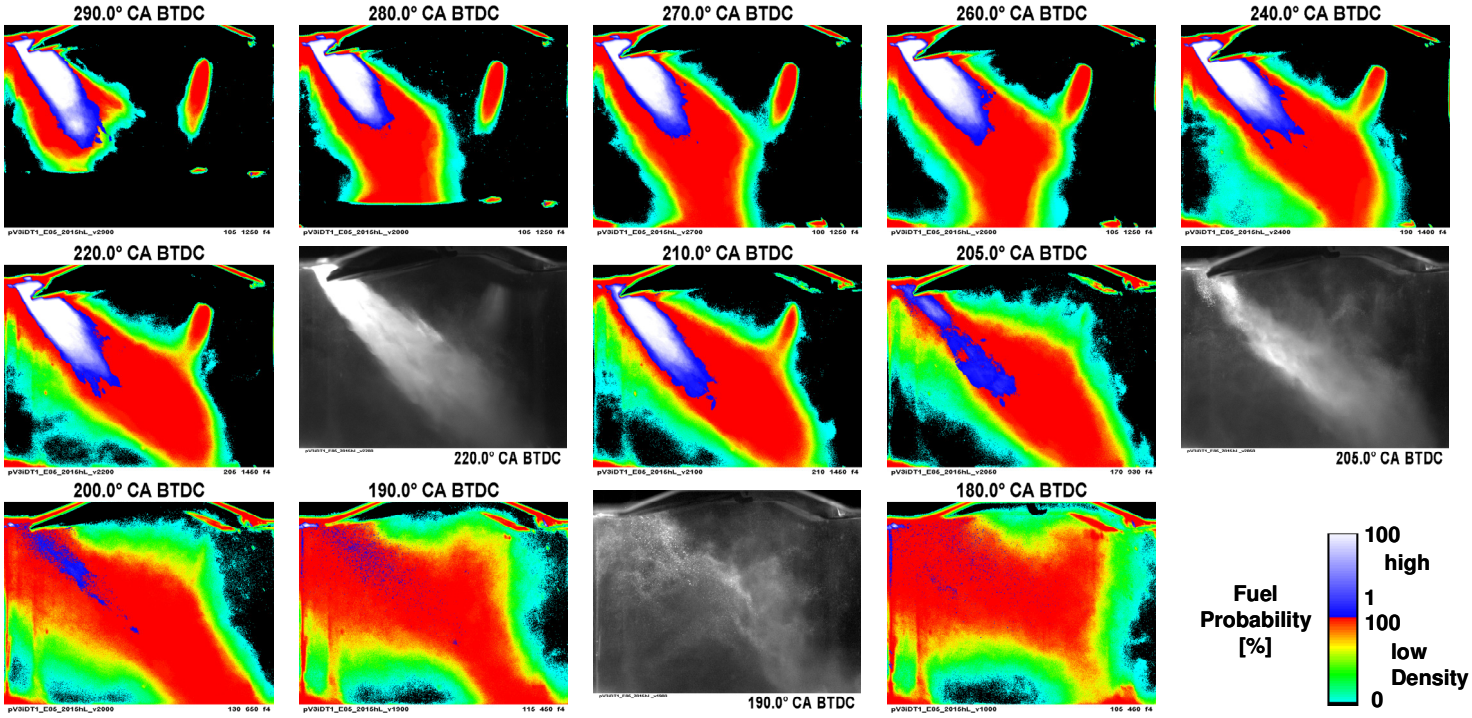

Figure 58 - Statistical and single fuel images at 2000 rpm full load with E85 for tumble ratio of 1.93 with start of injection timing 300°BTDC.

Summary/Conclusions

This SCE section presented work undertaken to design and optimize a new combustion system for a flex fuel turbocharged direct injection engine. This included: port design and development, fuel spray design and single cylinder and optical engine development.

Single cylinder testing allowed the combustion system to be developed months before multi-cylinder engine hardware was available, compressing program timing and reducing cost due to the reduced number of prototype parts required for development and reduced rebuild time. Optical engine development provided additional valuable insight into mixture preparation and combustion processes which showed the influences of tumble ratio, engine speed, fuel flow rate, injection timing, fuel rail pressure, injector spray pattern and differences between gasoline and E85 operation. This allowed a robust combustion system to be developed meeting all requirements, and combustion system changes were not required in subsequent program phases.

The main findings from the SCE optical and conventional engine test programs were:

- The use of LDA for port development allowed the quality of the tumble flow field to be assessed in addition to measurement of tumble ratio and flow coefficient. This was important to ensure that a centered and symmetric tumble field was created for more uniform flame propagation and reduced knock propensity.
- At part load, high tumble provided improved fuel/air mixing which reduced fuel consumption due to improved mixture homogeneity and reduced CO emissions.
- At full load with gasoline, high tumble reduced the propensity to knock improving combustion stability due to more advanced combustion phasing.
- Due to E85's high heat of vaporization and high octane number it was possible to operate knock free at very high BMEP. This results in high cylinder pressure, high rates of pressure rise and increased combustion noise. High tumble further increases rates of pressure rise due to increased burn rate,

however it is preferable to maintain high tumble and retard ignition timing to reduce rates of pressure rise as this results in higher efficiency than low tumble at MBT ignition.

- Operation with E85 provides a significant reduction in soot producing flames reducing smoke, primarily due to the high oxygen content of ethanol and its boiling point of 78°C.
- With a side injector configuration, tumble air motion helps deflect the fuel spray from the liner reducing or eliminating bore washing. High tumble is more effective at reducing bore washing than low tumble which is particularly important at low speed full load where the effective air motion is low but fuel flow rates remain high.
- The tumble air motion field is stronger earlier in the intake stroke, so earlier injection timing results in reduced bore washing and improved mixture preparation. However, earlier injection timing leads to an increase in smoke due to increased piston wetting. Therefore injection timing must be optimized to provide adequate mixture preparation, minimal bore washing and low smoke. Reduced fuel spray penetration can be an enabler for earlier injection timing, and E85 can be operated with earlier injection timing due to reduced smoke emissions.
- High tumble is just as beneficial for a flex-fuel turbocharged direct injection engine as for a gasoline or E85 only optimized turbocharged direct injection engine. While the octane benefits of high tumble are not required for E85 operation, there are mixture preparation and bore washing mitigation benefits which are even more important for E85 due to increased fuel flow rates. With gasoline, high tumble is required to minimize octane requirements, improve mixing, and reduce bore washing.
- Results from optical engine testing discerned differences between the two injectors tested - DT1 and DT2. During catalyst heating the top fuel spray plume from injector DT2 separated from the main spray and missed the piston bowl leading to reduced stratification and poorer combustion performance. These findings could have been used to re-design the fuel spray for improved combustion, however, injector DT1 met requirements.

Phase III – Advanced Development

Task 1.0 – Cylinder Head

As mentioned previously, the architecture for the cylinder head was based on a production Ford PFI head. This allowed for a foundation that had much more alignment with Ford's manufacturing strategies, offered some level of previous data and analysis to provide guidance, and also used some shared or similar hardware. From this initial starting point, a large percentage of the cylinder head was then redesigned to accommodate the combustion system changes, as well as high cylinder pressure and temperature requirements when running high boost and E85.

The original production PFI cylinder head was designed for a 92.2mm cylinder bore diameter. To gain the structure required for a robust engine and achieve a more optimal bore-stroke ratio for a turbocharged engine, the bore diameter was reduced to 88.5mm. This allowed for more material in the cylinder liners and bore bridges, and also reduced the loads from the firing pressures.

Piston Forces = Cylinder Pressure * Piston Area

The valve sizes were reduced to accommodate the smaller bore size. Some slight additional increase in valve sizes could have been achieved by relocating the valve locations and narrowing up the side-to-side distance between the valves. It was decided to leave the slightly larger spacing between the valves as it allowed for an improved water jacket to cool the bridges on both the intake and exhaust side. Typically the intake side valve bridge water jacket becomes too small to manufacture in the delicate sand cores, but this space was utilized to greatly improve the cylinder head cooling. A full 360° cooling jacket was enabled around the spark plug and a flow path between the intake ports and valves to allow for a proper cross flow cooling strategy in the cylinder head. This also provided a cooling path to and around the DI injector. Cross-sectional views of the cylinder head are shown in Figure 59 and Figure 60.

Section View – Valve Center

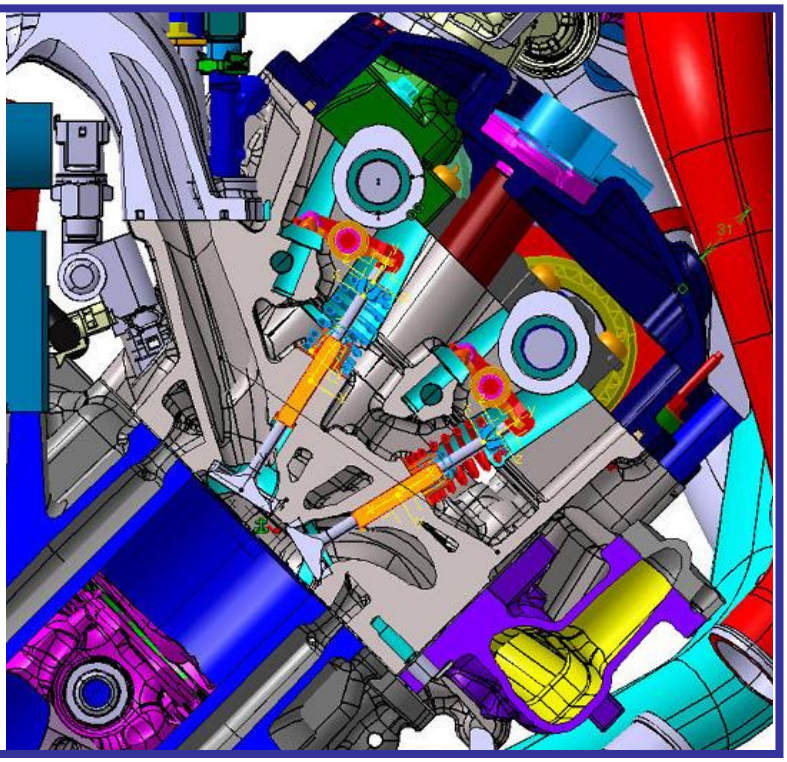

Features

-Valve Location c/o Production PFI

-Modified Valve Size for Bore 88.5

-Tumble Port

-Water around Exhaust Port and Spark Plug

Figure 59 - Cross-sectional view of cylinder head showing valvetrain.

Section View – Injector – Spark Plug

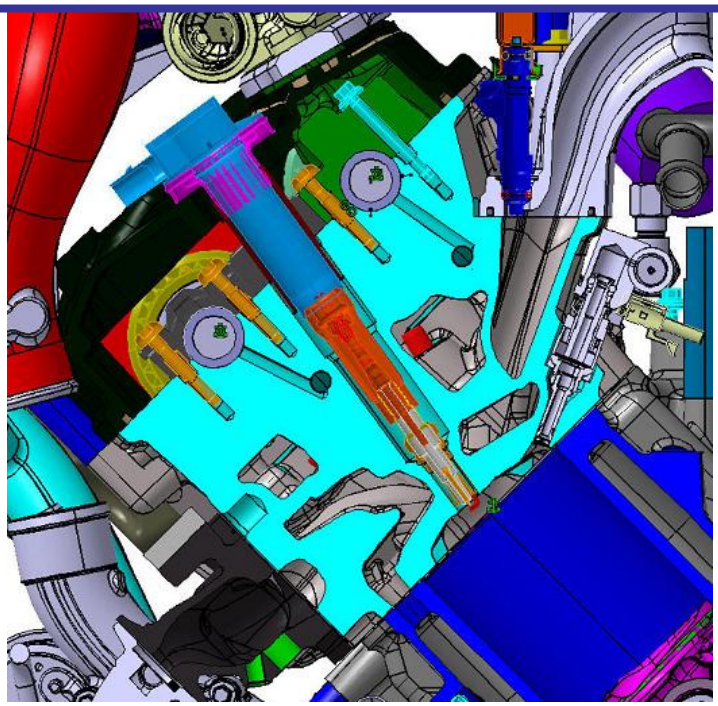

-Low Water Jacket

-Injector Close to Intake Port

-Cooling on Top Side of Injector

Figure 60 - Cross-sectional view of cylinder head showing DI injector and spark plug.

To achieve the desired cross flow and balance of coolant through the head, the water/coolant mixture is fed up from the cylinder block into the exhaust side of the cylinder head through metered holes in the head gasket. On the intake side, three exits were provided that could each be tuned for the desired flow rates across the cylinders and front to back. The front two outlets feed into a log manifold to the radiator in the front. The rear exit also leads to the radiator. As shown in Figure 61, the resulting temperatures in the cylinder head combustion chamber were very well controlled and near the targets of approximately 245-250°C.

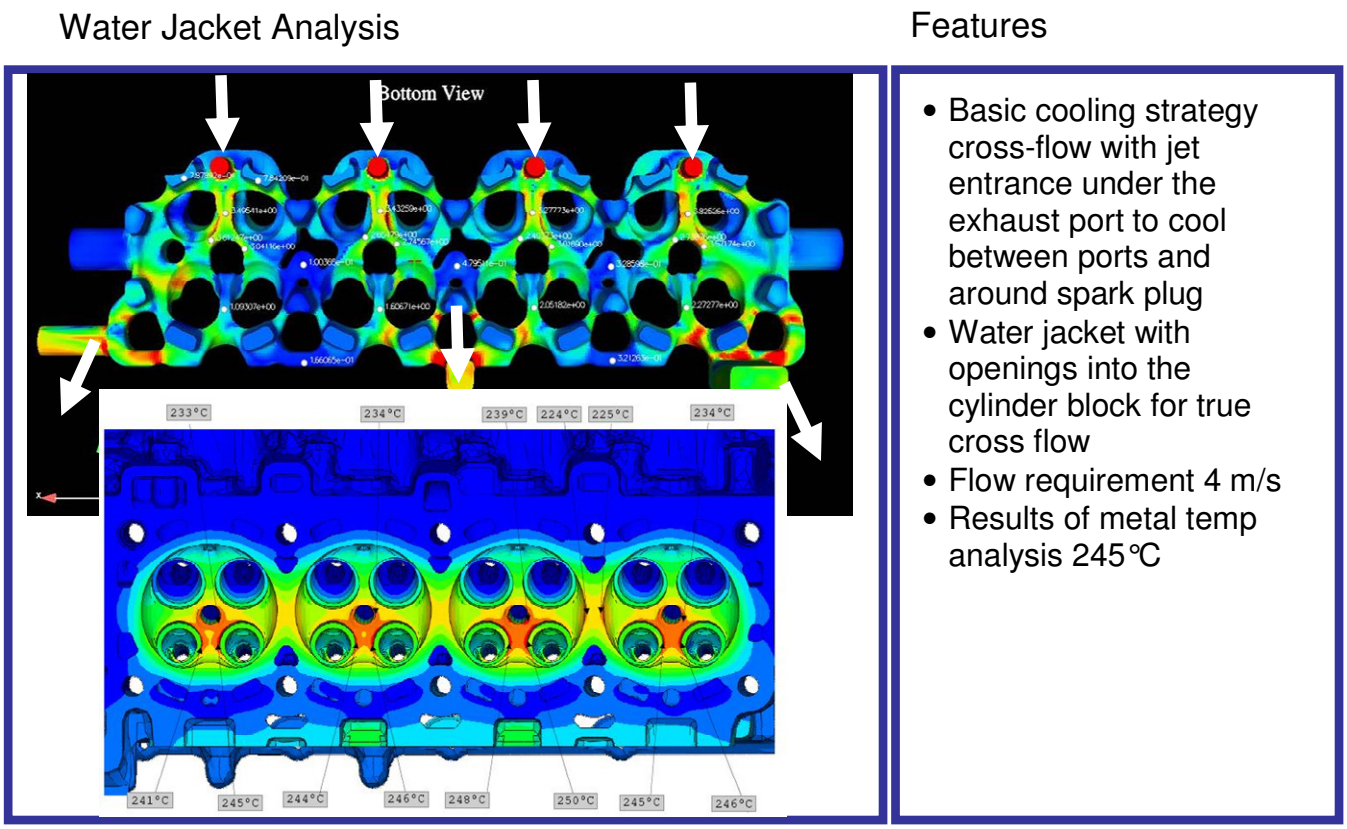

Figure 61 - Cylinder head water jacket analysis.

Valvetrain Design

Valvetrain geometry was carried over from an existing natural aspirated base engine design. However, due to ethanol fuel and boosted operating conditions, some valvetrain components were upgraded. Below are the components that were customized to meet the requirements of the boosted E85 engine.

- Valve spring
- Intake valves
- Exhaust valves, sodium cooled
- Exhaust seat insert
- Intake seat insert

Valve Spring

In order to overcome the typical high exhaust manifold backpressure waves from blowdown events, it was necessary to increase the exhaust spring installed load. This ensures the exhaust valve remains in the closed position on the camshaft base circle under higher exhaust backpressure.

Valves

The intake valve was optimized for air flow, and to be robust to E85 and rigid to cylinder pressure. The valve body was nitrided for E85 application. The valve head geometry was modified to withstand high in-cylinder pressure and ensure minimal valve head flexing.

The exhaust valve head diameter was also optimized to maximize the blowdown and scavenging processes. Since the exhaust valve is exposed to high gas temperature, in excess of 950℃, the stem was filled with sodium liquid. This is to dissipate heat from valve throat to stem preventing low cycle fatigue failure.

Valvetrain Dynamics Analysis

In addition to the upgraded components, valvetrain dynamics analyses were performed to predict key valvetrain performance metrics. A multi-body dynamics model was constructed by AVL based on the camdrive system shown in Figure 62 to evaluate the unique cam profiles optimized for E85.

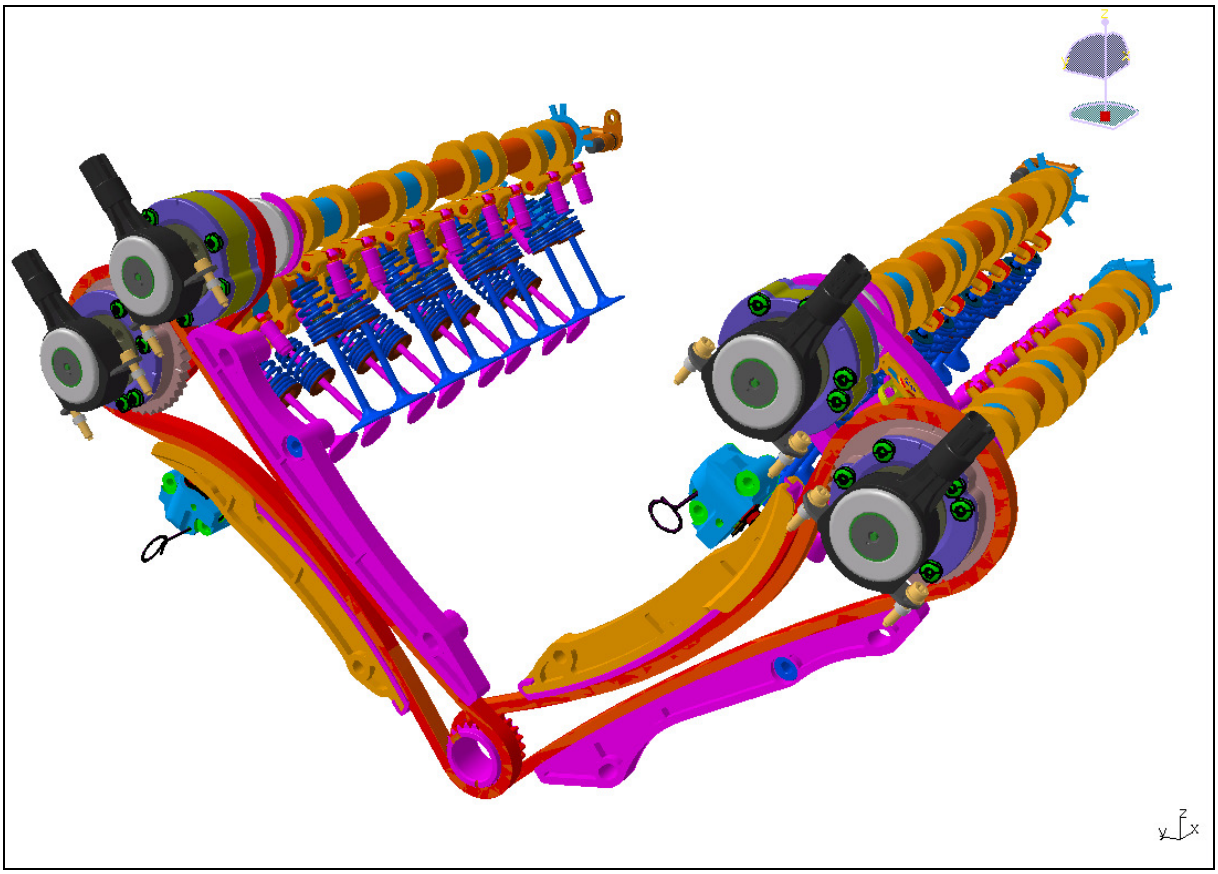

Figure 62 - Cam drive system.

Cam contact stress

Cam contact stresses were calculated for the right bank valvetrain configuration with and without cylinder pressure. In all cases, contact stress values are lower than maximum recommended design limits for both exhaust and intake valves, with and without gas pressure.

Valve seating velocity

The maximum seating velocities of exhaust and intake valves from 1000 to 5900rpm without cylinder pressure and with maximum values were calculated. In all cases, valve closing velocities are lower than the maximum allowable value.

Contact Loss

Contact loss between cam and roller finger follower is considered one of the most important durability criteria for valvetrain. Contact forces were calculated and no zero contact forces between the cam and its follower both with and without cylinder pressure were found. Therefore, no separation is expected between cam and follower.

Valve Consumed Life Prediction

Fatigue life of intake and exhaust valves was calculated based on estimated cylinder pressure and temperature. Figure 63 shows their predicted consumed life at the end of a 500 hr accelerated durability cycle. Based on this analysis it can be concluded that the valves are designed to withstand the mechanical and thermal loads. This analysis did not consider the wear and lubricity of valve and seat insert, but this was discussed earlier regarding their material selection.

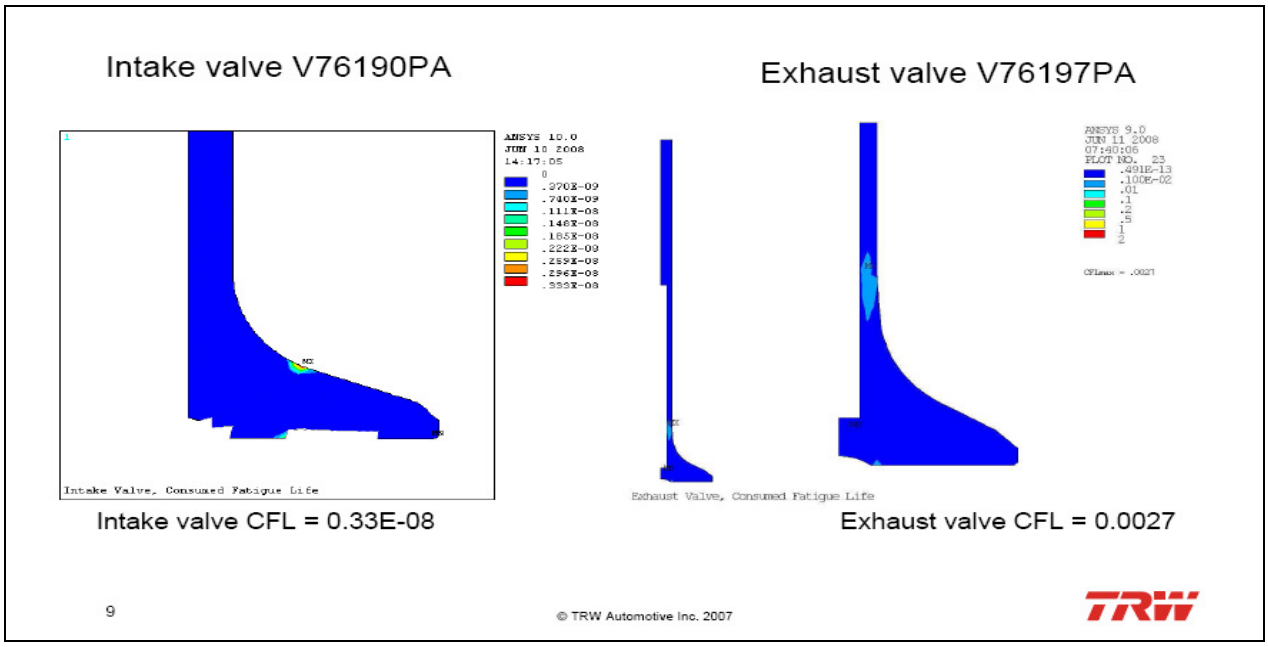

Figure 63 - Intake and Exhaust Valves Consumed Life.

Task 2.0 – Air System

The initial air path system includes conventional single scroll turbochargers mounted directly to log style exhaust manifolds on both sides of the engine. For packaging in the vehicle, the turbocharger locations are directly below the manifolds and tucked up tightly to the cylinder block. Proper attention was paid to the inlet and outlet plumbing for best air flow and for proper oil draining of the turbocharger center sections back to the oil pan. The exhaust manifold design features are shown in Figure 64.

Gen I Exhaust Manifold Design

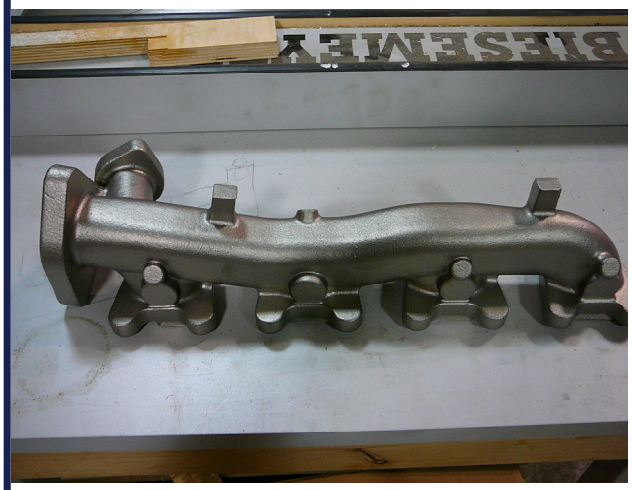

Design Features

- Log style manifold, packages turbos in conventional side locations
- Cast stainless steel capable of 1050°C operating temperature
- New high pressure casting process by WesCast produces high quality surface finish; potential to eliminate spot face machining for attachment bolts
- Three-bolt configuration per cylinder port
- Two-bolt and V-band clamp attachment features for turbochargers
- Two-bolt flange EGR take-off provision
- Cast bosses for heat shield mounting
- Incorporates cast bosses for thermocouples and pressure transducers
- Optimized design through GT-POWER and CFD analysis

Figure 64 - Exhaust manifold design features.

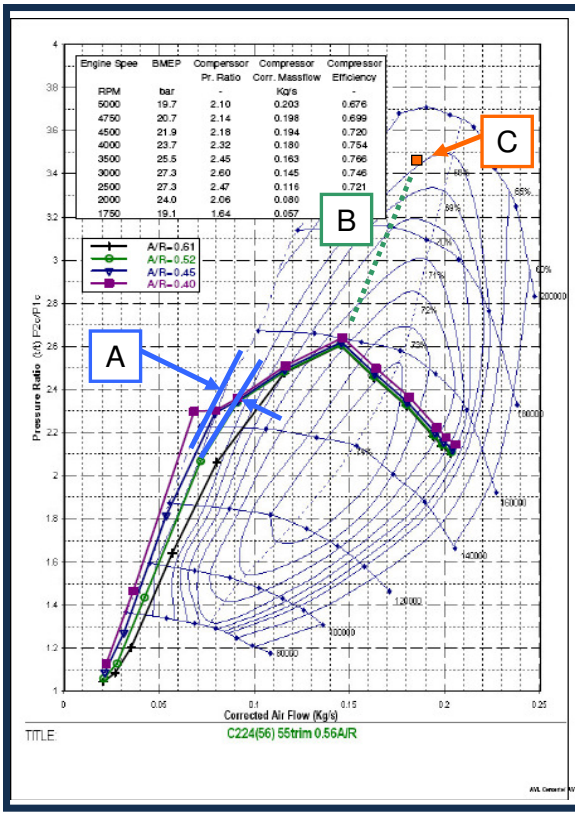

Compressor Stage
Honeywell GT2056 T55 0.56A/R

- Analytical Surge Margin ~ 13 %
- Estimated Altitude Capability ~ 10,900 ft
  Assumes 2% speed increase per 1000 ft altitude increase.
  Analysis conducted @ sea level.
  Maximum predicted turbo speed = 160 krpm
- 195 krpm turbo speed limit (compressor limit)
- Compressor bypass integrated into CAC outlet. Initial compressor out temperature predicted to be 170°C. Bypass valve operating temperature limited to 140°C. Initial compressor out temperature prediction based upon cold pipe temperature rise of 30°C (assumed hot air recirculation). More probable assumption when operating under full boost conditions would be 3°C temperature rise, from air filter to compressor inlet, similar to other programs.
- PWM wastegate control valve integrated into turbo compressor inlet tubes.

Figure 65 - Compressor map and design considerations.

Multiple compressor and turbine designs were analyzed to achieve the best balance of performance attributes for the engine. The compressor map and design considerations for the turbochargers are shown in Figure 65. Symmetry was kept as much as possible from side to side to avoid system imbalance. The compressor outlets feed upwards to twin intercoolers mounted over each valve cover. The outlets from the intercoolers then connect via a Y-section to feed the throttle body and intake manifold. The layout of the turbochargers and intercoolers is shown in Figure 66.

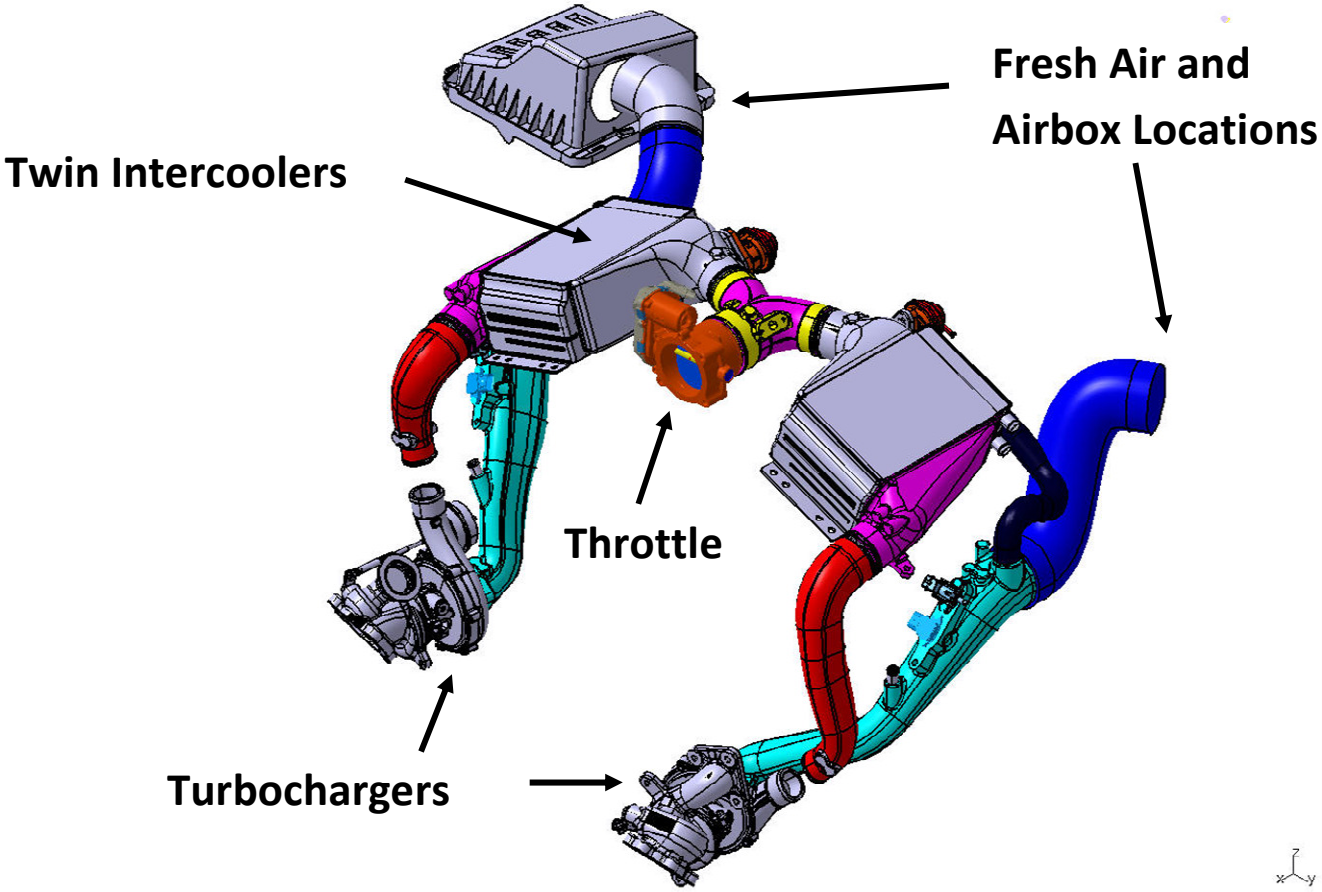

Figure 66 - Twin-turbocharger system.

A front feed intake manifold would be prime choice for a production design. This would provide for minimal package space and optimal air flow. For the prototype engines, a rear entry manifold to feed the intake runners was developed, and an additional inlet elbow was added for potential later introduction of EGR gas. The length of the inlet was chosen to allow for at least 200 mm for proper mixing of the EGR gases with fresh charge air. This first generation design of the intake manifold is shown in Figure 67.

Extensive modeling and analysis was performed on the design of the intake manifold. A full sweep of intake runner length and diameter was evaluated in GT-POWER to find the optimum combination for best BMEP and BSFC. For the 2000 rpm point, runner length and diameter had minimal effect on BMEP. However, longer runners showed a small but continual degradation in BSFC due to increased friction. For improved packaging and best balance, 122 mm long and 44mm diameter runners were selected. CFD was also performed to optimize the geometry for best flow and a 1D-3D analysis was done to evaluate firing order and wave dynamic effects.

Results from the 1D-3D analysis showed an imbalance in volumetric efficiency across the engine with cylinders 2 and 8 being noticeably lower for the case shown. The design of the cold air side was reviewed, including air

entry conditions and the CFD results, and no issues were found. The exhaust residual fraction was then evaluated for each cylinder. Due to the sequential firing order of cylinders 1 and 2 on the left bank and cylinders 6 and 8 on the right bank, the trapped exhaust masses are higher for cylinders 2 and 8. The high pressure pulse in the exhaust manifold from the previous firing cylinder during blowdown affects the backflow of exhaust gas into these cylinders during the overlap period. This phenomenon is known as "blowdown interference" and is discussed in detail later in this report.

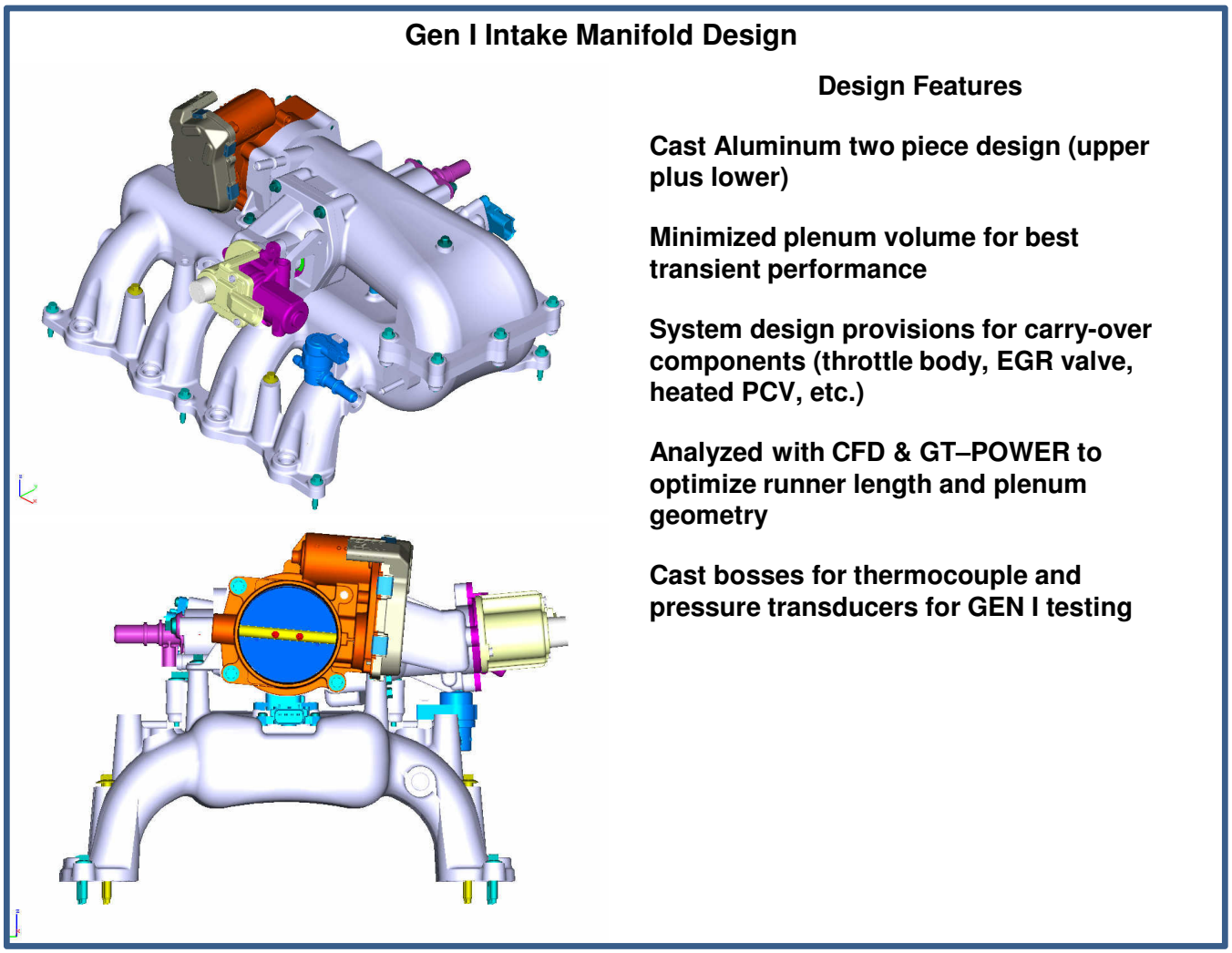

Figure 67 - Generation 1 intake manifold design and features.

Several alternative designs were considered to minimize this imbalance effect due to the V8 firing order. Cam strategies were investigated as well as various turbocharger and exhaust manifold configurations. One of the options that was tested and then chosen as the prime design was a split 2+2 exhaust manifold and twin scroll turbochargers. The early fabricated manifold and twin scroll turbocharger for the right bank is shown below. Cylinders 1 and 3 are paired together and separated from cylinders 2 and 4.

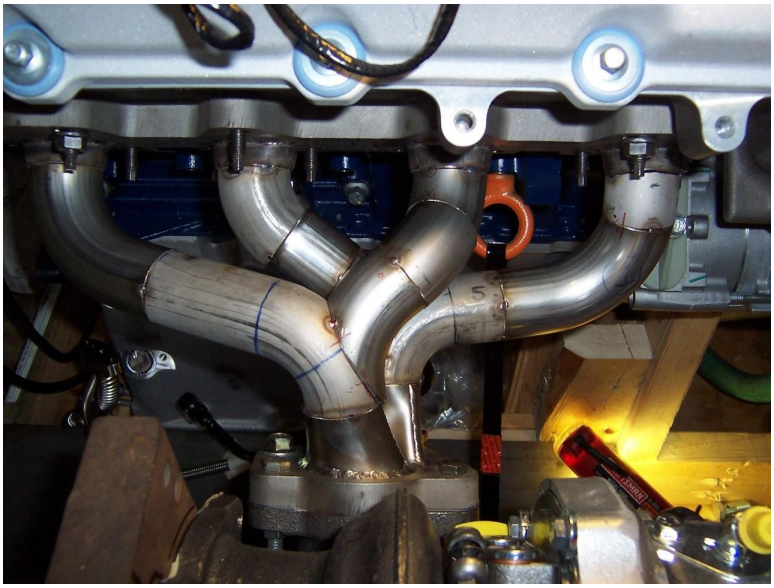

Figure 68 - Right bank exhaust manifold for twin scroll turbocharger.

After initial success when testing this new configuration, more robust cast stainless steel twin scroll manifolds were designed and procured. These new designs incorporated bosses for instrumentation and underwent several temperature and stress analyses to ensure longevity on the engine dynamometer (Figure 69 and Figure 70).

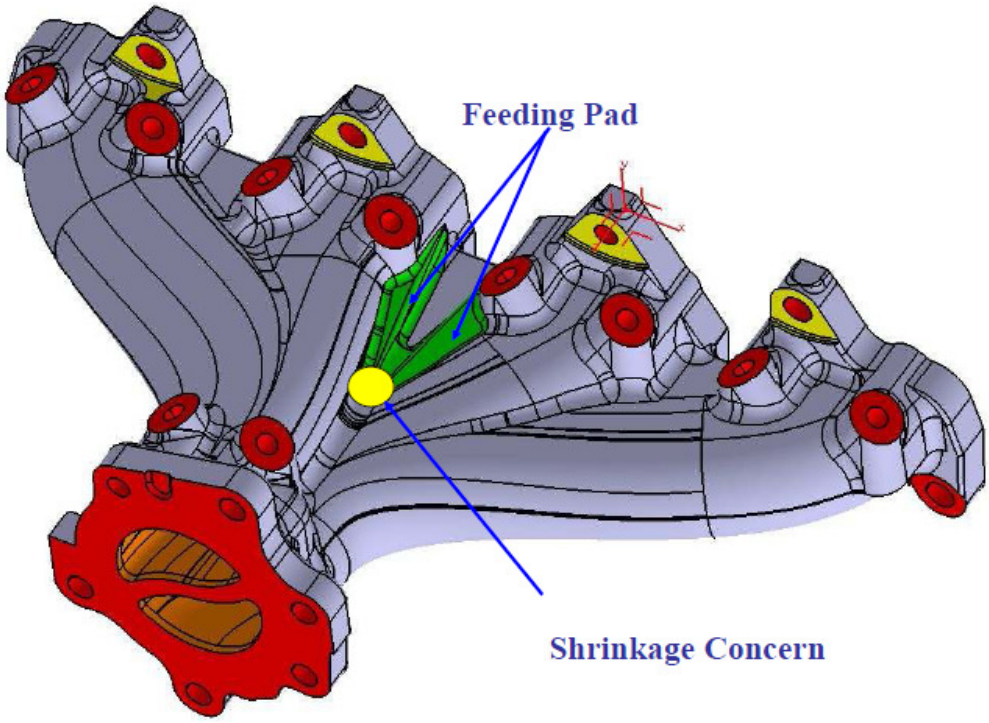

Figure 69 - Cast stainless steel exhaust manifold for twin scroll turbocharger.

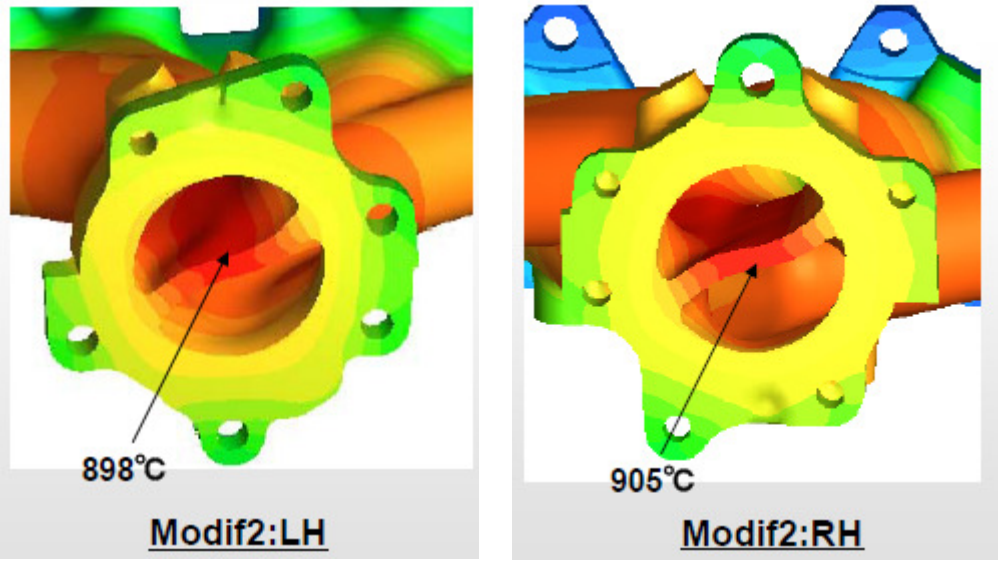

Figure 70 - Thermal analysis of exhaust manifold at twin scroll turbocharger inlet.

Task 3.0 – Fuel System

Placement of the DI injector for this engine was a critical design decision with the options of central or intake side location. A central injector location would be required should the engine need to operate in a stratified combustion mode for lean burn operation. However, the central location is the hottest location for the injector and the location that is most problematic in terms of packaging an adequate coolant jacket around the injector and spark plug, compounding injector packaging and cooling issues.

DI injector cooling was considered an important consideration for this engine, not only because of the high specific torque targets, but also because under the Dual Fuel operating regime fuel flow to the DI injector would be shut off at part load with fuel supplied by the PFI injector only. GDI injectors are temperature limited to reduce fouling, which can deteriorate spray, and rely on fuel flow through the injector to cool the injector tip, lubricate the tip, and ensure long term mechanical durability. Prior results have shown that operating conditions around mid-speed, light-load result in the hottest injector tip temperatures. At these conditions fuel flow through the injector is low relative to combustion temperatures and under Dual Fuel operation all fuel would be delivered by the PFI injector with zero flow through the DI injector.

To minimize cost, complexity, and increase migrateability, the decision was made to package the injector on the intake side. This location satisfied all current performance and emissions requirements with minimum risk to injector durability and tip temperature concerns.

The DI injector was packaged in the cylinder head with the tip located between the intake valves (Figure 72). The body of the injector was inclined to the gas face which was a satisfactory position to provide a 360° water jacket around the injector with a well-targeted fuel spray and minimum impact on the intake port. As the cylinder head and intake port design evolved, a requirement to reduce the installed injector angle was adopted to facilitate removal of the injector. This modification had no impact on injector spray targeting as the spray could be retargeted in the new position; however this compromised injector cooling as it closed off the area under the injector required for cooling underneath the injector body. Injector tip temperatures measured on the running engine are shown later in this report (page 88).

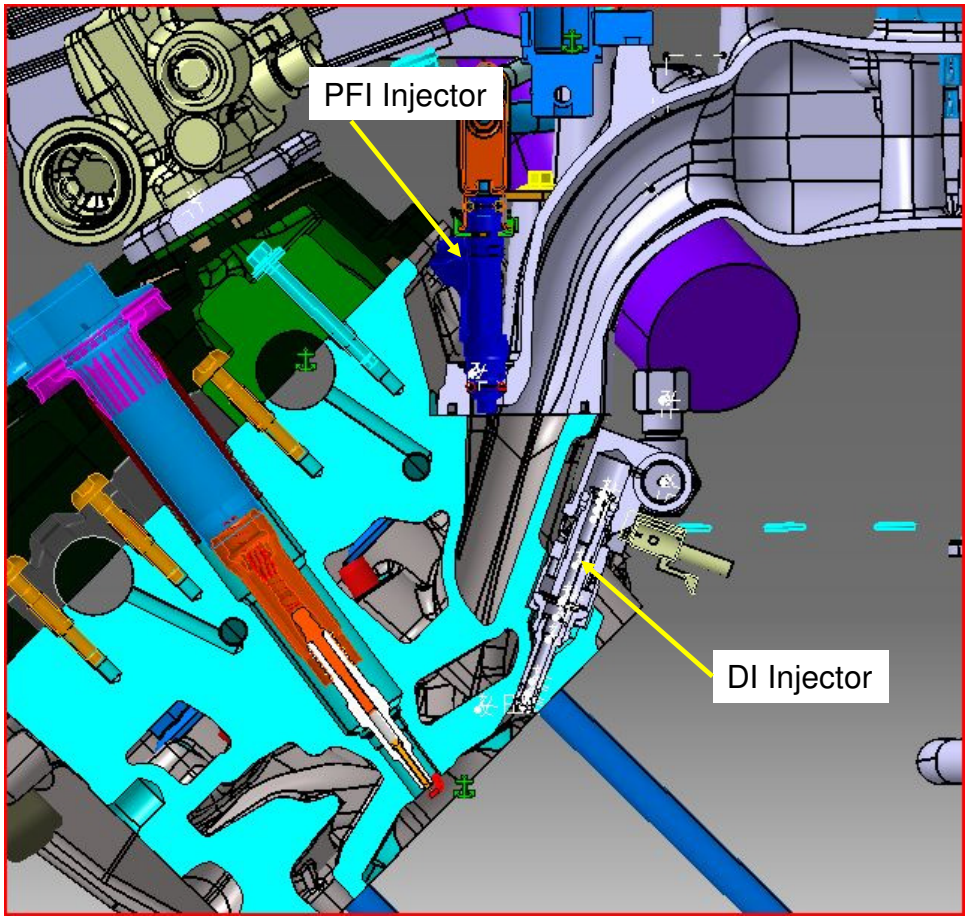

Figure 71 - Cylinder head and intake manifold cross-section showing location of PFI and DI injectors.

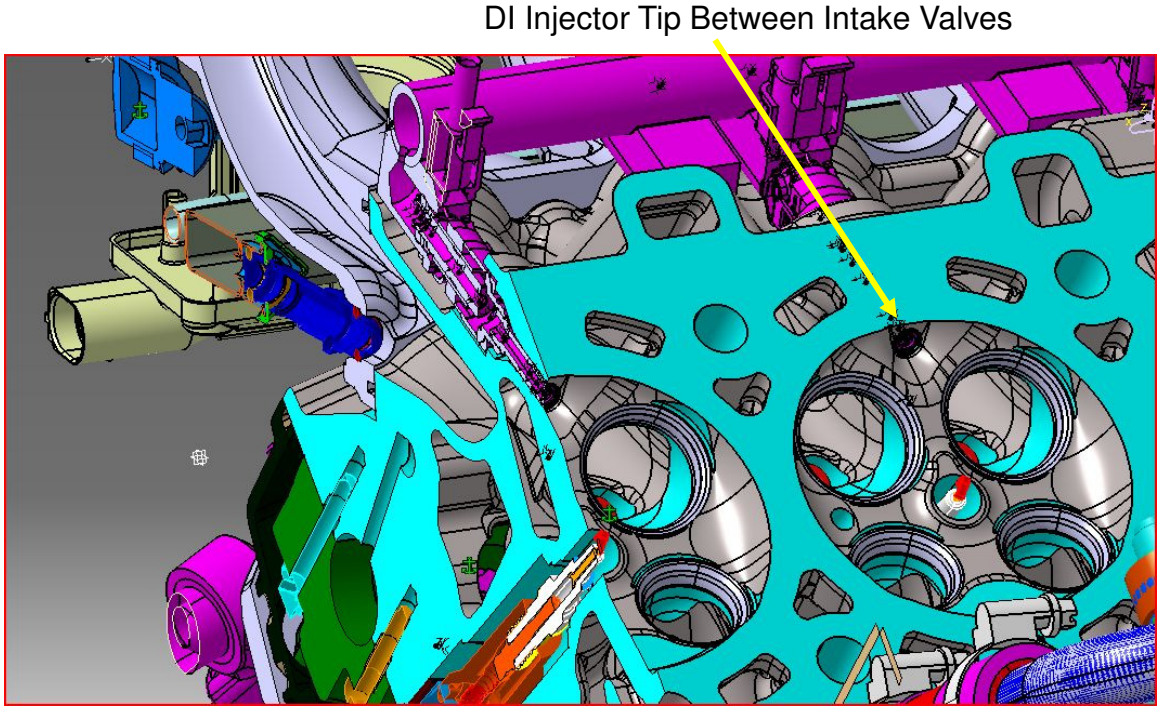

Figure 72 - Location of DI injector tip in the combustion chamber.

Injectors were sized using the maximum permissible injection duration under peak power conditions and the minimum injector duration required for idle operation. Sizing must ensure the injector operates in the linear region of its flow versus pulse width duration curve at all conditions with a high degree of cycle-to-cycle repeatability. The number of injector holes was optimized for the specified flow rate to maintain required L/D (L=length of each injector hole, D=hole diameter) limits which influences atomization and penetration.

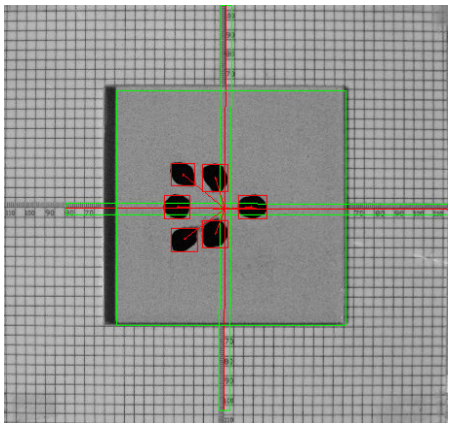

Spray Pattern & Targeting

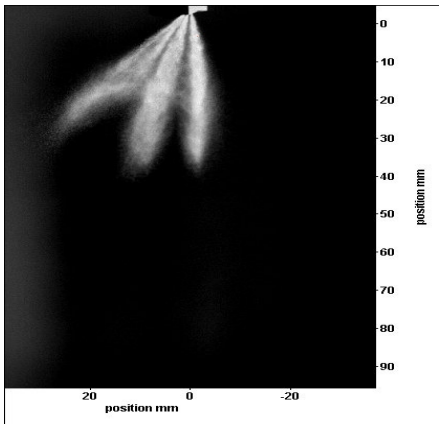

Atomization & Penetration

Figure 73 - DI injector spray characteristics.

Injector sprays were designed by AVL based on knowledge and experience gained from many other GDI programs and injector spray development in CFD and optical single cylinder engine and conventional engine development work. Two injector sprays were designed with variations of spray targeting based on two recent and similar other engine programs where the injectors had performed very well. The fuel injector supplier also provided an injector design derived from applying their standard methodologies.

Piston bowls were designed to work in combination with these injectors to support very late ignition timing for catalyst heating by creating a rich mixture at the spark plug with a split injection strategy. The piston bowl was designed to be as open as possible so as not to negatively impact normal homogenous combustion by hindering flame propagation.

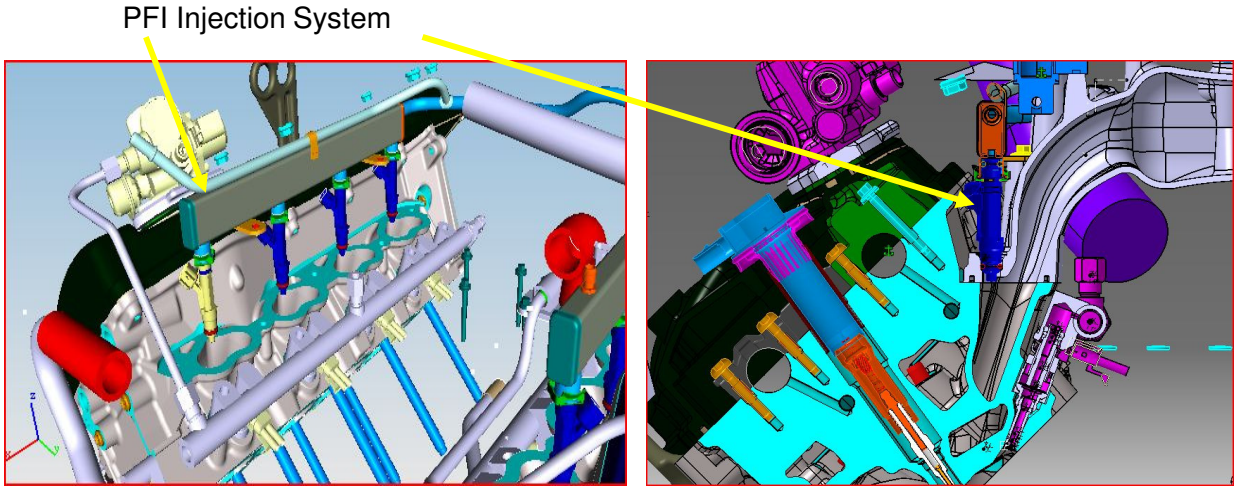

Figure 74 - PFI injection system.

PFI injector flow rate was influenced by Dual Fuel operation where it would operate at light load with the DI injector shut off. The PFI injector would contribute less than 50% of the total fuel requirement at full load where

the DI injector would deliver the majority of the fuel. The PFI injector specification, defined by assuming a maximum flow of half the total fuel flow at peak power, helped bias the PFI injector to a lower flow rate to improve fuel flow control at idle. A PFI spray pattern was selected from the range of available production injectors to target closed intake valves with a wide spray angle for best spray quality while minimizing port wetting. These initial 'off the shelf' injectors were used for the single cylinder development. Customized injectors were specified and optimized for the multi-cylinder engine. Location of the PFI injector is shown in Figure 74.

Fuel pump options were reviewed in terms of fuel flow requirements, pressure requirements, and ethanol compatibility. Three pumps that met the functional requirements were identified: a six-piston radial pump, a dual piston plunger pump, and two single piston plunger pumps. The two single piston plunger pumps mounted on the cam covers and driven by an additional lobe on each cam were chosen (Figure 75).

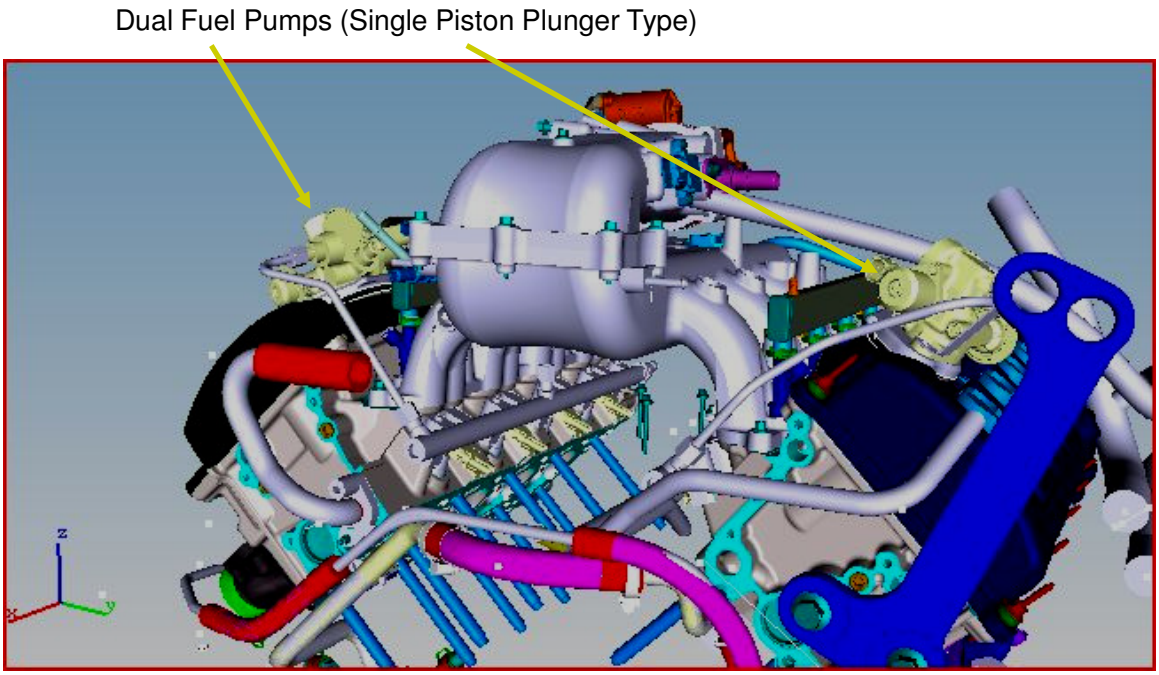

Figure 75 - Dual fuel pumps mounted on cam covers.

Task 5.0 – Multi-Cylinder Engine

Lower End

The lower end design was based on Ford's Modular V8 architecture. A careful study was undertaken to understand the design requirements, packaging space, and materials needed for each component in the system.

Design changes required with increasing cylinder pressure were assessed. The engine was expected to produce output torques over 100% greater than the naturally aspirated production version. Every major structural component had to be completely redesigned. The design target was chosen to be 150 bar peak cylinder pressure to allow for greatly improved spark advance and volumetric efficiency when running E85.

Cylinder Block

As mentioned, the cylinder block layout was based on Ford's Modular V8 architecture. Cylinder bank offset, head bolt pattern, deck height, and front and rear face of block planes are unchanged. However, much of the

rest of the cylinder block was modified significantly. Head and main bolt fastener sizes were increased for proper clamp loads at the higher cylinder pressures.

Compacted graphite iron (CGI) was chosen for the block material to handle the increased firing loads, to improve durability for the truck segment, and to minimize weight. A few new features were added to enable a much improved cooling system and revised cooling circuit. A pair of cooling logs were cast along the intake side of both cylinder banks to accept water out from the cylinder heads and provide for the desired cross flow through the head. A twin thermostat housing was added at the front of the block that would allow for a greater amount of coolant flow at minimal system restriction. The front water pump cavity was redesigned in conjunction with a new water pump to provide up to 150 gallons per minute (gpm) flow rate versus 96 gpm in the current production engine. All of the water jackets in the block were redesigned using CFD for optimum cooling and reduced metal temperatures. Design features of the cylinder block are shown in Figure 76.

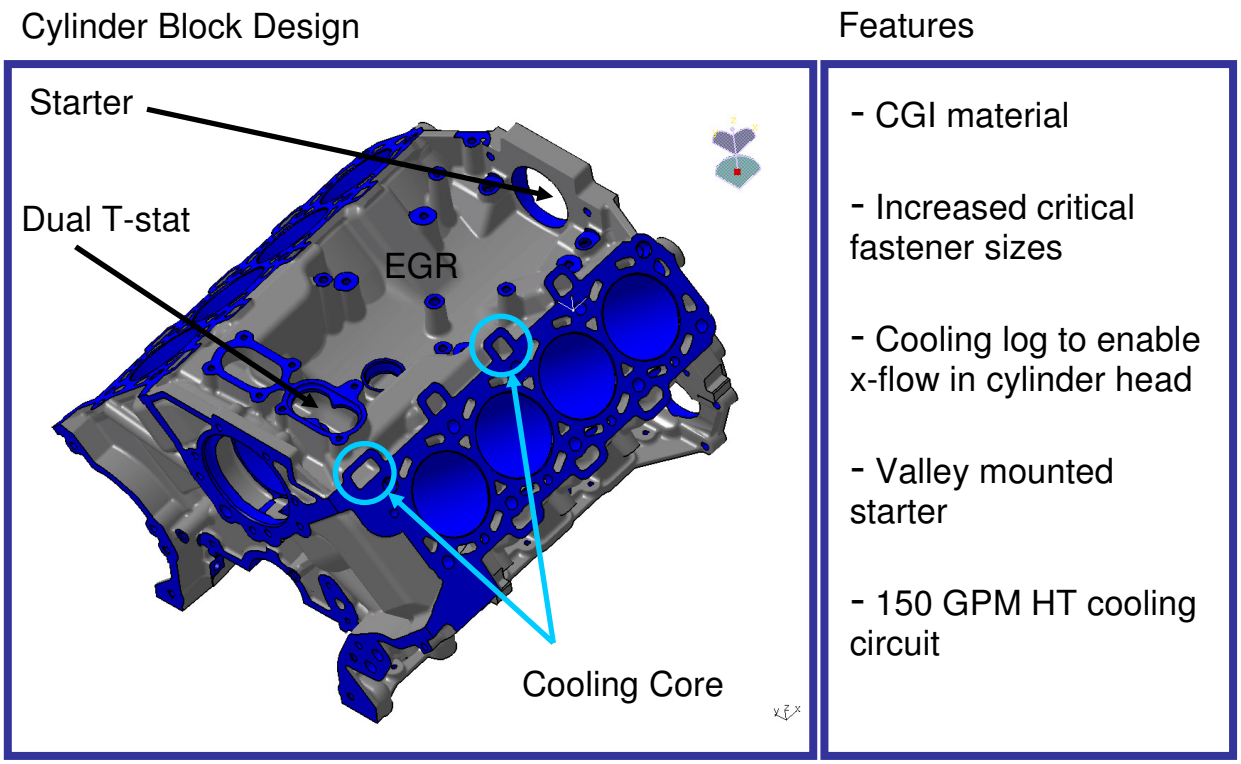

Figure 76 - Cylinder block design features.

FEA analysis was use to optimize the stresses in the 6 bolt main bearing cap design (Figure 77). A nodular iron cap was designed and the inner main fasteners increased from 10mm to 12mm diameter. The load paths to the cylinder head were also analyzed and the head bolts increased from 11mm to 13mm for proper clamp load on the gasket.

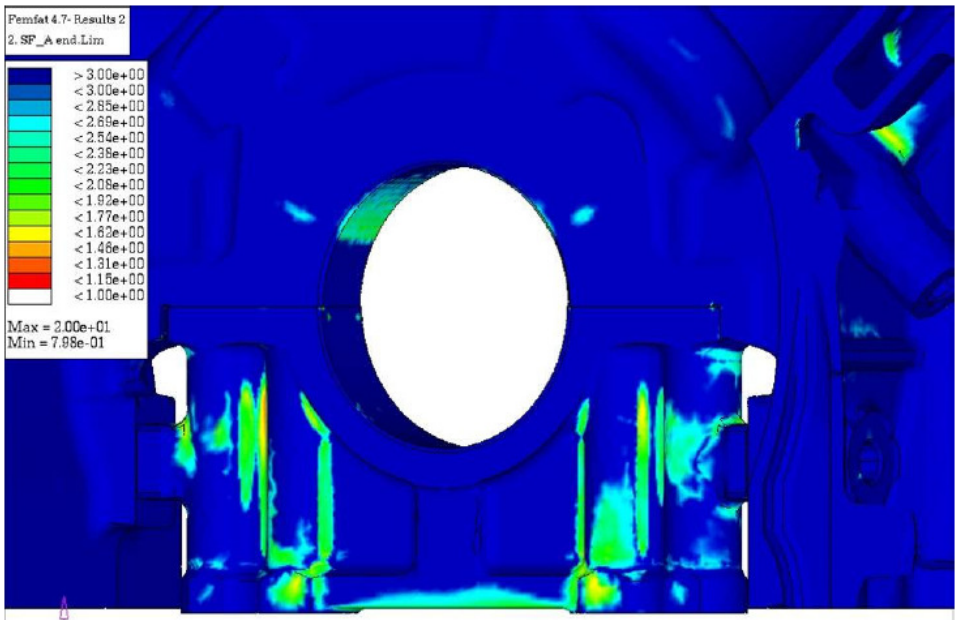

Figure 77 - FEA of main bearing cap.

Crankshaft

The crankshaft design was also new. An 8 counterweight design was chosen in order to minimize the main bearing loads. Due to the increased masses of the new piston and rods, full internal balance of the crankshaft was not possible. The new design has external balance in the crank damper and flywheel. The original production crank diameter was maintained which allowed the main bolt centerlines to remain constant for manufacturing. The bearings were widened slightly for proper oil film thickness under maximum loads. In order to increase the crank durability and stiffness, the rod journals were increased in diameter. This increased the overlap between the main bearings and rod pins. The rolling load in the pin fillets was increased and the post diameter was increased to handle the higher firing torsionals. Features of the crankshaft design are shown in Figure 78.

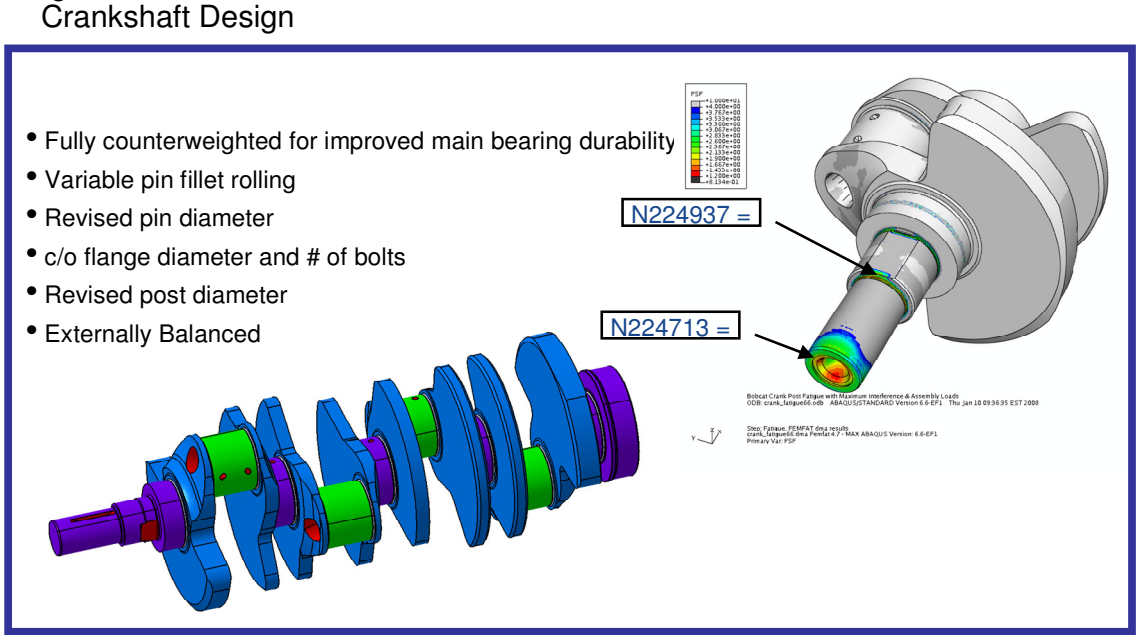

Figure 78 - Crankshaft design considerations.

Piston and Connecting Rod

A heavy duty piston and connecting rod design was utilized which incorporated features common with Diesel engines. The connecting rod is a powdered metal design, but manufactured for the program using 4340 billet steel. The 60mm diameter large end was split at a 45° angle to facilitate installation into the 88.5mm bore. The piston design incorporated a cooled oil gallery channel positioned behind the ring pack for heat removal from the piston top. A tubular oil squirter was designed for each cylinder aimed at a target entry hole into the gallery. An exit for the hot oil was provided on the opposite side. To withstand the high firing pressures, a high grade cast eutectic aluminum alloy was chosen and a Ni-ring insert was used for the top ring. A full stress and temperature analysis was performed by the supplier to ensure durability. Design features of the piston and connecting rod are shown in Figure 79.

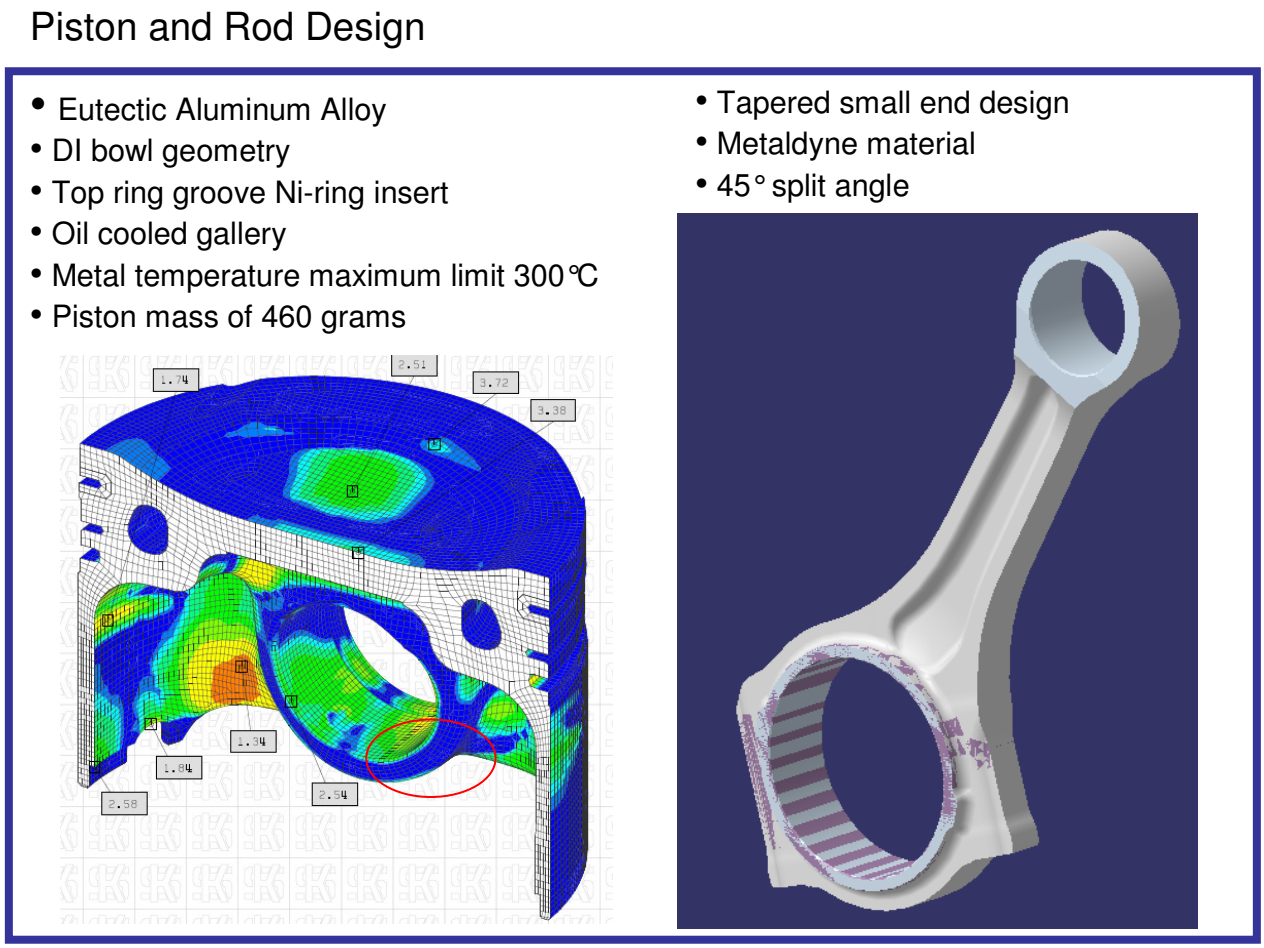

Figure 79 - Piston and connecting rod design features.

Engine Cooling

The engine cooling system was designed to meet the requirements of the 5.0L engine at worse-case, customer engine operating conditions. The cooling system has two loops, a High Temperature Loop (HTL) and a Low Temperature Loop (LTL). The HTL supports the base engine, oil cooler, twin-turbochargers, and vehicle heater core. The LTL supports the charge-air-coolers and transmission oil cooler. A schematic of the cooling system is shown in Figure 80.

The cooling system design and development was conducted using classical cooling system 1-dimensional and 3-dimensional analysis. The overall engine heat rejection requirements at the different engine operating conditions were determined using the engine energy balance method. A 1D flow network including the entire

cooling system was developed to generate the overall flow and pressure distribution input for CFD analysis. A 3D CFD analysis was conducted on the water pump to generate the inlet velocity profile to the cylinder block and head. Using the output from the water pump and 1D analysis, a 3D CFD analysis was conducted on both the right and left banks of the engine block and head to predict the flow distribution, overall total pressure drop across the engine, and gasket hole sizing strategy.

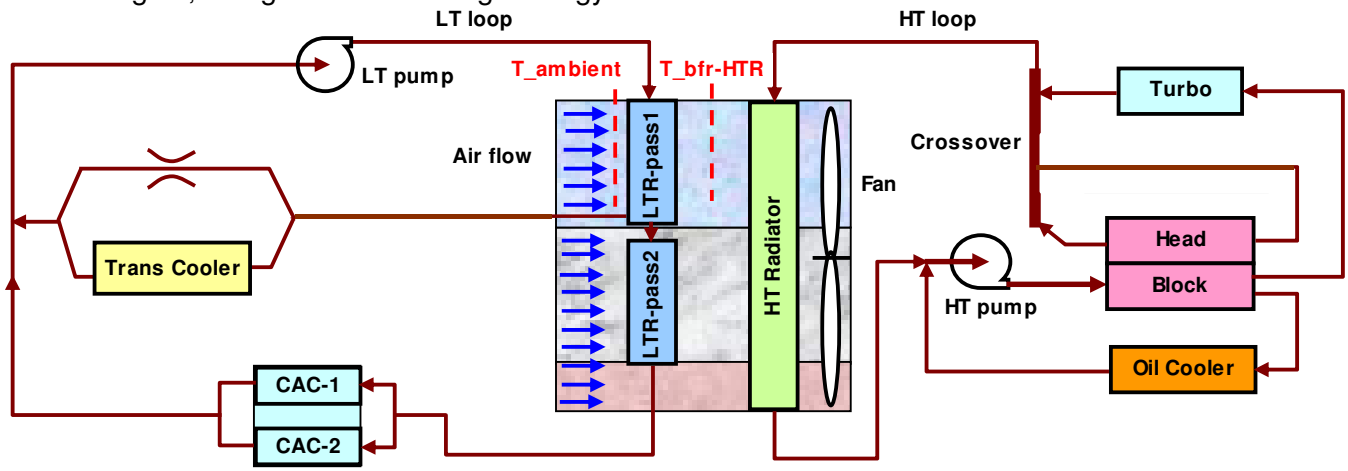

Figure 80 - Cooling system schematic.

The following cooling system assumptions were made:

- HTL water pump with dual layer impeller blades at 96mm diameter , carryover modular V8 engine location
- FEAD driven (150 GPM at rated engine speed)
- LTL water pump, with carryover impeller, housing integral with front cover, FEAD driven (24 GPM at rated engine speed)
- Hot side (exit), dual thermostat for flow requirements
- Front crossover internal to block with integrated thermostat housing
- Two external rear crossovers: block; bank to bank, cylinder head; right to left
- New heater core supply and return tubes
- Coolant: G0-5

Targets

Figure 81 and Figure 82 illustrate the engine target torque curves and power curves, respectively. The cooling system is design to support the worse-case in all three torque curves.

- GTDI:
  - 450 hp @ 4750 rpm; 500 ft lbf @ 1750 ~ 4500 rpm (17 bar BMEP)
- ETDI:
  - 550 hp @ 4750 rpm; 650 ft lbf @ 2000 ~ 4500 rpm (22 bar BMEP)
  - 550 hp @ 4750 rpm; 800 ft lbf @ 2500 ~ 3000 rpm (27-bar BMEP)

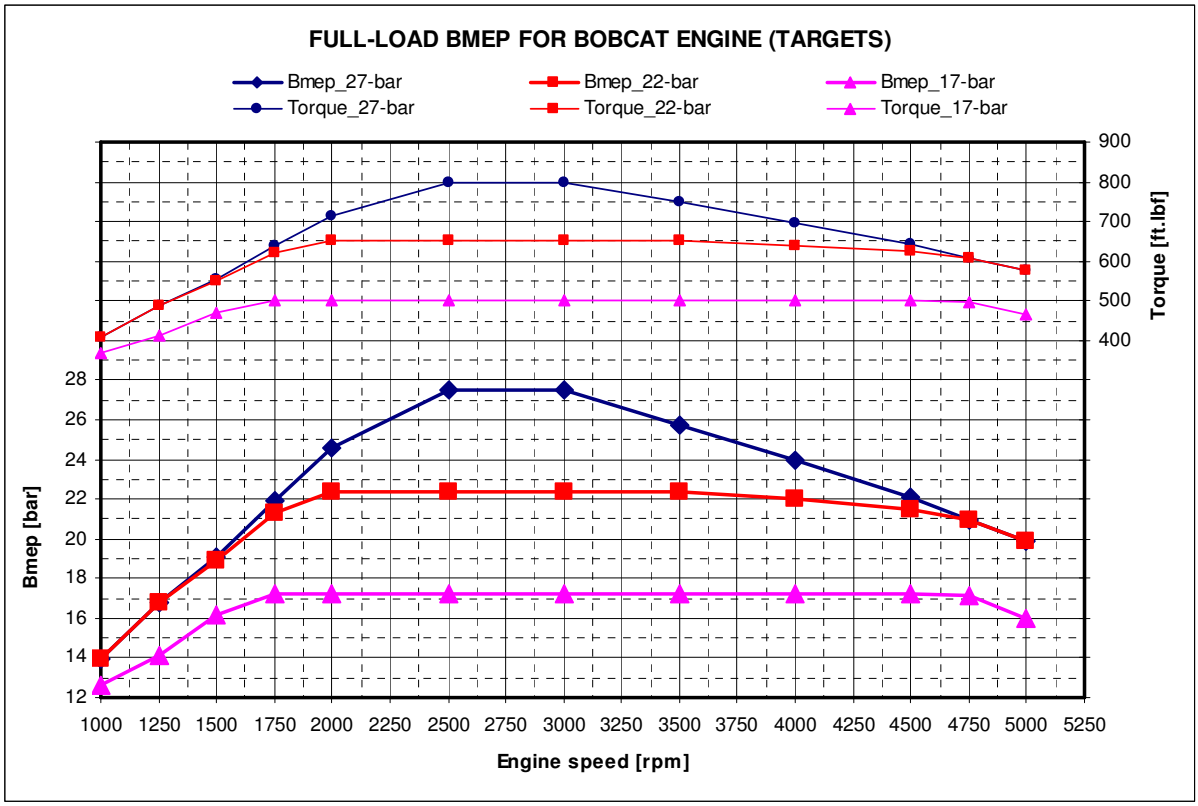

Figure 81 - Engine torque curve used for cooling system design.

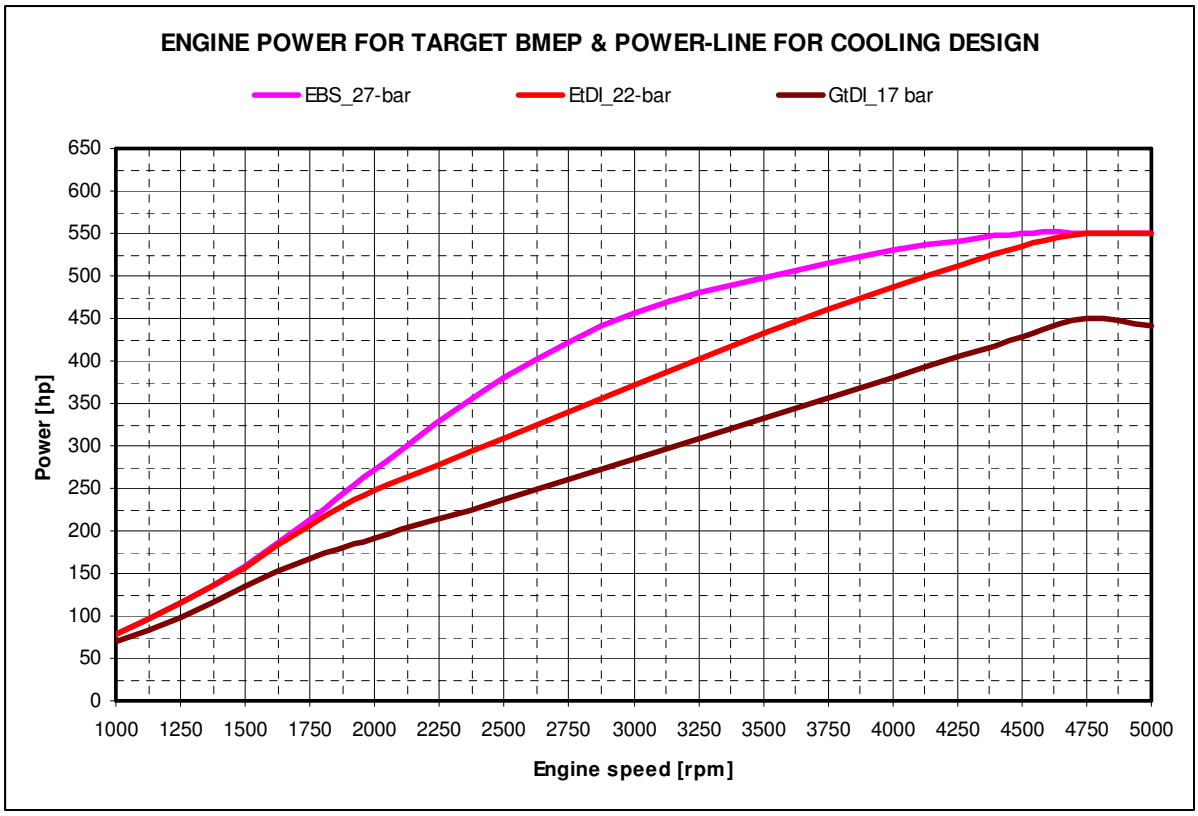

Figure 82 - Engine power curves used for cooling system design.

Predicted Engine Heat Rejection

The engine heat rejection is calculated using the following assumptions:

- Engine cooling on based on specific cooling load from reference GTDI engine test data
- EGR Cooler: ENSA U-flow for EGR
- DANA Charge-Air-Cooler
- 25°C ambient

Predicted HT/LT Pump Flows

Coolant flow targets are set for the worse-case condition for the various components.

- Required coolant flow for the engine is governed by Dual Fuel (max ΔT across engine ≤ 10°C).
- Required coolant flows for the oil cooler and charge-air-coolers are governed by Dual Fuel.

High Temperature Loop

The High Temperature Loop (HTL) delivers coolant to the base engine, oil cooler, twin-turbochargers, and vehicle heater core. The HTL is supported by a 180° dual-volute outlet water pump that provides 75 gpm of coolant to each bank. A symmetric cooling system has been developed to balance the engine's bank-to-bank cooling, see Figure 83. The oil cooler is fed from the crossover between the banks of the block.

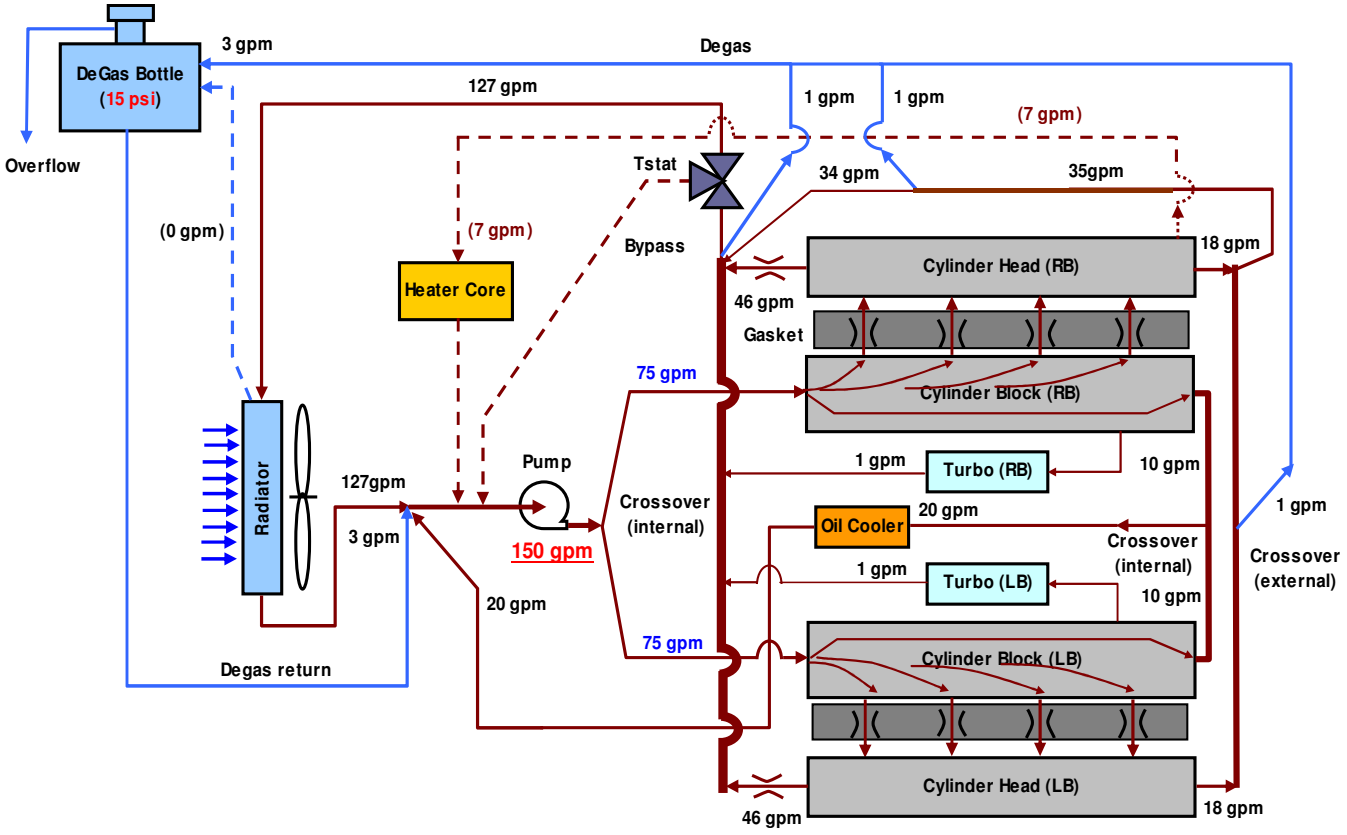

Figure 83 - High temperature loop cooling system.

Low Temperature Loop

The Low Temperature Loop (LTL) delivers coolant to the Charge-Air-Coolers, and the transmission oil cooler. The LTL has a two-pass radiator separate from the HTL radiator. A schematic of the LTL cooling system is shown in Figure 84.

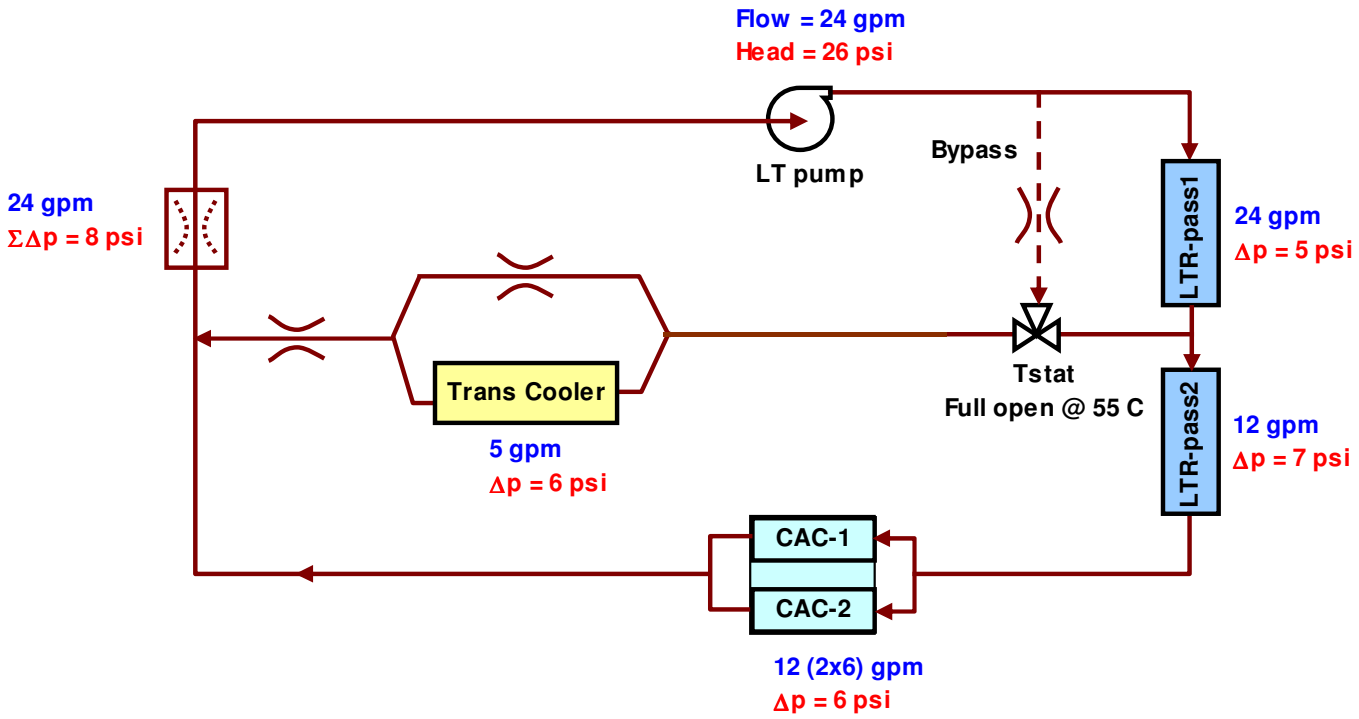

Figure 84 - Low temperature loop cooling system.

Ignition

To ensure that the ignition system was not a limiting factor, prototype hardware was procured and upgraded relative to the level typically utilized in a production GTDI application. The ignition coils used were prototype coil-on-plug with the following output as measured by SAE J973:

- Peak available voltage (into a 35pf load) = 45 kV
- Energy = 125 mJ
- Peak secondary current = 150 mA

The weakest link of the secondary ignition circuit from a dielectric perspective is the interface at the spark plug boot. This fact determined the peak available breakdown voltage. As a result, the spark plug gap needed to be very small. Initial testing was conducted with a 0.025 inch gap but at higher load operation (above ~ 700 ft lbs) it needed to be reduced to 0.015 inch. Spark plug gaps that were too large resulted in misfires.

The spark plugs used were a 14 mm (XL) conical seat design per ISO 28741. This is an industry standard design and it is utilized on most of Ford's recently designed production engines. The heat range of the plug was 425 IMEP per SAE J549. This is one HR colder than the 375 IMEP used on Ford's production GTDI applications. This colder HR is not currently considered production feasible due to the risk of spark plug fouling, but it was necessary to ensure that pre-ignition would not be a factor during testing. Historically most engine's light load stability degrades with small spark plug gaps below ~ 0.027 inch (0.7 mm). As such it is not considered production feasible given the current state of technology.

Multicylinder Engine

The multicylinder engines, as shown in Figure 85, were built at Ford's Beech Daly Technical Center in the prototype engine build area. Full measurement of all parts was completed at BDTC, Ford's Engine Manufacturing Development Operations (EMDO) center or via the supplier. All critical dimensions and interfaces were recorded such as final compression ratio, piston pin-to-bore clearance, and crankshaft end

play. The engine photo shown in Figure 86 is complete with wiring harnesses, boost system and intercoolers, and all required plumbing for hot testing. The engines are run at Ford's Engine Manufacturing and Development Operations facility prior to being fully instrumented and palletized for engine dynamometer. This ensures that there are no issues, including leaks, or mis-builds.

Figure 85 - Multi-cylinder engine with twin-turbochargers installed.

Figure 86 - Multi-cylinder engine with charge air coolers and throttle body installed.

Blowdown Interference

As part of this task, the effects of blowdown interference were investigated on the multi-cylinder engine and modeled using the GT-POWER 1-d simulation model. This work was documented in SAE 2010-01-0337[3], and this section of the report incorporates text and figures from that paper.

The issue of blowdown interference on the V8 engine is more problematic than on the I4 engine because of the V8's uneven firing interval. The cylinder numbering convention of the Ford V8 is shown by the schematic in Figure 87. In the schematic of Figure 88 [35], the cylinders are arranged from left to right 90° apart according to the firing order of 1 5 4 8 6 3 7 2 which is indicated by the solid arrows.

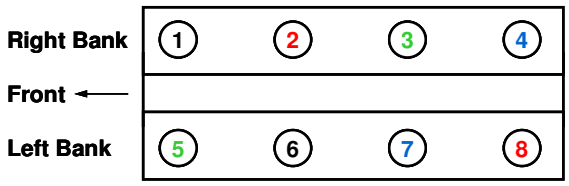

Figure 87 - Cylinder numbering convention of the Ford V8.

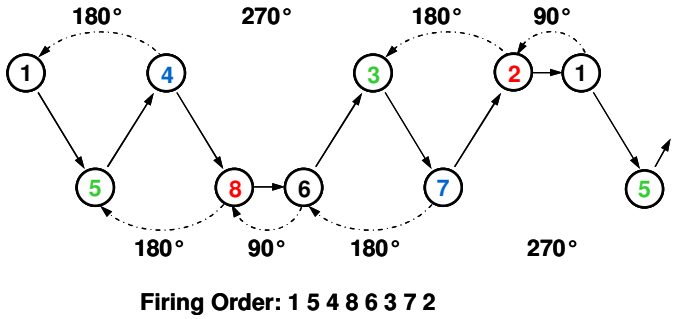

Figure 88 - Illustration of the uneven firing order on each bank of the 90 degree V8 engine.

Each bank has two 180° firing intervals, one 90° firing interval, and one 270° firing interval. Blowdown interference due to the 180° and 90° firing intervals is denoted by the dotted line arrows (the blowdown pulse of cylinder 4 interferes with cylinder 1, etc.). In Figure 87 and Figure 88, cylinder pairs (one cylinder on each bank) with identical preceding and following firing intervals are denoted by the same color: 1 & 6 (black), 2 & 8 (red), 3 & 5 (green), and 4 & 7 (blue).

Figure 89 shows the pressure measured in each cylinder's exhaust runner on the right bank of a turbocharged V8 engine at 2000 rpm, 17 bar BMEP. The pressures in the left bank manifold for paired cylinders are nearly identical. The exhaust manifolds are log style with very short runners (Figure 90) to provide for rapid turbocharger transient response. Because of the high speed of propagation of the pressure waves at exhaust gas temperature and the short travel distance in the exhaust manifold, the pressures in each exhaust runner are nearly identical at low engine speed.

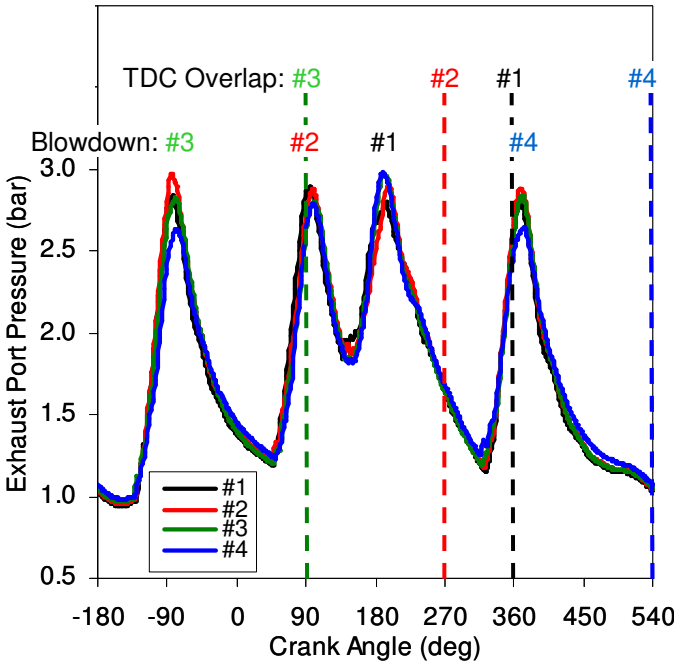

Figure 89 - Right bank exhaust pressure of V8 engine at 2000 rpm, 17 bar BMEP.

Figure 90 - Single scroll turbocharger log style exhaust manifold.

In Figure 89, the location of TDC overlap is denoted for each cylinder. As shown, the blowdown pulse of cylinder 4 occurs during overlap of cylinder 1 (at 360° crank angle). Similarly, the blowdown pulse of cylinder 2 occurs during overlap of cylinder 3 (at 90° crank angle). This is termed 180° interference since the following cylinder in the firing order is 180° CA later. Also as shown, the blowdown pulse of cylinder 1 occurs during the exhaust stroke of cylinder 2. This is termed 90° interference since the following cylinder in the firing order is 90° CA later. Cylinder 4 does not suffer from blowdown interference and has low pressure during overlap since the blowdown pulse from cylinder 3 occurs 270° CA later in the firing order, and arrives after the exhaust valves of cylinder 4 have closed. Corresponding cylinder pressure pumping loops for the right bank of the turbocharged V8 engine at 2000 rpm, 17 bar BMEP are shown in Figure 91. The pumping loops for the left bank paired cylinders are nearly identical.

Cylinders 1 & 6 and 3 & 5 suffer from 180° interference from the following cylinder in the firing order, which causes a high pressure blowdown pulse during overlap at low-medium engine rpm, similar to the I4 engine. Cylinders 1 & 6 additionally suffer from a 90° preceding interval in the firing order. The latter part of the exhaust flow from the 90° preceding cylinder (2 & 8) occurs during the early part of the exhaust stroke of the cylinder of interest (1 & 6) and causes increased pressure during the exhaust stroke, increasing pumping work. Cylinders 2 & 8 suffer from 90° interference from the following cylinder in the firing order. The blowdown pulse from this cylinder (1 & 6) increases the cylinder pressure during the exhaust stroke, increasing pumping work. Cylinders 4 & 7 do not have any issues with blowdown interference since the preceding interval is 180° and the following interval is 270°.

Cylinders 4 & 7 have positive pumping work because intake pressure is above exhaust pressure with no blowdown interference. Cylinders 2 & 8 have negative pumping work due to the 90° interference pulse of cylinders 1 & 6. The pumping work of cylinders 3 & 5 is less positive than that of cylinders 4 & 7 due to the 180° interference pulse. The positive pumping work of cylinders 1 & 6 is further reduced due to the effect of the 90° preceding cylinder exhaust flow.

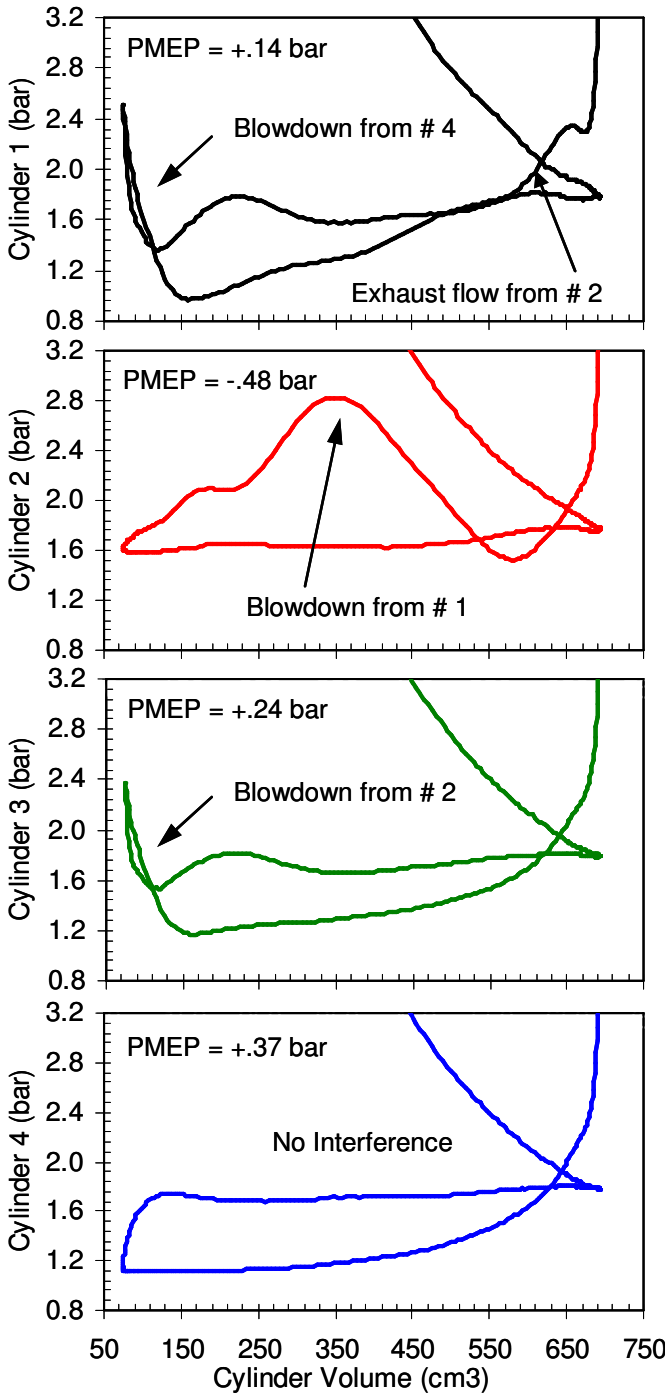

Figure 91 - Cylinder pressure pumping loops for the right bank of the V8 at 2000 rpm, 17 bar BMEP.

As shown in the pumping loops of Figure 91, cylinders 1 & 6 and 3 & 5 suffer from high exhaust pressure during overlap due to the 180° interference. As a consequence, these cylinders will have higher residual fraction than cylinders 4 & 7. This is illustrated in the corresponding GCA output shown in Figure 92. In these Figures, red lines denote exhaust and dotted blue lines denote intake. The top plots for each cylinder show exhaust flow out of the cylinder and intake flow into the cylinder. The bottom plots for each cylinder show intake and exhaust pressure profiles and the valve lift curves. These results were obtained at low overlap, which was used to minimize the impact of the interference. Nevertheless, the residual mass fraction (RMF) for cylinders 1 and 3 with 180° interference is about 5.5% as compared to 2.2% for cylinder 4 which does not suffer from interference.

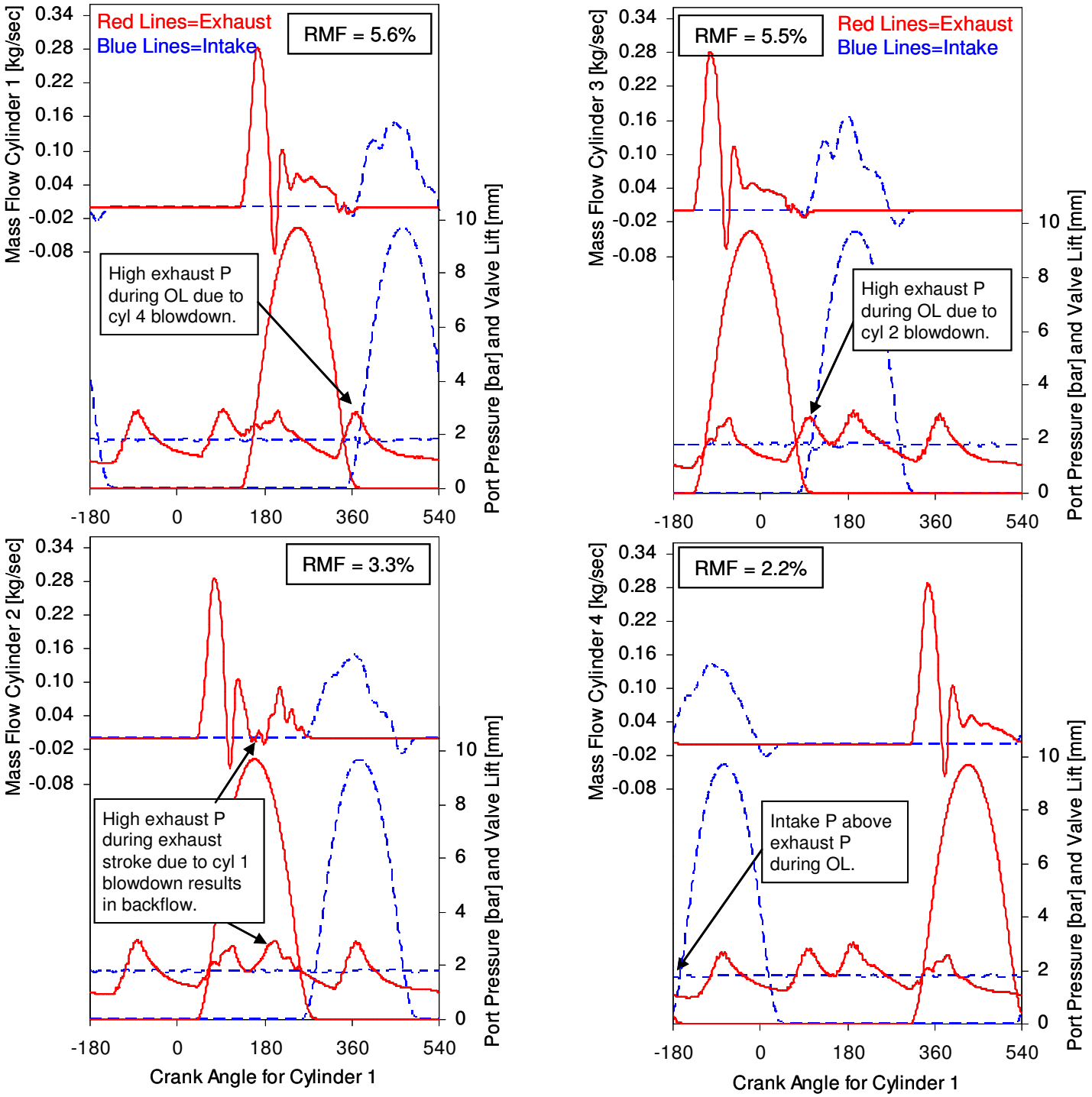

Figure 92 - GCA output for 2000 rpm, 17 bar BMEP illustrating blowdown interference on cylinders 1 and 2 (left) and cylinders 3 and 4 (right).

As engine speed is increased, the pressure wave travel time in the exhaust manifold becomes significant in terms of crank angle degrees. This causes the blowdown interference pulses to arrive later at the cylinder of interest, and paired cylinders for each bank no longer behave identically. Cylinder pressure pumping loops for the right bank of the V8 engine at 4750 rpm are shown in Figure 93.

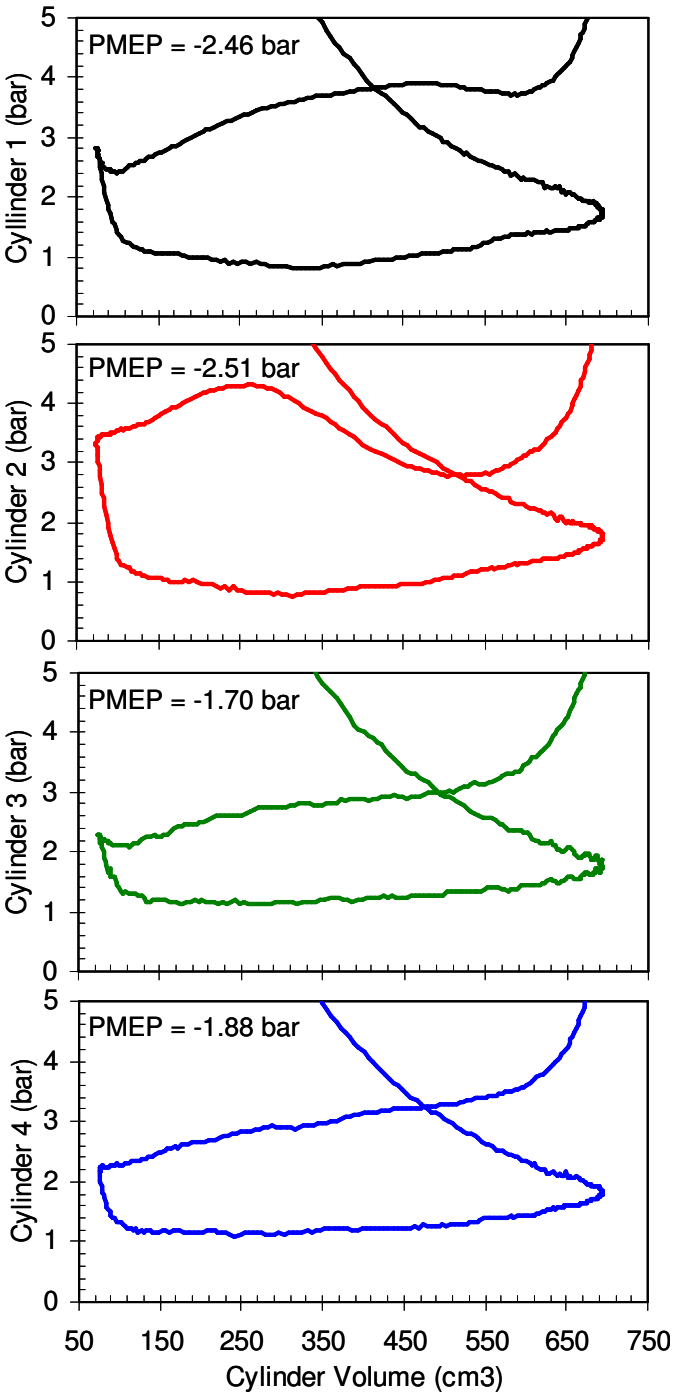

Figure 93 - Cylinder pressure pumping loops for the right bank of the V8 at 4750 rpm.

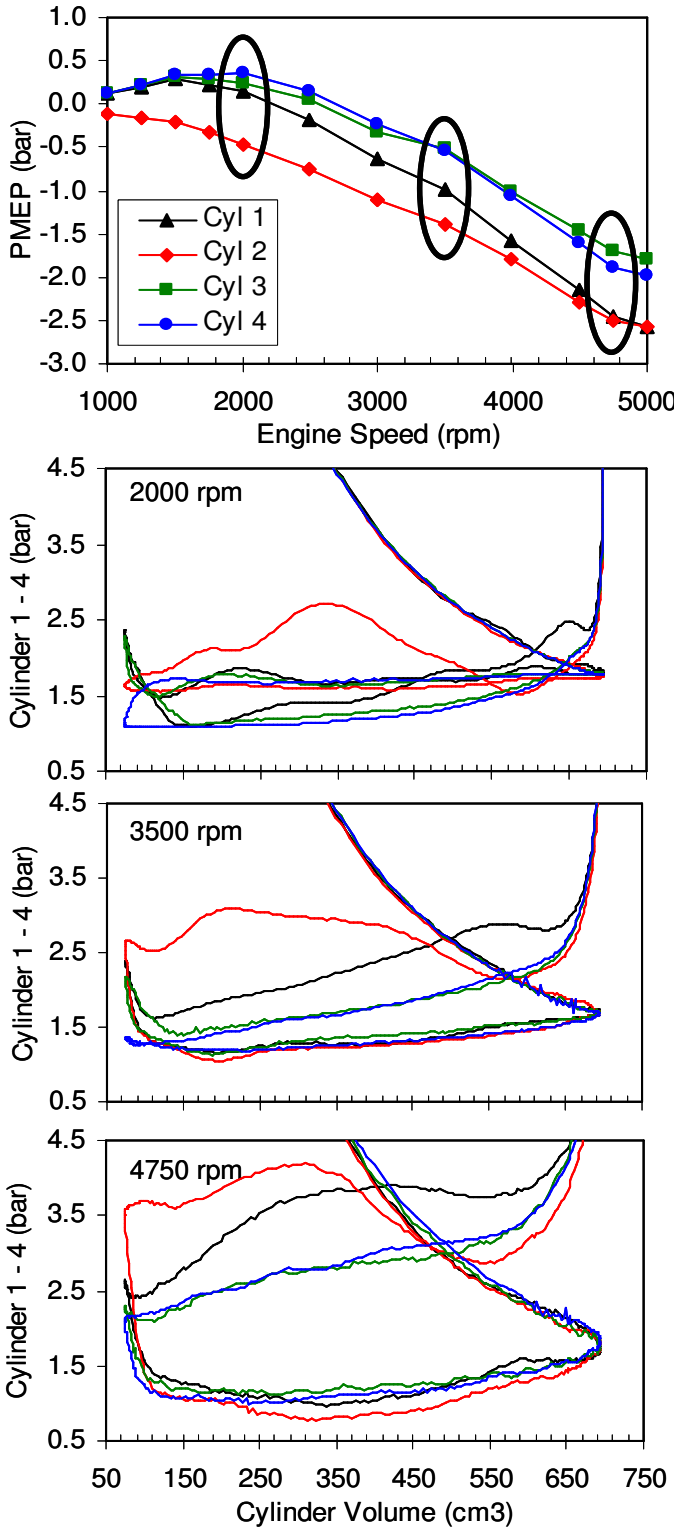

Figure 94 - PMEP and cylinder pressure pumping loops as a function of engine speed.

As previously explained, cylinders 4 & 7 do not suffer from blowdown interference. For cylinders 3 & 5, the 180° interference pulse from cylinders 2 & 8 arrives after exhaust valve closing at 4750 rpm and consequently the pumping loop is very similar to that of cylinders 4 & 7. For cylinders 1 & 6, the exhaust flow from the 90° preceding cylinder (2 & 8) causes increased pressure during the exhaust stroke, increasing pumping work.

Of primary interest at high speed is the effect of the 90° interference on cylinders 2 & 8. Because the 90° pulse arrives later in the cycle of cylinders 2 & 8, it not only increases exhaust stroke pumping work, but also increases the exhaust pressure during overlap, increasing residual fraction. As a consequence, cylinders 2 & 8 are more knock-limited at high engine speed than the other 6 cylinders.

An overlay of the cylinder pressure pumping loops as a function of engine speed is shown in Figure 94 along with the corresponding PMEP for each cylinder at the top of the figure. The pumping loops for 2000 rpm and 4750 rpm were previously shown individually in Figure 91 and Figure 93.

It is interesting to note that the effect of 180° interference on cylinders 1 & 6 and 3 & 5 is still present at 3500 rpm. Also, as noted for 4750 rpm, the 90° interference pulse arrives later at cylinders 2 & 8, increasing the exhaust pressure during overlap and residual fraction, as well as increasing exhaust stroke pumping work. Hence in summary, in contrast to the I4 engine, which has an even firing order and 180° interference on all cylinders, the V8 suffers from 90° interference on two cylinders, which significantly impacts residual fraction in those cylinders at medium and high speed, in addition to 180° interference on four cylinders.

EFFECT OF BLOWDOWN INTERFERENCE AT PART LOAD

At part load, blowdown interference causes imbalance in residual fraction between cylinders, particularly as variable camshaft timing (VCT) is applied. Residual fraction output from GCA is shown for the individual cylinders as a function of exhaust valve closing (EVC) timing at 1500 rpm, 9 bar BMEP in Figure 95.

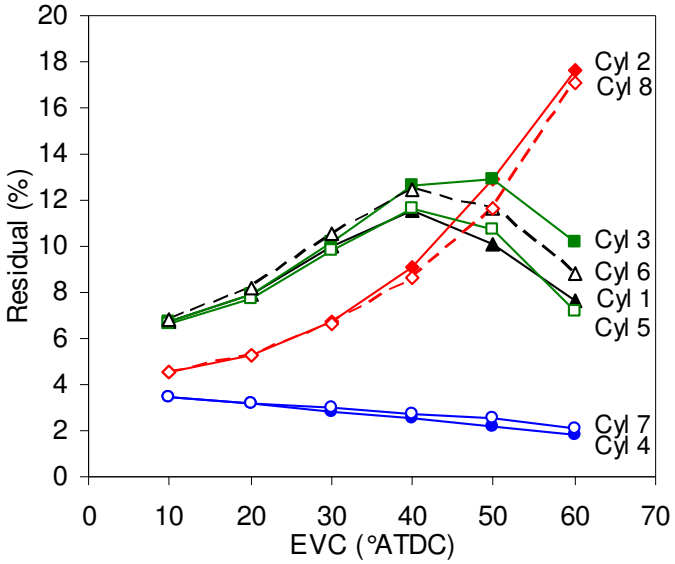

Figure 95 - Residual fraction as a function of EVC timing at 1500 rpm, 9 bar BMEP.

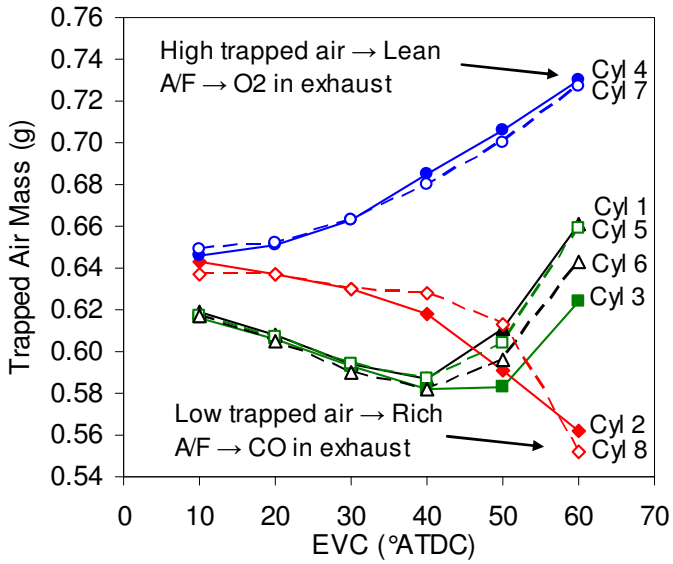

Figure 96 - Trapped air mass as a function of EVC timing at 1500 rpm, 9 bar BMEP.

As shown, the residual fraction differs dramatically between cylinders as overlap is increased. In the cylinders with high residual fraction, combustion instability and/or knock are encountered earlier than in the other cylinders. Figure 96 shows GCA output for the trapped air mass in the individual cylinders for this data set. Cylinders with higher residual fraction have lower trapped fresh air mass and richer air-fuel ratio, causing high CO in the exhaust. Conversely, cylinders with lower residual fraction have higher trapped air mass, causing high O2 in the exhaust. The presence of both CO and O2 in the exhaust will increase exothermic heat release in the catalyst. These effects will significantly limit the applicability of VCT strategies at part load, and consequently will limit the fuel consumption benefit of VCT which can be attained.

METHODS TO MITIGATE V8 BLOWDOWN INTERFERENCE

During this project, a number of methods to mitigate the effects of blowdown interference were investigated with 1D modeling using the GT-POWER code and with engine dynamometer data. These methods include using twin scroll turbochargers, using shorter exhaust camshaft duration on two cylinders on each bank (termed "2 x 2 cams"), and connecting the exhaust manifold banks with a balance tube. These investigations are described in the following sections.

TWIN SCROLL TURBOCHARGERS

The ultimate technical solution to V8 blowdown interference is embodied in the 4.4L BMW M-Series X6 [36], which uses inboard exhaust manifolds to allow routing of the appropriate cylinder pairs to twin scroll turbochargers (Figure 97). This layout provides an even firing interval of 360° to each scroll with low volume exhaust manifolds for optimum transient response, and is conceptually equivalent to the use of twin scroll turbochargers on two I4 engines [37]. Although this approach provides optimum resolution of blowdown interference, it appears to be quite expensive and may present thermal management challenges with underhood temperatures and thermal expansion of exhaust manifold and turbocharger components. It also is not applicable to adding turbocharging to an existing engine with outboard exhaust manifolds without requiring a new cylinder head architecture.

For the purpose of investigating the effect of twin scroll turbochargers on a V8 engine with outboard exhaust manifolds, prototype exhaust manifolds were fabricated as shown in Figure 98 to allow the use of twin scroll turbochargers available from a production vehicle application. The right bank manifold provides cylinder pairing of 1 with 3 to one scroll and 2 with 4 to the other scroll. The left bank manifold provides cylinder pairing of 6 with 5 to one scroll and 8 with 7 to the other scroll. Referring to Figure 5, this layout results in firing intervals of 270° and 450° to each scroll, and in theory should eliminate blowdown interference. In the actual hardware, the construction of the twin scroll turbine allows some limited communication between the two scrolls.

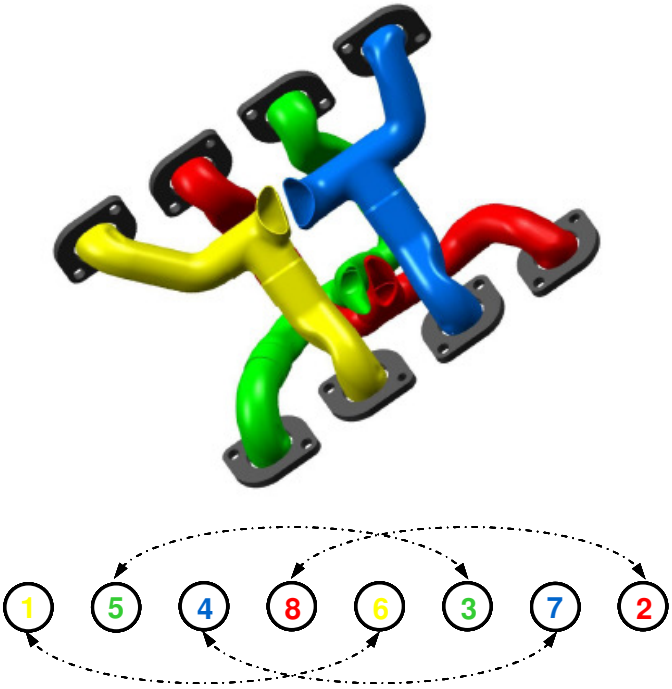

Figure 97 - BMW M-Series in-board exhaust manifolds and cylinder routing with twin scroll turbochargers.

Figure 98 - Prototype exhaust manifold layouts for twin scroll turbochargers.

Comparison of pumping loops for twin scroll and single scroll turbochargers for cylinder 1 at 1500 rpm, 14 bar BMEP are shown in Figure 99. As shown, twin scroll results in greatly diminished magnitude of the 180° interference pulse, as well as reduced effect of the exhaust flow from cylinder 2. Comparison of pumping loops for twin scroll and single scroll turbochargers for cylinder 2 are shown in Figure 100. As shown, twin scroll results in reduced magnitude of the 90° interference pulse, but not its complete elimination, due to the communication between scrolls.

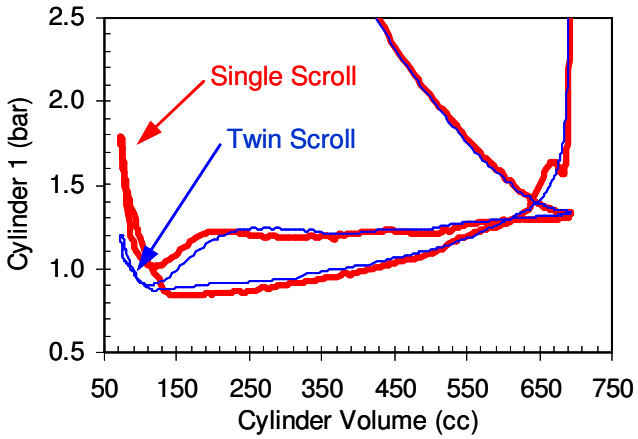

Figure 99 - Pumping loops for twin scroll and single scroll for cylinder 1 at 1500 rpm, 14 bar BMEP.

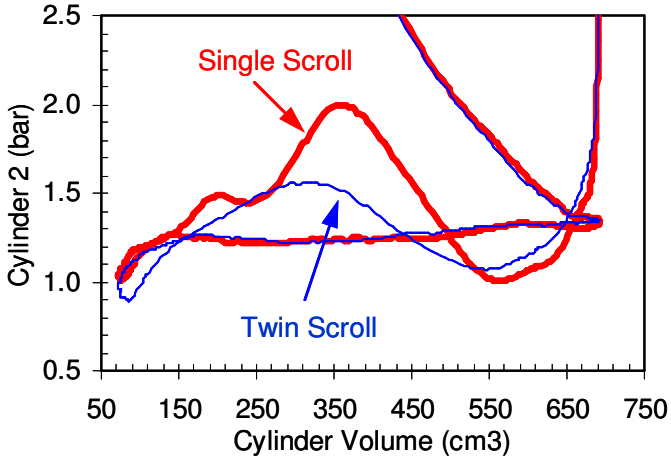

Figure 100 - Pumping loops for twin scroll and single scroll for cylinder 2 at 1500 rpm, 14 bar BMEP.

A comparison of residual gas fraction at 1500 rpm, 11 bar BMEP determined with GCA is tabulated in Table 1. This data was taken at high overlap conditions with an intake valve opening (IVO) timing of 40° bTDC and exhaust valve closing (EVC) timing of 30° aTDC. As shown, twin scroll significantly reduced the cylinder-to-cylinder variation of residual fraction, and brought the 180° interference cylinders (1 & 6 and 3 & 5) much closer to the cylinders without interference (4 & 7). It also improved the 90° interference cylinders (2 & 8), but at 1500 rpm, 90° interference is not as significant as 180° interference.

Table 3 - Comparison of residual fraction from GCA for single scroll and twin scroll at 1500 rpm, 11 bar BMEP with 40 bTDC IVO and 30 aTDC EVC.

		Residual Fraction (%)	
Cylinder	Interference Type	Single Scroll	Twin Scroll
1	180°	7.4	5.4
6	180°	7.7	5.6
3	180°	7.2	5.5
5	180°	7.2	5.6
2	90°	4.5	4.1
8	90°	4.5	4.0
4	None	4.0	3.5
7	None	3.8	3.6

The 1D code GT-POWER was used to model the twin scroll turbocharger arrangement with the communication between scrolls modeled as an orifice, as shown in Figure 101 and Figure 102 [37].

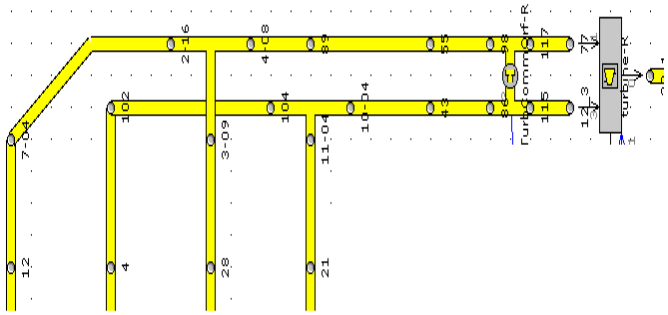

Figure 101 - Model of the right bank exhaust manifold and twin scroll turbine.

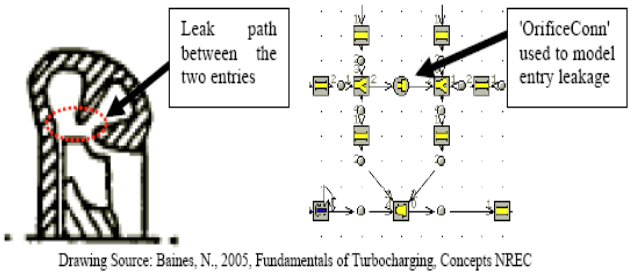

Figure 102 - Twin scroll cross-section schematic and communication orifice model.

As one step in the model calibration, the orifice size was adjusted until the exhaust manifold pressure profiles calculated by the model matched those measured on engine dynamometer at 1500 rpm, as shown in Figure 103. This calibration required an orifice diameter of 15 mm. The effect of twin scroll turbochargers on residual fraction compared to single scroll turbochargers at 1750 rpm is shown in Figure 104. As shown, twin scroll significantly reduces the residual fraction for the cylinders with 180° blowdown interference. The interference is not completely eliminated because of the communication between scrolls.

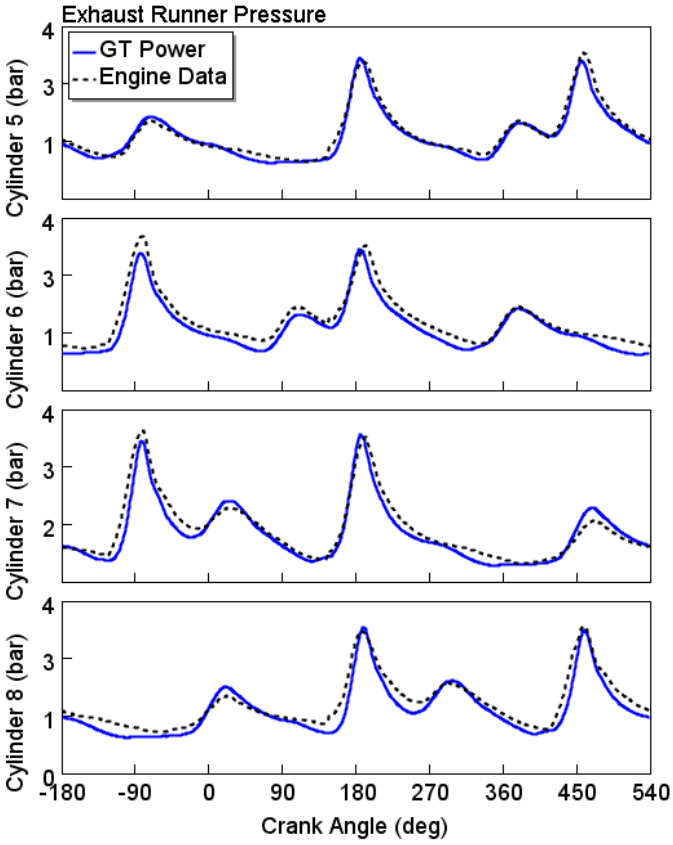

Figure 103 - Comparison of measured and modeled pressure for the left bank exhaust manifold.

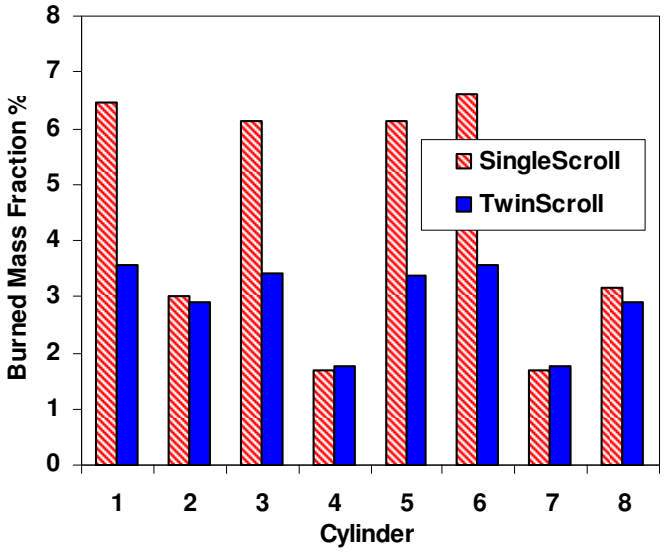

Figure 104 - Model results for the reduction of residual mass fraction with twin scroll turbochargers.

2 X 2 EXHAUST CAMSHAFTS

As discussed previously, 180° blowdown interference can be resolved at low to medium speed on the I4 turbocharged engine by using a short exhaust camshaft duration, with relatively late exhaust valve opening (EVO) timing. This technique cannot be directly applied to the V8 engine on all cylinders, because it would cause the blowdown pulse from cylinders 1 & 6 to arrive closer to the overlap of cylinders 2 & 8, increasing the severity of the 90° interference, as illustrated in Figure 23. Later EVO is also not required for cylinders 3 & 5, since these cylinders already follow 270° later in the firing order than cylinders 4 & 7. Hence, using shorter exhaust duration would cause an unnecessary penalty in high speed performance for these cylinders.

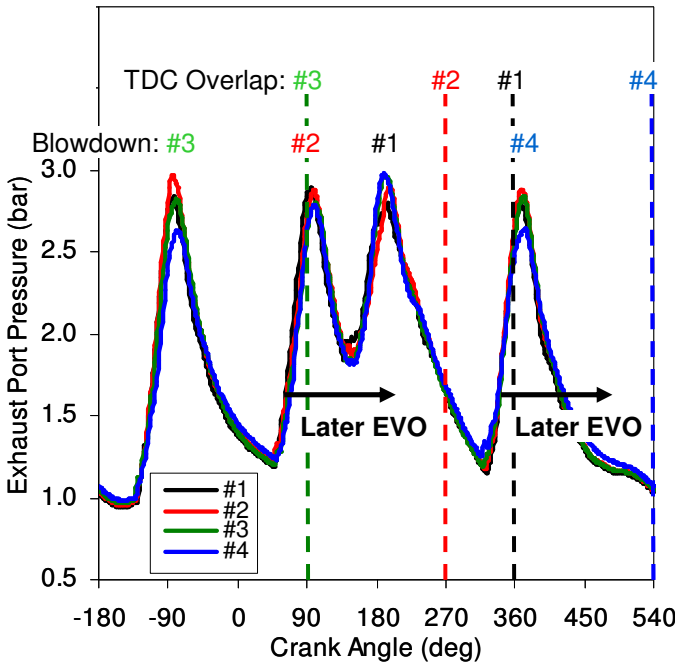

Figure 105 - Right bank exhaust manifold pressure.

Thus, 180° blowdown interference can be mitigated on the turbocharged V8 by using short exhaust cam duration on two cylinders per bank (2 and 4 on the right bank and 8 and 7 on the left bank), with the other two cylinders per bank retaining conventional duration. This concept is the subject of a patent issued to Porsche [35], and has been introduced in production by Porsche on their 4.8L V8 turbocharged Cayenne. This concept is termed "2 x 2 cams" in this report.

2 x 2 cams were investigated using the 1D GT-POWER model. As a first step, the model was calibrated to the baseline case with conventional exhaust camshafts and single scroll turbochargers. The results of this calibration are shown in Figure 106 for the right bank cylinders. As shown, the results of the calibrated model are in reasonably good agreement with the measured cylinder pressure data.

After model calibration, a sweep of exhaust cam duration for the two cylinders per bank with shorter exhaust event (2 and 4 on the right bank and 8 and 7 on the left bank) was conducted to determine the duration needed to avoid 180° interference at low speed. For this sweep, the exhaust valve closing was held constant, and hence shorter duration corresponds to later exhaust valve opening. The baseline exhaust cam duration was 254°. The results of this sweep along with the baseline case are shown in Figure 107 for the right bank.

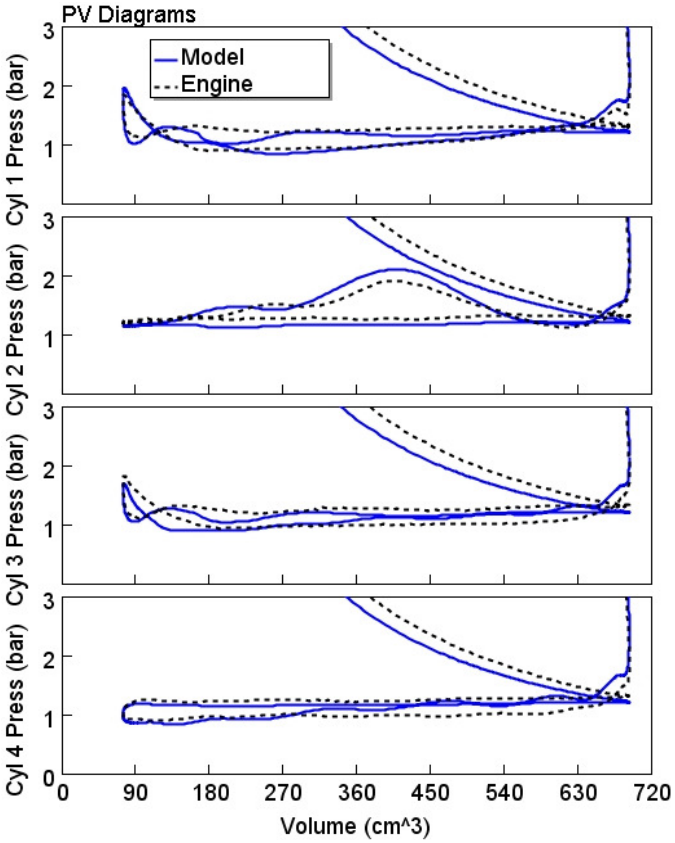

Figure 106 - Calibration of model results to engine data at 1500 rpm, 14 bar BMEP.

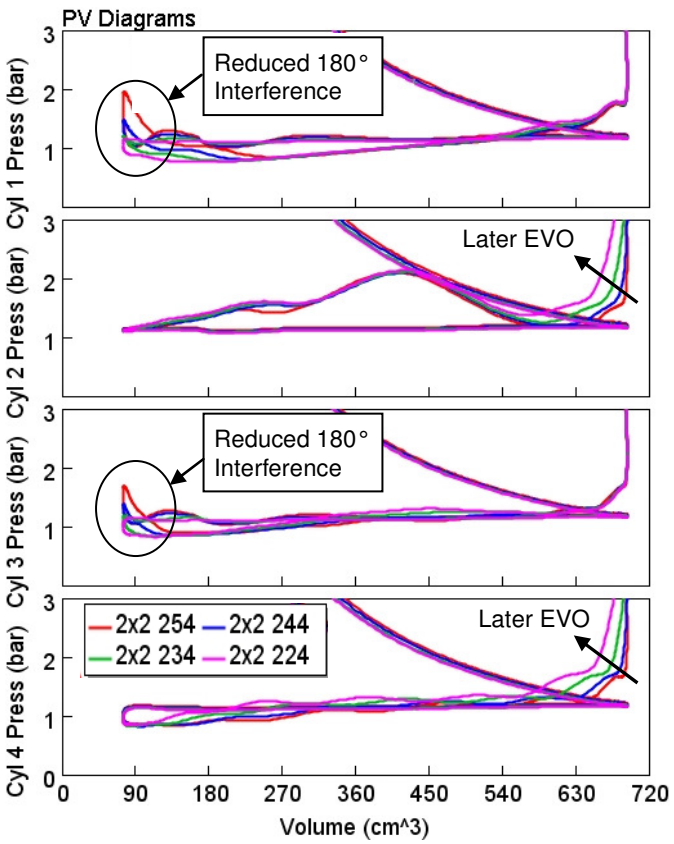

Figure 107 - Model results for 2 x 2 exhaust cam duration sweep at 1500 rpm, 14 bar BMEP.

Later exhaust valve opening (EVO) timing as the exhaust cam duration is shortened is evident for cylinders 2 and 4. Referring to the overlap region of cylinders 1 and 3, it appears that the exhaust cam duration for cylinders 2 and 4 must be a minimum of 20° shorter than the baseline duration in order to eliminate 180° interference at this speed-load condition. The residual fraction for the cylinders of the right bank is shown in Figure 108 for 2 x 2 cams with 224° duration on the cylinders with a short exhaust event and 254° duration on the other cylinders. As shown, the residual fraction for cylinders 1 and 3 with 180° interference is significantly reduced, and is within about 1% of that of cylinder 4 (which does not suffer interference) at this speed-load condition.

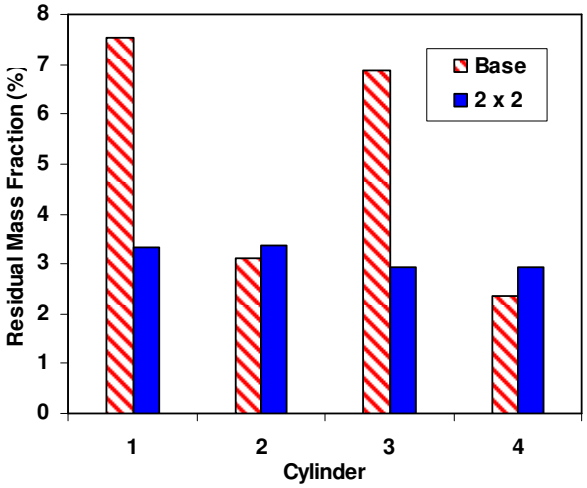

Figure 108 - Effect of 2 x 2 cams on residual mass fraction at 1500 rpm, 14 bar BMEP.

Next, the model was run with 2 x 2 cams at conditions corresponding to full load at low, medium, and high speed. These results are shown in Figure 109 through Figure 114. At 2000 rpm, there is no significant visible evidence of 180° blowdown interference in the pumping loops of Figure 109, and the residual fraction is reasonably consistent between cylinders, as shown in Figure 110.

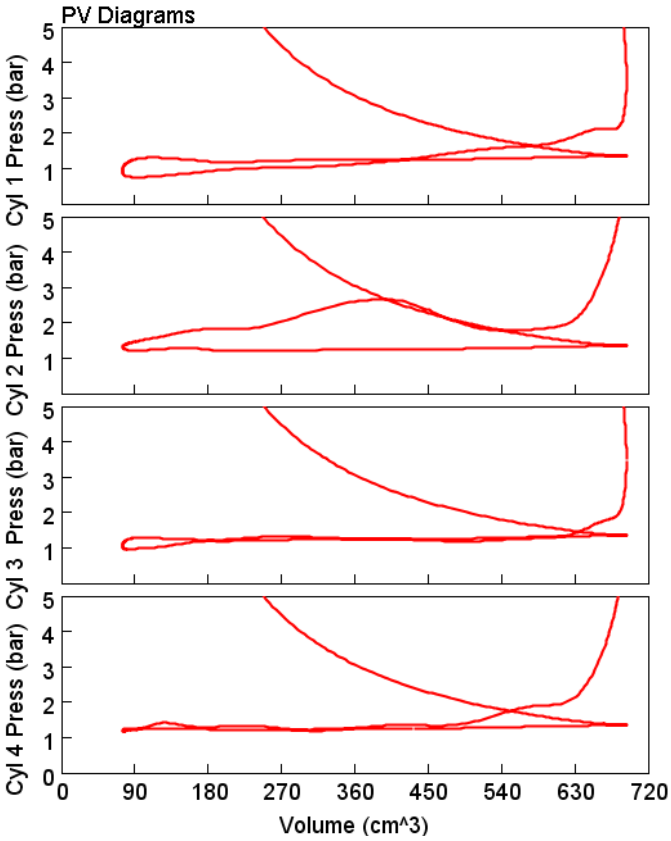

Figure 109 - Pumping loops for 2 x 2 exhaust cams at 2000 rpm, 17 bar BMEP.

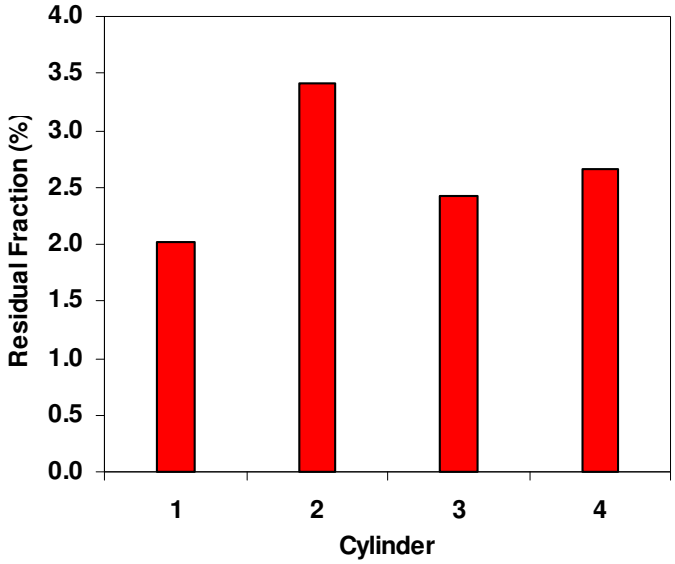

Figure 110 - Residual fraction for 2 x 2 exhaust cams at 2000 rpm, 17 bar BMEP.

Pumping loops for 3500 rpm and 4750 rpm are shown in Figure 111 and Figure 113. It is apparent from these pumping loops that 90° interference is present at medium and higher speeds on cylinders 2 & 8, as expected, since 2 x 2 exhaust cams only address 180° interference. As a consequence, the residual fraction for cylinders 2 & 8 is much higher than for the other cylinders, as shown in Figure 112 and Figure 114 for 3500 rpm and for 4750 rpm, respectively. It can also be observed in the pumping loops that EVO timing is excessively late at these engine speeds for cylinders 2 & 8 and 4 & 7, which increases exhaust stroke pumping work.

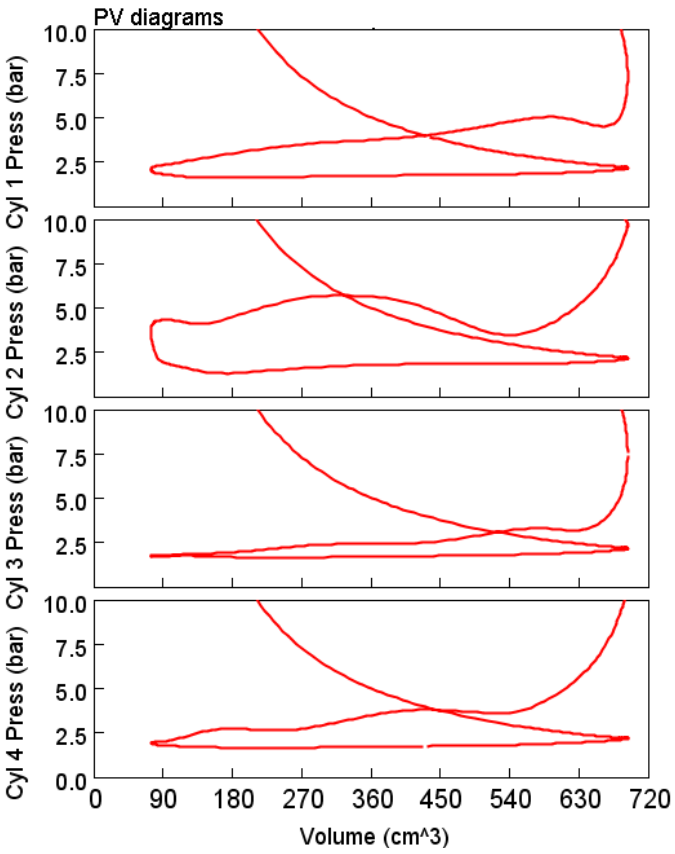

Figure 111 - Pumping loops for 2 x 2 exhaust cams at 3500 rpm, full load.

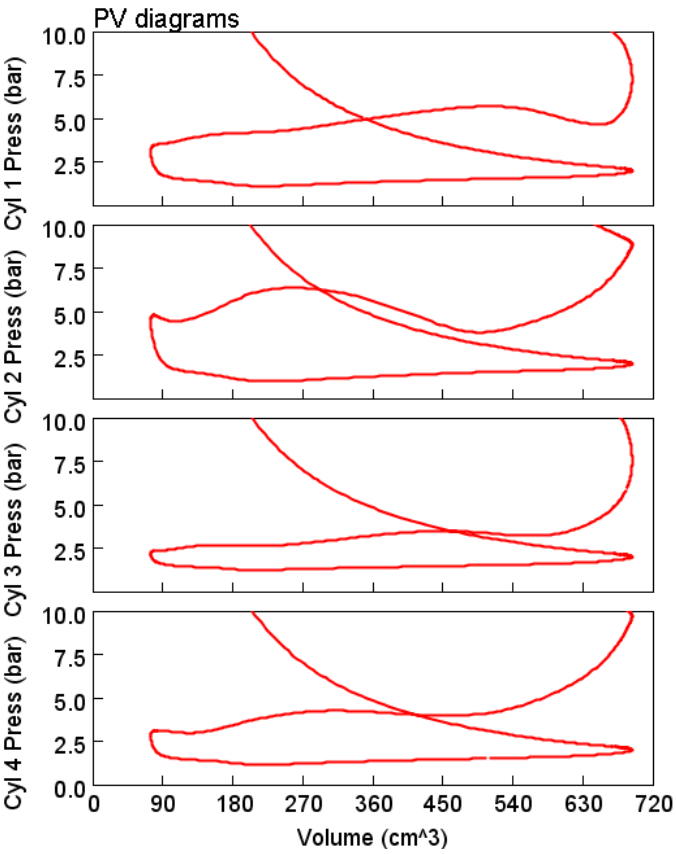

Figure 113 - Pumping loops for 2 x 2 exhaust cams at 4750 rpm, full load.

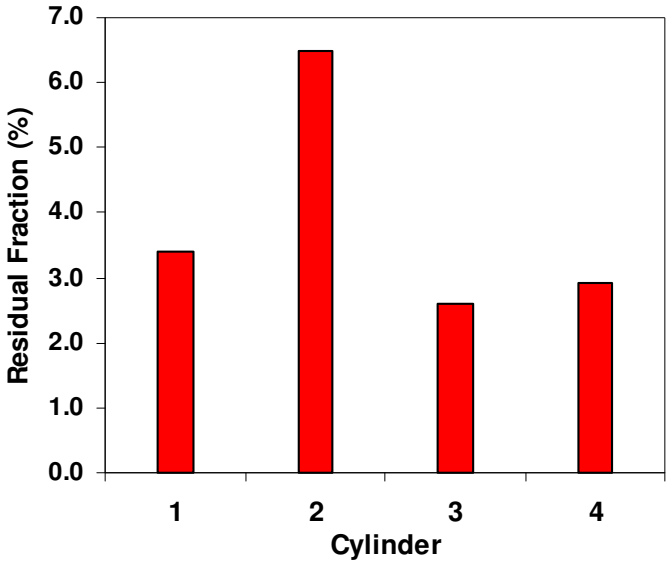

Figure 112 - Residual fraction for 2 x 2 exhaust cams at 3500 rpm, full load.

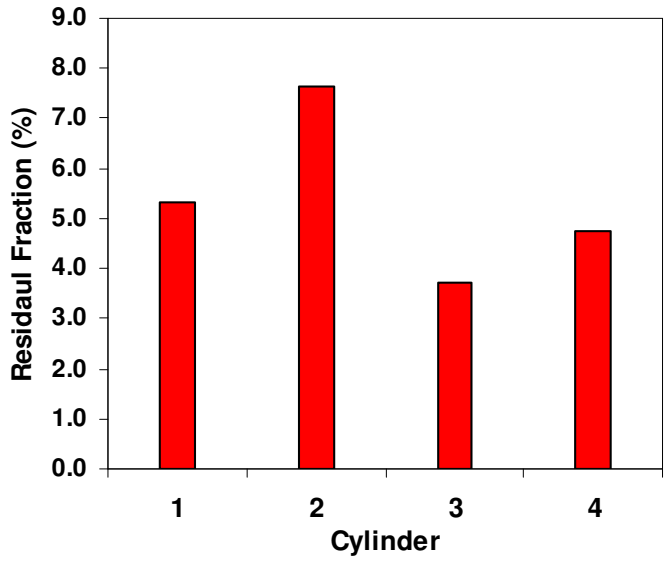

Figure 114 - Residual fraction for 2 x 2 exhaust cams at 4750 rpm, full load.

The model was then run at 1500 rpm, 14 bar BMEP to investigate if the reduction of 180° interference with 2 x 2 exhaust cams allows scavenging with more even distribution of fresh air and residual fraction between cylinders as overlap is increased. The results shown in Figure 115 indicate that scavenging will reduce

residual fraction on cylinders 1 & 6, 3 & 5, and 4 & 7, but cylinders 2 & 8 will limit EVC timing to about 40° ATDC due to the influence of 90° interference even at this low engine speed.

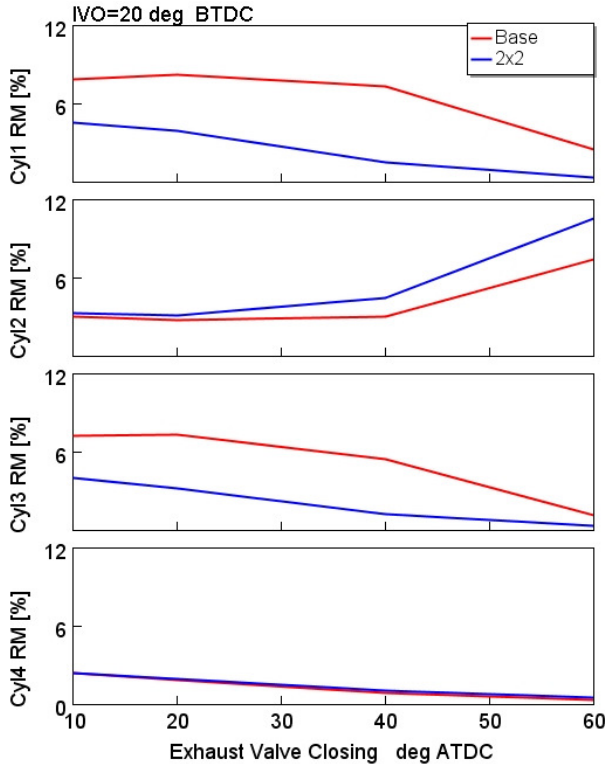

Figure 115 - Effect of EVC timing on residual fraction at 1500 rpm, 14 bar BMEP with 2x2 exhaust cams.

The above analyses clearly show the limitations of using 2x2 cams in the resolution of blowdown interference on a twin-turbocharged V8 engine. Thus, twin scroll turbochargers were utilized for the remainder of the project. A comparison of full load BMEP with GTDI for twin scroll turbochargers, 2 x 2 exhaust camshafts with single scroll turbochargers, and base camshafts with single scroll turbochargers is shown in Figure 116.

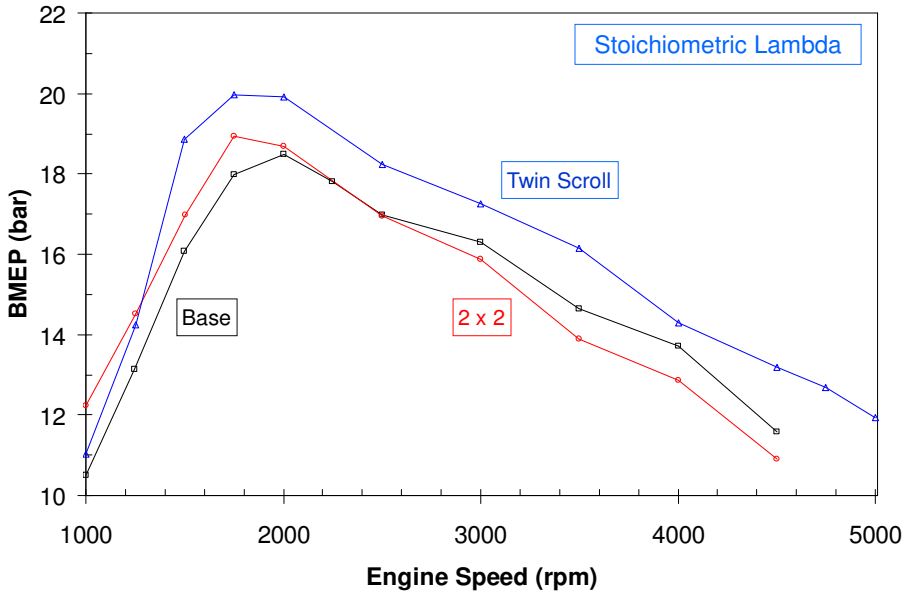

Figure 116 - Comparison of BMEP with GTDI for twin scroll, 2 x 2 exhaust camshafts, and the baseline.

Phase IV – Engineering Development

Task 1.0 – Cylinder Head

No cylinder head issues were discovered during the course of the multi-cylinder engine testing, therefore, no design updates or revisions were required.

Task 2.0 – Fuel System

In a conventional DI application, gasoline is always flowing through the injector (except in non-sustainable deceleration fuel shutoff conditions). In a Dual Fuel application with the primary gasoline fuel routed to the PFI system and the secondary E85 fuel routed to the DI system, the DI injector will not be flowing fuel at light load conditions where the engine is not knock-limited. Because fuel flow through the injector is an important mechanism for injector cooling, this creates potential injector cooling issues and the potential for deposit formation both external and internal to the injector tip. To investigate these potential issues, a PFI system was added to a production 3.5L TiVCT GTDI ("EcoBoost") engine to enable Dual Fuel operation.

Injector Tip and Fuel Pump Temperature Measurements

In order to quantify the temperatures and understand the cooling mechanisms for the DI injector and fuel pump, a thermocoupled injector and fuel pump were installed. The engine was tested at a variety of speed-load conditions, including the maximum load condition where the DI system is not flowing fuel and the overall highest load condition in Dual Fuel mode. The DI fuel injector in cylinder #3 was instrumented with thermocouples at the injector tip and chamber body locations (Figure 117), and a fuel pump was instrumented at the fuel pump inlet and chamber locations (Figure 118).

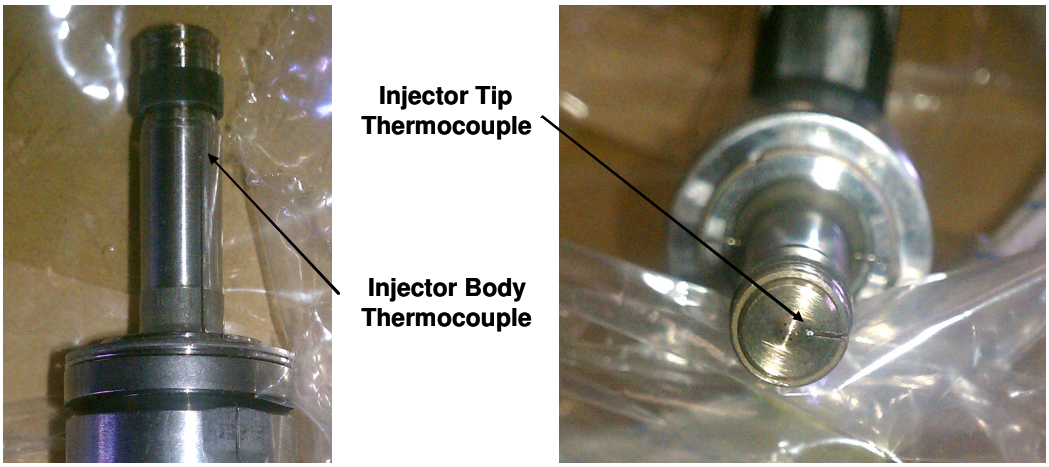

Figure 117 - Thermocouple locations for DI injector.

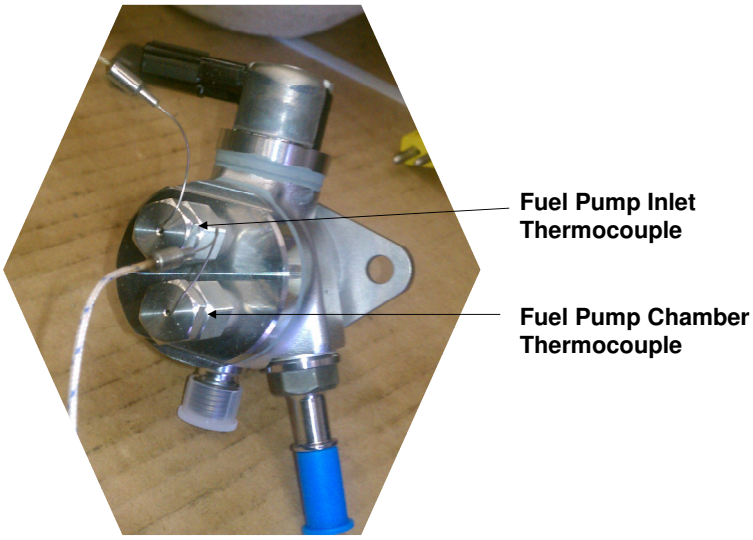

Figure 118 - Thermocouple locations for DI fuel pump.

As expected, the fuel injector and fuel pump temperatures are significantly reduced in the presence of fuel flow. Figure 119 and Figure 120 show the average temperatures observed at the maximum loads with and without direct injection of E85, respectively. The maximum engine load achievable using gasoline PFI is knock-limited at lighter loads, whereas the primary limiting factor using E85 DI is peak cylinder pressure. As expected, the injector tip temperature is appreciably higher when gasoline PFI is the sole source of fuel injection. The mechanical temperature limit of the injector tip is approximately 230 to 250° C. At engine speeds greater than 3000 rpm, the maximum load achievable using PFI alone begins to decrease, however, the average injector tip temperature continues to increase past the mechanical temperature limit. The maximum average injector tip temperature of 265°C is observed at 5000rpm, 7.5 bar BMEP.

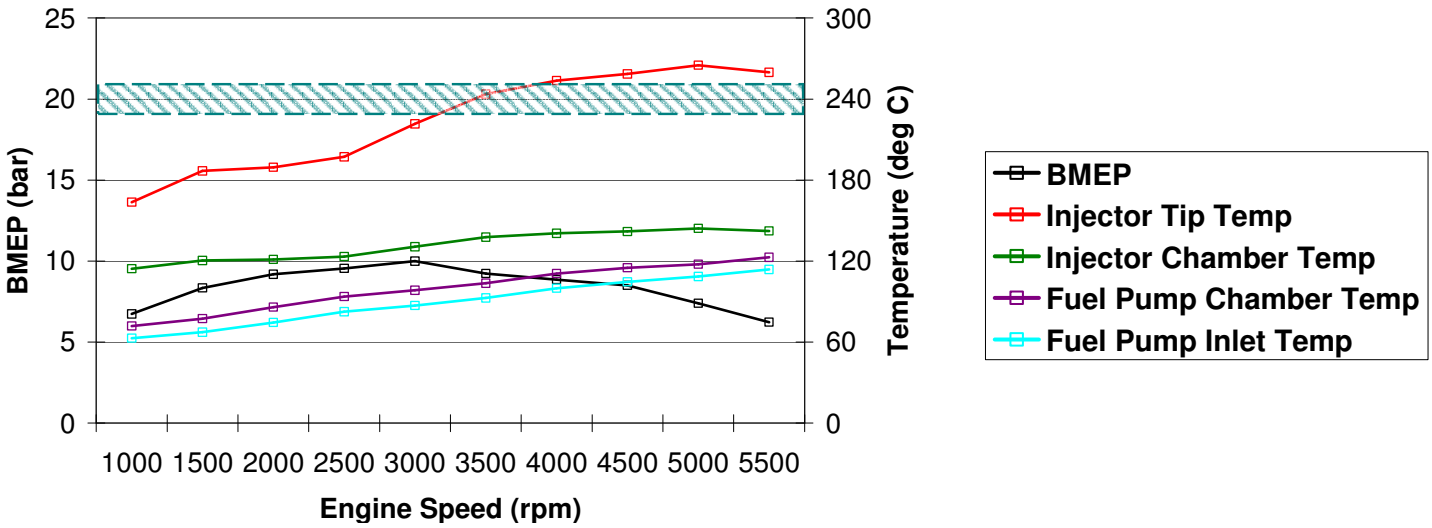

Figure 119 - Injector and fuel pump temperatures for PFI only mode.

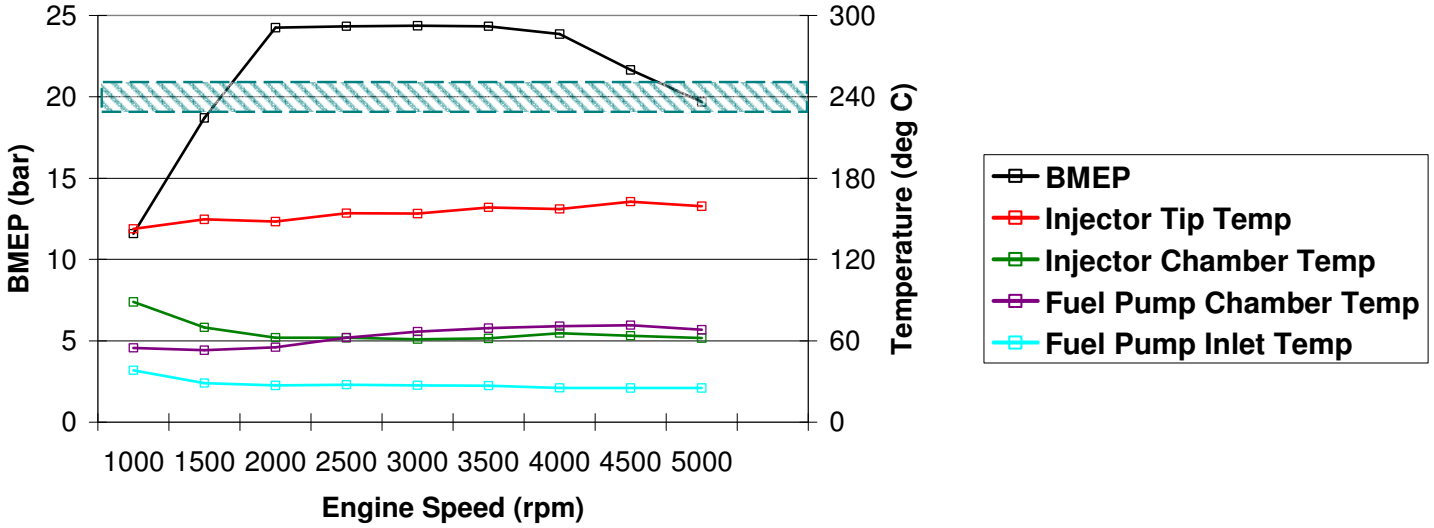

Figure 120 - Injector and fuel pump temperatures for E85 DI mode.

As E85 fuel flow is introduced into the DI system, the average injector temperature decreases rapidly. Figure 121 shows the impact of increasing the E85 mass ratio on fuel injector and pump temperatures. This data indicates the potential capability to control the fuel system temperatures through strategic injections of E85 fuel during extended PFI-only usage. The specific amount of E85 required to maintain temperature levels below the mechanical limit and outside of fuel deposit formation regions can thus be determined through further investigation.

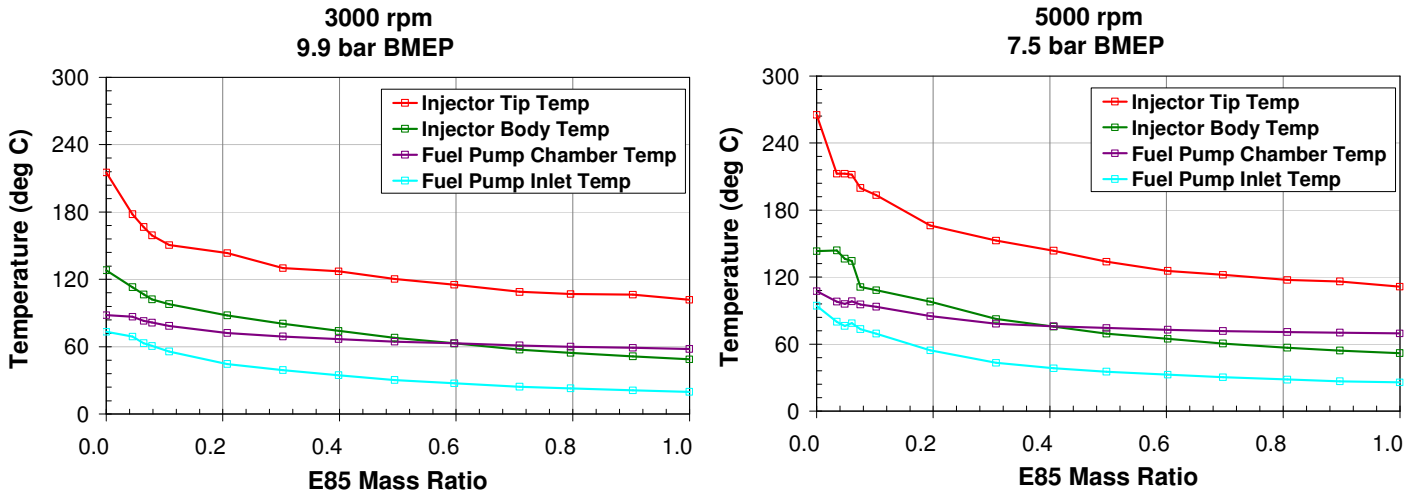

Figure 121 - Effect of E85 fuel flow on DI injector and fuel pump temperatures.

Injector Deposits

No issues with direct injector coking or deposits were encountered during the normal multi-cylinder engine development process with the Dual Fuel or the E85 FFV engines. In addition, deposit cycle testing was conducted to determine if deposit formation external or internal to the injector tip would be an issue. Preliminary testing indicated that no issues could be identified, presumably due to the cleaning properties of ethanol and the absence of particulate/soot formation with direct injection of E85. Longer term deposit testing will be performed to determine if deposit formation occurs for the Dual Fuel engine when fuel is not flowing through the injector over an extended time period, and if development of an injector cleanout cycle is necessary.

Multi-Cylinder Engine Development (Task 4.0)

Background

Selected properties of ethanol compared to gasoline are shown in Table 4. The first three properties cause ethanol to be an extremely knock resistant fuel in a direct injection engine. In addition to its RON value of 109, the high heat of vaporization (HoV) of ethanol results in substantial cooling of the charge with direct injection. In addition, the high sensitivity of ethanol results in an increase in effective octane as combustion phasing is retarded due to reduced unburned gas temperature [4].

As is well known, the Net Heating Value (NHV) per volume of ethanol is about 65% of that of gasoline. This causes a reduction in mpg fuel economy and in fuel tank range. The CO_2 emissions per unit heating value are 3% lower for ethanol than gasoline, while the CO_2 emissions per unit volume for ethanol are 64% of that of gasoline.

Table 4 - Properties of ethanol compared to gasoline.

	E100	Gasoline
RON	109	91
Sensitivity (RON minus MON)	17	~ 7
HoV (kJ/kg air at stoichiometry)	3.9 x base	base
Net Heating Value (MJ/L)	0.65 x base	base
CO_2 emissions (gCO_2/L)	.64 x base	base
CO_2 emissions (gCO_2/MJ)	.97 x base	base

A picture of the multi-cylinder engine along with lists of engine configuration information and engine operating constraints are shown in Figure 122.

Engine Configuration

5.0L 90 V8
Bore-stroke ratio: 0.88
Dual Fuel (DI and PFI)
Twin turbochargers
Compression ratio: 9.5:1 and 12:1
Twin Independent VCT

Engine Operating Constraints

Turbine inlet temperature = 950 °C
CA50 < 30 °ATDC
Max cylinder pressure = 150 bar

Figure 122 - Multi-cylinder engine configuration and operating constraints.

Because the engine was designed with both DI and PFI fuelling systems, various fuelling alternatives were utilized during the course of testing the multi-cylinder engine. These included:

- **GTDI**: Gasoline Turbocharged Direct Injection (100% gasoline DI)
- **ETDI**: Ethanol Turbocharged Direct Injection (100% E85 DI)
- **Dual Fuel**: E85 DI combined with 91 RON gasoline PFI

The first alternative replicates current "EcoBoost" engine technology, and was used to provide baseline data for this configuration. The second alternative is applicable for the E85 optimized FFV engine, and for full load performance of the Dual Fuel engine when running with 100% E85 DI to obtain maximum torque. The last alternative is applicable for the Dual Fuel engine, where E85 is used only as required to avoid knock, either at MBT (CA50 ~ 7 aTDC) or at a specified CA50.

As shown in Figure 123, two alternative paths were investigated for the Dual Fuel engine, maintaining the CR the same as the baseline GTDI engine, and increasing CR to take advantage of the high knock resistance of E85.

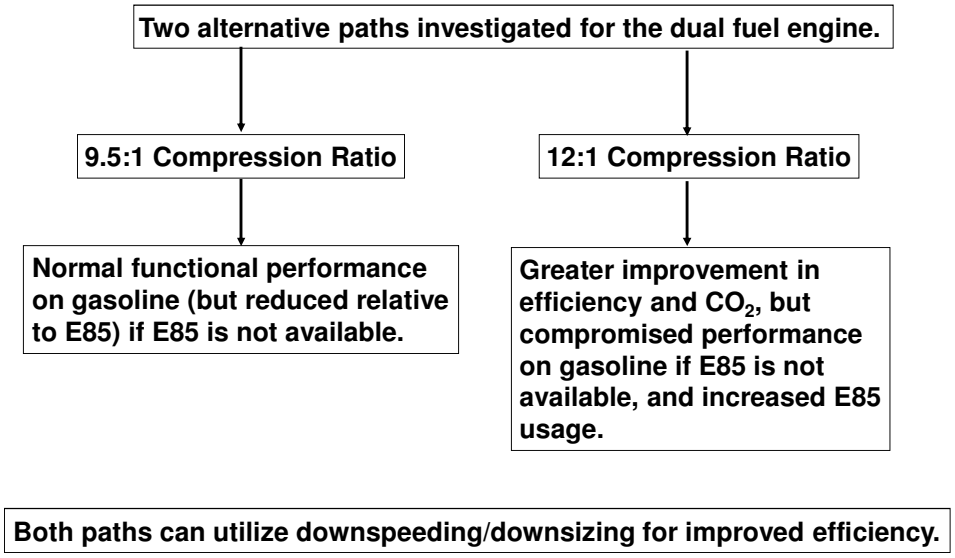

Figure 123 - Alternative compression ratio paths investigated for the Dual Fuel engine.

Full Load Performance

Single Scroll Turbochargers at 9.5:1 Compression Ratio

As a consequence of the high knock resistance of E85, the knock-limited BMEP with direct injection of E85 (ETDI) is much greater than that with direct injection of 91 RON gasoline (GTDI), as shown in Figure 124 for the single scroll turbocharger configuration at 9.5:1 CR. Peak BMEP with GTDI is 18 bar at stoichiometry and 23 bar with enrichment of lambda = 0.8 compared to 31.8 bar with ETDI at stoichiometry. Brake thermal efficiency (BTE) is higher for E85 than for gasoline at stoichiometry due to lower burned gas temperatures which result in reduced heat transfer losses and due to combustion phasing which is closer to optimum. When GTDI is run with enrichment to improve full load BMEP, then BTE is degraded. The consequent BSFC for gasoline at lambda = 0.8 is within 6% of the BSFC for E85 at stoichiometry, even though E85 has 29% lower heating value per unit mass than gasoline.

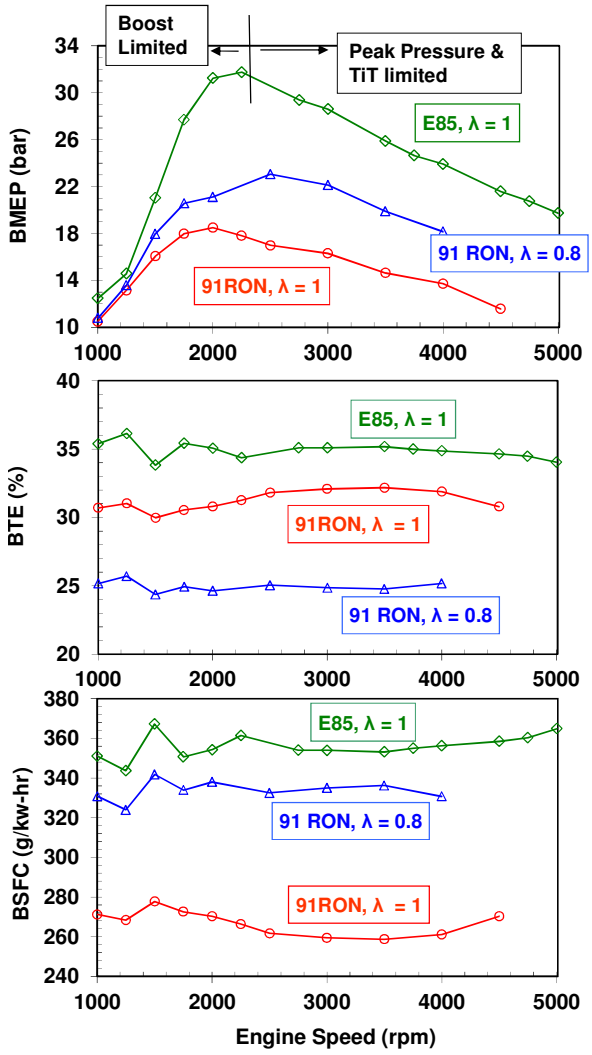

Figure 124 - Comparison of full load BMEP, brake thermal efficiency, and BSFC for ETDI at lambda = 1 and for GTDI at lambda = 1 and 0.8.

The operating constraints for this data set are shown in Figure 125. At engine speeds below 2250 rpm, the BMEP for ETDI is limited by the available boost of the turbocharger system. At engine speeds above 2000 rpm, the BMEP for ETDI is limited by the turbine inlet temperature constraint of 950° C and by the 150 bar peak pressure limit of the engine. The BMEP with GTDI is limited by knock at all engine speeds and by the turbine inlet temperature constraint above 2250 rpm at stoichiometry and above 3000 rpm at lambda = 0.8.

As shown in Figure 126, the degradation in BMEP with E85 is significantly less than for gasoline, especially on a percentage basis. The engine is knock-limited with gasoline and operating with enrichment provides an extension of the knock limit. With E85, the engine is not knock-limited, but operating with enrichment reduces turbine inlet temperature so that combustion phasing can be retarded to control peak pressure at the limit as boost is increased. Because ETDI provides very high BMEP even at stoichiometric air-fuel ratio, it is feasible to maintain stoichiometry over the entire engine operating range, and thereby enable three way catalyst (TWC) function and a very large emissions reduction for all off-cycle conditions.

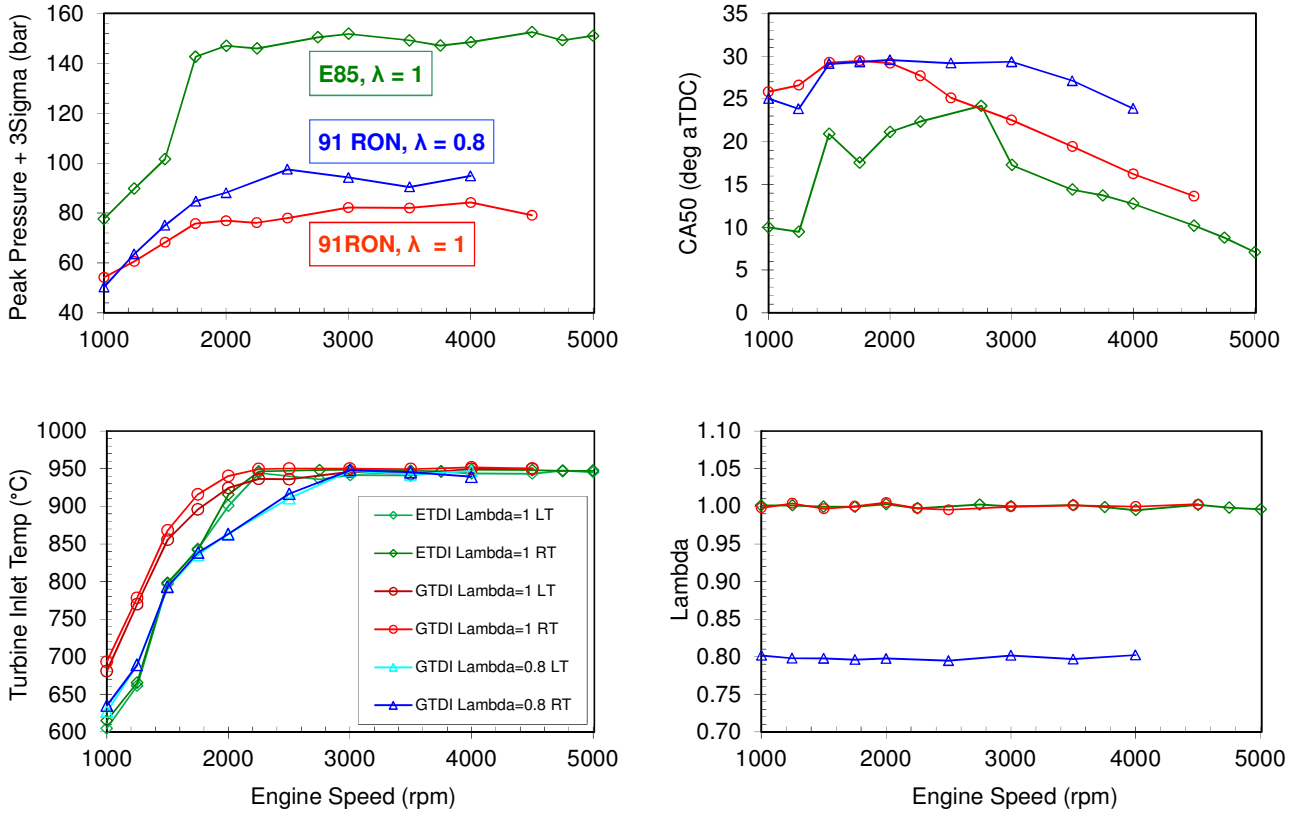

Figure 125 - Operating constraints for the data shown in Figure 124.

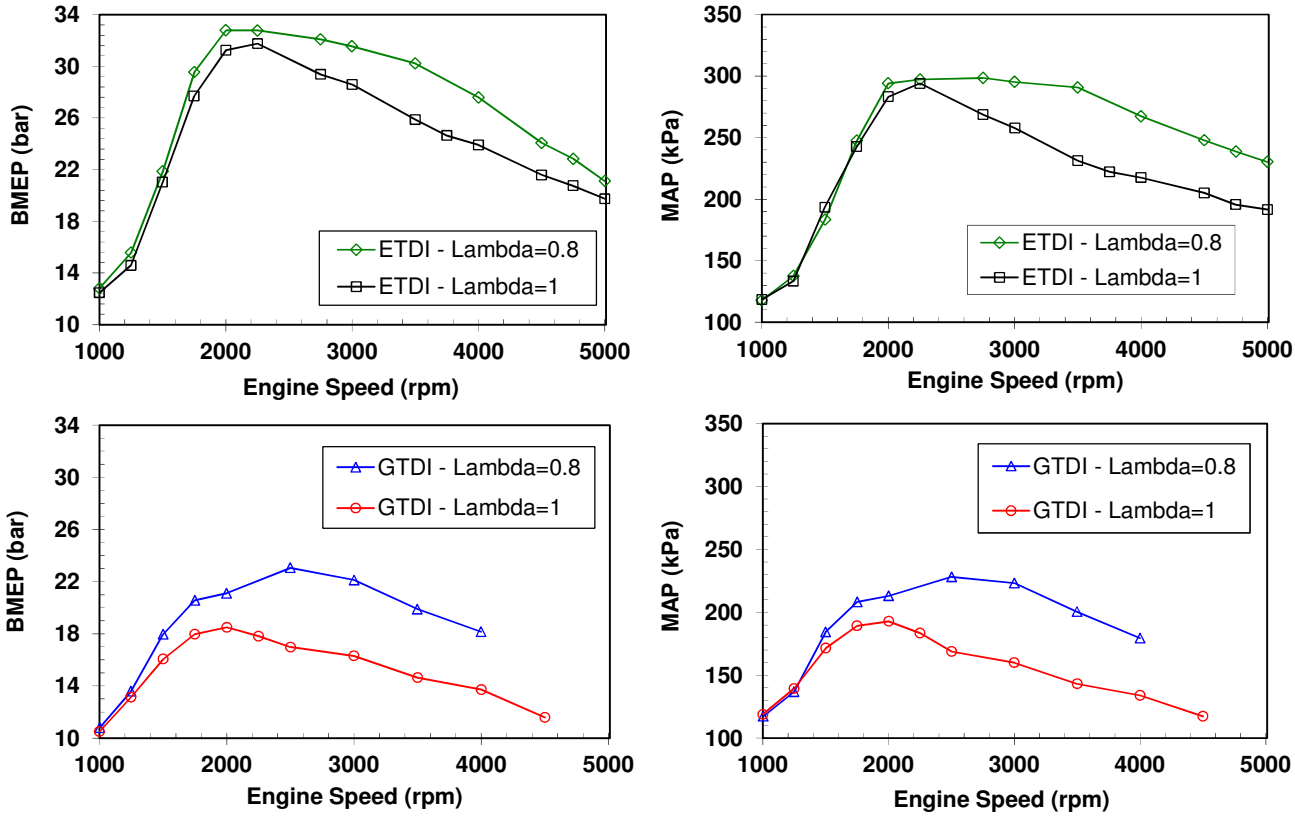

Figure 126 - BMEP comparison for GTDI and ETDI for lambda = 1 and 0.8 at 9.5:1 CR.

At low engine speed where only limited boost is available from the turbocharger system, increasing E85 ratio above the minimum required to avoid knock results in a substantial increase in BMEP, as shown in Figure 127. E85 has a stoichiometric air-fuel ratio of 9.8:1, whereas the stoichiometric air-fuel ratio for gasoline is about 14.6:1. Thus increased mass flow of fuel is required with E85 for a given quantity of air. Vaporization of E85 also results in substantial cooling of the charge prior to intake valve closing, which increases the density of the fresh air, which further increases the fuel flow required for stoichiometry. Thus, increasing E85 ratio increases the mass flow to the turbine, which increases turbine speed and work available to drive the compressor, increasing boost.

As shown in Figure 127, manifold absolute pressure (MAP) is increased 18 kPa as E85 ratio is increased from .65 to .95, resulting in a 3 bar increase in BMEP, from 23.2 bar to 26 bar. This increase in boost does not result in loss of surge margin (left side of Figure 127) because boost pressure and air flow increase following the same slope as the surge line. The increase in boost pressure for this data set is illustrated in the pumping loop comparison of Figure 128.

Since vehicle launch is a typical constraint which limits the minimum engine displacement for a turbocharged application, running 100% E85 DI at low engine speed is desirable in a Dual Fuel engine in order to enable increased downsizing of the engine displacement.

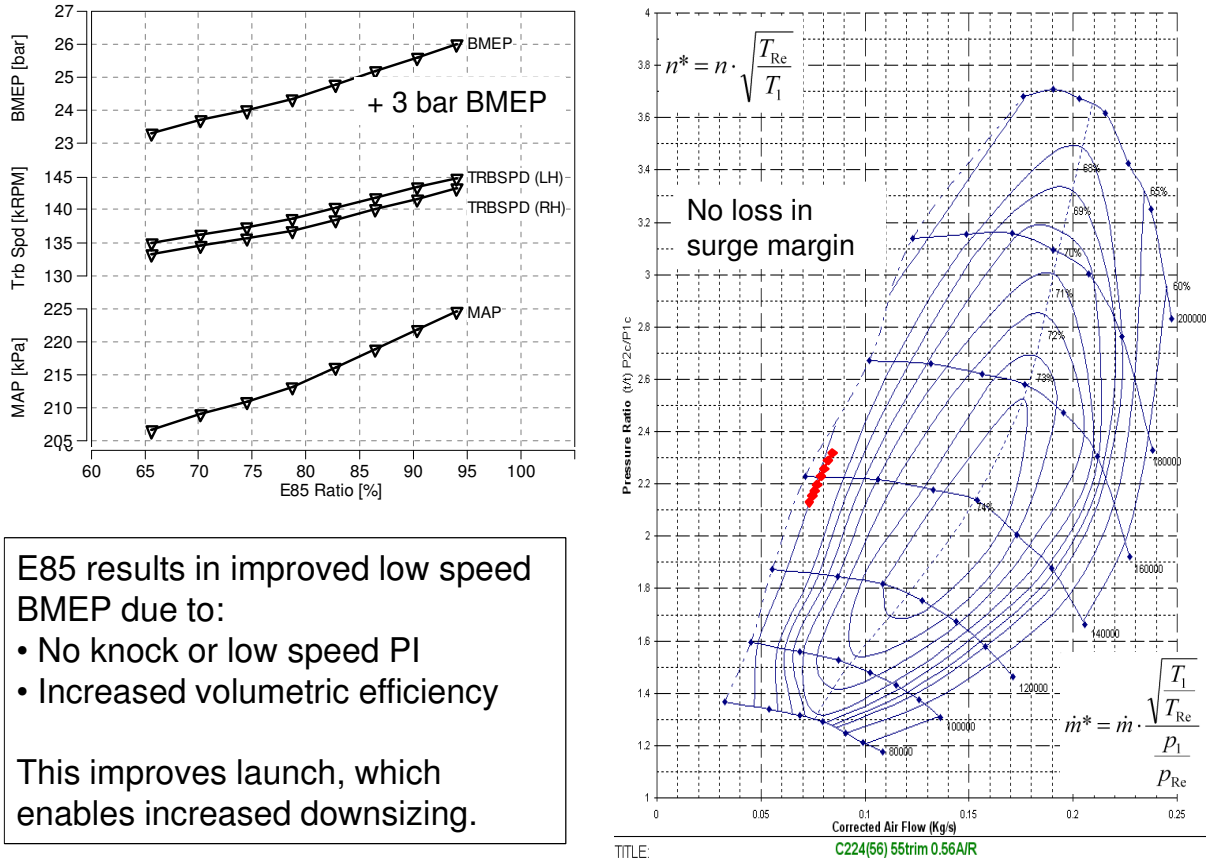

Figure 127 - Effect of E85 ratio on low speed BMEP.

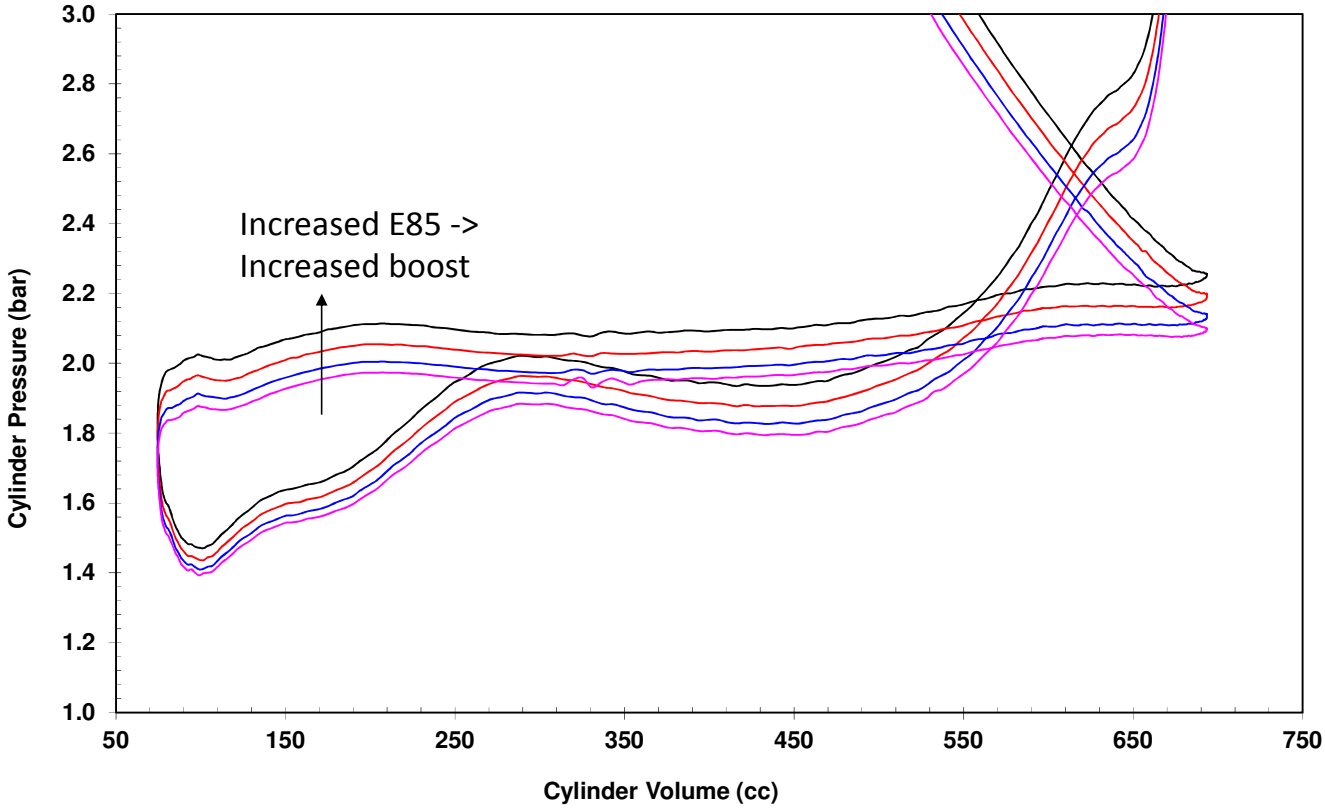

Figure 128 - Pumping loop comparison illustrating effect of E85 ratio on low speed boost.

Effect of Peak Pressure Limit

Although the engine for this program was designed for a peak cylinder pressure limit of 150 bar in order to take advantage of the knock resistant properties of ethanol, only a moderate loss in full load performance is associated with a peak cylinder pressure limit of 130 bar compared to 150 bar. 130 bar is achievable within conventional spark ignition engine design practice. A comparison of full load BMEP for peak pressure limits of 150 bar and 130 bar at stoichiometry is shown in Figure 129. At low engine speed, BMEP is limited by the available boost from the turbocharger system. At 2000 rpm and above, the BMEP is limited by the peak pressure constraint. Decreasing the peak pressure constraint from 150 bar to 130 bar requires retarding of combustion phasing and a reduction in boost level in order to simultaneously satisfy the turbine inlet temperature and peak pressure limits.

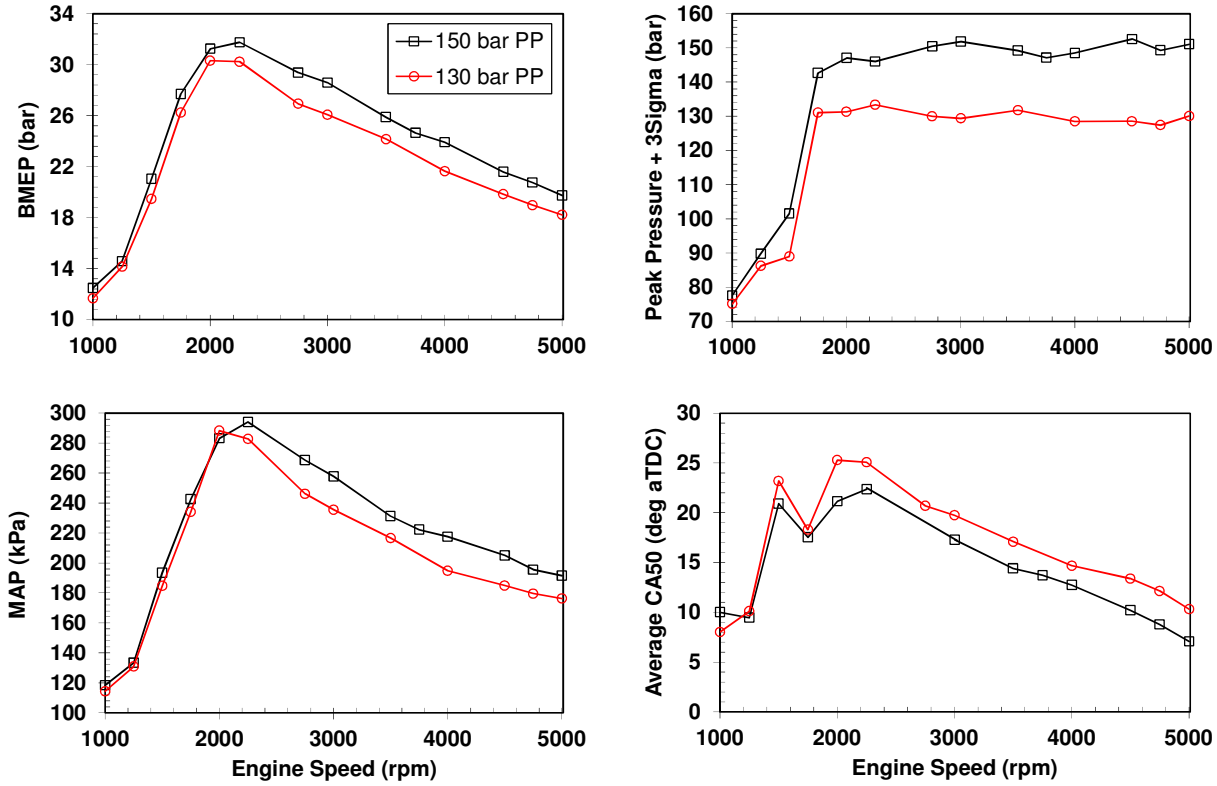

Figure 129 - BMEP for ETDI at 150 bar and 130 bar peak cylinder pressure limits.

Twin Scroll Turbochargers at 12:1 CR

As mentioned previously, twin scroll turbochargers were utilized to minimize the effects of V8 exhaust blowdown interference. An available twin scroll turbocharger from a production I4 engine application was used. The specifications for this turbocharger supplied by the manufacturer indicated that the turbocharger would be reasonably well matched for the 5.0L V8 application. However, the compressor surge line on the running engine was found to lie significantly within the surge line supplied by the manufacturer. This was not a limit for GTDI, since the low speed BMEP is constrained by knock, but was a significant limit for low speed BMEP for ETDI.

GTDI

Full load performance for GTDI at 12:1 CR with twin scroll turbochargers for lambda = 1 and lambda = 0.8 is shown in Figure 130. As shown, at 12:1 CR, the engine is extremely knock-limited with 91 RON gasoline, and consequently stoichiometric air-fuel ratio requires a drastic reduction in boost level and severe loss in BMEP. A comparison of 12:1 CR and 9.5:1 CR at lambda = 0.8 is shown in Figure 131. In this comparison, the 12:1 CR data was taken with twin scroll turbochargers and the 9.5:1 CR data was taken with single scroll turbochargers. In spite of this advantage in reduced blowdown interference effects, 12:1 CR still results in a severe degradation in boost levels and BMEP, even when running with enrichment.

Vehicle simulation analysis for GTDI was based on data acquired at 9.5:1 CR. Although the BMEP at 0.8 lambda is significantly degraded at 12:1 CR, it should be sufficient for driveability with reduced performance if E85 is not available (17.2 bar BMEP at 2500 rpm) for an E85 optimized FFV engine.

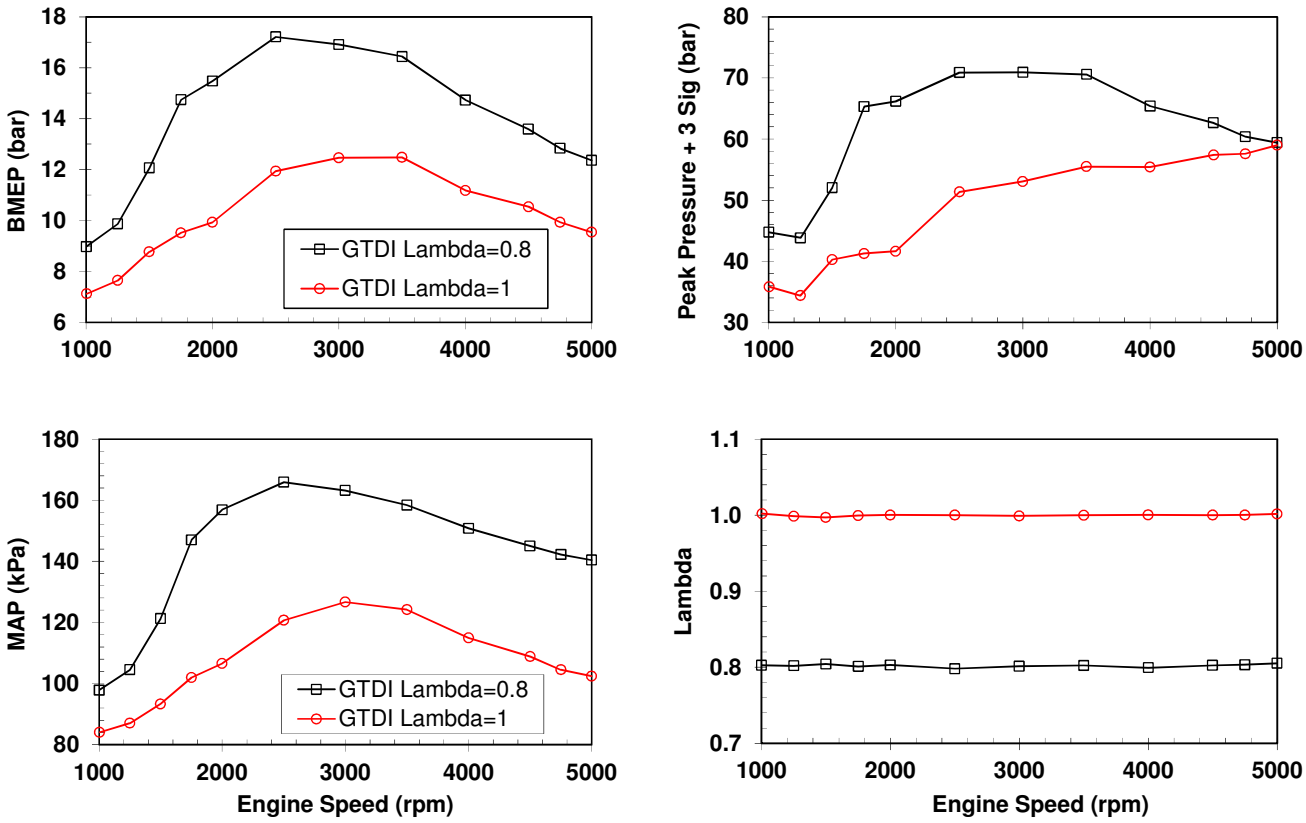

Figure 130 - Full load for GTDI at 12:1 CR with lambda = 1 and 0.8.

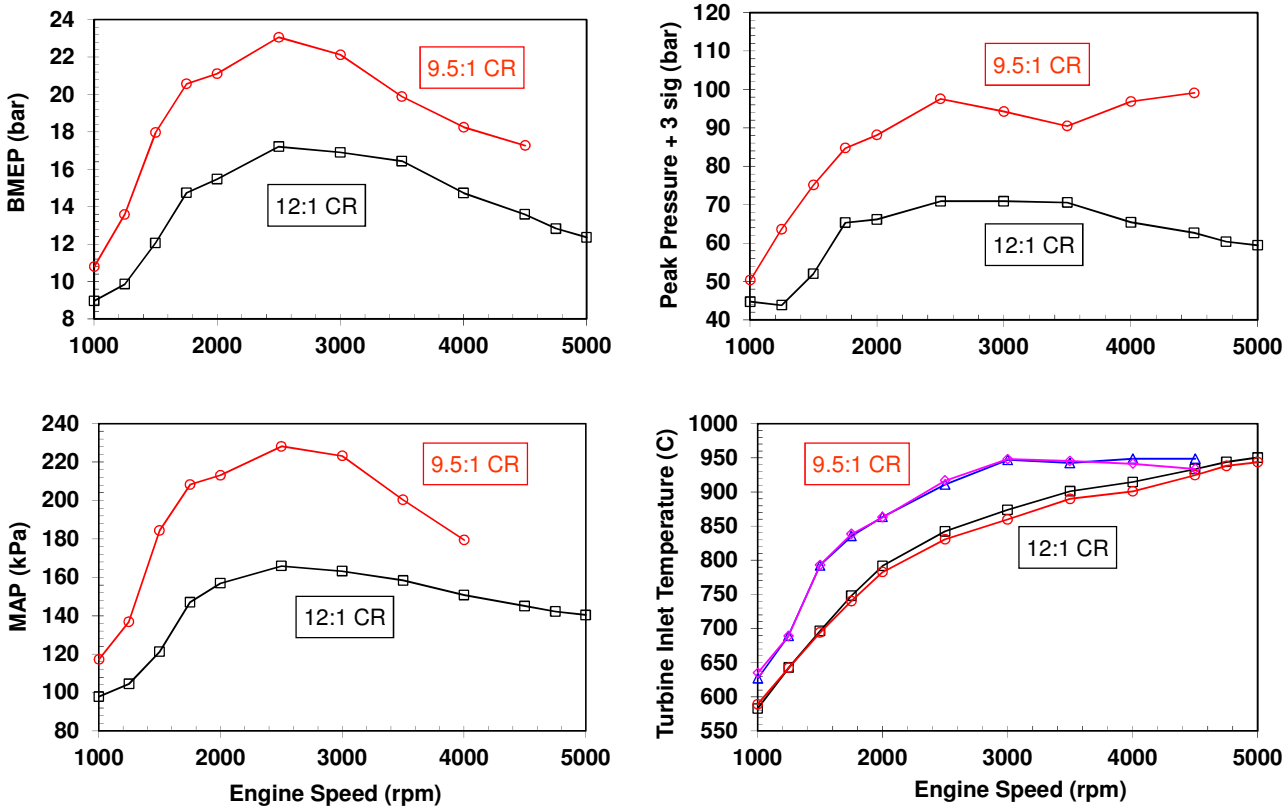

Figure 131 - Full load performance for GTDI at lambda = 0.8 for compression ratios of 12:1 and 9.5:1.

ETDI

As mentioned previously, the data for ETDI with twin scroll turbochargers was affected by compressor surge at low engine speeds. A comparison of full load performance with ETDI for 9.5:1 and 12:1 CR with twin scroll turbochargers is shown in Figure 132. At equal combustion phasing, increasing compression ratio results in reduced exhaust enthalpy due to increased expansion ratio, which results in reduced turbine work and boost levels at low engine speeds. In principle, this loss in low speed exhaust enthalpy could be recovered with spark retard, but this was precluded by compressor surge. As shown in Figure 133, the surge line observed on the engine was significantly inside the surge line of the map supplied by the turbocharger supplier.

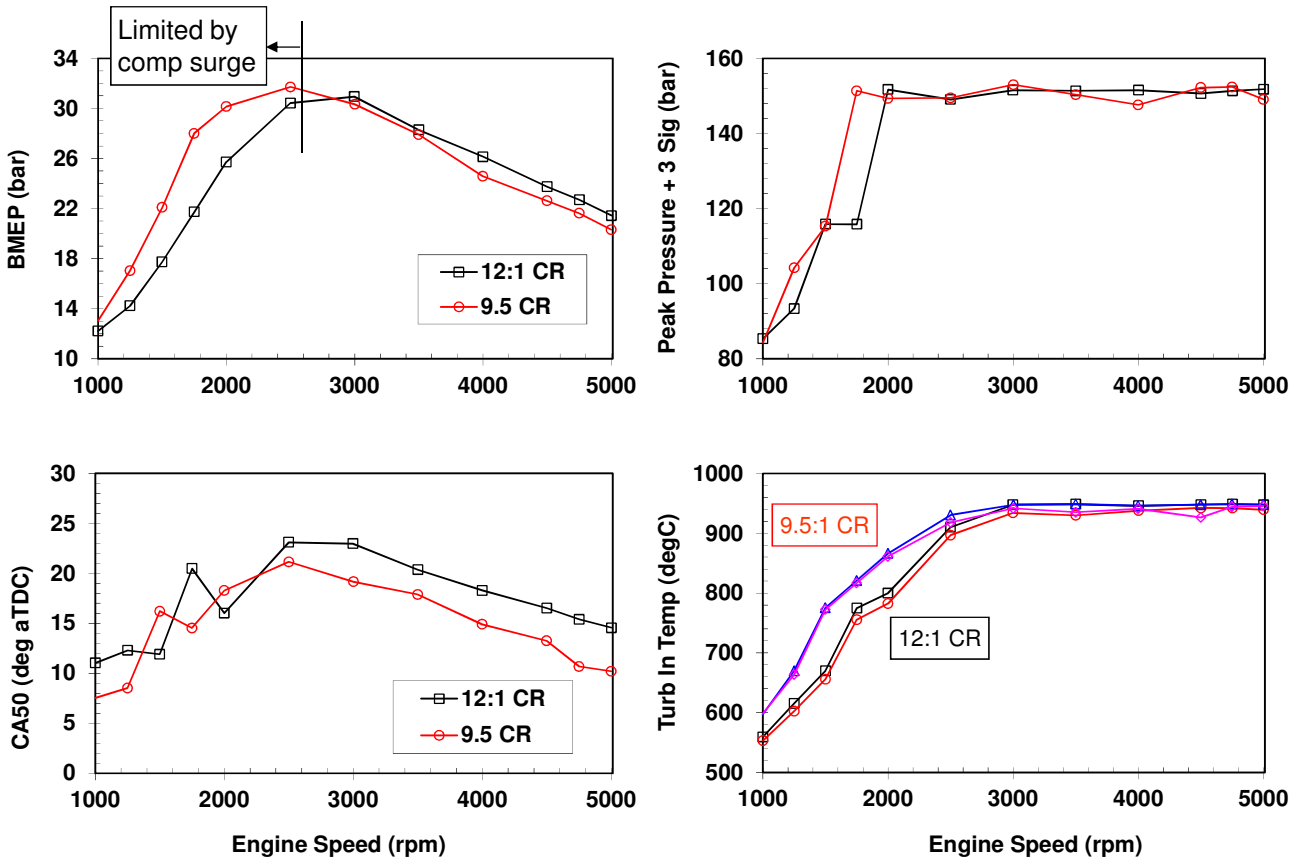

Figure 132 - BMEP comparison for ETDI at 12:1 CR and 9.5:1 CR at stoichiometry.

Analysis with the GT-POWER model indicates that with a properly specified compressor the low speed BMEP for 12:1 CR will be slightly greater than for 9.5:1 CR, similar to the behavior at medium to high engine speeds. In stark contrast with gasoline, increasing CR to 12:1 with E85 resulted in slightly improved performance at 3000 rpm and above, even at the peak pressure and turbine inlet temperature limits. Increased compression ratio results in increased expansion ratio with an associated reduction in turbine inlet temperature, which at higher engine speeds where the engine is at the turbine inlet temperature limit allows additional combustion phasing retard to hold the peak pressure limit.

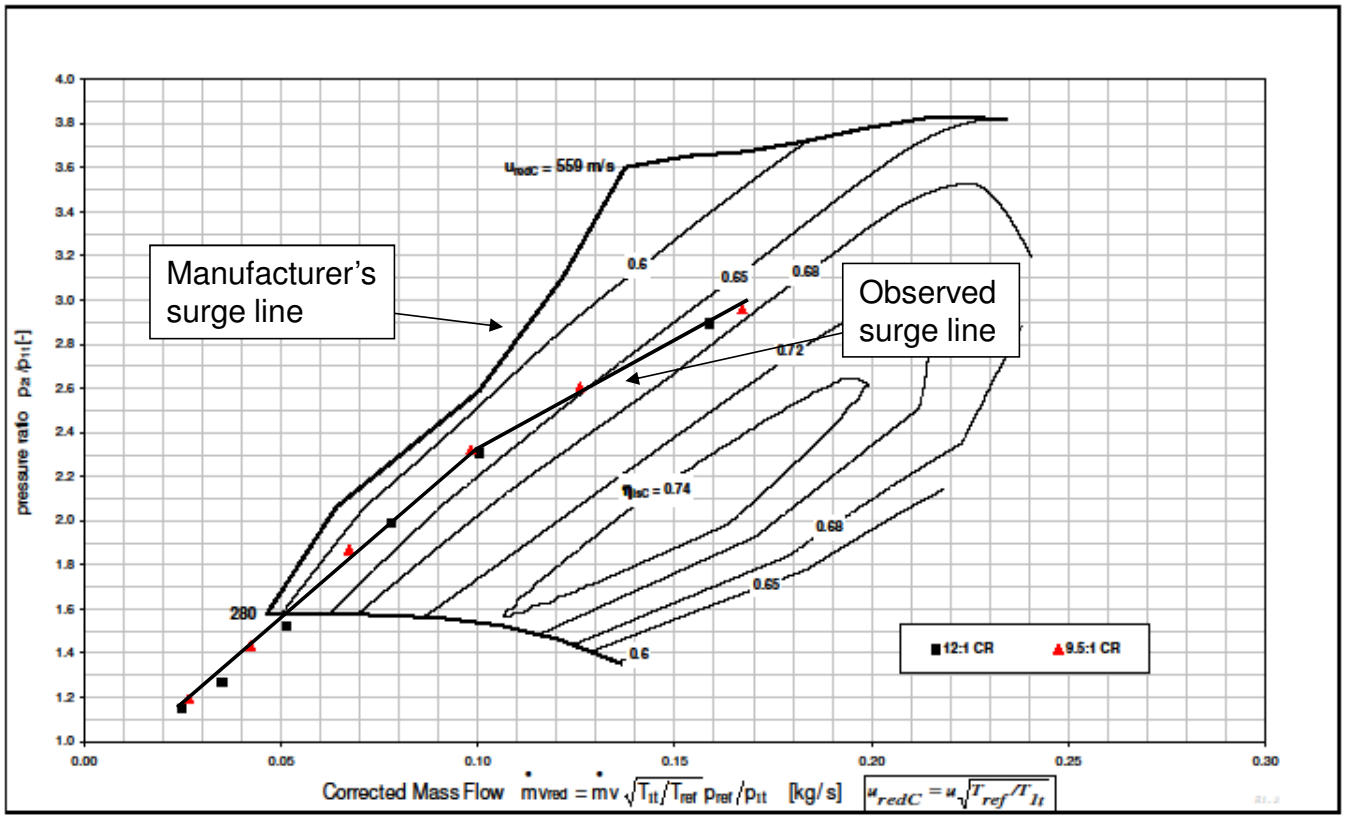

Figure 133 - Compressor map for twin scroll turbocharger illustrating discrepancy in the surge line.

It is noteworthy that during the course of multi-cylinder engine testing, no issues with low speed pre-ignition were encountered with the Dual Fuel engine or the E85 FFV engine, presumably due to the absence of particulate/soot formation with E85 and the charge cooling effect associated with direct injection of E85. In addition, no issues with injector coking/deposits were encountered with the Dual Fuel engine or the E85 FFV engine, due to the cleaning properties of ethanol and the absence of particulate/soot formation.

Part Load

Steady state engine dynamometer data was taken at part load to provide data for vehicle level projections using AVL's CRUISE vehicle simulation model (see Phase IV – Engineering Development, Vehicle Simulation Analysis). As shown in Figure 123, both 9.5:1 CR and 12:1 CR were investigated, and twin scroll turbochargers were utilized to minimize the effects of V8 blowdown interference (see Phase III – Advanced Development, Blowdown Interference). For each configuration, injection timing sweeps were performed to determine optimum fuel injection timing for direct injection of E85, and camshaft timing sweeps were performed to determine the optimum camshaft timing settings (Figure 134) for best BTE using twin independent variable camshaft timing (TiVCT) utilizing a dual retard strategy [6].

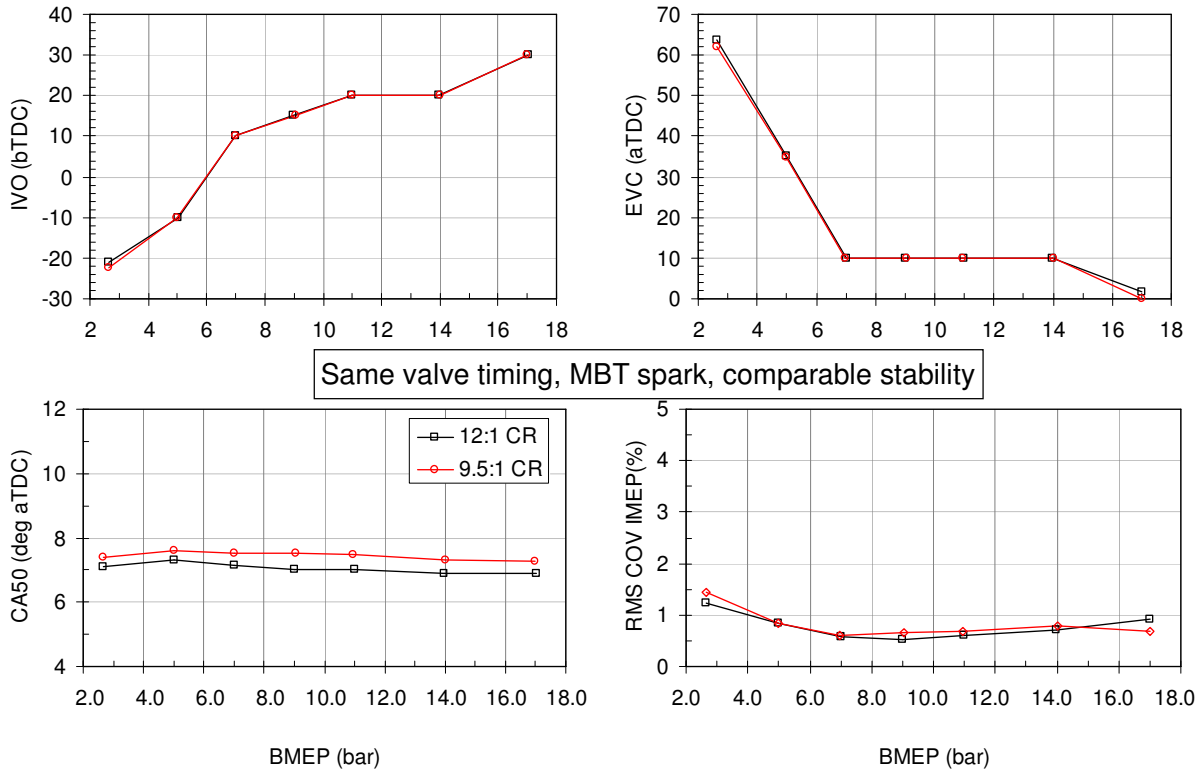

Figure 134 - Engine conditions for BMEP sweep at 2500 rpm.

Figure 135 and Figure 136 show BMEP sweeps at 1500 rpm and 2500 rpm, respectively, for 12:1 CR and 9.5:1 CR at MBT spark timing (CA50 of 7° aTDC) at the optimum camshaft and injection timings. As shown, the amount of E85 required to avoid knock increases substantially with increasing CR, as expected. Also as expected, brake thermal efficiency (BTE) improves with higher CR. Total BSFC is the combined BSFC for E85 and gasoline, calculated as (E85 mass fuel flow + gasoline mass fuel flow)/ brake power). At low BMEP when E85 is not required to avoid knock, total BSFC is better for 12:1 CR than for 9.5:1 CR, due to improved BTE. At high BMEP when E85 is required to avoid knock, the heating value per mass penalty of E85 more than offsets the BTE improvement associated with higher CR, and total BSFC is higher for 12:1 CR than for 9.5:1 CR.

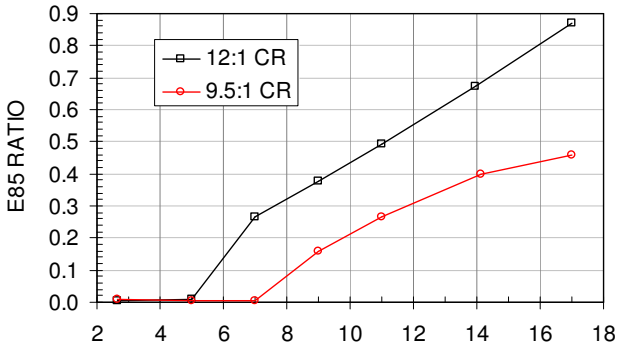

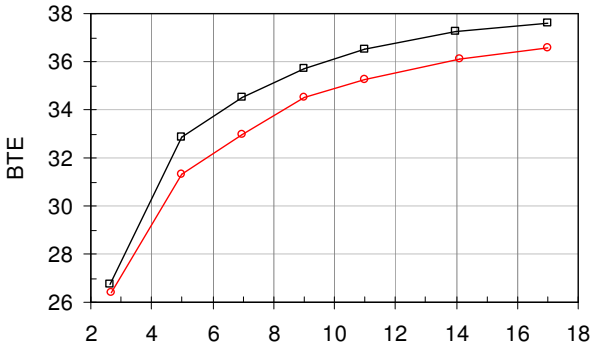

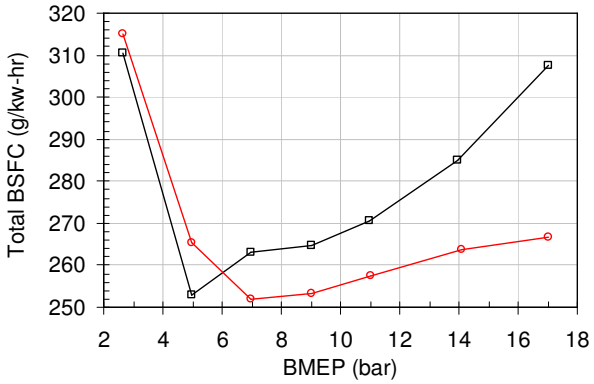

12:1 vs. 9.5:1 CR

- Improved BTE
- Increased E85 ratio
- Better total BSFC at light load; worse at high load at MBT

Figure 135 - Dual Fuel BMEP sweep at 1500 rpm for 9.5:1 and 12:1 CR.

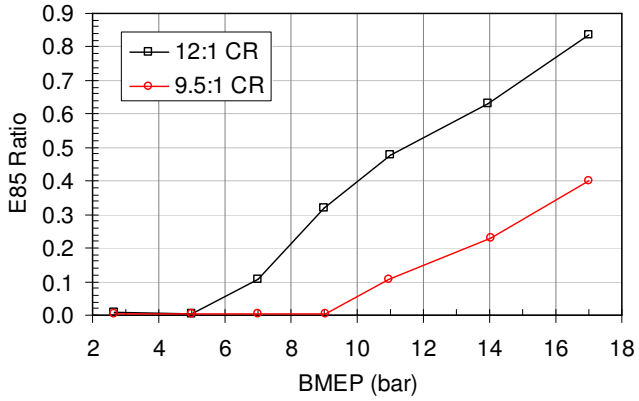

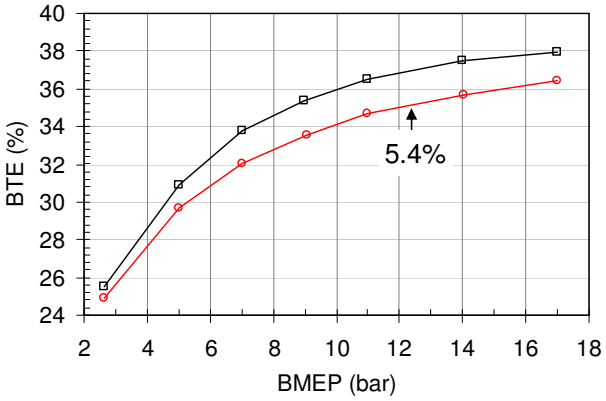

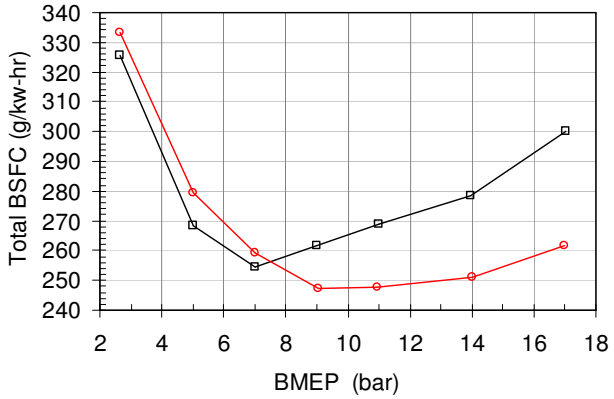

12:1 vs. 9.5:1 CR

- Improved BTE
- Increased E85 ratio
- Better total BSFC at light load; worse at high load at MBT

Figure 136 - Dual Fuel BMEP sweep at 1500 rpm for 9.5:1 and 12:1 CR.

Spark retard from MBT significantly reduces the amount of E85 required to avoid knock, as shown in the lower left plot of Figure 137. Initially spark retard has a very limited effect on thermal efficiency but a large effect on the peak unburned gas temperatures which govern knock kinetics. As spark is retarded and the amount of E85 is reduced, the amount of gasoline must be increased, and the brake thermal efficiency of the engine degrades due to non-optimal combustion phasing. However, because of E85's low heating value per mass compared to gasoline, the combined mass quantity of fuel initially decreases as the spark is retarded. This results in a minimum combined BSFC at moderate spark retard. With further retard, the combined BSFC degrades because of the increasing effect of spark retard on thermal efficiency.

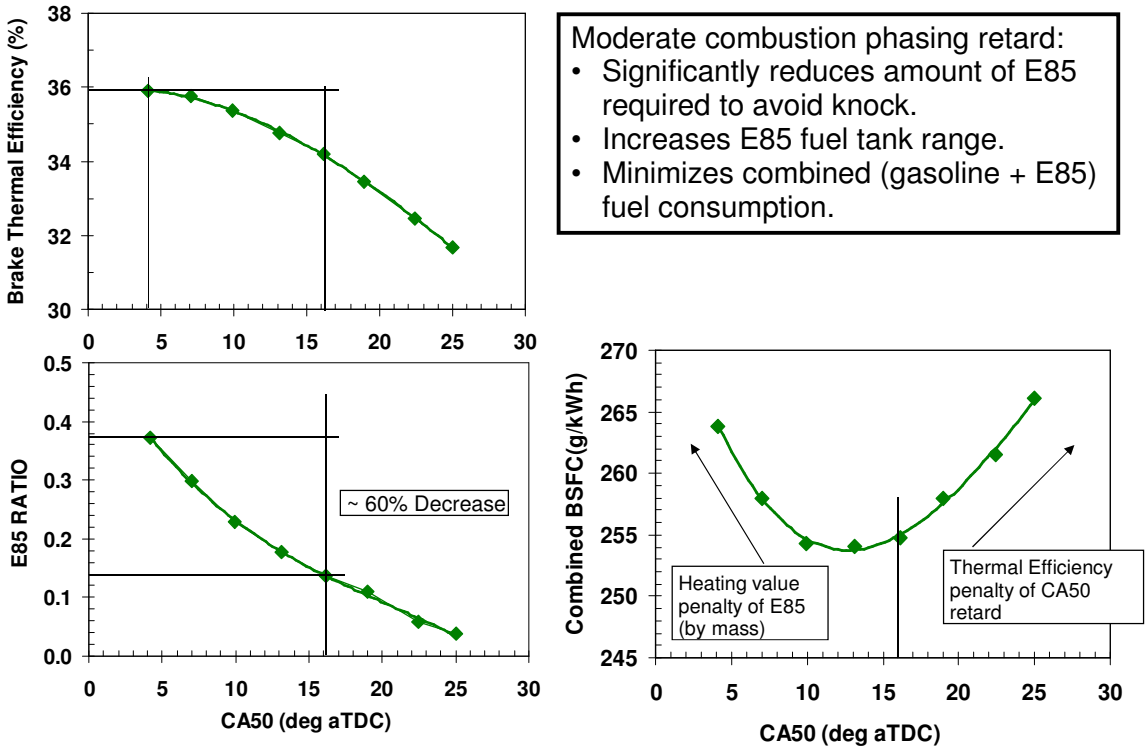

Figure 137 - Effect of combustion phasing retard on BTE, E85 Ratio, and combined BSFC.

To minimize the total fuel flow used in the vehicle simulations for the Dual Fuel engine, spark sweeps were run at each rpm-BMEP point of Figure 135 and Figure 136. From these spark sweeps, the combustion phasing for minimum total BSFC was determined at each rpm-BMEP point, and the corresponding E85 ratio and BTE were quantified. This data is shown in Figure 138 and Figure 139, and was used as input to the vehicle simulation program for the Dual Fuel engine. Since the E85 optimized FFV engine uses 100% E85, data at MBT combustion phasing was used as input to the vehicle simulation program for that configuration to provide the lowest fuel and energy consumption and CO_2 emissions.

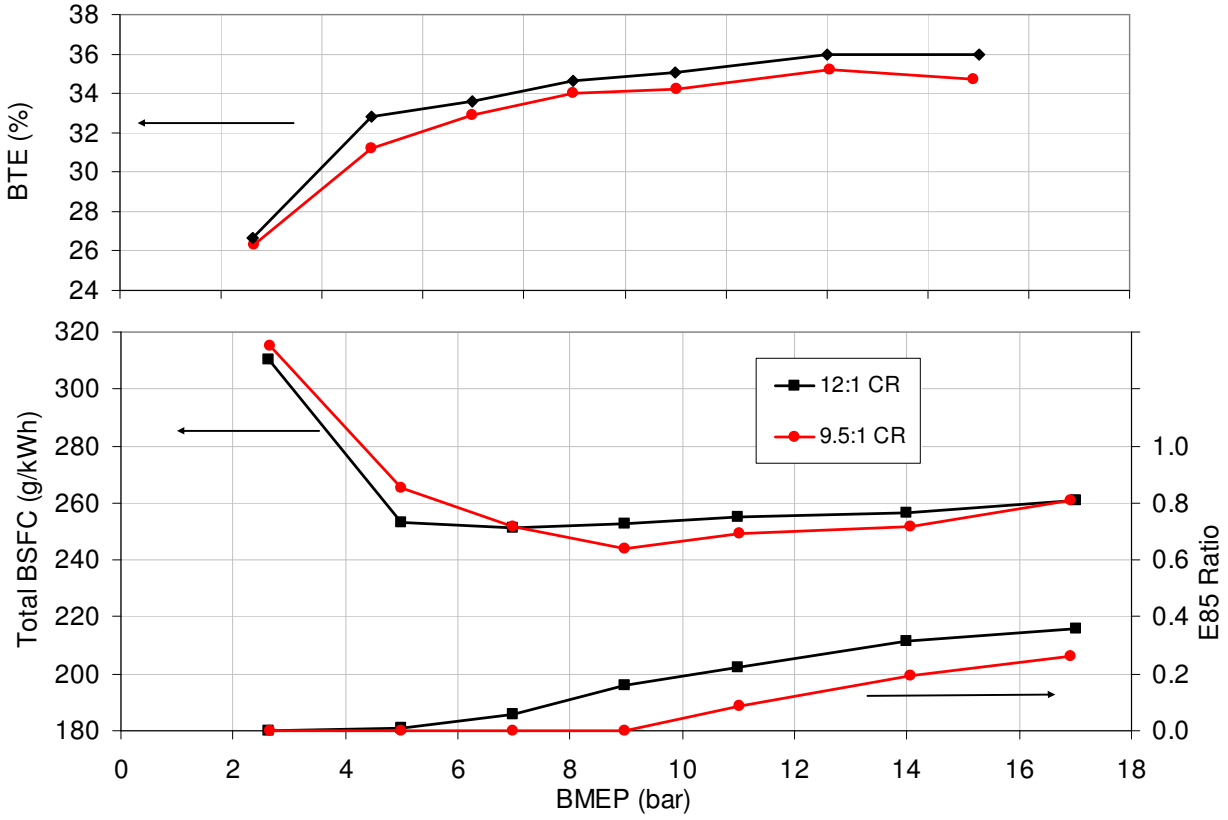

Figure 138 - Brake thermal efficiency, total BSFC, and E85 ratio vs. BMEP at 1500 rpm.

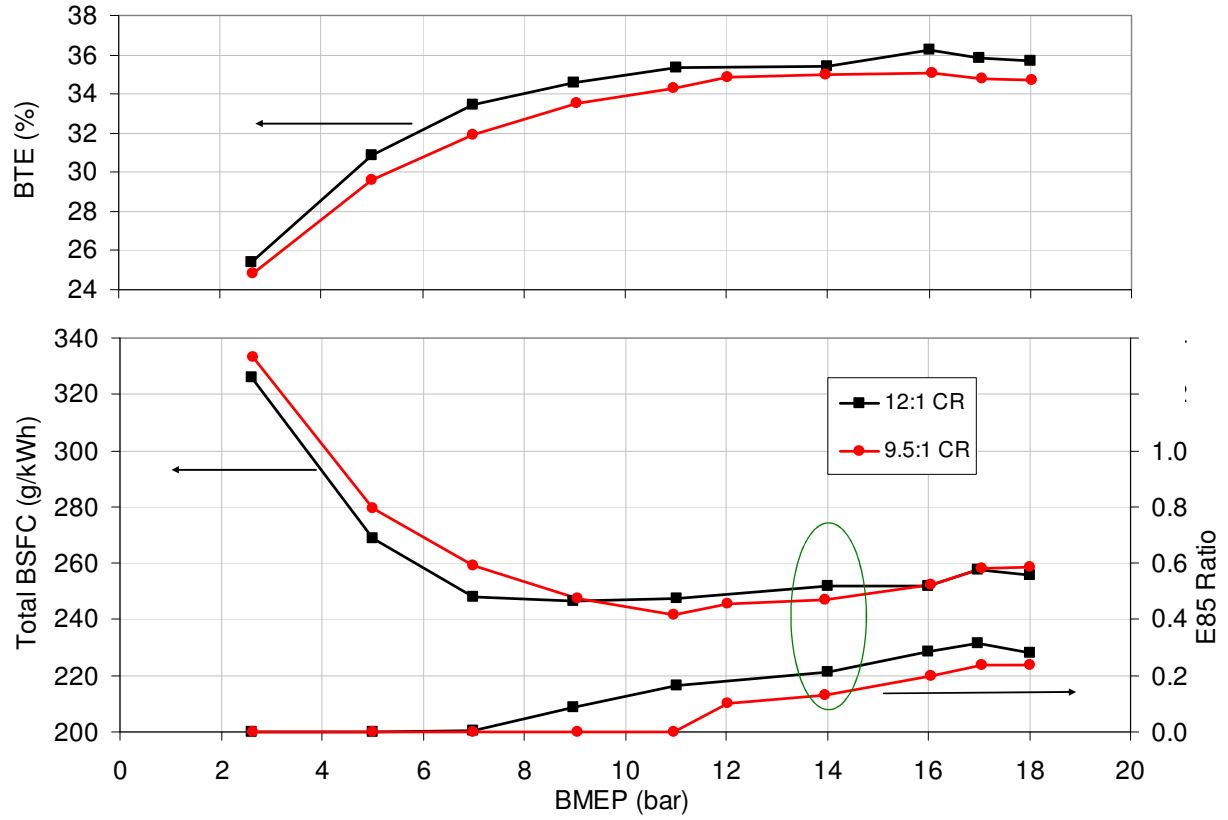

Figure 139 - Brake thermal efficiency, total BSFC, and E85 ratio vs. BMEP at 2500 rpm.

Trailer Towing

Because trailer towing is an important attribute for the F-Series pickup, trailer towing with a Dual Fuel engine was investigated in detail. Figure 140 and Figure 141 show data for a combustion phasing sweep for 9.5:1 CR and 12:1 CR at 2500 rpm, 14 bar BMEP. This rpm-BMEP point corresponds to towing a 10,000 pound trailer at 65 mph up a 1% grade with a 3.0L engine in a F150. Detailed analysis of data at this point is shown to illustrate the effects of both CR and combustion phasing retard on E85 consumption and brake thermal efficiency (BTE) under heavy load conditions.

As shown in Figure 140 and Figure 141, 12:1 CR results in improved BTE and lower CO_2 emissions at a given combustion phasing. Also at a given combustion phasing, the amount of E85 required to avoid knock is greater at 12:1 CR. Because of the increased E85 mass flow rate and the heating value per mass penalty of E85 relative to gasoline, the combined BSFC is higher for 12:1 CR than for 9.5:1 CR until a combustion phasing corresponding to a CA50 of about 17° aTDC. At this point, the thermal efficiency benefit of higher CR is directly offset by the heating value per mass penalty of greater E85 mass flow rate.

It is interesting that the slope of the E85 mass flow vs. CA50 curve in Figure 140 is greater for 12:1 CR than for 9.5:1 CR. This is a consequence of the high sensitivity of ethanol to unburned gas temperature [4]. As combustion phasing is retarded, unburned gas temperature is reduced. Because of the non-linearity of knock kinetics to temperature, this reduction in temperature has a greater effect at increased CR. Due to the higher slope of E85 mass flow rate as a function of combustion phasing, the minimum combined BSFC occurs at later CA50 for 12:1 CR than for 9.5:1 CR.

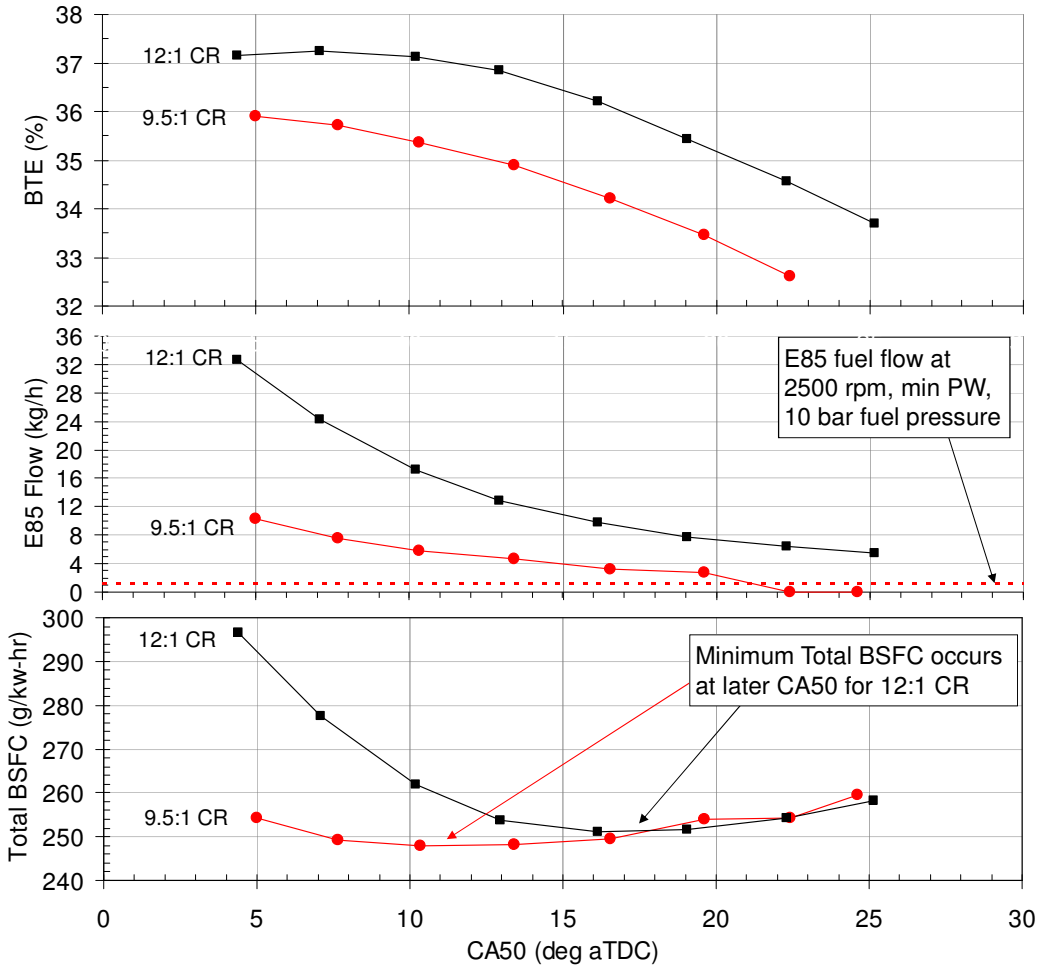

Figure 140 - Brake thermal efficiency, mass flow rate of E85, and total BSFC at 2500 rpm/14 bar BMEP.

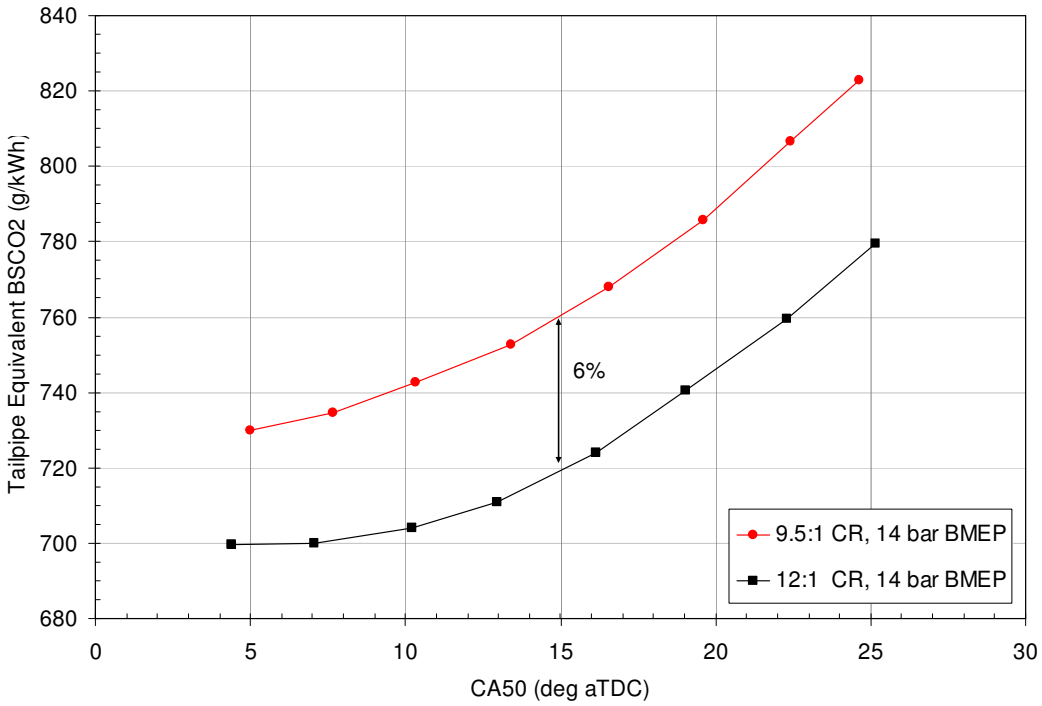

Figure 141 - CO_2 emissions for 2500 rpm, 14 bar BMEP for 9.5:1 and 12:1 CR.

The E85 mass fuel flow rate data of Figure 140 is plotted as the E85 ratio in Figure 142, where the E85 ratio is defined as the mass flow rate of E85 divided by the total mass fuel flow rate (E85 + gasoline). As shown, at the combustion phasing for minimum total BSFC, E85 ratio is increased from about 0.15 to about 0.25 as CR is increased form 9.5:1 to 12:1.

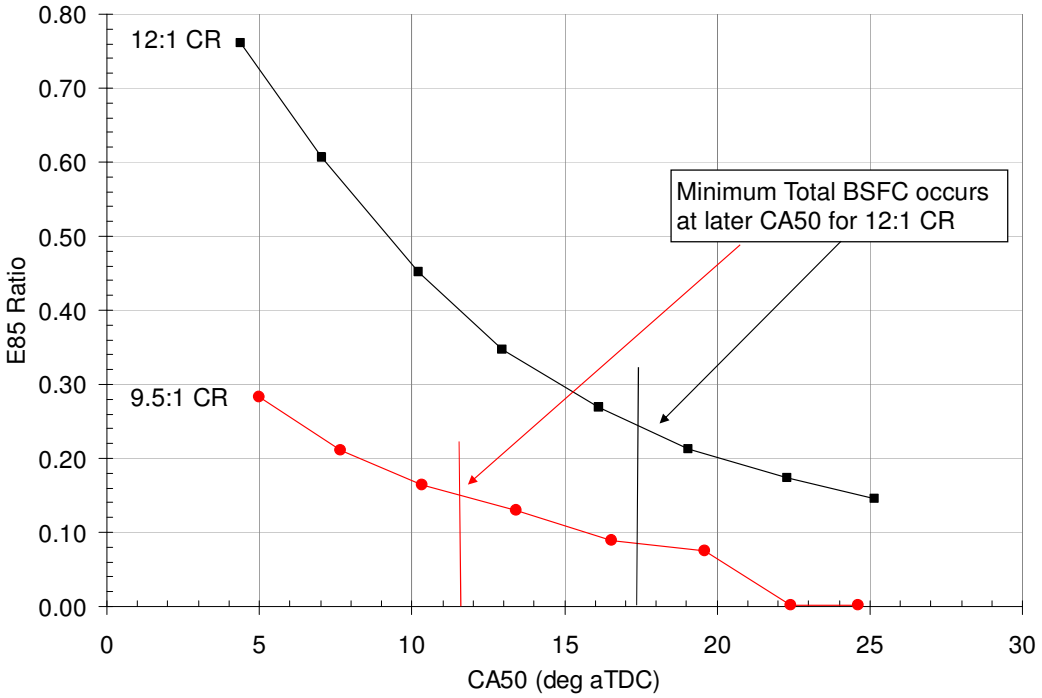

Figure 142 - E85 ratio vs. CA50 at 2500 rpm, 14 bar BMEP for 9.5:1 and 12:1 CR.

The tank range ratio (TRR), which is defined as the range on the E85 tank divided by the range on the gasoline tank, is an important factor for customer acceptance of the Dual Fuel engine concept. For a given ratio of tank sizes, the TRR is a simple function of the E85 mass ratio, as shown by the green line in Figure 143 for an E85 tank which is one-third the size of the gasoline tank (for example, a 9 gallon E85 tank and a 27 gallon gasoline tank).

Data for 2500 rpm, 14 bar BMEP at 9.5:1 CR is shown by the open red circles in Figure 143, at combustion phasings corresponding to MBT, minimum total BSFC, and minimum E85 fuel flow. The latter is determined by the minimum pulse width at reduced fuel rail pressure, and is shown by the dotted red line in the middle plot of Figure 140. A similar set of points is shown by the open black squares for 12:1 CR in Figure 144, except in this case the minimum E85 fuel flow is determined by the maximum combustion phasing retard which is still within the combustion stability limit. For this purpose, a CA50 limit of 30° aTDC has been used as a guideline.

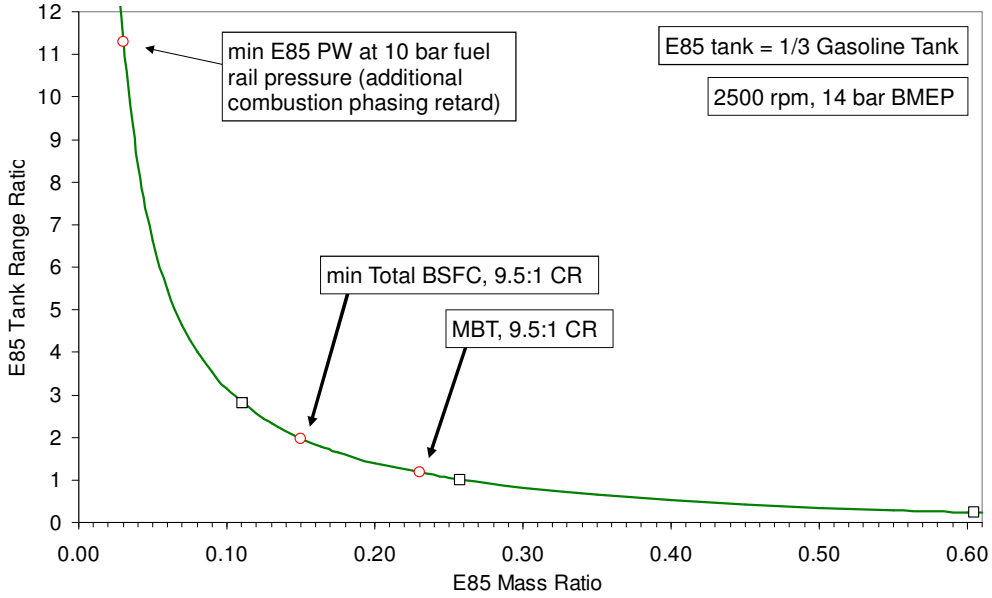

Figure 143 - E85 tank range ratio vs. E85 mass ratio for 9.5:1 CR at 2500 rpm, 14 bar BMEP.

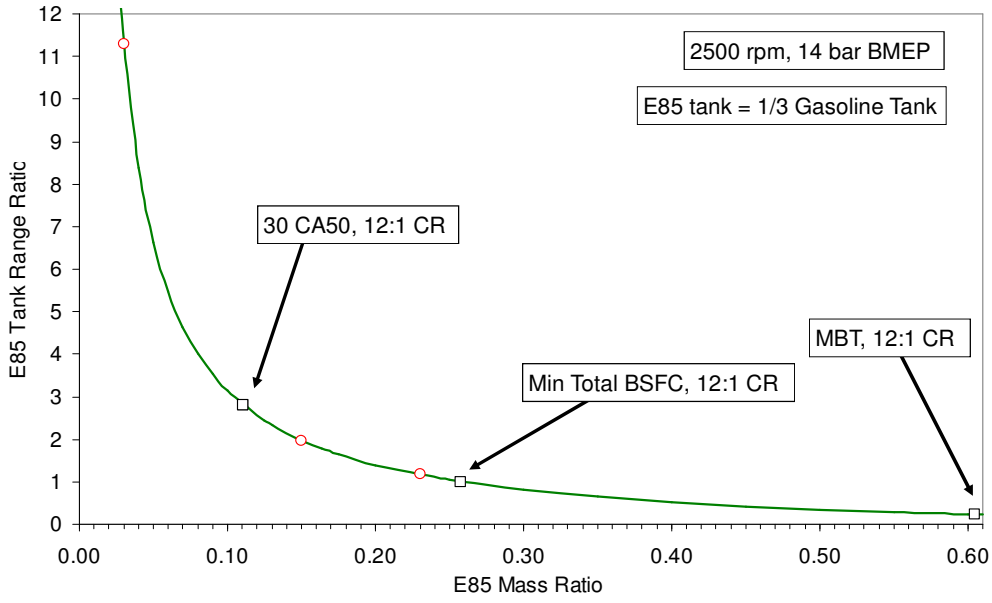

Figure 144 - E85 tank range ratio vs. E85 mass ratio for 12:1 CR at 2500 rpm, 14 bar BMEP.

Retarding combustion phasing beyond the phasing for minimum total BSFC is associated with a degradation in total BSFC, as shown in the middle plot of Figure 140. This total BSFC penalty can be plotted vs. the TRR, as shown in Figure 145. As shown, at 9.5:1 CR a TRR of over 11 can be achieved with only a 2% penalty in total BSFC. At 12:1 CR, a TRR of only about 3 can be achieved, and it is associated with a 5% total BSFC penalty.

Therefore, depending on the price and availability of E85, maintaining the CR at the level of the GTDI engine (9.5:1 CR in this case) may be desirable in order to obtain an acceptable TRR. For this reason, the fuel economy, energy consumption, and CO_2 emissions for the Dual Fuel engine shown in this report were evaluated at 9.5:1 CR.

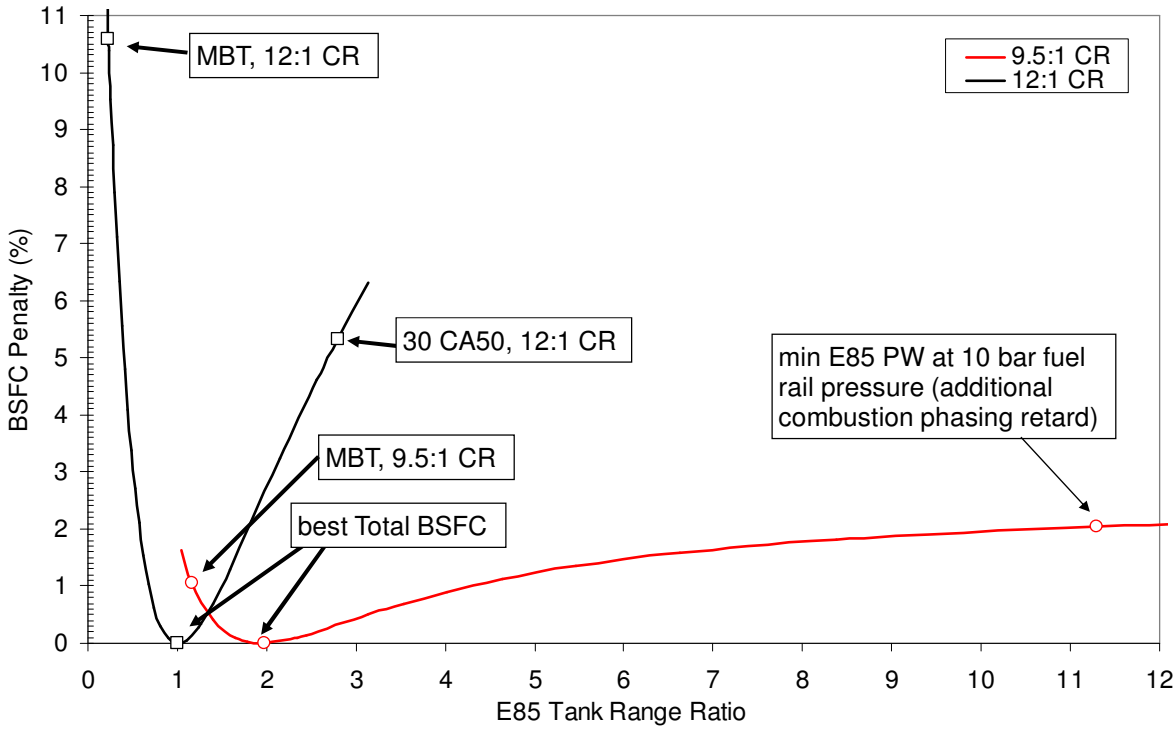

Figure 145 - Total BSFC penalty for combustion phasing advance/retard relative to min total BSFC phasing.

Performance and Fuel Economy Analysis (Task 3.0)

Vehicle Simulation Analysis

AVL-CRUISE vehicle simulation toolset was used to estimate vehicle level performance and fuel economy for the F150 pickup. Maps of fuel consumption as a function of engine speed and torque were developed based on the steady state data taken on the 5.0L V8 multi-cylinder engine (Task 4.0 - Multi-Cylinder Engine). Because the full load performance of the 5.0L V8 Dual Fuel and FFV engines far exceeds that of the baseline 6.2L naturally aspirated engine, maps were created for various displacement hypothetical V6 Dual Fuel and FFV versions of the engine, as well as a hypothetical 3.5L V6 GTDI engine. These maps were generated using the assumption that all engine variants have equal BSFC at equal BMEP and rpm as the 5.0L V8, and that the full load BMEP vs. engine speed is the same as the 5.0L V8, using the same fueling configuration as the particular variant.

A larger displacement 6.2L naturally aspirated engine was selected as the baseline comparator for the Dual Fuel and E85 optimized FFV engines. As a point of reference, the fuel economy and performance of the Dual Fuel and E85 optimized FFV engines are also compared to a hypothetical 3.5L GTDI engine. The fuel

economy map and full load performance of the hypothetical 3.5L GTDI engine which is based on the 5.0L V8 data varies somewhat from that of the production 3.5L GTDI "EcoBoost" engine in the F150. However, for relative comparisons of the Dual Fuel and E85 optimized FFV engines to a hypothetical 3.5L GTDI engine, the most accurate approach is to use engine maps and full load performance values based on data taken on the same engine, as illustrated in the Table 5.

Table 5 – Engines analyzed with vehicle simulation of F150 (NA = Naturally Aspirated, DF = Dual Fuel). 3.5L "EcoBoost" used for reference only.

	Data Source	DI	PFI
6.2L NA	production map	-	Gasoline
3.5L GTDI	scaled from 5.0L	Gasoline	-
3.5L/3.0L/2.5L DF	scaled from 5.0L	E85	Gasoline
3.5L/3.0L/2.5L FFV	scaled from 5.0L	E85	-
3.5L EcoBoost (reference only)		Gasoline	-

AVL-CRUISE analysis was performed for various drive cycles, including FTP74, Highway, US06, 70 mph cruise, and 70 mph cruise pulling a 10,000 pound trailer. FTP74 was run in place of FTP75 because the vehicle model was not configured to simulate the cold start portion of the FTP75 using stabilized warmed-up data as input. However, for the purpose of relative comparisons, FTP74 was used in place of FTP75 in combination with the Highway cycle to calculate M-H values.

Full Load Performance

Figure 146 and Figure 147 show full load performance metrics for the hypothetical 3.5L GTDI engine, various displacement hypothetical Dual Fuel engines, and the baseline naturally aspirated 6.2L engine (the engine configuration is shown along the top of each figure). The FFV variants are not shown in Figure 146 and Figure 147 since the Dual Fuel engines and the FFV engines both use E85 fuel at full load, and therefore the full load performance of these two engines is the same at the same displacement.

Figure 146 shows gradeability metrics for the F150. Gradeability denotes the maximum grade which can be sustained for the specified conditions, for example, "65 mph Max Grade in 6GL" is the maximum grade which can be sustained at 65 mph in 6th gear with the torque convertor locked. Similarly, Figure 147 shows acceleration metrics for the F150 for the same series of engines. Acceleration time denotes the time required for the vehicle to accelerate from the specified starting vehicle speed to the specified ending vehicle speed. For example, "40-60 mph with 10K Trailer" denotes the time required to accelerate from 40 mph to 60 mph while towing a 10,000 pound trailer.

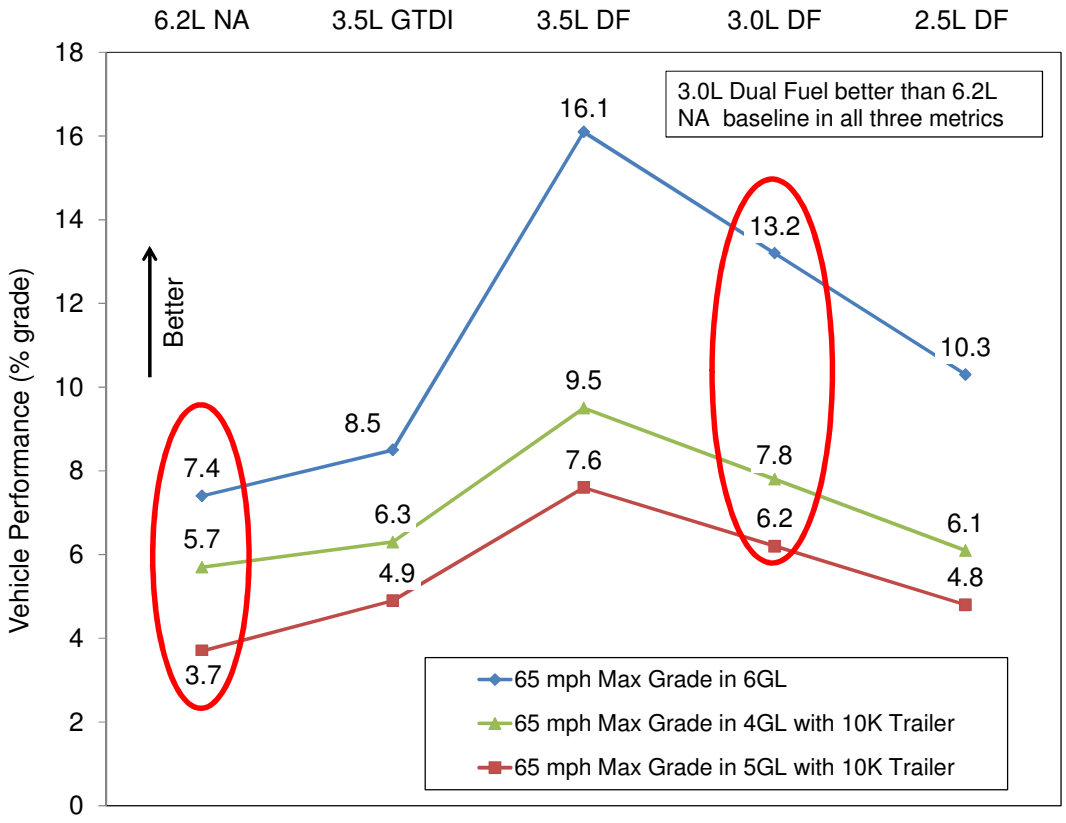

Figure 146 - Vehicle performance gradeability metrics for F150.

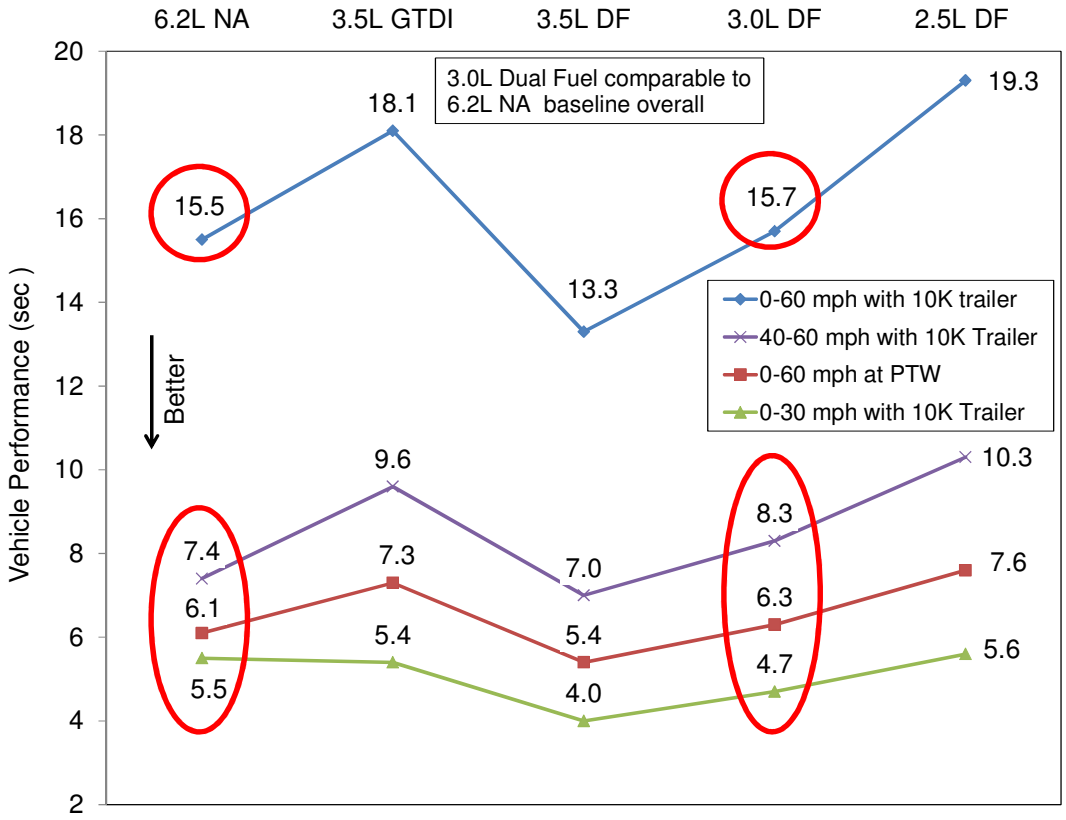

Figure 147 - Vehicle performance acceleration metrics for F150.

As shown in Figure 146 and Figure 147, a 3.0L Dual Fuel engine performs significantly better than the 6.2L baseline engine for gradeability metrics, and is comparable to the 6.2L baseline engine for acceleration metrics. Considering both sets of metrics, the overall performance of a 3.0L Dual Fuel engine is judged to be somewhat better than the baseline 6.2L naturally aspirated engine. To be conservative, 3.0L Dual Fuel and E85 optimized FFV engines are compared on the basis of equivalent vehicle performance to the 6.2L baseline engine for fuel economy, energy consumption, and CO_2 emissions. Note that the full load performance of the Dual Fuel engines is based on data taken at stoichiometry, whereas the performance of the baseline 6.2L and 3.5L GTDI engines is based on data taken with enrichment.

As shown in Figure 146 and Figure 147, the 3.0L Dual Fuel engine performs better than the 3.5L GTDI engine for all gradeability and acceleration metrics shown. The 3.5L GTDI shown in these figures is based on scaled data from the 5.0L engine for consistency with the Dual Fuel and E85 optimized FFV engines, and thus does not represent the performance of the production 3.5L "EcoBoost" engine.

Fuel Economy

The CRUISE vehicle simulation model was also used to estimate fuel economy in mpg for various drive cycles, including M-H, US06, 70 mph cruise, and 70 mph cruise towing a 10,000 pound trailer. Results are shown in Figure 148 for the 3.5L GTDI and Dual Fuel engines at 9.5:1 CR, and for the E85 optimized FFV engines at 12:1 CR. As will be discussed later in this report, the range on the E85 tank with the Dual Fuel engine is significantly reduced with increased CR. Therefore, to increase customer acceptance of the concept, the CR is maintained at the level of the baseline GTDI engine for the assessment of the fuel economy, energy consumption, and CO_2 emissions of the concept. The results for the E85 optimized FFV engine are at 12:1 CR because increasing CR is required to optimize the engine for use with E85 due to its very high effective octane. The implications of this high CR on performance with gasoline are discussed later.

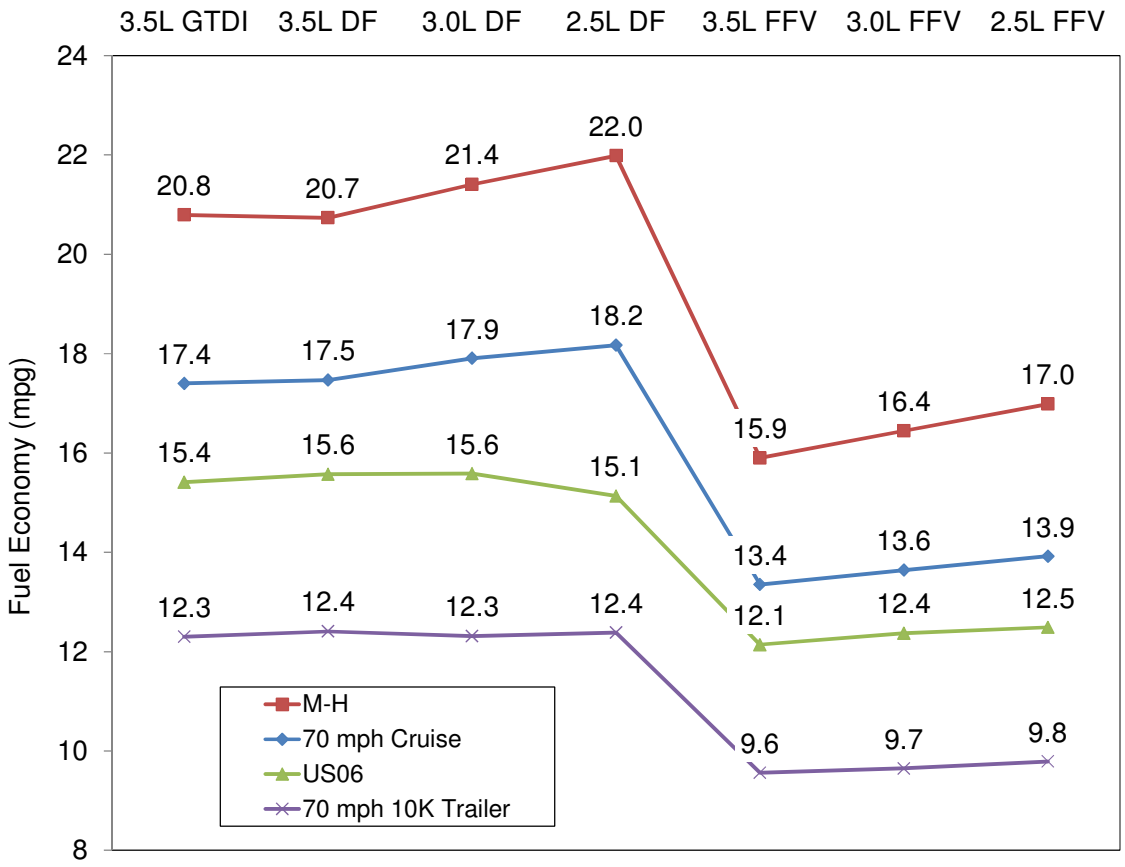

Figure 148 - Projected fuel economy for F150 for various drive cycles.

The 3.5L Dual Fuel engine would be expected to result in the same or slightly better fuel economy compared to the 3.5L GTDI engine at the same compression ratio. The slight degradation in fuel economy (0.1 mpg) shown in Figure 148 for the 3.5L Dual Fuel engine relative to the 3.5L GTDI engine is due to variability of the measured engine dynamometer data used to create the fuel consumption maps. As the Dual Fuel engine is downsized from 3.5L, fuel economy improves for the M-H cycle and for the 70 mph cruise condition. For the 70 mph cruise with a 10,000 pound trailer and for the US06 cycle, fuel economy is relatively unaffected by downsizing from 3.5L. This occurs because these latter two cases are heavily loaded, so the engine is not operating at light load conditions where additional downsizing would provide a fuel consumption benefit. For the 2.5L Dual Fuel engine, fuel economy in mpg degrades slightly for the US06 cycle. This occurs because the engine is operating at high BMEP where E85 consumption is increased, and the lower net heating value of E85 compared to gasoline results in a slight mpg degradation.

Figure 148 includes results for the E85 optimized FFV versions of the engine at 12:1 CR. The fuel economy in mpg is degraded for the FFV engines compared to the Dual Fuel and 3.5L GTDI engines due to the net heating value per volume penalty of E85 relative to gasoline of approximately 29%. Since the engine is using only E85, fuel economy continues to improve slightly as the FFV engine is downsized to 2.5L for all drive cycles.

Comparison of the 3.0L Dual Fuel and E85 optimized FFV engines to the 3.5L GTDI engine is based on the results of Figure 148 which used self-consistent engine dynamometer data as input. As shown in Table 6, the E85 optimized FFV engine using E85 results in a mpg fuel economy penalty of about 8% relative to the baseline 6.2L naturally aspirated engine. This compares favorably with the reduced energy content per gallon of E85 relative to gasoline of 29%. The 3.0L Dual Fuel engine at 9.5:1 CR results in mpg fuel economy improvements of about 20% relative to the baseline 6.2L engine and about 3% relative to the 3.5L GTDI engine.

Table 6 - M-H fuel economy for 3.0L Dual Fuel (9.5:1 CR) and E85 optimized FFV (12:1 CR) engines.

Engine	M-H Fuel Economy (mpg)	Change (%)
6.2L Naturally Aspirated	17.8	base
3.5L GTDI (scaled from 5.0L data)	20.8	16.6
3.0L Dual Fuel (scaled from 5.0L data)	21.4	20.0
3.0L FFV E85 (scaled from 5.0L data)	16.4	- 7.8

Energy Consumption

Energy consumption for the various drive cycles is shown in Figure 149 for the same series of engines. One of the initial project objectives was to “Reduce FTP 75 energy consumption by 15% - 20% compared to an equally powered vehicle with a current production gasoline engine”. As previously done for fuel economy in mpg, the improvement in energy consumption in MJ per mile was calculated for the Dual Fuel and E85 optimized FFV engines relative to the 6.2L baseline engine and the results are shown in Table 7. As shown, the energy consumption for the 3.0L Dual Fuel and E85 optimized FFV engines is reduced about 21% and 26%, respectively, relative to the baseline 6.2L naturally aspirated engine, exceeding the project objective of 15 – 20% reduction.

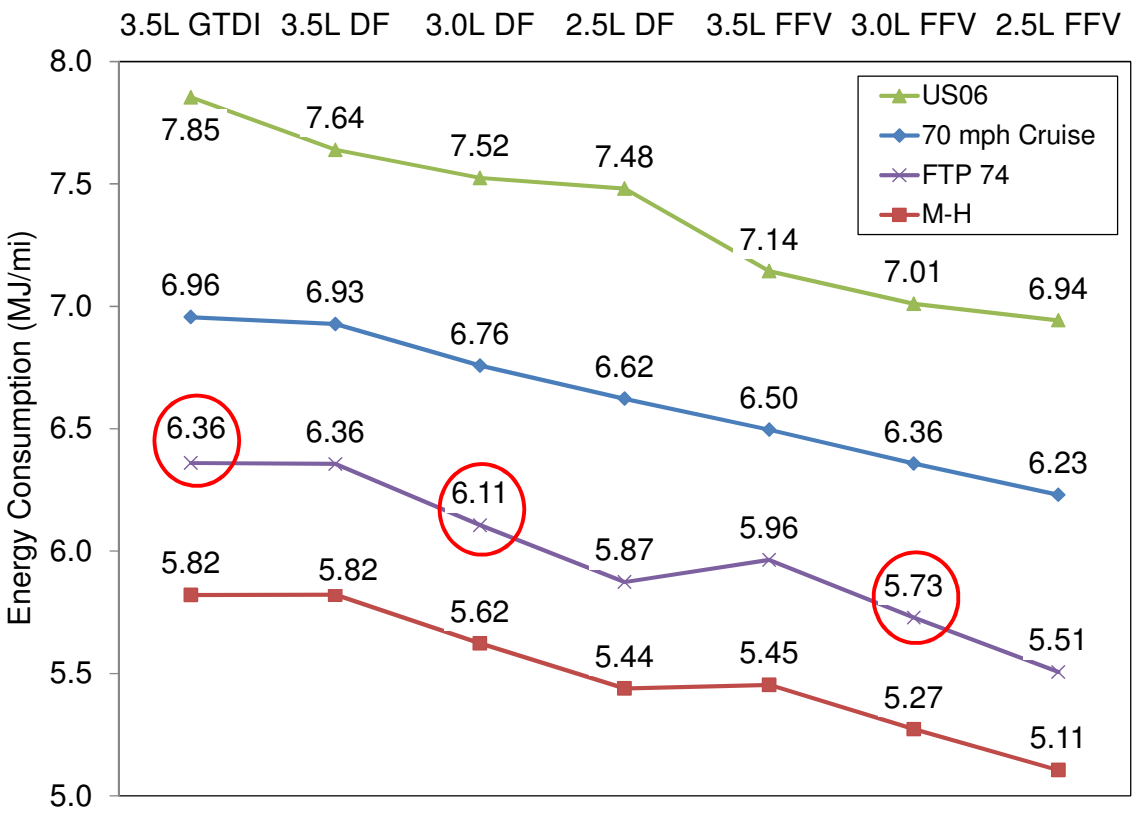

Figure 149 - Energy consumption for F150 for various drive cycles.

Table 7 - FTP74 energy consumption for 3.0L Dual Fuel and E85 optimized FFV engines.

Engine	FTP74 Fuel Economy (mpg)	FTP74 Energy Consumption (MJ/mi)	Improvement (%)
6.2L Naturally Aspirated	15.7	7.73	base
3.5L GTDI (scaled from 5.0L data)	19.0	6.36	17.8
3.0L Dual Fuel (scaled from 5.0L data)	19.8	6.11	21.1
3.0L FFV E85 (scaled from 5.0L data)	15.1	5.73	25.9

CO2 Emissions

CO_2 emissions for the M-H cycle calculated in the same manner are shown in Table 8. As shown, the 3.0L Dual Fuel and E85 optimized FFV engines result in CO_2 emission reductions of about 17% and 24%, respectively, relative to the 6.2L baseline gasoline engine.

Table 8 - CO_2 emissions for 3.0L Dual Fuel and E85 optimized FFV engines.

Engine	M-H CO_2 (g/mi)	Improvement (%)
6.2L Naturally Aspirated	495	base
3.5L GTDI (scaled from 5.0L data)	424	14.2
3.0L Dual Fuel (scaled from 5.0L data)	410	17.1
3.0L FFV E85 (scaled from 5.0L data)	379	23.5

E85 Tank Range for Dual Fuel Concept

For the Dual Fuel engine, an important consideration for customer acceptance of the concept is the refill frequency of the E85 tank relative to the gasoline tank. An output of the CRUISE vehicle simulation for the Dual Fuel engine for the various drive cycles is the fuel economy in mpg for both gasoline and E85. From these values, the tank range ratio (TRR) can be calculated. The TRR is the ratio of the number of miles which can be driven on a tank of E85 divided by the number of miles which can be driven on a tank of gasoline, which is equivalent to the ratio of the refill frequency for the two tanks. For example, a TRR of three means that the E85 tank will need to be refilled every third time that the gasoline tank is filled. For customer acceptance of the Dual Fuel concept, a high TRR is desirable.

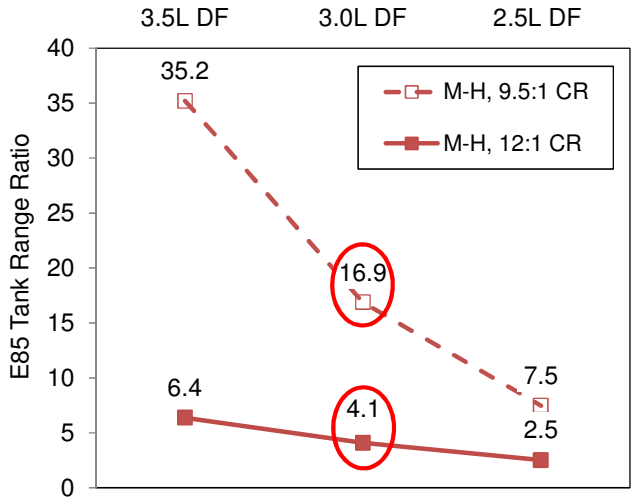

Figure 150 - Tank range ratio for M-H cycle.

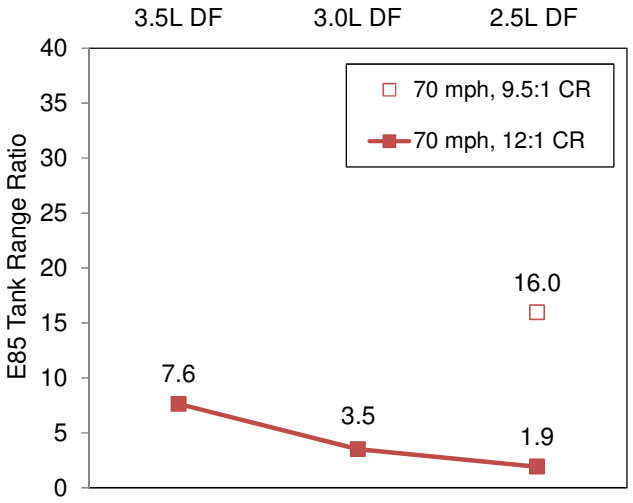

Figure 151 - Tank range ratio for 70 mph cruise.

Tank range ratios for the M-H cycle are shown in Figure 150 for Dual Fuel engines at 9.5:1 CR and 12:1 CR. As shown, decreasing engine displacement and/or increasing CR results in a significant reduction of TRR since a larger amount of E85 is required to avoid knock. For a 3.0L Dual Fuel engine, the TRR is reduced from 16.9 to 4.1 as CR is increased from 9.5:1 to 12:1. The TRR for a 70 mph cruise is shown in Figure 151. E85 is not required to avoid knock at 9.5:1 CR for 3.5L and 3.0L Dual Fuel engines at this condition, and therefore the TRR is infinite for these two cases. The TRR for towing conditions is discussed in detail in Task 4.0 – Multi-Cylinder Engine. As shown in that section, the TRR for towing conditions is significantly reduced for 12:1 CR compared to 9.5:1 CR. Therefore, depending on the price and availability of E85, maintaining the CR at

the level of the GTDI engine (9.5:1 CR in this case) may be desirable in order to obtain an acceptable TRR. For this reason, the fuel economy, energy consumption, and CO_2 emissions for the Dual Fuel engine shown in this report were evaluated at 9.5:1 CR.

Full Load Performance of E85 Optimized FFV Engine Using Gasoline

As stated previously, the fuel economy, energy consumption, and CO_2 emissions of the E85 optimized FFV engine were evaluated at 12:1 CR in order to utilize the high effective octane of E85 fuel. However, the performance of this FFV engine will be adversely affected by the high CR when the engine is operated on gasoline. The degradation in performance metrics for a 3.0L E85 optimized FFV engine operating on 91 RON gasoline relative to operating on E85 is shown in Figure 152. For reference, performance metrics are also shown for the 3.5L GTDI engine at 9.5:1 CR. Due to this significant degradation in performance, implementation of an E85 optimized FFV engine at high CR would be dependent upon the availability of E85.

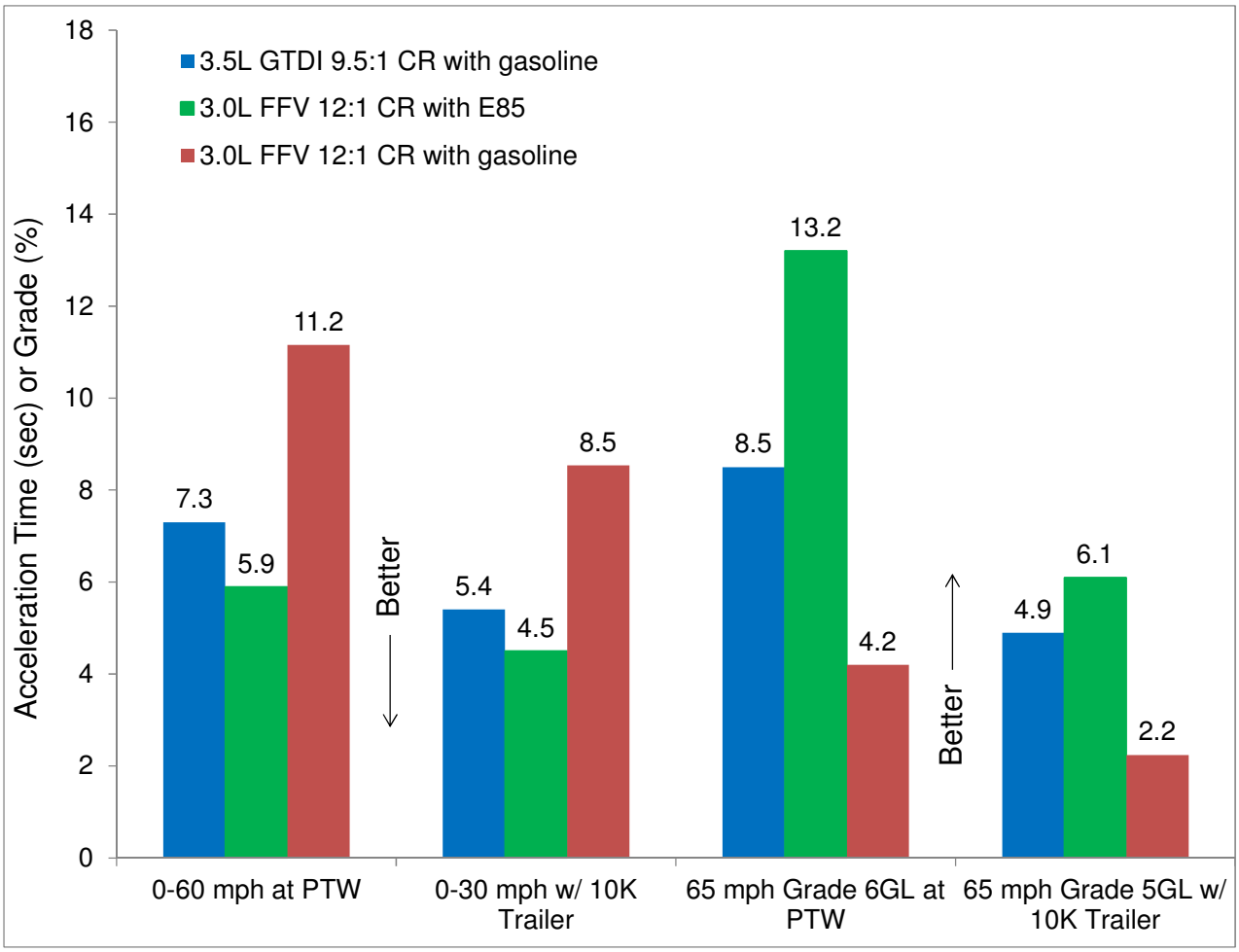

Figure 152 - Performance metrics for 3.0L FFV and 3.5L GTDI engines.

Leveraging of Ethanol to Replace Gasoline

Because direct injection of E85 enables very high BMEP and downsizing of the engine displacement, gasoline is used more efficiently in the vehicle, thereby leveraging the benefit of ethanol in reducing the consumption of gasoline. This is illustrated in Figure 153 for the vehicle simulation results for the F150 on the M-H cycle for the hypothetical engines which were scaled from 5.0L engine dynamometer data. The bars in Figure 153 represent the quantity of gasoline and ethanol which would be consumed driving the M-H cycle over and over for 1,000 miles. As shown, the 3.0L Dual Fuel engine at 9.5:1 CR consumes 0.9 gal of E85 in 1000 miles, but uses 2.3 less gallons of gasoline compared to the 3.5L GTDI engine. This is equivalent to one gallon of E85 replacing 2.5 gallons of gasoline.

The 3.0L E85 optimized FFV engine at 12:1 CR uses 60.8 gallons of E85 in 1000 miles, whereas the 3.5L GTDI engine uses 48.1 gallons of gasoline. This is equivalent to one gallon of E85 replacing 0.8 gallon of gasoline. Note that this is still a significant improvement compared to the heating value of E85 relative to that of gasoline; on an equal heating value basis, one gallon of E85 would replace 0.71 gallons of gasoline. The improvement from 0.71 to 0.8 is due to the increase in thermal efficiency in the vehicle as a result of higher CR and downsizing of the engine displacement.

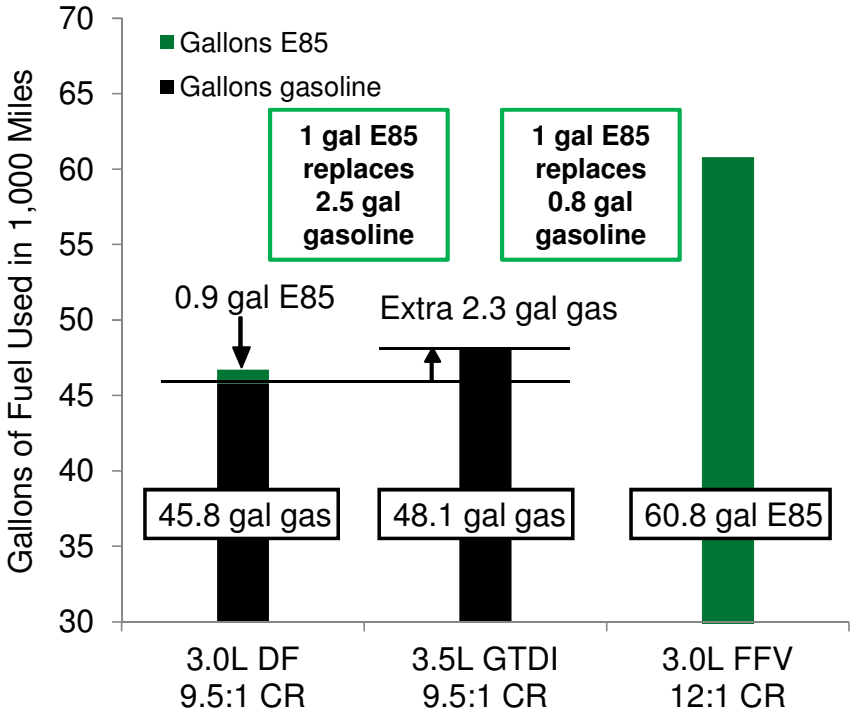

Figure 153 - Leveraging of E85 to replace gasoline for F150 on M-H cycle .

Cold Start Emissions Assessment (Task 4.0)

Summary

One of the primary project objectives was to meet at least ULEV emissions, with a stretch target of ULEV II/Tier II Bin 4. This section focuses on this objective by exploring the emissions capability of the Dual Fuel engine (PFI gasoline and DI E85). To facilitate this work and provide a baseline production vehicle emissions level, a PFI system was added to a production 3.5L TiVCT GTDI (EcoBoost) engine. Three cold start scenarios were investigated: 1) DI gasoline only (baseline GTDI), 2) DI E85 only (FFV engine using E85 fuel), and 3) Dual Fuel (DI E85 and PFI gasoline).

Typically, E85 worsens cold start capability at low ambient temperatures and increases cold start feedgas hydrocarbons. PFI gasoline can produce low feedgas emissions with good stability at relatively low exhaust enthalpy conditions, but at the higher exhaust enthalpy required to achieve timely catalyst activation in a turbocharged application, PFI-gasoline typically demonstrates unacceptable combustion stability.

Testing on an engine only dynamometer with a 150,000 mile equivalent aged Three Way Catalyst (TWC) system showed that Dual Fuel engine cold starts have the capability of meeting ULEV II/Tier II Bin 4 emissions standards and are generally equal to or better than the other cold start scenarios in terms of emissions and engine stability. The Dual Fuel engine and E85 optimized FFV engine provide near zero particulate emissions, but the cold start NMOG emissions for the E85 optimized FFV engine are higher than the baseline GTDI engine. A feasible calibration scenario for a dual injection/dual fuel cold start application was also developed.

Hardware

A production 2011MY F-Series 3.5L TiVCT GTDI EcoBoost engine (Figure 154) was modified to accept the intake manifold and fuel injectors from a 3.7L V6 PFI engine (Figure 155). Due to cylinder head design commonality, the 3.7L PFI intake manifold could be directly bolted on the 3.5L GTDI engine.

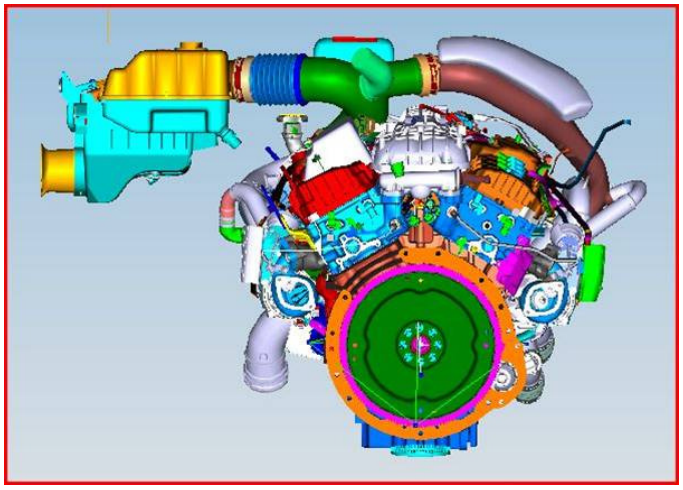

Figure 154 - Rear view of 3.5L TiVCT GTDI engine.

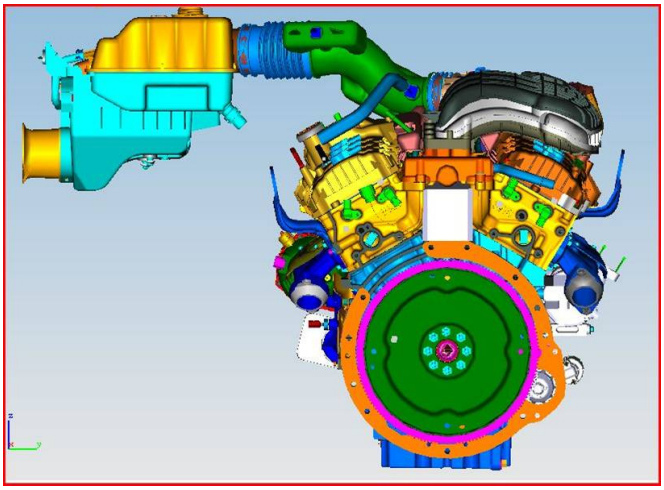

Figure 155 - Rear view of 3.7L PFI engine.

A small addition of welded material was required on the cylinder head intake flange to ensure adequate sealing of the intake manifold. Additionally, an injector pocket cutout for the PFI fuel injector was required to provide clearance for the injector and spray (Figure 156). Injector layout was a compromise between wetting of the port near the injector tip (the "doghouse") and ideal spray targeting on the back of the intake valve. The final PFI targeting is shown in Figure 157. This less than ideal, but acceptable, injector targeting shows part of the spray contacting the port floor while avoiding excessive wetting of the doghouse.

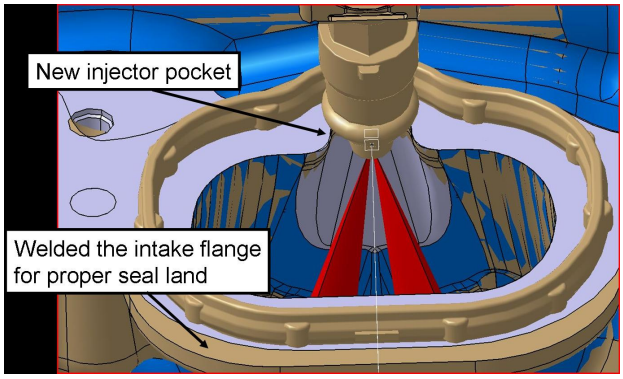

Figure 156 - Cylinder head modifications.

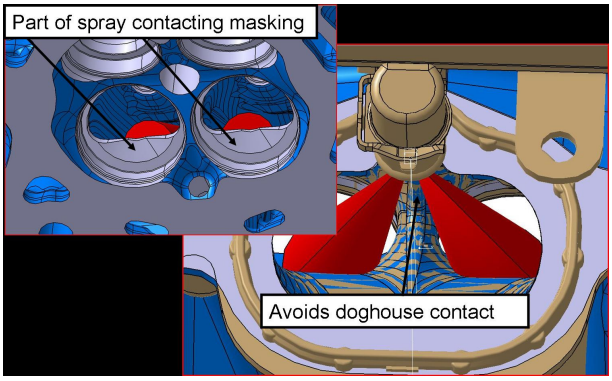

Figure 157 - PFI injector targeting.

Dynamometer Cold Start Optimization

Test hardware consisted of a modified 3.5L TiVCT GTDI with a 3.7L PFI intake manifold and injectors. Three fueling scenarios were evaluated: 1) DI gasoline (EcoBoost baseline), 2) DI E85 (Flex Fuel) and 3) DI E85 + PFI gasoline (Dual Fuel). Cold start testing was conducted at Ford's Dearborn Dynamometer Laboratory in an engine only dynamometer test room. To eliminate the inertia of the electric dynamometer, the engine was outfitted with a bell housing and clutch to allow the engine to be decoupled from the dynamometer during start. A 12 Volt electric starter was installed to replicate the engine cranking performance in a vehicle. A hydraulic load pump was added to the front end accessory drive (FEAD) system to allow simulation of the engine FEAD and other parasitic loads experienced by the vehicle during engine start up and idle. Exhaust catalysts that were aged to a simulated 150,000 miles were installed on the engine so that catalyst activation and post-catalyst (tailpipe) emissions could be evaluated.

Test cell instrumentation included pre-catalyst and post-catalyst emissions benches, pre-catalyst FFID (Fast Flame Ionization Detector), and a particulate mass measurement system capable of measuring transients. Emissions bench measurements included THC (total hydrocarbons), NO_X, CO and CO_2. Emission bench and FFID measurements were taken after the turbine just in front of the first catalyst brick. Tailpipe measurements were taken just after the light-off catalyst. The transient particulate measurement was taken only on the right bank about 685 mm downstream of the light-off catalyst. The end of the light-off catalyst is 460 mm from the manifold collector. Temperature measurements for exhaust enthalpy calculations were taken from individual port measurements with 1/16" thermocouples on each bank of the engine, as illustrated in Figure 158. The catalyst was also instrumented with a thermocouple in the midbed location, defined as 25.4 mm downstream of the front brick face in the centroid of the cross section. The location of the catalysts is shown in Figure 159.

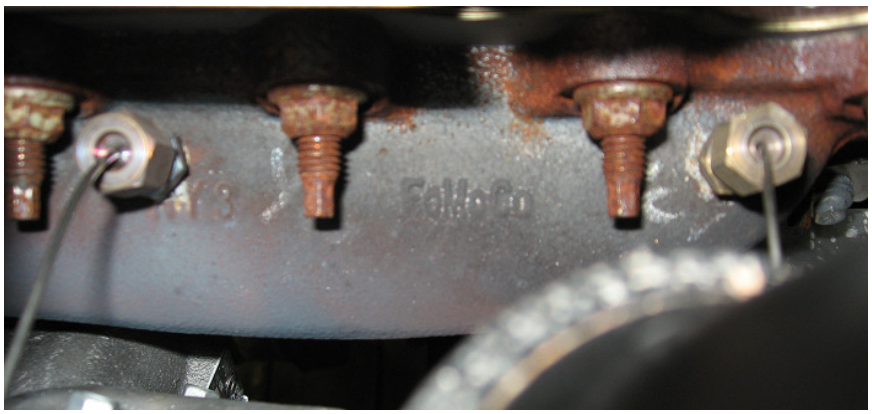

Figure 158 - Exhaust manifold with exhaust port thermocouples (cylinders 1 & 2).

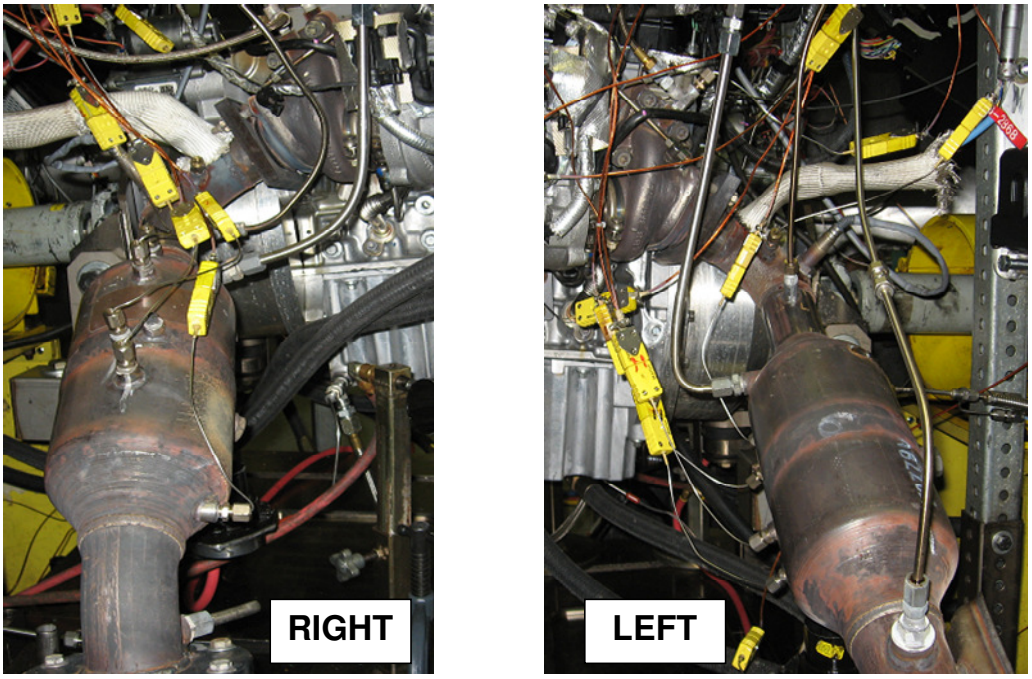

Figure 159 - Right and left exhaust system, turbocharger outlet, and catalyst.

For this testing a cold start is defined as a starter motor cranked start after all powertrain and exhaust aftertreatment components have been soaked to 20º C ± 2°. The challenge of a cold start is to minimize the emissions and generate sufficient exhaust enthalpy for catalyst activation, while maintaining acceptable combustion stability, during the initial idle after start.

A DI engine strategy calibration during engine start and warm-up has a high number of degrees of freedom with respect to control parameters for best emission, catalyst heating, and combustion stability performance during the initial idle. Adding a PFI system increases the dimensions of possible solutions. A means to expedite this process is necessary. Given the large number of parameters to calibrate on a DI engine, steady state cold fluids mapping was conducted to find optimal values for DI related fuel system parameters. The DI cold start initial idle (region 3 in Figure 164) calibration parameters were characterized/optimized using cold fluids mapping. Cold fluids mapping is a steady state test where the calibration parameters are varied while the engine emissions and stability performance are measured with the engine coolant and oil temperatures maintained near 20ºC. Cold fluids mapping facilitates the optimization of the large degrees of freedom of a DI engine.

Parameters swept during cold fluids testing include:

- SOI (Start Of Injection) of the intake stroke injection
- EOI (End Of Injection) of the compression stroke injection
- Split ratio, percent of total fuel mass in the intake stroke injection
- FRP (Fuel Rail Pressure)
- Intake cam advance from base position
- Exhaust cam retard from base position
- Exhaust heat flow (varied by adjusting mass flow in conjunction with spark timing to maintain constant BMEP)

Figure 160 and Figure 161 show injection timing and cam timing sweeps for Direct Injection (DI) only when running gasoline (E0 – Indolene Clear). Figure 162 and Figure 163 show injection timing and cam timing sweeps for Direct Injection (DI) only when running E85. Injection timing and cam timing trends are very similar for both test fuels, although Smoke/PM (FSN) is not a relevant constraint when running E85.

Turbine In Heat Flow (watts / L)	Fuel Rail Pressure (psi)	Split Ratio	SOI1 (° BTDC)	EOI2 (° BTDC)
7000	800	70 / 30	Variable	Variable

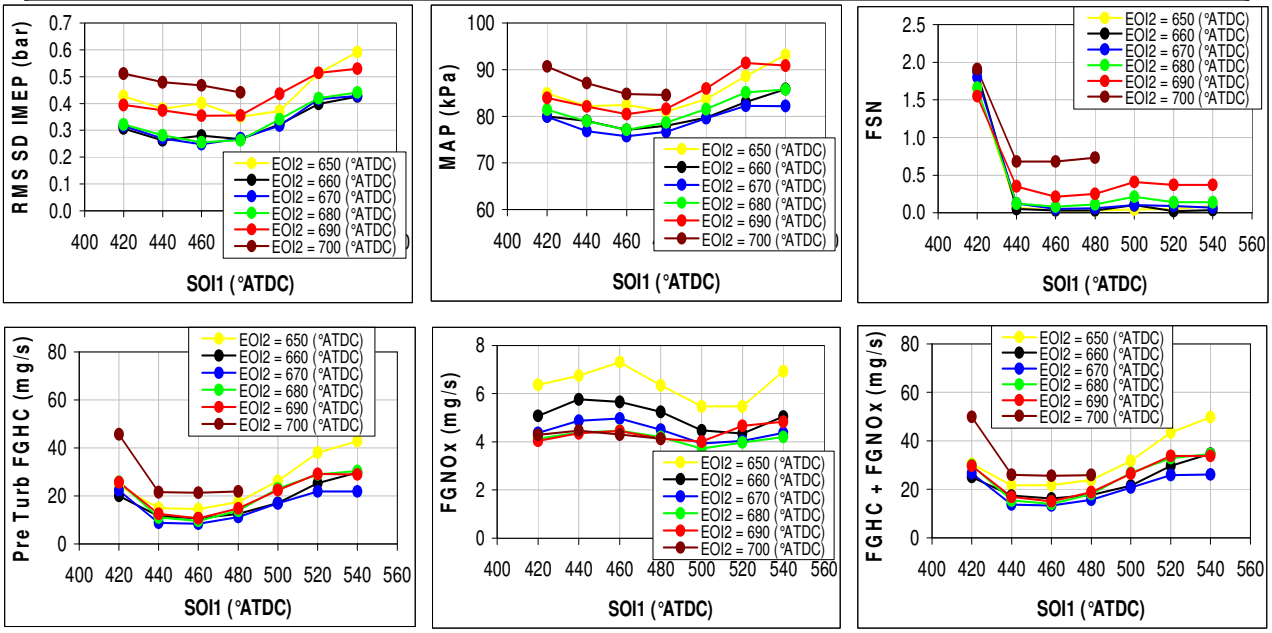

NMEP (bar)	Engine Speed (rpm)	A/F E0	Intake Cam Advance (° from base)	Exhaust Cam Retard (° from base)
1.7	1250	14.6:1	0	0

Figure 160 - Cold fluids injection timing sweeps for split injection with gasoline.

Turbine In Heat Flow (watts / L)	Fuel Rail Pressure (psi)	Split Ratio	SOI1 (° BTDC)	EOI2 (° BTDC)
8000 - 9000	800	70 / 30	460	675

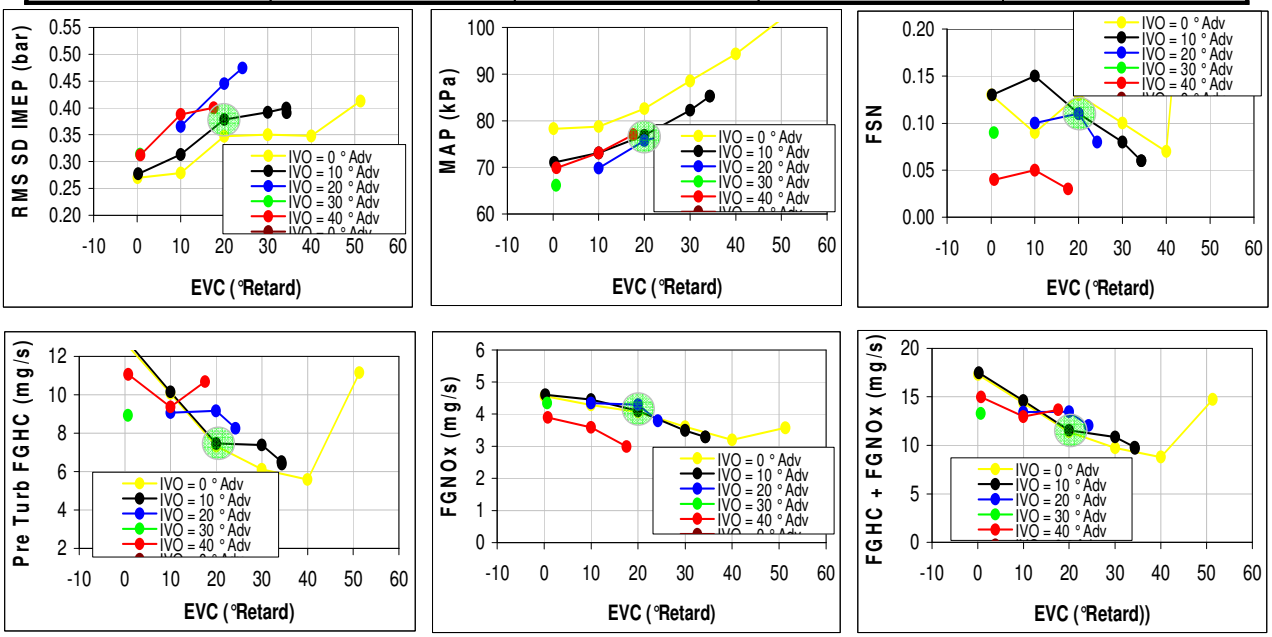

NMEP (bar)	Engine Speed (rpm)	A/F E0	Intake Cam Advance (° from base)	Exhaust Cam Retard (° from base)
1.7	1250	14.6:1	Variable	Variable

Figure 161 - Cold fluids cam timing sweeps for split injection with gasoline.

Turbine In Heat Flow (watts / L)	Fuel Rail Pressure (psi)	Split Ratio	SOI1 (° BTDC)	EOI2 (° BTDC)
7000	800	70 / 30	Variable	Variable

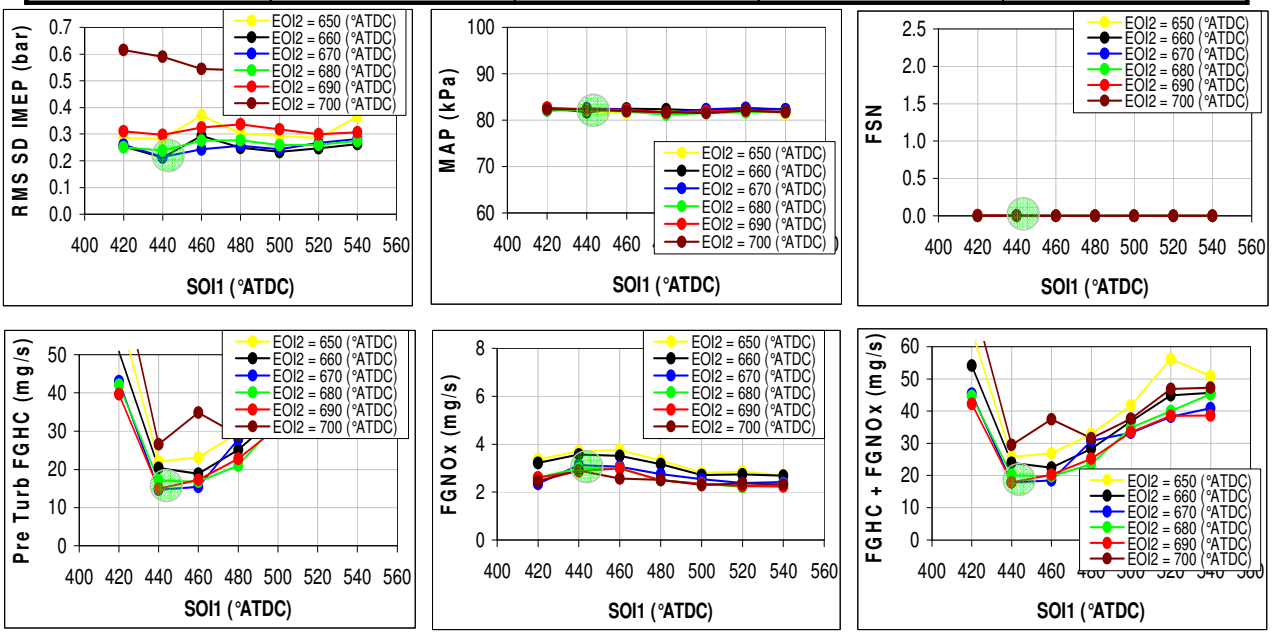

NMEP (bar)	Engine Speed (rpm)	A/F E85	Intake Cam Advance (° from base)	Exhaust Cam Retard (° from base)
1.7	1250	9.7:1	0	0

Figure 162 - Cold fluids injection timing sweeps for split injection with E85.

Turbine In Heat Flow (watts / L)	Fuel Rail Pressure (psi)	Split Ratio	SOI1 (° BTDC)	EOI2 (° BTDC)
8000 - 9000	800	70 / 30	440	670

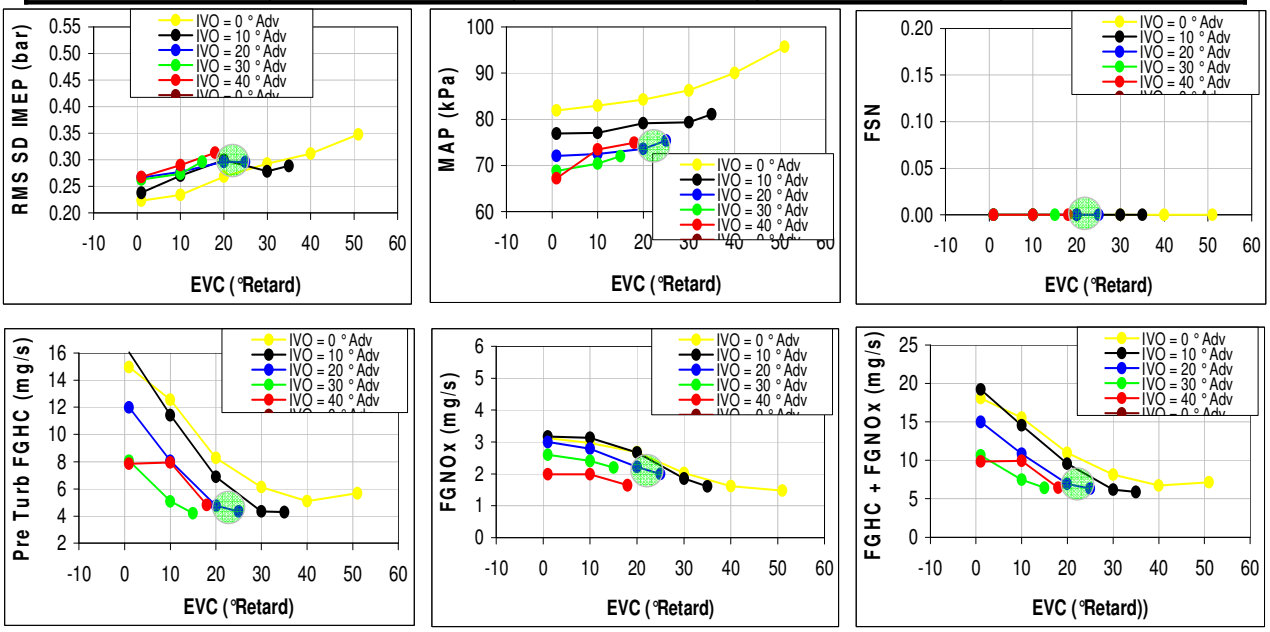

NMEP (bar)	Engine Speed (rpm)	A/F E85	Intake Cam Advance (° from base)	Exhaust Cam Retard (° from base)
1.7	1250	9.7:1	Variable	Variable

Figure 163 - Cold fluids cam timing sweeps for split injection with E85.

It has been shown that the emission and stability trends (i.e., optimal values for SOI, EOI, FRP etc.) found with cold fluids mapping are valid when compared to actual cold start tests, although the magnitude of the emissions, especially PM, are not accurate. Thus actual cold starts need to be run as a final assessment of cold start performance. In addition, cold fluids mapping is inappropriate for PFI testing because the fuel preparation is significantly different from a cold start. Therefore the optimization of the additional PFI parameters must be done with actual cold starts.

To simplify analysis, Figure 164 shows the cold start broken into smaller time intervals such as crank, run-up and flare, and stabilized neutral cold idle. Crank ends at the first combustion event for each cylinder. Run-up and flare is the transition period after each cylinder has fired once until the desired idle speed is achieved.

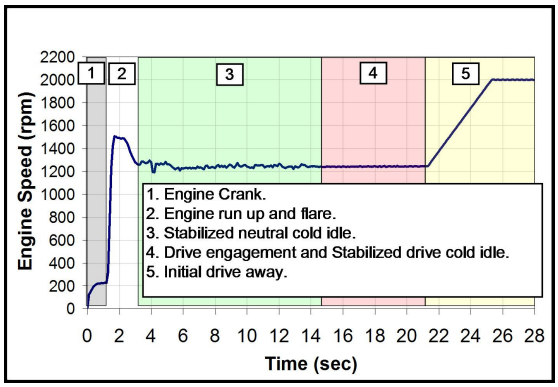

Figure 164 - Cold start regions.

A majority of the tailpipe emissions are generated during the initial cold start and idle phase, regions 1-4, while emission requirements are for an entire test. To establish pre-catalyst emission targets for regions 1-4, assumptions based on historical data are made for the portion of the tailpipe emissions for the overall cycle that are emitted in bag 1. Making reasonable assumptions for catalyst conversion efficiency, the tailpipe contribution can be converted into a pre-catalyst target. The assumptions are cross-checked against existing T2B4 capable vehicles. These emission targets are then used to assess the capability of the hardware and calibration to meet the total cycle emission requirements. The 0-20 second emission targets for the Tier II Bin 4 emissions standard are shown in Figure 165.

0-20 second Cumulative T2B4 FTP Feedgas Emission Targets		
NMOG (mg)	CO (mg)	NOx (mg)
583	13492	153

Figure 165 - 0-20 seconds emission targets for Tier II Bin 4.

Cold Start Test Plan

The DI candidate calibrations from the cold fluids work (region 3) were trialed while the DI crank and run-up (regions 1 and 2) were optimized. Through cold starts, both a DI gasoline only and a DI E85 only optimum calibration were determined. The DI gasoline calibration serves as a baseline for comparison with the various Dual Fuel/dual injection scenarios. The DI gasoline scenario meets T2B4 emissions as a production application, and therefore this comparison is a further indication of emissions compliance. The DI E85 cold start serves as a possible cold start solution for the Dual Fuel/dual injection package, provided emissions and other attribute targets are met. In addition, the DI gasoline and DI E85 calibrations serve as excellent starting points for the evaluation of cold starts with the addition of the PFI system. All PFI injections were with

gasoline, and other than the baseline DI gasoline scenario, all DI injections were with E85. The total mass of fuel injected was distributed by percentage and augmented by a multiplier for fuel type. The test points were classed by percent mass per fuel system. Although numerous PFI and DI fuel injection ratios were investigated, Figure 166 shows a summary of the most reasonable iterations that were evaluated.

Fuel Injection					Responses		
PFI (%)*	Intake DI (%)*	Comp DI (%)*	Intake DI (%)*	Comp DI (%)*	0-20s HC (mg)	0-20s NOX (mg)	5-15s SDIMEP (bar)
E0	E0		E85				
	70	30			BASELINE		
			70	30			
75				25			
35			35	30			

* = % of total fuel injected on a mass basis

Figure 166 - Dual Fuel / dual injection test matrix.

"Intake DI" represents fuel injected during the intake stroke, when the intake valve is open. "Comp DI" represents fuel injected during the compression stroke, once the intake valve is closed and the piston is moving toward TDC. All PFI injections occurred as closed valve injections during the end of the exhaust stroke, just before the intake valves are opened.

Cold Start Test Results

Test results consisted of multiple test samples (at least 3), for each test scenario shown in the test matrix. In addition each scenario was tested at a high enthalpy or heat flow (6500 Watts/liter of engine displacement) and a low enthalpy or heat flow (4200 Watts/liter) based on exhaust port temperatures. The two heat flows bracket the range of typical heat flows for V6 EcoBoost application and were used to assess the heat flow requirement to achieve adequate catalyst activation by the 20 second drive away. It was found with this post-turbocharger catalyst package that the high heat flow is required. Results for the high catalyst heat flow case are shown in Figure 167. As shown, Dual Fuel with 35% PFI (E0), 35% Intake DI (E85), 30% Compression DI (E85) yields a well-balanced solution for emissions and combustion stability. This scenario yields the lowest feed gas HC, with feed gas NOx and combustion stability near baseline levels.

Fuel Injection					Responses		
PFI (%)*	Intake DI (%)*	Comp DI (%)*	Intake DI (%)*	Comp DI (%)*	0-20s HC (mg)	0-20s NOX (mg)	5-15s SDIMEP (bar)
E0	E0		E85				
BASELINE	70	30			357	66	0.480
			70	30	**800**	**44**	**0.443**
75				25	283	**137**	**0.636**
35			35	30	**224**	72	0.468

* = % of total fuel injected on a mass basis

Figure 167 - High catalyst heat flow results.

Figure 168 is a bar graph depicting the cumulative emission results for the 0 – 20 second period of the test (regions 1 – 4) from Figure 167, along with the T2B4 targets from Figure 165.

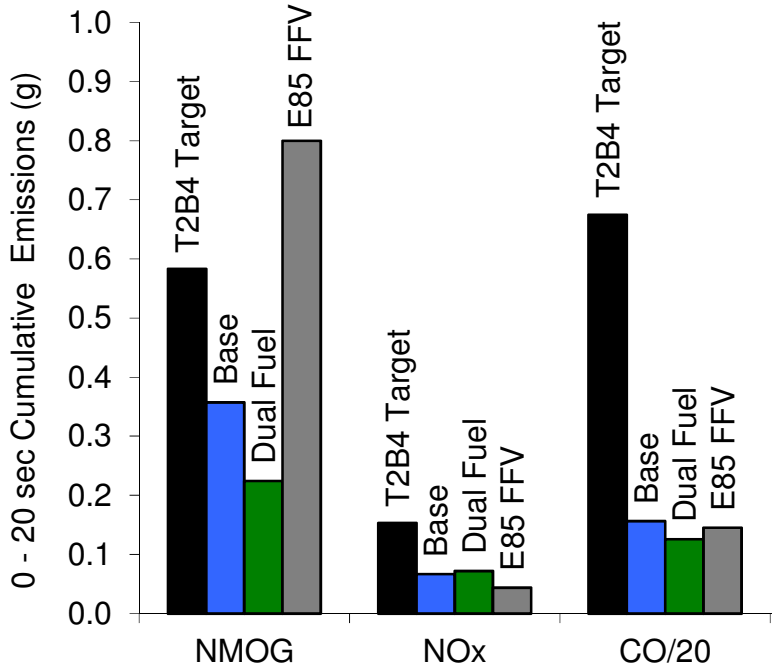

Figure 168 - Cumulative cold start emissions (0 – 20 sec) for high catalyst heat flow for baseline GTDI, Dual Fuel (35/35/30), and E85 FFV. Targets for Tier II Bin 4 are shown for reference.

Results for the low catalyst heat flow case are shown in Figure 169. As shown, the Dual Fuel case with 35% PFI (E0), 35% Intake DI (E85), 30% Compression DI (E85) yields a well-balanced solution for emissions and combustion stability. This scenario yields the lowest feedgas HC, with feedgas NOx and combustion stability near baseline levels. It was found with this post turbocharger catalyst package that the low heat flow was not adequate to achieve catalyst activation by the 20 second drive away.

Fuel Injection					Responses		
PFI (%)*	Intake DI (%)*	Comp DI (%)*	Intake DI (%)*	Comp DI (%)*	0-20s HC (mg)	0-20s NOX (mg)	5-15s SDIMEP (bar)
E0	E0		E85				
BASELINE	70	30			460	36	0.459
			70	30	**941**	**23**	0.347
75				25	270	**58**	**0.471**
35			35	30	**243**	35	0.445

* = % of total fuel injected on a mass basis

Figure 169 - Low catalyst heat flow test results.

Comparing Figure 167 and Figure 169, the DI only scenario (E0 or E85) yields lower feedgas HC as heat flow is increased, highlighting the significant post-cylinder oxidation and combustion improvement due to charge stratification that is possible with DI systems. This DI attribute is one of the reasons why DI hardware is being used for engine applications with turbochargers, which require significant heat flow to achieve adequate catalyst activation quickly.

Figure 167 and Figure 169 also show that the Dual Fuel 35/35/30 injection scenario allows combustion stability to be maintained across the low and high heat flow range, whereas the 75/25 case does not. This result highlights the charge stratification afforded by both the DI compression and DI intake injections, a phenomenon that has also been demonstrated through combustion modeling.

Scaling of Results to 5.0L Displacement

This work has demonstrated that a Dual Fuel/dual injection (DI and PFI) hardware scenario is a viable alternative for meeting current emission standards. Because this testing was performed on a 3.5L V6 engine, the project targets required scaling of this data to ensure compliance on a 5.0L V8 engine. The scaled data is shown in Figure 170. Comparing the targets in Figure 165 to the scaled numbers in Figure 170, it can be seen that both heat flow scenarios easily meet the T2B4 0-20 second emissions targets, although the high heat flow scenario would be required to achieve catalyst midbed temperature targets and ensure adequate catalyst conversion efficiencies during the rest of the FTP test cycle. As mentioned previously, meeting the 0-20 second target provides high confidence for meeting the overall cycle standard.

Scaled Dual Fuel Emissions Results*			
	NMOG (mg)	CO (mg)	NOx (mg)
Low Heat Flow	347	3807	50
High Heat Flow	320	3579	103

***NOTE:** The 35% E0 PFI , 35% E85 int-DI, 30% E85 comp-DI Dual Fuel data is scaled by the factor (5.0 / 3.5), to account for the displacement difference of the surrogate cold start engine.

Figure 170 - 0-20 second scaled emissions results for 35% E0 PFI , 35% E85 int-DI, 30% E85 comp-DI.

Summary

A 5.0L V8 twin-turbocharged direct injection engine was designed, built, and tested for the purpose of assessing the fuel economy and performance in the F-Series pickup of the Dual Fuel engine concept and of an E85 optimized FFV engine. Additionally, production 3.5L gasoline turbocharged direct injection (GTDI) "EcoBoost" engines were converted to Dual Fuel capability and used to evaluate the cold start emissions and fuel system robustness of the Dual Fuel engine concept. All project objectives were met or exceeded.

Full Load Performance
The Dual Fuel and E85 optimized FFV engines provides greatly increased full load torque and power compared to an equal displacement GTDI engine due to the highly knock resistant properties of E85. Peak BMEP (a measure of torque per unit of engine displacement) increased from 23 bar with gasoline running with enrichment to 32 bar with E85 at stoichiometry (Figure 171). This enables downsizing of the engine displacement and/or downspeeding (running lower engine speed), which moves the engine operating range in the vehicle to a more efficient region, providing improved vehicle fuel economy.

Brake thermal efficiency (BTE) is higher for E85 than for gasoline at stoichiometry due to lower burned gas temperatures which result in reduced heat transfer losses and due to combustion phasing which is closer to optimum. When GTDI is run with enrichment to improve full load BMEP, then BTE is degraded.

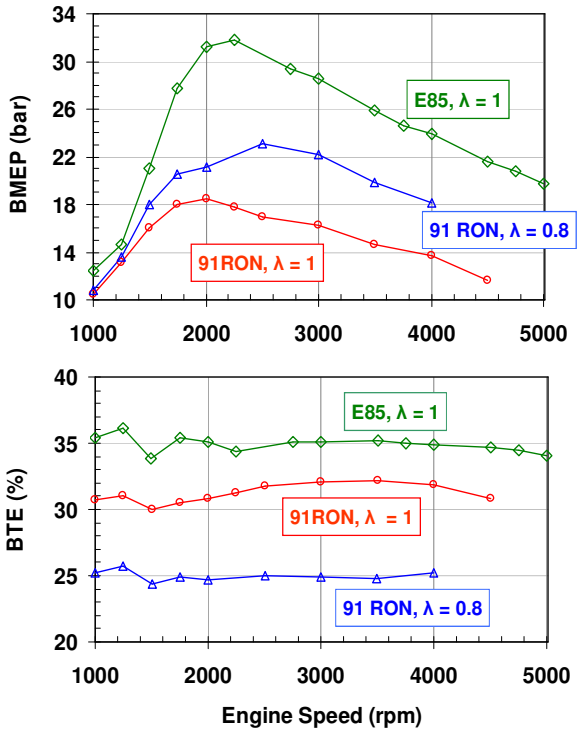

Figure 171 - Full load BMEP for ETDI and GTDI.

Fuel Economy

Using 5.0L engine dynamometer data scaled to various engine displacements as input, vehicle simulation analysis for the F150 indicates that a 3.0L Dual Fuel or E85 optimized FFV engine can replace the 6.2L displacement naturally aspirated gasoline engine (the baseline at project initiation) and provide equivalent or greater vehicle acceleration and towing performance, with the following results (Figure 172):

- The E85 optimized FFV engine using E85 fuel results in a mpg fuel economy penalty of about 8% on the combined M-H cycle. This compares favorably with the reduced energy content of E85 compared to gasoline of 29%.
- The Dual Fuel engine results in a mpg fuel economy improvement of about 20% on the combined M-H cycle.
- The E85 optimized FFV engine using E85 fuel and the Dual Fuel engine result in reductions of energy consumption on the FTP75 cycle of 26% and 21%, respectively, exceeding the project objective of 15 - 20%.
- The E85 optimized FFV engine using E85 fuel and the Dual Fuel engine result in reductions of CO_2 emissions on the M-H cycle of 23% and 17%, respectively.

For reference, simulation results for a 3.5L GTDI engine based on scaled 5.0L engine data are also shown in Figure 172.

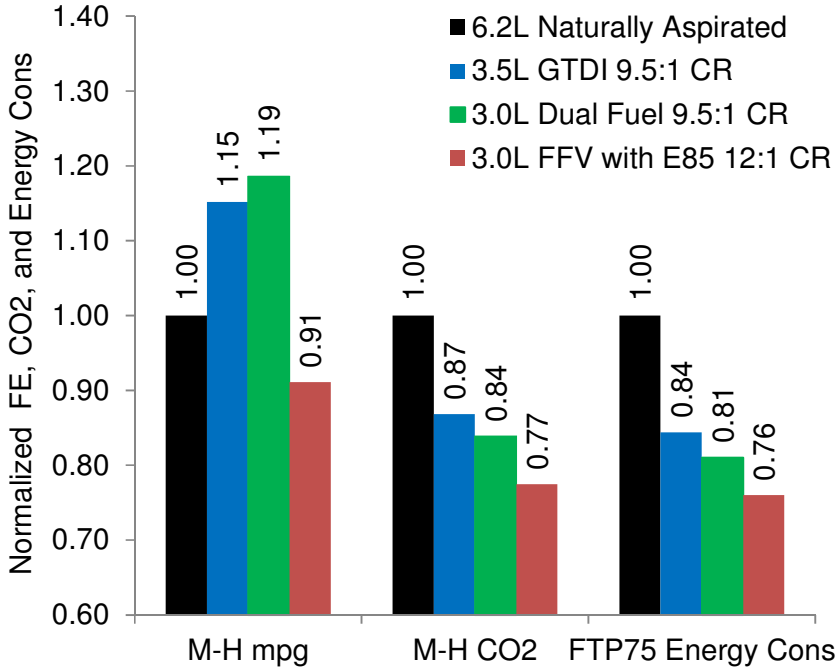

Figure 172 - M-H fuel economy, M-H CO_2 emissions, and FTP75 energy consumption normalized to values for 6.2L naturally aspirated baseline engine.

The above results assume the Dual Fuel engine maintains the compression ratio of the baseline GTDI engine (to increase driving range on the E85 fuel tank, as described below), and that the E85 optimized FFV engine has an increased compression ratio of 12:1(to utilize the high effective octane of E85 fuel). However, the performance of the E85 optimized FFV engine will be adversely affected by the high compression ratio when the engine is operated on gasoline, and thus implementation of an E85 optimized FFV engine at high compression ratio would be dependent upon the availability of E85.

Leveraging of Ethanol to Replace Gasoline

Because direct injection of E85 enables very high BMEP and downsizing of the engine displacement, gasoline is used more efficiently in the vehicle with the Dual Fuel engine concept, thereby leveraging the use of ethanol in reducing the consumption of gasoline. For the vehicle simulation results for the F150 on the M-H cycle, the reduction in gasoline consumption for the 3.0L Dual Fuel engine compared to the 3.5L GTDI engine is equivalent to one gallon of E85 replacing 2.5 gallons of gasoline (Figure 173).

The reduction in gasoline consumption for the 3.0L E85 optimized FFV engine is equivalent to one gallon of E85 replacing 0.8 gallon of gasoline. Note that this is still a significant improvement compared to the heating value of E85 relative to that of gasoline; on an equal heating value basis, one gallon of E85 would replace 0.71 gallons of gasoline. The improvement from 0.71 to 0.8 is due to the increase in thermal efficiency in the vehicle as a result of higher CR and downsizing of the engine displacement.

Thus, the Dual Fuel engine concept provides greater leveraging of ethanol in reducing gasoline consumption and greater mpg fuel economy than the E85 optimized FFV engine. The E85 optimized FFV engine provides lower CO_2 emissions and energy consumption than the Dual Fuel engine (Figure 172), but full load performance is more severely degraded due to higher CR if E85 is not available.

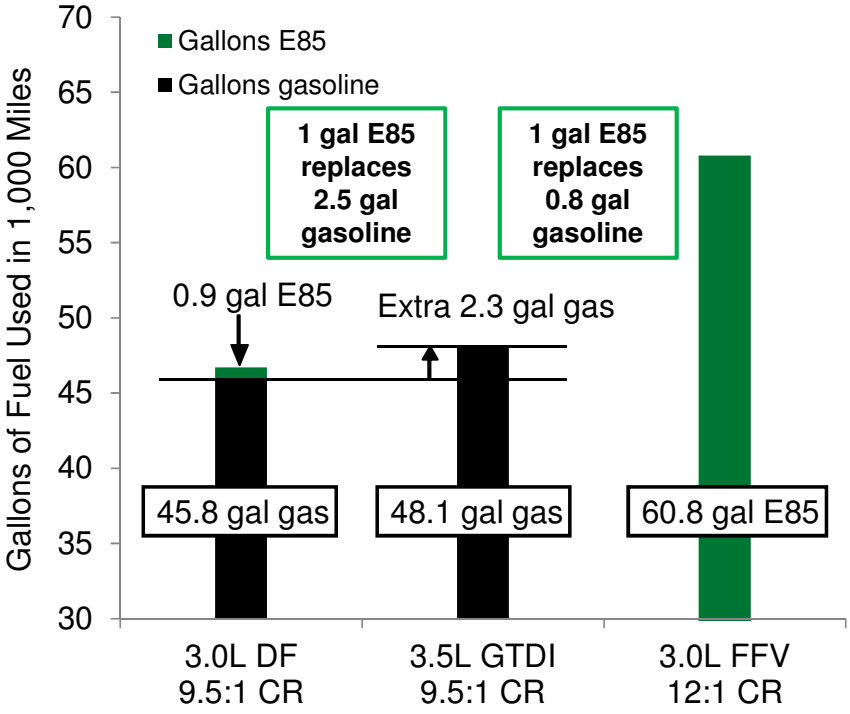

Figure 173 - Dual Fuel engine leveraging of ethanol to reduce gasoline consumption.

Emissions

The Dual Fuel engine concept provides cold start NMOG and NOx emissions comparable to a well-developed "EcoBoost" gasoline turbocharged direct injection (GTDI) baseline engine and meets the cold start emission targets for the project stretch objective of ULEV II / Tier II Bin 4. The Dual Fuel engine and E85 optimized FFV engine provide near zero particulate emissions, but the cold start NMOG emissions for the E85 optimized FFV engine are higher than the baseline GTDI engine (Figure 174).

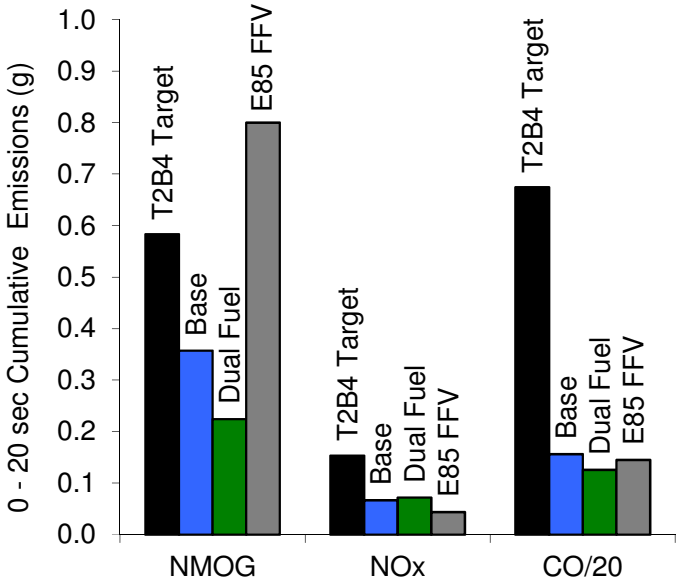

Figure 174 - Cold start emissions for base GTDI, Dual Fuel, and E85 FFV.

The Dual Fuel and E85 FFV engines are also able to run with stoichiometric air-fuel ratio over the entire engine operating range, which enables three way catalyst function for all operating conditions, including off-cycle. This is in contrast to gasoline engines which run with significant enrichment at full load.

E85 Tank Range for Dual Fuel Concept

The E85 tank for a 3.0L Dual Fuel engine in a F-Series pickup would need to be filled about every 17th time that the gasoline tank is filled for driving conditions typical of the M-H cycle and about every 11th time for towing a 10,000 pound trailer at 65 mph up a 1% grade, with the following assumptions:

- The E85 tank is one third the size of the gasoline tank.
- Moderate combustion phasing retard is applied to reduce E85 usage under heavy load conditions such as towing a trailer.
- The compression ratio of the engine is maintained at that of the baseline GTDI engine.

Increasing compression ratio improves the fuel efficiency and CO_2 emissions of the engine in the vehicle, but dramatically increases E85 usage and the refill frequency of the E85 tank relative to that of the gasoline tank. Thus, selection of compression ratio for a Dual Fuel engine will be dependent upon the duty cycle of the intended vehicle application and the availability of E85. Additionally, the above refill frequencies only include the use of E85 for knock suppression, and do not take into account other uses of E85 such as for the reduction of cold start emissions, use of 100% E85 fuelling for enhancement of turbocharger response and vehicle launch performance, and potential use of additional E85 for direct injector robustness. The cumulative effect of these uses of E85 for an actual vehicle implementation of the concept has not yet been quantified.

Durability/Robustness

No technical issues have been encountered to date which would preclude implementation of the Dual Fuel concept. However, production of the concept would require assessment of long term durability/reliability and analysis of potential failure modes in addition to those investigated during this project.

References

1. Stein, R.A., House, C.J., and Leone, T.G., "Optimal Use of E85 in a Turbocharged Direct Injection Engine," SAE paper 2009-01-1490, SAE Int. J. Fuels Lubr. 2(1): 670-682, 2009.
2. Whitaker P., Shen Y., Spanner, C., Fuchs, H., Agarwal A., Byrd, K., "Development of the Combustion System for a Flexible Fuel Turbocharged Direct Injection Engine", SAE 2010-01-0585, SAE Int. J. Engines 3(1): 326-354, 2010.
3. Agarwal, A., Jung, H., Stein, R.A., Kassem, A., Whitaker, P., Spanner, C., “Blowdown Interference on a V8 Twin-Turbocharged Engine’, SAE 2010-01-0337, April 2010.
4. Stein, R.A., “E85 Optimized Engine“, USDA Teleseminar, March 29, 2011.
5. Stein, R.A., Polovina, D., Roth, K., Foster, M. et al., "Effect of Heat of Vaporization, Chemical Octane, and Sensitivity on Knock Limit for Ethanol - Gasoline Blends," SAE Int. J. Fuels Lubr. 5(2):2012, doi:10.4271/2012-01-1277.
6. Jung, H.H., Stein, R.A., Leone, T.G., “Comparison of Dual Retard VCT to Continuously Variable Event Valvetrain, SAE 2004-01-1268, April 2004.
7. Zhao, F., Harrington, D.L., and Lai. M.D., Automotive Gasoline Direct-Injection Engines, SAE International, 2002.
8. Van Basshuysen, R., Gasoline Engine with Direct Injection, Vieweg+Teubner | GWV Fachverlage GmbH, Wiesbaden, 2009.
9. Ikoma, T., Abe, S., Sonoda, Y., et al., "Development of V-6 3.5-liter Engine Adopting New Direct Injection System," SAE Technical Paper 2006-01-1259.
10. Marriott, C.D., Wiles, M.A., Gwidt, M.J., and Parrish, S.E., "Development of a Naturally Aspirated Spark Ignition Direction-Injection Flex-Fuel Engine," SAE Technical Paper 2008-01-0319.
11. Yang, J. and Kenney, T., "Some Concepts of DISI Engine for High Fuel Efficiency and Low Emissions," SAE Technical Paper 2002-01-2747.
12. VanDerWege, B.A., Han, Z., Lyer, C.O., et al., "Development and Analysis of a Spray-Guided DISI Combustion System Concept," SAE Technical Paper 2003-01-3105.
13. Hadler, J., Szengel, R., Middendorf, H, et al., "Minimum Consumption - Maximum Force: TSI Technology in the New 1.2L Engine from Volkswagen," 30. Internationales Wiener Motorensymposium, 2009.
14. Honda, T., Kawamoto, M., Katashiba, H., et al., "A Study of Mixture Formation and Combustion for Spray Guided DISI," SAE Technical Paper 2004-01-0046.
15. Bandel, W., Fraidl, G.K., Kapus, P.E., et al., "The Turbocharged GDI Engine: Boosted Synergies for High Fuel Economy Plus Ultra-Low Emissions," SAE Technical Paper 2006-01-1266.
16. Fraidl, G.K., Kapus, P.E., Prevedel, K., and Fürhapter, A., "GDI Turbo: The Next Step," 28. Wiener Motorensymposium 2007.
17. Fuchs, H., Hopfner, W., Kapus, P., and Winklhofer, E., "Methods and Criteria for Fuel Injector Integration in Boosted Gasoline Direct Injection Engines," IMechE: Injection Systems for IC Engines, London, 2009.
18. Lang, O., Habermann, K., Krebber-Hortmann, K., et al., "Potential of the Spray-Guided Combustion System in Combination with Turbocharging," SAE Technical Paper 2008-01-0139.
19. Alger, T., Chauvet, T. and Dimitrova, Z., "Synergies between High EGR Operation and GDI Systems," SAE Technical Paper 2008-01-0134.
20. Kulzer, A., Christ, A., Rauscher, M., et al., "Thermodynamic Analysis and Benchmark of Various Gasoline Combustion Concepts," SAE Technical Paper 2006-01-0231.
21. Zhang, Y., He, B.Q., Xie, H., and Zhao, H., "The Combustion and Emission Characteristics of Ethanol on a Port Fuel Injection HCCI Engine," SAE Technical Paper 2006-01-0631.
22. Nakata, K., Utsumi, S., Ota, A., et al., "The Effect of Ethanol Fuel on a Spark Ignition Engine," SAE Technical Paper 2006-01-3380.
23. Gnannam, G., Sobiesiak, A., Reader, G., and Zhang, C., "An HCCI Engine Fuelled with Iso-octane and Ethanol," SAE Technical Paper 2006-01-3246.
24. Cohn, D.R., Bromberg, L. and Heywood, J.B., "Direct Injection Ethanol Boosted Gasoline Engines: Biofuel Leveraging For Cost Effective Reduction of Oil Dependence and CO_2 Emissions," MIT 2005.

25. Kapus, P.E., Fürhapter, A., Fuchs, H., and Fraidl G.K., "Ethanol Direct Injection on Turbocharged SI Engines - Potential and Challenges," SAE Technical Paper 2007-01-1408.
26. Hirooka, H., Mori, S., and Shimizu, R., "Effects of High Turbulence Flow on Knock Characteristics," SAE Technical Paper 2004-01-0977.
27. Lumley, J.L., Engines: An Introduction, Cambridge University Press, 1999.
28. Glanz, R., "Differential Measurement of Tumble Flows," MTZ Worldwide, January, 2000.
29. Anderson, M.K., Assanis, D.N., and Filipi, Z.S., "First and Second Law Analyses of a Naturally-Aspirated, Miller Cycle, SI Engine with Late Intake Valve Closure," SAE Technical Paper 980889.
30. GCA - Gas Exchange and Combustion Analysis Software: https://www.avl.com/gca-gas-exchange-and-combustion-analysis-software;jsessionid=380823936F65D8230F38EE73BDDCF61E.avlwp47.
31. Fairbrother R., Leifert T., Moreno Nevado F., "Measurement Supported Thermodynamic Analysis of Cylinder Internal Processes under Transient Conditions", AVL Combustion Diagnostics Symposium, Baden, June 2008.
32. Fairbrother R., Leifert T., Moreno Nevado F., "Advanced Thermodynamic Analysis with AVL GCA Efficiently Supports Development and Calibration of Internal Combustion Engines", Engine Process Simulation and Supercharging, Berlin, June 2007.
33. Fairbrother R., Leifert T., Moreno Nevado F., "Genaue Bestimmung wichtiger Ladungswechselparameterdirekt am Prüfstand auf Basis vorhandener Messwerte", Ladungswechsel im Verbrennungsmotor, Stuttgart, November 2007.
34. Prevedel K., Pinter A., Wolkerstorf J., Haimann A.,"Fahrspaß trotz Hubraumverkleinerung: eine lösbare Herausforderung durch Aufladung?", 8th Supercharging Conference, Dresden, 2002.
35. E. Rutschmann, C. Bruestle, "Multiple Cylinder Internal Combustion Engine", U.S. Patent No. 6,397,802 B1, June 4, 2002.
36. R. Diez, H. Kornherr, F. Pirntke, J. Schmidt, "Efficiency Increase Through Cross-Cylinder Bank Exhaust Manifold", MTZ (71) 05122010, pp 348-352, 2010.
37. H. Drangel, H. Nordin, P. Johansson, A. Koenigstein, "Charging System for a High Performance SI-Engine - Technology and Methods", Aufladetechnische Konferenz 2007.
38. GT-POWER v.7.0 Flow Theory Manual, Gamma Technologies, Westmont, IL 60559, USA.

Statement of Project Objectives

E85 Optimized Engine

A. OBJECTIVES

The overall objectives of this project are to:

- Develop a roadmap and demonstrate a minimized fuel economy penalty (mpg) for a F-Series pickup truck FFV with a highly boosted high compression ratio spark ignition engine optimized for running with ethanol blends up to E85.
- Achieve a reduction of energy consumption of 15% - 20% along FTP 75 compared to an equally powered vehicle with a current production gasoline engine.
- Meet at least ULEV emissions, with a target of ULEV II / Tier II Bin 4.

B. SCOPE OF WORK

Ethanol is an excellent fuel for highly turbocharged engines due to its fuel characteristics. From previous work it is known that down-sizing /down-speeding concepts can achieve a considerable fuel consumption reduction in drive cycle and real customer use. Thus a logical approach for reducing fuel consumption with ethanol fuel is to design and develop a highly turbocharged engine with high low-end torque and combine it with optimized transmission ratios. This results in typical drive cycle and customer operation at lower engine speeds, with consequent improvement in fuel consumption.

The scope of work also includes an overlay of the Ethanol Boosting Systems (EBS) concept, which combines gasoline port fuel injection (PFI) with E85 direct injection (DI), where gasoline PFI is used for starting/cold start emissions and low-medium load operation and the amount of ethanol is increased as a function of load to prevent knock. A fundamental advantage of the EBS concept is that E85 is only used as required at high loads to avoid knock. Therefore from an environmental and societal point of view, the beneficial impact of using the available E85 to improve engine efficiency can be achieved over a much broader number of vehicles.

Specifically, the scope of work entails:
Phase 1 - Define the overall engine system and conduct modeling analysis of vehicle fuel economy. Define the cylinder head architecture and design hardware for conventional and transparent single cylinder engines.
Phase 2 - Conduct optical and conventional single cylinder engine dynamometer studies to optimize the combustion system design. Initiate design of multi-cylinder engine components.
Phase 3 - Complete design and analysis of multi-cylinder engine components. Build multi-cylinder engines and conduct engine dynamometer testing to optimize cam timing, turbocharging matching, compression ratio, etc. Demonstrate full load torque capability and fuel efficiency at vehicle mapping points.
Phase 4 - Conduct base engine mapping and calibration optimizing for attributes focusing upon fuel efficiency. Optimize cold starting strategy on transient engine dynamometer. Demonstrate overall program objectives at a vehicle level for the E85 optimized engine using vehicle simulation results based on engine dynamometer data.

C. TASKS TO BE PERFORMED

Budget Period (BP) 1
Phase I and Phase II

Milestones to be achieved to complete Phase 1:

- Engine system definition, including cylinder head architecture (direct injector location, valvetrain layout, etc.), boost system configuration (turbochargers, intercooler, etc.), direct fuel injection system (number

and type of high pressure pumps, etc.), and engine structural considerations for an E85 optimized engine.

- Analytical predictions of engine full load performance and vehicle fuel efficiency for E85 optimized FFV and EBS engines.
- Component design for single cylinder transparent (for optical studies) and conventional engines.

Milestones to be achieved to complete Phase II:

- Combustion system (intake port design, injector fuel spray, and piston bowl) definition to optimize for operation on E85 based on optical and conventional single cylinder tests.

PHASE I - CONCEPT DEFINITION

Concept design (3D models with low level details) of all parts to convert the existing V8 engine to an E85 optimized direct injection turbocharged engine. Main systems considered are outlined in the tasks below.

Task 1.0 - Cylinder Head

Layout cylinder head geometry for a new roller finger follower 4-valve per cylinder valvetrain, incorporating direct injection and port fuel injection (for the EBS variant), and dual independent variable cam timing.

Task 2.0 – Air System

Analysis of the intake port geometry of the cylinder heads will be carried out. The intake and exhaust port will be tested on the stationary flow test bench. For the exhaust port, only the flow coefficients are determined. For the intake port, the flow structures are measured with LDA (Laser Doppler Anemometry), in a plane half a bore diameter below the fire deck and the flow coefficients and tumble ratios will be determined. Mean values (mean flow coefficient, tumble number) will be calculated by integrating the flow parameter ratios over crank angle, using a simple incompressible calculation and the valve lift curve. The results will be compared to available statistics. Port shape changes and different valve seat geometries are evaluated. 3D CAD design of modified intake ports will be developed to manufacture an intake flow box to perform experimental port flow development and optimization as required.

Task 3.0 – Fuel System

- Determine optimum direct injector location (side or central) for the E85 optimized engine, including consideration of the EBS engine concept (port fuel injection of gasoline combined with direct injection of E85). Factors to be considered include injector tip temperature, structural requirements for an E85 optimized engine, spark plug dielectric strength for high boost levels and compression ratios (14 mm vs. 12 mm diameter), and technology futuring.
- Determine direct injector dynamic range requirements and determine injector flow rate characteristic.
- Determine high pressure pump requirements and define pump type, number of pumps, and pump drive method.

Task 4.0 – Performance Development and Analysis

A 1-d thermodynamic simulation of the engine will be carried out using the GT Power model to determine:

- Initial definition of valve timing and valve lift profiles
- Preliminary turbocharger matching
- Full load performance estimates

The requirements from the gas exchange process may lead to adapted cam profiles. If required new cam profiles will be checked in view of specific evaluation criteria.

Vehicle simulations will be carried out on F-Series vehicles using the thermodynamic simulation results. The main objective of this simulation task is to predict cycle fuel consumption of the target vehicles for the E85 optimized engine.

Calibrate engine results with a knock model that combines realistic engine information from GT-POWER with the fuel chemistry of the CHEMKIN kinetics code. Temperatures and pressures of the end-gas will be calculated in GT-POWER with adequate modeling of the turbocharging, residuals, intercooling, ethanol charge cooling (including finite evaporation rates), etc. These results will be used to determine the auto-ignition characteristics of the fuel in a kinetic calculation using CHEMKIN, with the PRF (Primary Reference Fuel) mechanism that includes ethanol. In collaboration with Ford, a vehicle model will be also used to investigate implications of the knock model on ethanol consumption over different cycles, fuel efficiency (in addition to engine efficiency results from GT-POWER), for different type vehicles. If resources allow, simulation of thermal stratification using CFD codes (FLUENT) will be used to try to determine whether stratification is a practical means to minimize ethanol consumption.

Task 5.0 – Single Cylinder Engine

Components specific to the conventional single cylinder optical single cylinder engines will be designed. The purpose of the conventional single cylinder engine is to evaluate and verify the function of the combustion system prior to the design and procurement of multi-cylinder components.

Procurement of components for the single cylinder engines (including tooling), setup of the single cylinder engine test cell, and fuel for initial testing. The work prior to the engine tests comprises of:

- Cylinder head design adaptations
- Parts procurement and cylinder head modification
- Assembly of the modified head
- Engine functionality tests.

Task 6.0 – Optical Engine
The purpose of the transparent engine is to conduct optical studies to enable the visualization of the interaction of the ethanol fuel spray with the in-cylinder tumble motion induced by the intake ports.

Task 7.0
Setup of the optical engine in the test cell.

Task 8.0 – Program Management and Reporting
This task includes project tracking and management throughout Phase I, and documentation of the project status at regular intervals.

Phase I Decision Point (Go/No-Go)
The recipient shall prepare a draft topical report at the completion of Phase I describing the Phase I technical progress. This report shall include discussion on topics including, but not limited to, description of the work performed and the anticipated practicality, durability, reliability, and maintainability of the technology, results of any analyses, numerical simulations, and/or laboratory or field validations. After review and comment by the appropriate DOE representatives, the recipient shall modify the draft report to address the comments in the Phase I Topical Report.

The Recipient shall not proceed with subsequent Budget Period activities before receiving written authorization from the DOE Contracting Officer. No Government funds may be expended for subsequent Budget Period activities before receiving a written continuation authorization from the DOE Contracting Officer. Such authorization is dependent on the availability of funds, recipient's success in achieving technical milestones and on the recommendation of the DOE Project Officer. In the event that the recipient is not authorized to proceed with subsequent budget period activities the topical report shall become the final report.

PHASE II - SINGLE CYLINDER EXPLORATORY DEVELOPMENT
Phase II also includes layout and initial design of multi-cylinder engine components in parallel with the single cylinder investigations, but the end of Phase II is defined by the completion of the single cylinder work.

Task 1.0 - Cylinder Head
Following concept definition detail design will commence (3D models and 2D detail drawings for prototype manufacturing) of the Phase 1 defined parts and components. The main systems are as described previously. Piston tops will be designed (in combination with the cylinder head combustion chamber) for 12:1 compression ratio for the E85 optimized engine, including valve-to-piston clearance allowing for an intake valve opening (IVO) of 40°BTDC and an exhaust valve closing of 60° ATDC. Piston bowls will be designed and procured for evaluation of cold start catalyst heating with E85 on the optical and conventional single cylinder engines.

Task 2.0 – Air System
Layout of the intake manifolding, exhaust manifolding, turbochargers, and intercooler system will be conducted. Vehicle packaging of the above systems will be carried out for the F-Series vehicle / transmission combination. Packaging will be performed at a level suitable to ensure installation in a demonstrator vehicle is feasible.

Task 3.0 – Fuel System
The drive system for the high pressure direct injection pump(s) will be designed. Layout of the fuel injector rail incorporating consideration of production assembly will be conducted.

Task 4.0 – Performance Development and Analysis
Refinement of the 1-d GT-Power model will continue, including incorporation of modifications for ethanol combustion. Turbocharger matching studies will also continue, with consideration of compressor and turbine maps to cover the range of potential fuels and associated boost levels for the FFV version of the E85 optimized engine.

Task 5.0 – Single Cylinder Engine
The conventional single cylinder engine will be used to evaluate and verify the function of the combustion system prior to the design and procurement of multi-cylinder components.

The conventional single cylinder engine will work in concert with the optical single cylinder engine, where the optical engine is use to gain insights and the conventional engine is used to acquire operating engine data and evaluate modifications.

Task 6.0 – Optical Engine
The specific project objectives of this activity comprise the analysis of:

- Minimized fuel wall wetting
- Optimized double injection capability
- Optimized cold start capability
- Minimum soot formation.

For this purpose, the following will be identified:

- Fuel injection and spray interaction with head, liner and piston
- Fuel spray interaction with intake airflow
- Combustion quality evaluation on basis of premixed versus diffusion flame combustion
- Soot in combustion.

Above phenomena are documented with spray and flame photography with laser illumination for fuel vapor imagining by means of laser induced fluorescence. Image evaluation and data reduction is accomplished with standardized evaluation techniques.

Engine operating points will especially focus on:

- Low speed high load. Engine speed is limited to 2500 rpm maximum
- Part load reference points
- Dual injection modes for partial stratification
- Cold start (first injections at cranking speed during cold start).

Results of the engine variants tests are used to specify:

- Injector and injection pressure requirements
- Operation for minimum fuel wall wetting (fuel in oil)
- Operation for minimum soot in combustion
- Dual injection modes to support partial stratification in catalyst heating mode
- Injection strategy for cold start.

Task 7.0 – Program Management and Reporting
This task includes project tracking and management throughout Phase II, and documentation of the project status at regular intervals.

Task 8.0 - Topical Report and Continuation Application
The recipient shall prepare a draft topical report, as a part of the continuation application, describing the Phase 1 and Phase 2 technical progress. This report shall include discussion on topics including, but not limited to, description of the work performed and the anticipated practicality, durability, reliability, and maintainability of the technology, results of any analyses, numerical simulations, and/or laboratory or field validations. After review and comment by the appropriate DOE representatives, the recipient shall modify the draft report to address the comments in the Phase 2 Topical Report. If the government/recipient elects not to continue with the remaining effort, the Phase 2 Topical Report will become the Project Final Report.

The Recipient shall not proceed with subsequent Budget Period activities before receiving written authorization from the DOE Contracting Officer. No Government funds may be expended for subsequent Budget Period activities before receiving a written continuation authorization from the DOE Contracting Officer. Such authorization is dependent on the availability of funds and on the recommendation of the DOE Project Officer. In the event that any Budget Period is not authorized, the topical report shall become the final report.

Budget Period (BP) 2
Phase III

Milestones to be achieved to complete BP2:

- Design and analysis of multi-cylinder engine components for the E85 optimized FFV and EBS engines completed.
- Multi-cylinder engine parts procured and engines built.
- Cam timing, compression ratio, turbocharger matching, etc. optimized by conducting multi-cylinder engine dynamometer development.

PHASE III- Advanced Development

Task 1.0 - Cylinder Head
Design and analysis of all cylinder head components will be finalized, including valvetrain, water jackets, camshafts, and variable cam timing. Supporting thermo-mechanical analysis will be carried out covering:

- Coolant CFD of cylinder head
- Finite element analysis of cylinder head
- Dynamic analysis of complete timing drive and valvetrain including the high pressure fuel pump drive and variable cam timing (VCT).Valve bridge dimensions and cylinder head structure will be designed to be capable of 150 bar peak cylinder pressure, to provide the required strength for the boost level and compression ratio of an ethanol optimized engine. Water jackets will be designed with particular attention to direct injector cooling.

The cylinder head will incorporate dual independent variable cam timing. Camshafts will be designed for dual independent variable cam timing (VCT), utilizing to the extent possible the naturally aspirated camshaft and cam phaser design features.

Task 2.0 – Air System
The design of air system components will be completed, including turbocharger system (including intercooler), inlet air system, and intake manifolding. Analysis of component flow losses and cylinder-to-cylinder air distribution will be performed.

Task 3.0 – Fuel System
Fuel system component design will be completed, including the high pressure fuel pump(s) and drive system, direct injectors, port fuel injectors (for the EBS variant), and fuel rails.
Issues with respect to transient response of the injectors, infrastructure issues and tank design will be investigated. Dual-fuel injectors concepts, as well as dual fuel tanks, will be explored. Infrastructure issues will be explored, including exploring means of introducing the technology in test fleets. CFD codes will be used to simulate the injector. Issues with respect to the fuel tank, such as means to minimize evaporative emissions, ways to minimize the cost of the tank, and best means of fueling the tank (one tank neck with internal valving, multiple filling necks), will be explored.

Task 4.0 – Performance Development and Analysis
As multi-cylinder data becomes available, the above described models will be further validated and used to conduct optimization studies to allow more efficient multi-cylinder optimization of turbocharger matching, variable cam timing strategy, and ethanol consumption for the EBS variant.

Task 5.0 – Multi-Cylinder Engine
The procurement of prototype parts and components will be carried out with technical support during the procurement process. Three prototype engines will be built, two for conventional steady state multi-cylinder testing, and one for multi-cylinder transient cold start development. Before the assembly all parts will be measured according to the inspection list and all values documented in the relevant inspection sheets. The main components will be pressure tested. After the inspection the engine parts will be released for the assembly. All measurement results, the pick list etc. will be gathered in the build log. The build log will be stored and a copy of the build log will be kept with the engine.

The engine will be set up on an engine dynamometer test bed and put into operation. The full and part load engine development will be carried out on a steady state engine test bed in order to achieve the targets of performance, fuel consumption and emissions.

The following ethanol-specific issues will be considered in the development program:

- The higher octane number, the lower caloric value and the higher heat of evaporation in comparison to gasoline will change the combustion system of the engine.
- Fuel properties can lead to pre-ignition, therefore a spark plug temperature measurement will be required.

Initial measurements are carried out on steady state engine test bed to determine the requirements and limits for hardware components (flow capacity of injector, fuel pump) as well as to have first assessment on engine performance on ethanol fuel operation.

Based on the findings from initial measurement an extended program shall be performed to cover the most relevant engine operation modes:

- Full load, complete curve
- Part load, homogeneous, specific points out of mini-map
- Idle, start of injection variation for 550 rpm

These measurements are focused to investigate the potential for optimizing emissions and soot, as well as improving fuel consumption.

The spark plug temperature measurement will be carried out with support of the spark plug supplier on the engine dynamometer test bed.

Task 6.0 – Program Management and Reporting
This task includes project tracking and management throughout Phase III, and documentation of the project status at regular intervals.

Task 7.0 - Topical Report and Continuation Application.
The recipient shall prepare a draft topical report, as a part of the continuation application, describing the Phase 3 technical progress. This report shall include discussion on topics including, but not limited to, description of the work performed and the anticipated practicality, durability, reliability, and maintainability of the technology, results of any analyses, numerical simulations, and/or laboratory or field validations. After review and comment by the appropriate DOE representatives, the recipient shall modify the draft report to address the comments in the Phase 3 Topical Report. If the government/recipient elects not to continue with the remaining effort, the combined Phae 1, Phase 2 and Phase 3 Topical Reports will become the Project Final Report.

The Recipient shall not proceed with subsequent Budget Period activities before receiving written authorization from the DOE Contracting Officer. No Government funds may be expended for subsequent Budget Period activities before receiving a written continuation authorization from the DOE Contracting Officer. Such authorization is dependent on the availability of funds and on the recommendation of the DOE Project Officer. In the event that any Budget Period is not authorized, the topical report shall become the final report.

Budget Period (BP) 3
Phase IV

Milestones to be achieved to complete BP3:

- Multi-cylinder full load performance and fuel efficiency at vehicle mapping points demonstrated for the E85 optimized FFV and EBS engines.

- Cold starting strategy optimized for emissions and combustion stability for E85 optimized FFV and EBS engines.

- Mapping and calibration for optimized fuel efficiency for the E85 optimized FFV and EBS engines .

- Demonstration of vehicle level attributes (fuel economy, emissions, and performance) for the E85 optimized FFV and EBS engines, based on vehicle simulation using transient and steady state engine dynamometer data as input.

PHASE IV - Engineering Development

Task 1.0 - Cylinder Head
This task includes any required design updates/revisions that are required as a result of issues discovered during the course of the multi-cylinder engine testing.

Task 2.0 – Fuel System
This task encompasses modeling to optimize ethanol consumption for the EBS concept variant of the engine, working in concert with the multi-cylinder mapping of Task 7.
Issues related to injector coking with deposits and/or injector tip temperature will also be investigated, with emphasis on the EBS variant where the DI injectors do not flow fuel at light loads. For example, this may involve working with the injector supplier to develop novel injector sealing techniques which improve heat transfer from the injector tip.
This task also includes resolution of fuel system issues which arise during the course of the multi-cylinder testing. An example would be issues which arise due to injector rail dynamic pressure pulsations.

Task 3.0 – Performance Development and Analysis
Vehicle simulation analysis using the steady state engine dynamometer data of Task 7.0 will be performed to developed vehicle level fuel economy and performance results, both for the FFV version of the engine and for the EBS variant. This analysis will be performed for various standardized drive cycles.
Vehicle level tailpipe emissions will be assessed based upon cold starts performed on a transient dynamometer using a full aftertreatment system and Ford's TWC simulation model.

Task 4.0 - Multi-Cylinder Engine
Upon completion of the thermodynamic development in Phase III, mapping of the engine on the engine dynamometer will be performed to optimize operating parameters such as fuel injection timing and pressure, variable cam timing settings, combustion phasing, and knock control. For the EBS variant, the E85 quantity required to avoid knock will be determined as a function of combustion phasing to allow optimization of vehicle fuel consumption. (Moderate retard of combustion phasing reduces the E85 requirement and the total mass flow of fuel required.)

Optimized calibrations for cold start (20°C) emissions, combustion stability, and catalyst light-off will be developed to demonstrate the capability of the technology to meet ULEV/T2B4 emissions. A surrogate engine equipped with a catalyst system will be employed, with results scaled to reflect equivalent results of the project engine. This will be performed for both gasoline and E85 DI, followed by EBS using gasoline PFI combined with E85 DI. Parameters to be investigated and optimized are:

- Crank Time
- Potential for split injection (1 induction and 1 compression injection per cycle)
- Fuel pressure, injection timing/s, split factor (in the case of more than 1 injection/cycle) and cam timings
- Combustion stability
- HC and NOx feedgas emissions
- Heat flux (mass flow times temperature) for catalyst heating

For EBS, opportunities presented by combining gasoline PFI and E85 DI will be investigated.

Task 5.0 – Program Management and Reporting
This task includes project tracking and management throughout Phase IV, and documentation of project results in a final report.

D. CRITICAL PATH PROJECT MILESTONES (MILESTONE PLAN/STATUS)

As a part of the approved SOPO, the Recipient will develop a Milestone Plan that will serve as the baseline for tracking performance of the project and will identify critical path project milestones (no less than 2 per calendar year) for the entire project.

During project performance, the Recipient will report the Milestone Status as part of the required quarterly Progress Report as prescribed under Attachment 4, Reporting Requirements Checklist. The Milestone Status will present actual performance in comparison with Milestone Plan, and include:

(1) the **actual** status and progress of the project,
(2) specific progress made toward achieving the project's critical path milestones, and,
(3) any proposed changes in the projects schedule required to complete critical path milestones.

E. DELIVERABLES

The periodic, topical, and final reports shall be submitted in accordance with the attached "Federal Assistance Reporting Checklist" and the instructions accompanying the checklist.

Topical Reports required at the completion of each Budget Period.

F. BRIEFINGS/TECHNICAL PRESENTATIONS

The Recipient shall prepare detailed briefings for presentation to the Project Officer at the Project Officer's facility located in Pittsburgh, PA or Morgantown, WV. Briefings shall be given by the Recipient to explain the plans, progress, and results of the technical effort.

The Recipient shall provide and present a technical paper(s) at the DOE/NETL Annual Contractor's Review Meeting to be held at the NETL facility located in Pittsburgh, PA or Morgantown, WV.